Cape Peninsula University of Technology

# Mechanism of enantiomeric resolution

By

Mawonga N. Mei

Thesis submitted in fulfilment of the requirements for the degree of PhD in Chemistry in the Faculty of Applied Sciences at the Cape Peninsula University of Technology.

Supervisor: Prof. Ayesha Jacobs

Co-supervisor: Prof. Luigi R. Nassimbeni

Bellville, Cape Town, 2021

# Declaration

I, Mawonga Newton Mei, declare that the contents of this thesis represent my own unaided work, and that the thesis has not previously been submitted for academic examination towards any qualification. Furthermore, it represents my own opinions and not necessarily those of the Cape Peninsula University of Technology.

Signed: Date:

# Abstract

Selected racemic mixtures were resolved using the four *Cinchona* alkaloids; cinchonine (**CINC**), cinchonidine (**CIND**), quinine (**QUIN**) and quinidine (**QUID**) in a series of solvents. The resultant crystalline products were analyzed with the ultimate objective of establishing the mechanism of enantiomeric resolution. The effect of the choice of solvent on the chiral resolution outcome was also investigated.

Several racemates were used in the study but only the following five gave rise to suitable crystalline material; citronellic acid (**3.1**), malic acid (**3.2**), *trans*-9,10-dihydro-9,10-ethanoanthracene-11,12-dicarboxylic acid (**3.3**), 9,10-dihydro-9,10-ethanoanthracene-11-carboxylic acid (**3.4**) and 2-chloropropanoic acid (**3.5**). Crystals were obtained from the slow evaporation of mixtures of the racemate and the resolving agent in a 1:1 ratio. The desolvation temperatures and melting points of the crystalline materials were determined using differential scanning calorimetry (DSC). The mass loss percentages of the incorporated solvents were obtained from thermogravimetry (TGA). Single crystal X-ray diffraction was used to determine the crystal structures. The crystal packing and hydrogen bond data of the resultant salts were analyzed. In selected cases, FT-IR spectroscopy was used to confirm salt formation by determining the carboxylate frequencies. The CrystalExplorer program was employed to determine the intermolecular interactions involved in stabilising the molecular packing. The Cahn-Ingold-Prelog system was used to establish the configurations of the isolated enantiomers, based on the known configurations of the resolving agents.

Suitable crystals resulted from slow evaporation of solutions from the following solvents; acetone, acetonitrile mixed with water, methanol, pentanol, toluene, and water. Fourteen diastereomeric salts and their crystal structures were obtained in the study. These include eleven crystal structures where one enantiomer was preferred; **P1** (*S*-**3.1**$^-$)(**CIND**$^+$)•**H$_2$O, P2** (*D*-**3.2**$^-$)(**CINC**$^+$)•**2H$_2$O, P3** (*L*-**3.2**$^-$)(**CIND**$^+$)•**2H$_2$O, P4** (*R*,*R*-**3.3**$^-$)(**CINC**$^+$)•**ACE**, **P5** (*R*,*R*-**3.3**$^-$)(**CIND**$^+$), **P6** (*S*,*S*-**3.3**$^-$)(**QUID**$^+$)•**2MeOH, P7** (*R*,*R*-**3.3**$^-$)(**QUIN**$^+$)•**2MeOH, P8** (*S*,*S*-**3.3**$^-$)(**CINC**$^+$)•**H$_2$O, P9** (*R*-**3.4**$^-$)(**QUIN**$^+$)•**MeOH, P10** (*R*-**3.4**$^-$)(**QUID**$^+$) and **P11** (*S*-**3.5**$^-$)(**QUIN**$^+$)•**H$_2$O.** Mixtures of enantiomers were also found in three crystal structures involving **3.5, P12** (0.4*S*-**3.5**$^-$)(**QUID**$^+$)•**H$_2$O, P13** (0.8*S*-**3.5**$^-$)(**CINC**$^+$)•**H$_2$O** and **P14** (0.6*S*-**3.5**$^-$)(**CIND**$^+$)•**H$_2$O.** Attempts to obtain more material of **P5** and **P10** resulted in powders, **P5a** and **P10a**. All of the salts were obtained in a 1:1 ratio with transfer of protons from the carboxylic acids to the bases and some of the salts were solvated. The crystal structures were dominated by N—H···O, O—H···O and O—H···N hydrogen bonds and weak hydrogen bonds in the form

of C—H···O interactions. The close contacts were established by the CrystalExplorer program as O···H, H···H, C···H, N···H and Cl···H (in the case of **3.5**).

# Acknowledgements

I would like to thank my supervisor, Prof Ayesha Jacobs, for her support and guidance in this project. She gave me the opportunity to think independently, build, and experiment without restrictions. Thanks also go to Profs Nassimbeni and Bàthori for their insight and participation in this research project. I really appreciate their time and attention given to this project.

I would particularly like to thank the following colleagues who have not only been great technical resources, but also made working in the labs fun, Gillian, Zandile, Siya, Andiswa, Kallie and the rest. I wish them all the best of luck and success in their future careers.

My colleagues deserve countless acknowledgements for their support and generous nature. They gave me the opportunity to learn and concentrate on my studies and assisted when approached for assistance.

Thanks to the late Prof. Edwin Weber for the two roof shaped compounds used in the study.

Finally, I would like to thank my family, especially my better half, Deliwe, my siblings, for their support through this endeavour in my life. I dedicate this PhD to my late parents and brother, who were sources of inspiration, Mbutho and Nonkosamabhele Mei, and Mfundo Mei.

The financial assistance of NRF and CPUT towards this research is acknowledged. Opinions expressed in this thesis and the conclusions arrived at, are those of the author, and are not necessarily to be attributed to the National Research Foundation and CPUT.

Table of contents

List of chapters

## List of figures

## List of tables

## List of schemes

**CIND** in water and toluene, **P11 (*S*-3.5$^-$)(2.3$^+$)·$H_2O$, P12 (**0.45*S*-**3.5$^-$)(2.4$^+$)•$H_2O$**, P13 (**0.8*S*-**3.5$^-$)(2.1$^+$)·2$H_2O$** and **P14 (**0.6*S*-**3.5$^-$**)(2.2$^+$)·$H_2O$.**

## Abbreviations

| | |
|---|---|
| AC | Absolute configuration |
| **ACE** | Acetone |
| ACL | α-Amino-ε-caprolactam |
| API | Active pharmaceutical ingredient |
| *et al.* | And others |
| BINOL | 1,1'-Bi-2-naphthol |
| BNDA | 1,1'-binaphthyl-2,2'-dicarboxylic acid |
| BnBr | Benzylbromide |
| BNP | Binaphthylphosphoric acid |
| Bp | Boiling point |
| nBu | Butyl |
| CAHB | Charge assisted hydrogen bond |
| Cat | Catalyst |
| **CINC** | Cinchonine |
| **CIND** | Cinchonidine |
| CCDC | Cambridge Crystallographic Data Centre |
| CDK | Cyclin-dependent kinase |
| CMPA | Chiral mobile phase additives |
| CRL | *Candida rugosa* Lipase |
| CSD | Cambridge Structural Database |
| CSP | Crystal structure prediction |
| CYDTA | *Trans*-1,2-Cyclohexanediaminotetraacetate |
| DCR | Dielectrically controlled resolution |
| de | Diastereomeric excess |
| DEA | 9,10-Dihydro-9,10-ethanoanthracene |
| DMF | Dimethyl formamide |
| DMPPA | Dimethyl-3phenylpentanoic acid |
| DMSO | Dimethylsulphoxide |

| | |
|---|---|
| DNA | Deoxyribonucleic acid |
| DSC | Differential scanning calorimetry |
| EDDA | N,N'-Ethylenediaminediacetate |
| EDTA | Ethylenediaminetetraacetate |
| ee | Enantiomeric excess |
| Et | Ethyl |
| En | Ethylenediamine |
| $Et_2O$ | Diethyl ether |
| ENL | Erythema nodosum leprosum |
| EtOAc | Ethyl acetate |
| EU | European Union |
| EtOH | Ethanol |
| FDA | Food Drug Administration |
| FT-IR | Fourier transform infrared |
| GSK | GlaxoSmithKline |
| HPLC | High performance liquid chromatography |
| HCl | Hydrochloric acid |
| HSM | Hot stage microscopy |
| IDA | Iminodiacetatate |
| IUPAC | International Union of Pure and Applied Chemistry |
| IND-SAC | Indomethacin-saccharin |
| ISA | Indole-3-succinic acid |
| iBu | Isobutyl |
| iPr | Isopropyl |
| MA | Mandelic acid |
| Me | Methyl |
| MeOH | Methanol |
| Mp | Melting point |
| MPRD | Methylpyrrolidine |
| NGA | Naphthyl glycolic acid |
| NMR | Nuclear magnetic resonance |
| OMe | Methoxy |
| Oy | Optical yield |

| | |
|---|---|
| PeOH | Pentanol |
| Ph | Phenyl |
| nPr | Propyl (linear chain) |
| Ox | Oxalate |
| PhMe | Phenylmethane |
| PTC | Phase transfer catalysts |
| PTE | Phenyl-2-*p*-tolyl ethanamine |
| PXRD | Powder X-Ray diffraction |
| *Rac* | Racemic |
| RT | Room temperature |
| **QUIN** | Quinine |
| **QUID** | Quinidine |
| RA | Resolving agent |
| SMB | Simulated moving bed |
| SPINLO | 1,1'-Spirobiindane-7,7'-diol |
| TADDOL | α,α,α',α'-Tetraaryl-2,2-disubstituted 1,3-dioxolane-4,5-dimethanol |
| *Tert* | Tertiary |
| TGA | Thermo-gravimetric analysis |
| THF | Tetrahydrofuran |
| TLC | Thin layer chromatography |
| TMP | Trimethoprim |
| TA | Tartaric acid |

## Symbols

| | |
|---|---|
| α | Alpha |
| Θ/ϕ | Angles |
| Å | Angstrom |
| *S* | Assigned to a chiral centre whose configuration is left handed |
| *R* | Assigned to a chiral centre whose configuration is right handed |
| *β* | Beta |
| Cal | Calories |
| C | Celcius |

| | |
|---|---|
| cm | Centimetre |
| D | Dimension |
| *D*/*d* | Distances |
| º | Degrees |
| *M* | Description of a left handed helix |
| *P* | Description of a right handed helix |
| *d* | Dextrorotatory |
| ε | Dielectric constant |
| K | Kelvin |
| k | Kilo |
| *l* | Levorotatory |
| M | Molarity |
| Mol | Mole |
| p$K_a$ | Measure of acid strength |
| mg | Milligram |
| ml | Millilitre |
| Min | Minute |
| *o*-, *m*-, *p*- | Ortho-, meta- and para- |
| % | Percent |
| π | Pi |
| S | Resolution efficiency |
| [α] | Specific rotation |
| T | Temperature in Kelvin |
| τ | Torsion angle |

# Chapter 1

# Introduction

## 1.1. Stereochemistry

Stereochemistry is the field of chemistry that is concerned with the 3-dimensional aspects of molecules. This includes molecules that have their atoms linked in the same order but differ in 3-dimensional orientation, such compounds are called stereochemical isomers or stereoisomers. The order of atom connections is the same, but the atoms differ in their spatial orientation, e.g. *cis*- and *trans*- dimethylcyclopropane (*cis*-**1.1** and *trans*-**1.1**).[1(a)]

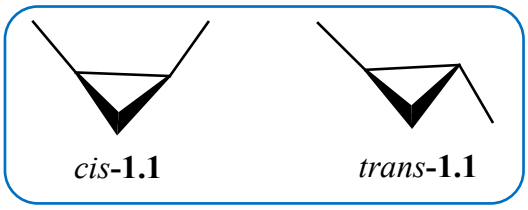


### 1.1(a) Enantiomers

Molecules of the type $CH_3A$, $CH_2AB$ are identical to their mirror images, but CHABC is not. A CHABC molecule is related to its mirror image just like the right hand is related to the left hand (Figure 1.1)

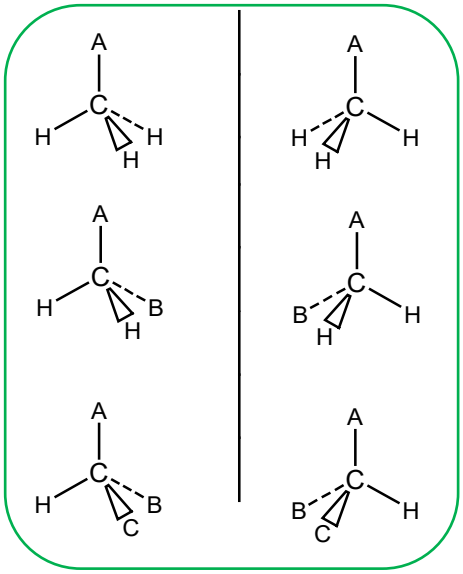


Figure 1.1 Mirror images of the type $CH_3A$, $CH_2AB$ and CHABC molecules.

By using molecular models, it is impossible to superimpose CHABC on its mirror image (as one cannot superimpose the left hand on the right hand), because they are not the same. The $CH_3A$ and $CH_2AB$ molecules are identical to their mirror images and therefore are not handed. Their atoms coincide when you superimpose one on its mirror image. The compounds that are

dissimilar to their mirror images are called enantiomers (from the Greek word *enantio*, meaning opposite). 2-Hydroxypropanoic acid (lactic acid) (**1.2**) exists as a pair of enantiomers since it has four dissimilar substituents joined to the carbon atom (Figure 1.2).[1(a)]

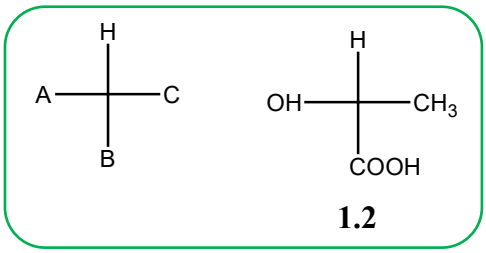


Figure 1.2 Lactic acid: a molecule of the general formula CHABC.[1(a)]

These enantiomers are (+)- and (-)-2-hydroxypropanoic acids ((+)-**1.2** and (-)-**1.2**) (Figure 1.3) and are found in sour milk, but the (+)-enantiomer occurs in muscle tissue.

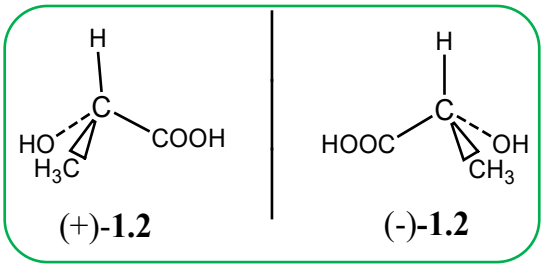


Figure 1.3 Mirror images of **1.2**.

1.1(b) Chirality (handedness)

A chiral compound is a compound that is not identical to its mirror image and does not have a plane of symmetry. A compound that has a plane of symmetry is non-chiral or achiral (Figure 1.4).[1(a)]

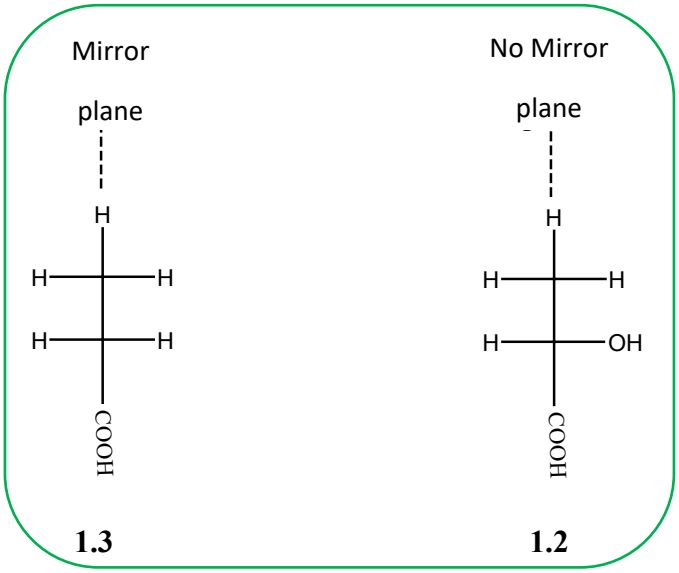


Figure 1.4 An example of compounds with and without a mirror plane.[1(a)]

Propanoic acid (**1.3**) is achiral when lined up as in Figure 1.4 while 2-hydroxypropanoic acid (**1.2**) has no plane of symmetry and is chiral. Central C atoms bonded to four different substituents are called chiral centres, stereocentres, asymmetric centres or stereogenic centres. A chiral centre is the cause of chirality and chirality is the property of the whole compound.

1.1(c) Optical activity

Generally, enantiomers have similar properties, but are dissimilar in their ability to rotate plane-polarized light. Light consists of a series of vibrating waves that are oriented in all possible directions and in an even distribution, ie the waves are unpolarized. Light can be passed through a polarizing filter to give rise to plane-polarized light that consists of waves oriented only in one direction (Figure 1.5).

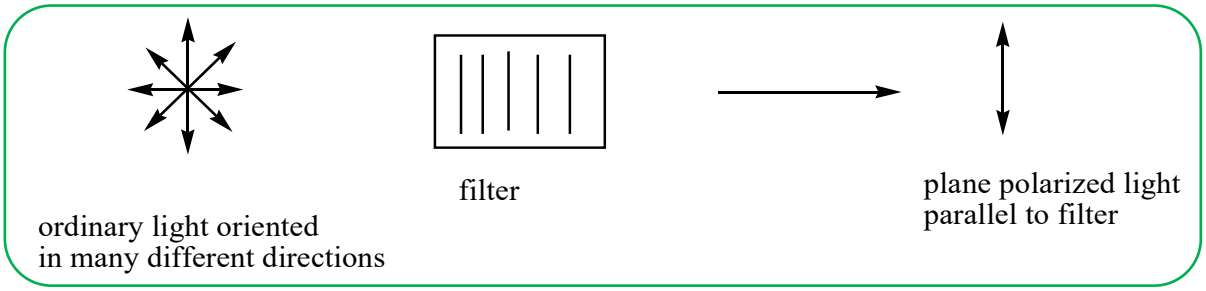


Figure 1.5 Plane-polarized light.

Solutions of chiral compounds rotate plane-polarized light that is passed through them either to the right [(clockwise) and are said to be dextrorotatory (*d*)] or to the left [(anticlockwise) and are said to be levorotatory *(l*)] after emerging from them, i.e. the angle of the light plane gets tilted to the right or to the left. Such solutions are said to be optically active (Figure 1.6).

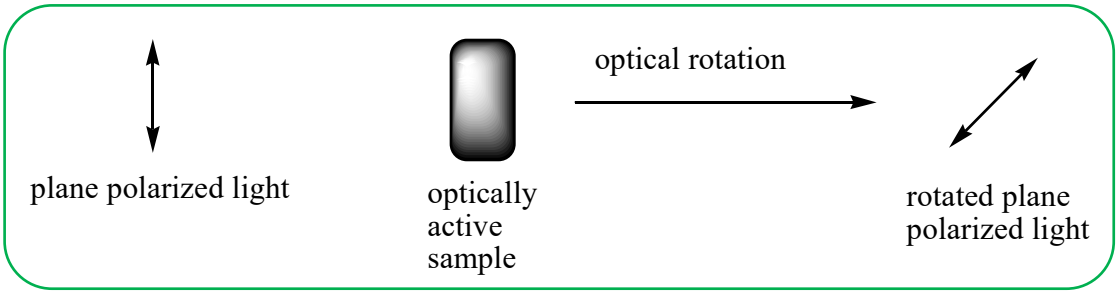


Figure 1.6 Rotation of plane-polarized light by active compounds.

Rotation to the right is given the (+) sign and rotation to the left the (-) sign.

The extent of rotation depends on the number of optically active molecules the light passes through, and this number depends on sample concentration (c) and the sample path length (l). $[\alpha]_D^{20}$ of a molecule is the observed rotation when a light of 589 nm wavelength is used (subscript D refers to the D-line of sodium and the superscript 20 refers to the temperature at

which the analysis was done in degrees Celcius) with a sample path length of 1 dm and a sample concentration of 1 g/cm$^3$, giving rise to the equation:

$\alpha = [\alpha] \times 1 \times c$,

α is the observed rotation in degrees. This specific rotation is a physical constant characteristic of a given optically active molecule, eg (+)-2-hydroxypropanoic acid has $[\alpha]_D = +3.82$ and (-)-2-hydroxypropanoic acid $[\alpha]_D = -3.82$. The two enantiomers rotate the light in opposite directions. Other examples include penicillin $[\alpha]_D = +233$ and cholesterol $[\alpha]_D = -31.5$.[1(a),(b)]

1.1(d) Configuration

Configuration is the 3-dimensional arrangement of substituents at a chiral centre. The Cahn-Ingold-Prelog rules are used to rank the four substituents joined to the chiral centre. The 1st rule states that the 4 atoms directly attached to the chiral centre are ranked according to their atomic numbers. The atom of the highest atomic number has the highest ranking and the one with the lowest atomic number has the lowest ranking. This is demonstrated in Table 1.1.

Table 1.1 Ranking of atoms based on their atomic numbers.[1(a)]

| Atomic no | 35 | 17 | 16 | 15 | 8 | 7 | 6 | 1 |
|---|---|---|---|---|---|---|---|---|
| Higher ranking | Br | Cl | S | P | O | N | C | H |

The second rule distinguishes between atoms that are of the same ranking. In such cases the ranking is established on the 2nd, 3rd, 4th or 5th atoms away from the chiral centre until a difference is found. A $–CH_2CH_2CH_3$ substituent and a $–CH_2CH_3$ substituent are equivalent based on rule one, but the propyl group ranks higher than the ethyl by rule 2. Other examples differentiating the substituents are $—CH_3 < —CH_2CH_3$, $—OH < —OCH_3$, $—CH(CH_3)_3 > —CH_2CH_3$ and $—CH(NH_2)CH_3 < —CH_2Br$.

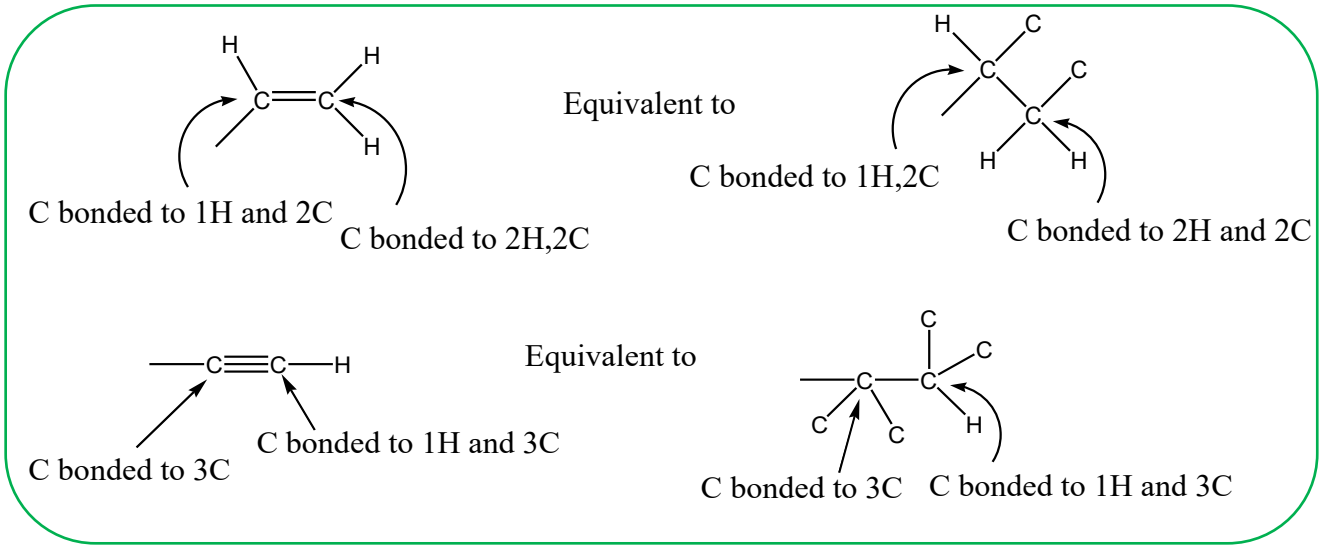


Figure 1.7 Illustration of the equivalence of double and triple bonded carbons.[1(a)]

The third rule involves multiply-bonded atoms. These are identical to the number of single bonded atoms. A C doubly bonded to another C is equivalent to a C singly bonded to two other C's as illustrated in Figure 1.7.

The stereochemical configuration around the C is described by orientating the molecule so that the substituent with the lowest ranking (4) is directly in-line with the eye of the observer, situated behind the remaining three substituents which are on the circumference of the steering wheel. The remaining three substituents will appear to radiate from the lowest ranked atom as in Figure 1.8.[1(a)]

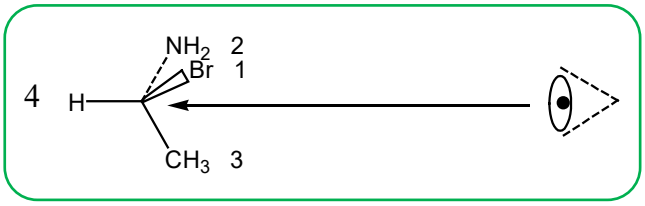


Figure 1.8 Ranking of the substituents on a chiral C.

If the H and $CH_3$ bonds are in the plane of a paper, $NH_2$ on the right of the observer and Br on the left of the observer, on counting from 1 to 3, the counting will be clockwise, therefore the chiral centre has the *R* configuration (Latin *rectus*, meaning right). If the counting is counterclockwise or to the left, the chiral centre has the *S* configuration (Latin *sinister*, meaning left). The sign of optical rotation (+) or (-) is not related to the *R,S* designation. (*S*)-Glyceraldehyde (**1.4**) happens to be levorotatory (-) and (*S*)-alanine (**1.5**) happens to be dextrorotatory (+) (Figure 1.9).[1(a)]


Figure 1.9 Two different compounds with the same configuration and different optical rotations.

1.1(e) Diastereomers

A compound with x chiral centres can have up to $2^x$ stereoisomers. 2-Amino-3-hydroxybutanoic acid has two chiral centres C2 and C3, therefore it has four possible isomers 2*R*,3*R*; 2*S*,3*S* (enantiomers) and 2*R*,3*S*; 2*S*,3*R* (enantiomers). The 2*R*,3*R* is the mirror image of the 2*S*,3*S* stereoisomer, and the 2*R*,3*S* stereoisomer is the mirror image of the 2*S*,3*R* stereoisomer. The 2*R*,3*R* and the 2*R*,3*S* isomers are not mirror images of each other. They are stereoisomers, but not enantiomers, therefore they are termed as diastereomers, they are stereoisomers that are not

mirror images. The relationship between enantiomers is like the left hand and the right hand of a person. The relationship of diastereomers is like that of hands from different people.

Enantiomers have different configurations at all chiral centres yet diastereomers have different configurations at some (1 or more) chiral centres but the same at others (Figure 1.10)

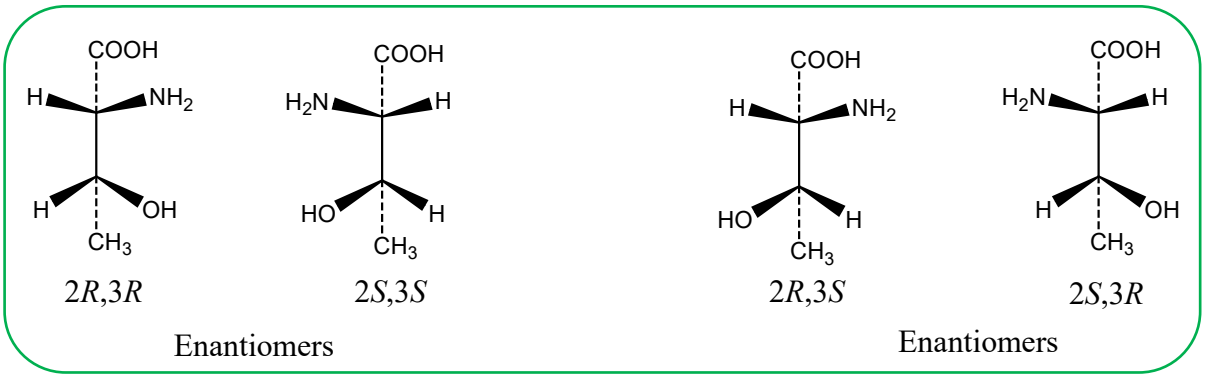


Figure 1.10 2-Amino-3-hydroxybutanoic acid stereomers.[1(a)]

Epimers are diastereomers that are different at only one chiral centre and are the same at all the other centres. Cholestanol (**1.6**) and coprostanol (**1.7**) are epimeric at carbon 5. These are found in human faeces and have 9 chiral centres.[1(a)]

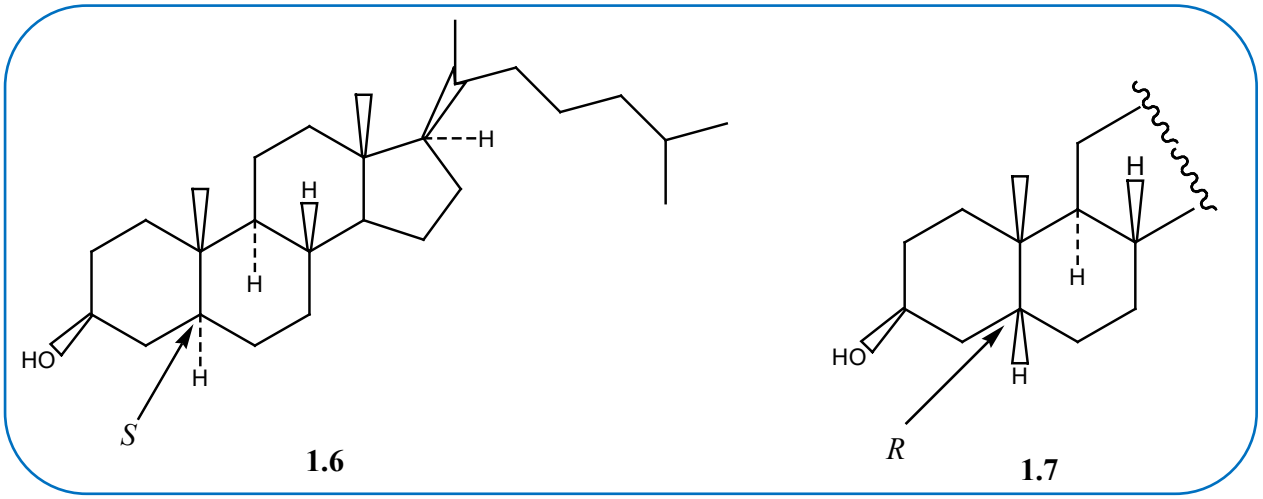


1.1(f) Meso Compounds

These are molecules that are achiral yet contain chiral centres. The 2*R*,3*R* and the 2*S*,3*S* stereoisomers of tartaric acid are enantiomers, but the 2*R*,3*S* and 2*S*,3*R* are superimposable, therefore they are indistinguishable, and the molecule possesses a plane of symmetry through the C2-C3 bond, making the acid achiral (Figure 1.11(c)).

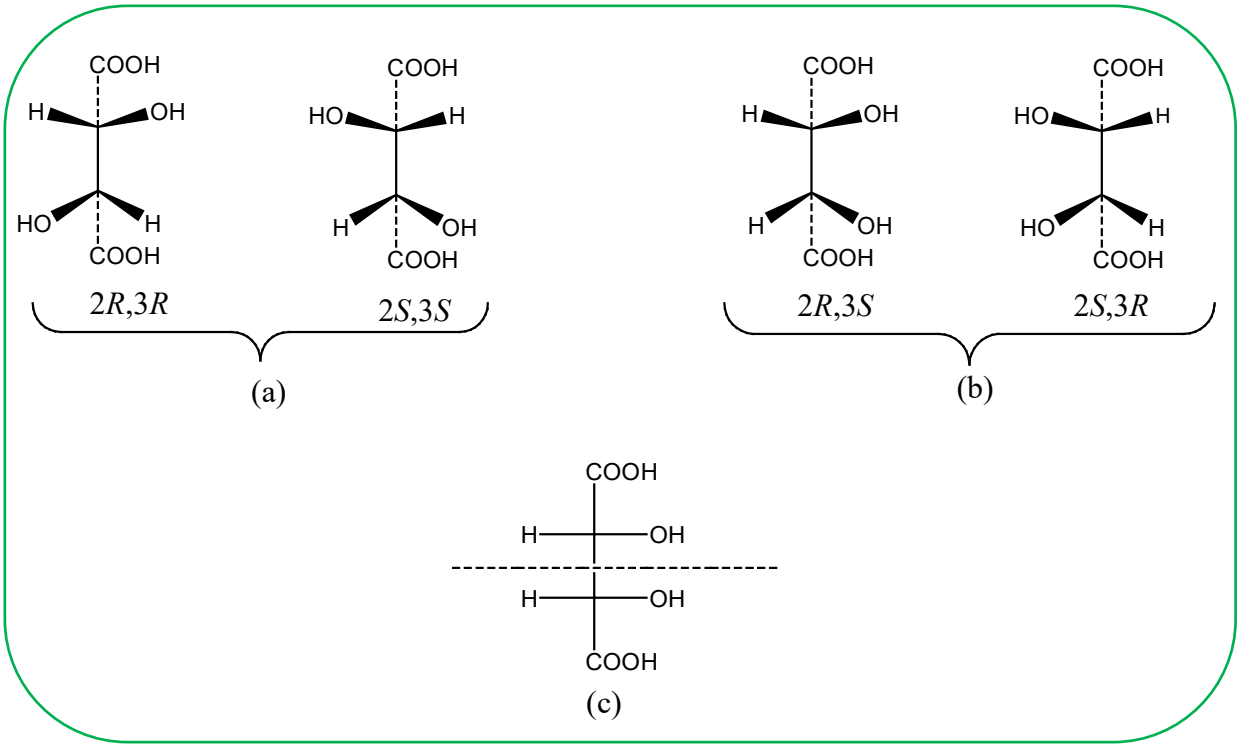


Figure 1.11 Tartaric acid stereoisomers.[1(a)]

This acid exists in three stereoisomeric forms, two enantiomers Figure 1.11 (a), and one meso form, Figure 1.11(b). The enantiomers have similar melting points, solubilities and densities but they have different optical rotations, one is dextrorotatory and the other one levorotatory. The meso form is optically inactive and has different physical properties.

1.1(g) Racemic modifications and the resolution of enantiomers

A racemic compound contains a 50:50 mixture of the two chiral enantiomers, and the mixture is called a racemate (racemic modification). It is denoted by (+/-) or the prefix *d,l*. Racemates have no optical rotation because the (+) rotation cancels the (-) rotation. Pasteur separated/resolved the racemic tartaric acid into its (+) and (-) enantiomers.

A common resolution method uses an acid-base reaction to yield a salt (Figure 1.12)

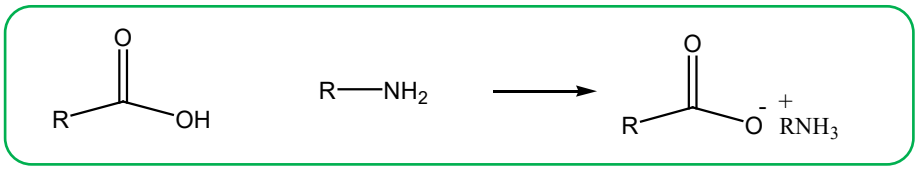


Figure 1.12 The reaction of an acid with a base to form a salt.[1(a)]

When a racemic mixture of lactic acid reacts with *R*-1-phenylethanamine, it gives rise to two dissimilar compounds. The *R*-lactic acid + *R*-1-phenylethanamine gives rise to an *R*,*R*-salt and the *S*-lactic acid gives rise to an *S*,*R*-salt, and the two salts are diastereomers (Figure 1.13).

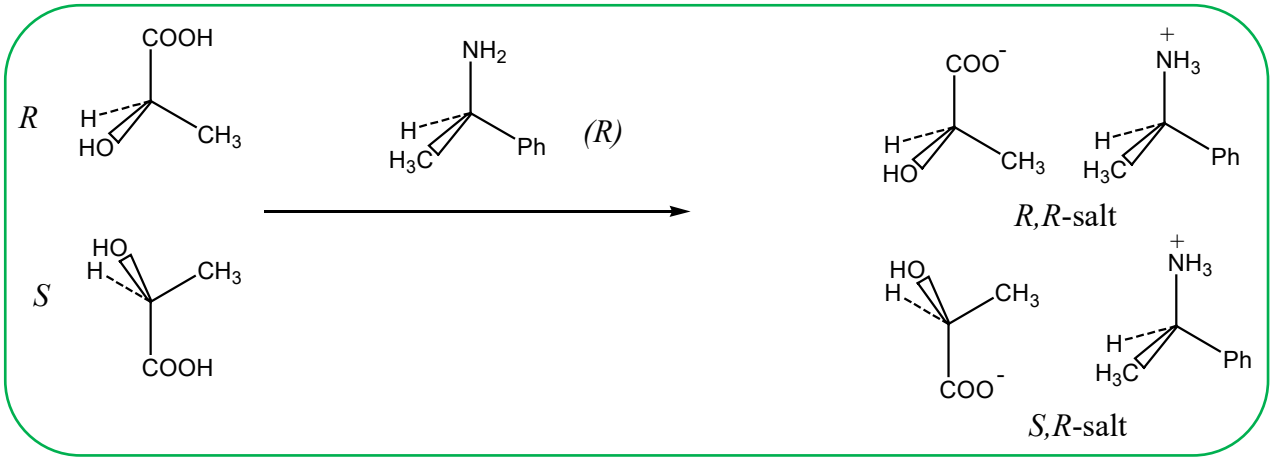


Figure 1.13 The reaction of racemic lactic acid with *R*-1-phenylethylamine.[1(a)]

Acidification of the two salts using a strong acid separates the two pure enantiomers of lactic acid. Treating racemic lactic acid with MeOH in the presence of an acid gives rise to a racemic mixture of mirror image enantiomeric products (Figure 1.14).

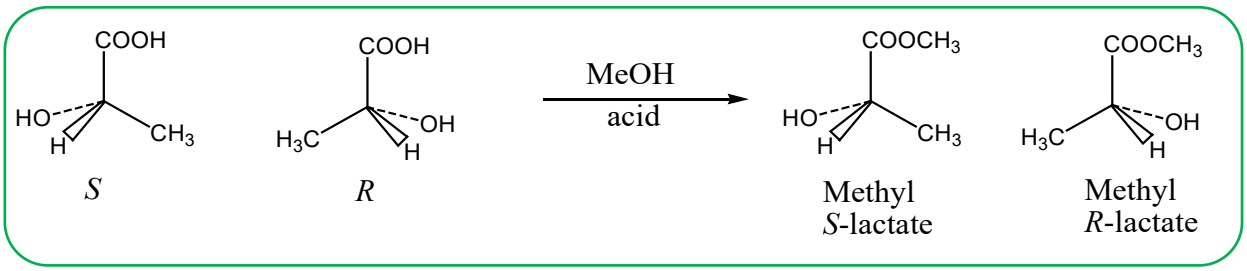


Figure 1.14 The reaction of racemic lactic acid with MeOH.[1(a)]

## 1.1(h) Chirality at other atoms

The most common cause of chirality is the presence of 4 different substituents attached to a tetrahedral atom. In certain cases, N, P and S can also be chiral centres, and these atoms are encountered in organic molecules. For example trivalent N is tetrahedral with its lone pairs of electrons acting as the 4$^{th}$ substituent.[1(a),(c),(d)]

## 1.1(i) Chirality in nature

Enantiomers usually have different biological properties. (+)-limonene (**1.8**) has the odour of oranges and lemons where (-)-limonene (**1.9**) has the odour of pine trees.

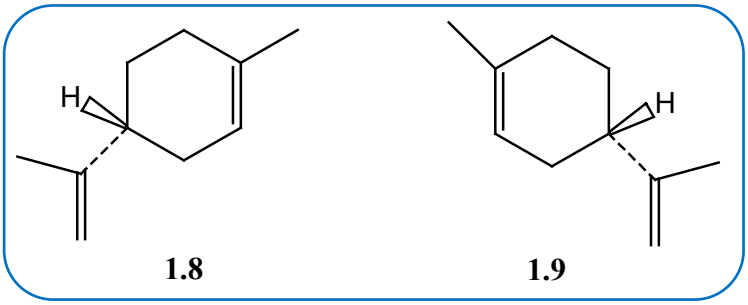

Chirality in drugs affect the biological properties of molecules. Racemic fluoxetine (Prozac) is an antidepressant but is inactive against migraine, and (*S*)-fluoxetine (**1.10**) prevents migraine. A substance needs to fit into an appropriate receptor that has similar complementary shape for it to have a biological effect. Biological receptors are chiral, therefore only one enantiomer can be accommodated.[1(a),(e),(f)]

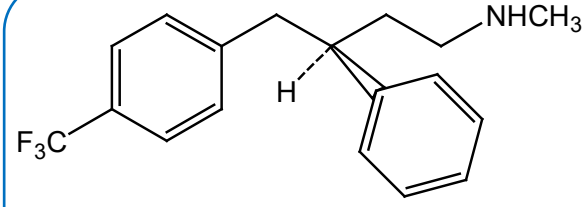


**1.10**

The enantiomeric excess (ee) is a measure of the quantity of one enantiomer present in a racemate in comparison to the other one. In a sample constituting of 40% ee in *R*, the other 60% constitutes a racemate having 30% *R* and 30% *S*, and the total amount of *R* is therefore 70%. A 70/30 (*R*/*S*) mixture has a 70 – 30 = 40% ee of *R*. This is obtained by dividing the observed optical rotation by the optical rotation of the pure enantiomer and multiplying by 100 to give rise to a percentage value.

## 1.1(j) Racemic modifications

A mixture of enantiomers results in a racemic modification.[2] The choice of marketing a pure enantiomer or a racemic drug relies on many factors. A pair of enantiomers often possess different or opposite pharmacological activities, in some cases one enantiomer can be toxic.[3] In the Martindale's Extra Pharmacopoeia 39 *beta*-blockers are listed and 14 are recognized as racemic drugs. Of the unrecognized drugs two have four isomers and one has eight isomers. A system of naming stereoisomeric drugs has been suggested.[4-7]

Drugs are administered in solid forms, as suspensions or inhalation dosage forms. The solid state characteristics of racemic mixtures and racemic compounds are likely to be different from their pure enantiomers. Another racemic modification that occurs in the solid state is the pseudoracemate.[8]

Racemic mixture- each enantiomer (isomer) crystallizes in different phases.

Racemic compound- each isomer has more affinity for compounds of the opposite form than for its own kind. The unit cell contains an equal number of molecules of each isomer.

Pseudoracemate or mixed crystal is a racemic solid solution where the two enantiomers are present in a random arrangement.[8]

Differential scanning calorimetry (DSC) can be used to characterize these racemic modifications, based on their melting point (mp) behaviours.[9-13]

The melting point of a racemic mixture is lower than those of the pure components and the racemic mixture is more soluble than its individual enantiomers. Density, powder X-ray diffraction patterns and IR spectra are similar to those of the pure constituents.

The melting point of a racemic compound may be higher or lower than the mp of the pure enantiomers, while the solubility maybe greater or lower than that of the pure enantiomers.[8, 14-16] The powder X-ray diffraction patterns and IR spectra of a racemic compound are different from those of the corresponding enantiomers.

The melting point of pseudoracemates vary, either having the same mp as the pure enantiomers, or having a minimum or maximum for the 1:1 mixture.[8]

## 1.2. Co-crystal formation

Crystal engineering and supramolecular chemistry play a key role in the preparation of co-crystals.[17] Poor bio-pharmaceutical properties are the predominant reasons why less than 1% of active pharmaceutical products appear in the marketplace.[18] Solubility is the key issue among these bio-pharmaceutical properties, with drugs discarded during production as a result of their low solubility. The pharmaceutical industry is challenged to better the solubility of drugs. The approaches that have been adopted to improve the aqueous solubility include micronisation,[19,20] salt formation,[21] emulsification[22] and solubilization using co-solvents.[23] These techniques have enhanced the oral bio-availability, but their success is reliant on the particular physicochemical nature of the compounds being investigated. [24]

A pharmaceutical co-crystal can be designed by crystal engineering to enhance the physicochemical properties of an active pharmaceutical ingredient (API) without affecting its basic functions. Crystal engineering is an application of the concepts of supramolecular chemistry to the solid state with the understanding that crystalline solids are demonstrations of self-assembly.[25] It involves the modification of the crystal arrangement of a solid material by altering intermolecular interactions that organize the formation and breaking of non-covalent

bonds.[26] These co-crystals are generally formed from intermolecular interactions eg hydrogen bonding, van der Waals interactions, and π-π stacking interactions.

Supramolecular synthons are structural units within the supramolecules that can be constructed or assembled by established synthetic operations involving intermolecular contacts.[27] These are spatial arrangements of intermolecular contacts and crystal engineering focuses on recognizing and designing synthons that are strong, leading to the formation of one, two or three-dimensional network frameworks. Figure 1.15 shows some common hydrogen bonds used in crystal engineering.

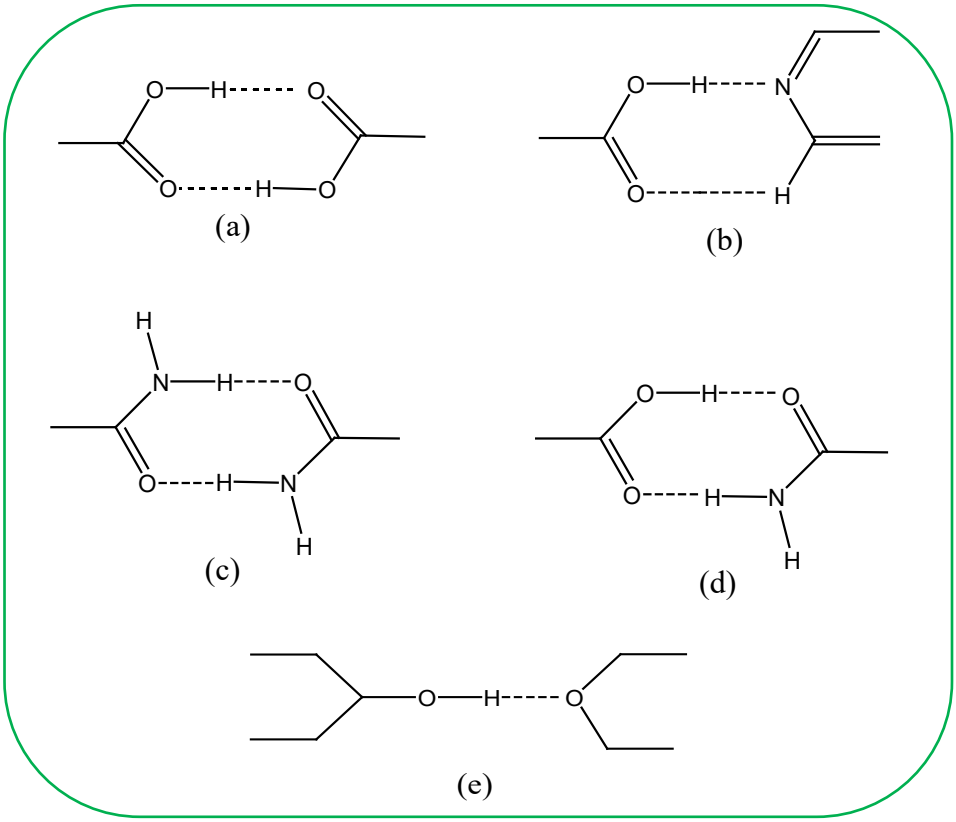


Figure 1.15 Hydrogen bonds used in crystal engineering include the (a) carboxylic acid dimer, a homosynthon, (b) a carboxylic acid-pyridine heterosynthon, (c) an amide dimer, a homosynthon, (d) a carboxylic acid heterosynthon and (e) an alcohol-ether heterosynthon.[27]

Acceptable co-crystal formers that are able to crystallize with the active pharmaceutical ingredients (APIs) include alcohols, carbohydrates, carboxylic acids, amides and amino acids.

The carboxylic acid functional group exists widely in drugs. The formation of the common carboxylic acid homosynthon in Figure 1.15(a) is *via* the C=O···H—O hydrogen bond.[28] The homosynthon, amide dimer in Figure 1.15(c) forms co-crystals through the C=O···H—N

hydrogen bond. The heterosynthons are carboxylic acid-pyridine, Figure 1.15(b), carboxylic acid amide, Figure 1.15(d) and the alcohol-ether, Figure 1.15(e).[27]

Heterosynthons are generally preferred compared to homosynthons due to energy considerations, with the acid-amide heterosynthon favoured over the other homosynthons.[29] The Cambridge Structural Database (CSD) may be used to obtain information on published organic molecules' crystal structures.[30(a)] Bis *et al*.[30(b)] analyzed the CSD and showed that the hydroxyl-cyano heterosynthons are greatly preferred compared to the hydroxyl-hydroxyl homosynthon. Weyna *et al*.[31] and Steiner *et al*.[32] have shown that the most broadly used synthons involve O—H···N hydrogen bonds. A CSD study indicated that the carboxylic acid-pyridine heterosynthons are preferred over the carboxylic acid homosynthons. These practical conclusions on the hierarchy of supramolecular synthons are essential for co-crystal design.

Basavoju *et al*. obtained a co-crystal of indomethacin (IND) and saccharin (SAC) by slow evaporation from ethyl acetate. The formation of the carboxylic acid homosynthons led to the formation of the 1:1 indomethacin-saccharin co-crystal (Fig. 1.16). The physical characteristics of the co-crystal were dissimilar from those of the starting materials, indomethacin and saccharin, and revealed its uniqueness.[33]

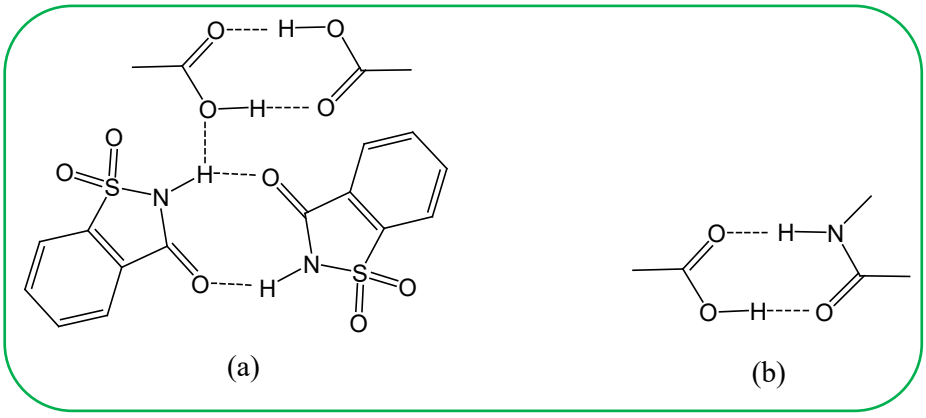


Figure 1.16 IND-SAC co-crystal structure.[33]

The crystal structure shows that the indomethacin carboxylic acid dimers interact *via* a weak N—H···O bond with the saccharin imide dimer, Figure 1.16(a), instead of the preferable heterosynthon, Figure 1.16(b).

## 1.3. Development of chiral drugs

In 1961 an event causing great suffering was reported due to the drug thalidomide, and its usage was later stopped in many countries because of its catastrophic teratogenicity.[34(a)] The drug usage was reported to have resulted in congenital heart defects, damaged ocular structures, cranial nerves, ears, kidneys, intestines and genitalia. The drug was formulated as a racemic

mixture; however, it was later shown that the (*S*)-enantiomer was tetragenic. The enantiomers of thalidomide undergo racemization *in vitro* and *in vivo*.[34(b)-(d), (f)] In 1998 Reist *et al*. reported the chiral inversion of thalidomide to be due to electrophilic substitution that involved particular and common basic catalysts. [34(e)] This example highlights the importance of the enantiomeric composition of marketed drugs and that the different enantiomers should be carefully studied.

In 1992 regulatory governing of chiral drugs was initiated in the US with the announcement of official protocols on the advancement and preparation of chiral drugs in a written communication entitled "Policy Statement for the Development of New Stereoisomeric Drugs", the European Union (EU) made a follow up with the "Investigation of Chiral Active Substances" in 1994.[35]

The prevalence of single enantiomer drug compounds continued to grow worldwide, with the market share of enantiomeric drugs' dosage form increasing from 27% in 1996, to an estimated 39% (2002).[33]

The top 10 single enantiomer blockbuster drugs listed by Caner *et al*.[35] in 2004 were Atorvastatin calcium (Pfizer), Simvastatin (Merck), Pravastatin sodium (Bristol-Meyers Squibb), Paroxetine hydrochloride (GSK), Clopidogrel bisulfate (Sanofi-Synthelabo/Bristol-Meyers Squibb), Sertraline hydrochloride (Pfizer), Fluticasone propionate and salmeterol xinafoate (GSK), Esomeprazole magnesium (AstraZeneca), Amoxicillin and potassium clavulanate (GSK), and Valsartan (Norvatis). The usage and structures of these enantiomers are in Appendix A.

Caner *et al*.[35] evaluated the advancement of chiral and achiral drugs and examined the effect of this on industrial drug advancement and drug control worldwide. In their survey of worldwide authorized drugs, they classified drugs as being achiral, single enantiomer or racemate, with racemates including diastereomeric mixtures.

The report revealed that single enantiomers and achiral drugs dominated whereas racemates were in the minority at 23% of the worldwide authorized drugs. In the period 1999-2002 the proportion of racemates decreased to 8% in comparison to the earlier decreases. In 2001 no racemates were authorized and two racemic drugs were authorized in 2002 in Japan and in South Korea. In 1998 the use of single enantiomers increased to 50%, increasing to more than 60% between the years 2000 and 2001. The guidelines of the regulatory agencies influenced these trends, which favoured and encouraged the advancement of single enantiomer drugs compared to racemates. The pharmaceutical companies' interests then shifted to the

manufacturing of the safer single enantiomer drugs and achiral drugs compared to the questionable racemic drugs.[35]

Drugs that were manufactured in the 1980s are still available in the racemic form, and the new ones are marketed as single enantiomers. When the old drugs get to the end of their patent life, companies manufacturing the drug market the single enantiomer analogues, and this is called "chiral switching".[36]

## 1.4. Resolved drugs

In 1999 Kozma *et al.*[37] reported the optical resolution of 2-(methylamino)-1-phenylpropane (**1.11**) *via* diastereomeric salt formation with 2*R*,3*R*-*O*,*O*'-di-*p*-toluoyltartaric acid (2*R*,3*R*-**1.12**). **1.11** is the key intermediate in the formation of Jumex®, (**1.13**) which is an anti-Parkinson agent. Industrially the optically active forms of **1.11** are prepared by forming the diastereomeric salt with tartaric acid (**1.14**) or with *O*,*O*'-dibenzoyltartaric acid (**1.15**).[38,39] There are three different ways to accomplish optical resolution *via* diastereomeric salt formation.[40]

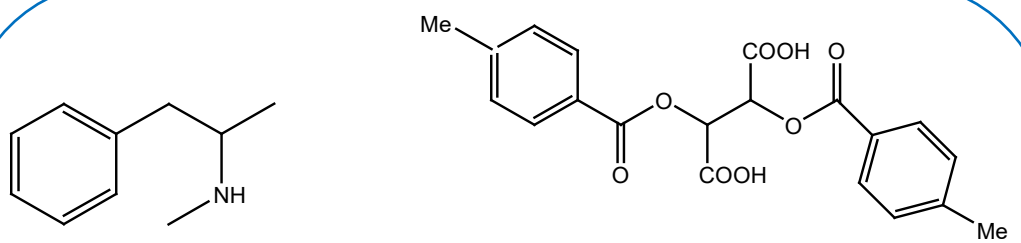


**1.11**




**1.12**

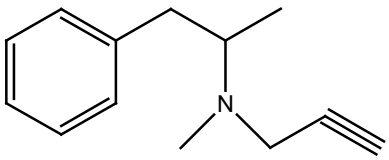


**1.13**

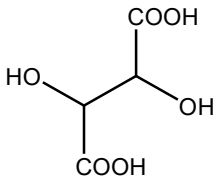


**1.14**

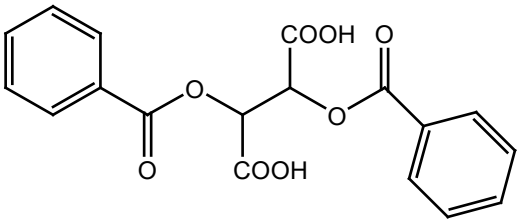


**1.15**

With the Pasteurian resolution method, a 1:1 mole ratio of the molecule to be resolved is reacted with the resolving reagent:

$$dl + 2R \rightleftharpoons dR + lR$$

*d* and *l* serve as the enantiomer of the racemate and *R* is the resolving agent

The Marckwald method involves using the nonstoichiometric ratio (1:0.5) of the racemate and the resolving agents:

$$dl + R \rightleftharpoons dR + l$$

The Pope-Peachy method forms an achiral salt of the unreacted enantiomer when the solubility problems occur during the Marckwald method.

$$dl + R + A \rightleftharpoons dR + lA$$

Kozma *et al*. applied the three methods and were able to resolve the base (**1.11**), and the results agreed with their predictions, since the Marckwald method provided the highest optical purity.[38,39]

Tartaric acid gives rise to acidic salts with **1.11**, Kozma *et al*. established that the *O*,*O*'-di-*p*-toluoyltartaric acid formed neutral salts with **1.11**. With the formation of neutral salts there is no potential for hydrogen tartrate anion chain formation, compared to other diastereomeric salts. They then concluded that irrespective of the two resolving agents having similar structures, the mechanism of the resolution ought to be different. The effectiveness of their resolution was in the same range as with tartaric acid but only a quarter molar equivalent of the resolving agent was needed for the resolution of one mol base.[37,38]

In 2000 Kim *et al*.[41] resolved the racemic piperidone **1.16** *via* a very well organized dynamic kinetic resolution in 75.9% yield resulting in an enantiopure piperidone **1.17**. Piperidone is an intermediate in the synthesis of flavopiridol, **1.18**, (a cyclin-dependent kinase (CDK) inhibitor) analogues, thio- and oxoflavopiridols that contain a sulphur (**1.19)** or oxygen (**1.20)** atom linker between the chrome ring and the hydrophobic side chain. Analogues **1.19** and **1.20** prevent the colony-forming action of multiple human tumor cell lines and possess an unusual antiproliferative profile compared to **1.18.**

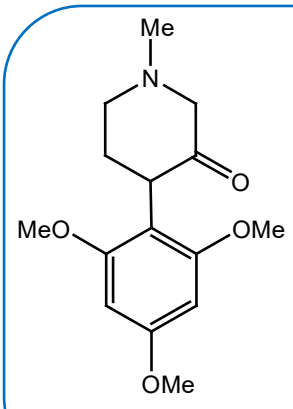


**1.16**

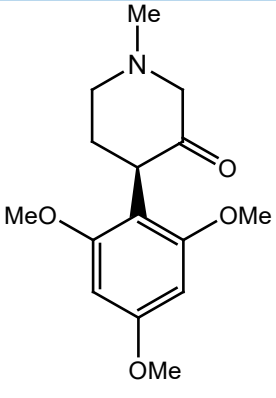


**1.17**

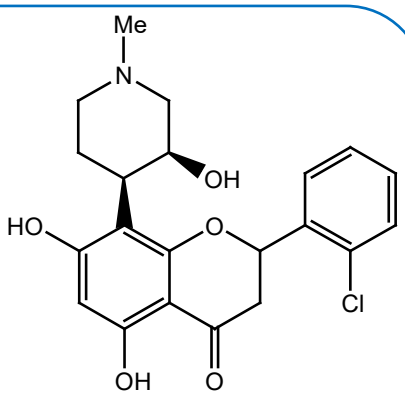


**1.18**

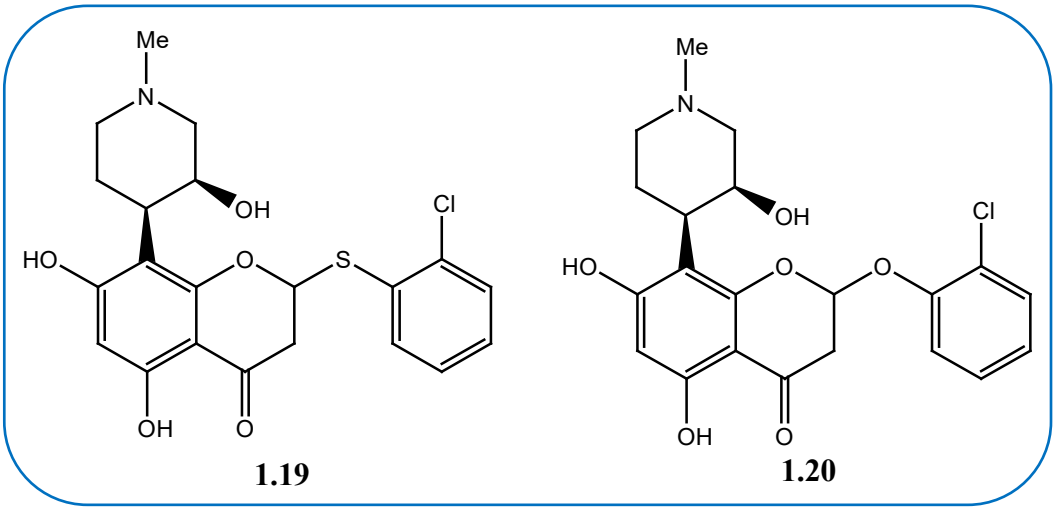


**1.19** **1.20**

5-Methoxy-2-{[(4-methoxy-3,5-dimethyl-2-pyridinyl)methyl]sulfinyl}-1H-benzimidazole, common name omeprazole (**1.21**), is a strong gastric acid secretion preventor. It was first sold by Astra in 1988, available as two enantiomers, (*S*)- and (*R*)-omeprazole as a result of the existence of a stereogenic centre at the sulphur atom.[42]

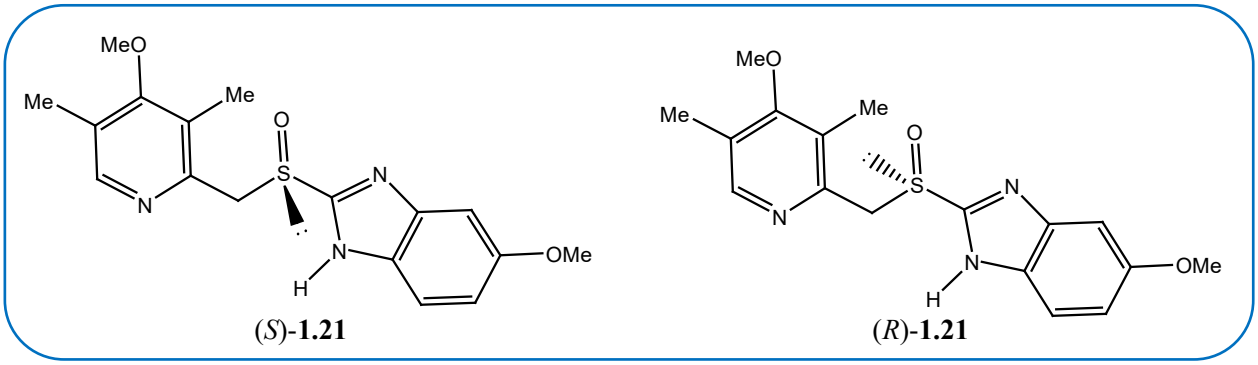


(*S*)-**1.21** (*R*)-**1.21**

**1.21** is a chiral sulfoxide that was initially resolved analytically in 1984 by chromatography employing bovine serum albumin. In 1991 it was resolved preparatively by chromatography on a *tris*phenylcarbamoycellulose-based stationary phase.[43]

von Unge *et al*.[43] tried to resolve omeprazole *via* diastereomerically N-substituted omeprazole derivatives, and the process involved the complex isolation and cleavage of the N-substituents. The compound **TADDOL** (**1.22**) was unsuccessful in resolving omeprazole. In 2000 Deng *et al*.[79] resolved omeprazole by inclusion complexation with a chiral host 2,2'-dihydroxy-1,1'-binaphthyl (**BINOL**) (**1.23**). An inclusion complex (-)-**1.21**-(-)-**1.23** or (+)-**1.21**-(+)-**1.23** was formed from the racemic omeprazole with chiral host (*S*)-(-)- or (*R*)-(+)-**BINOL** in high selectivities and the enantiomerically pure omeprazole enantiomers were formed by direct resolution with more than 95% enantiomeric excess.

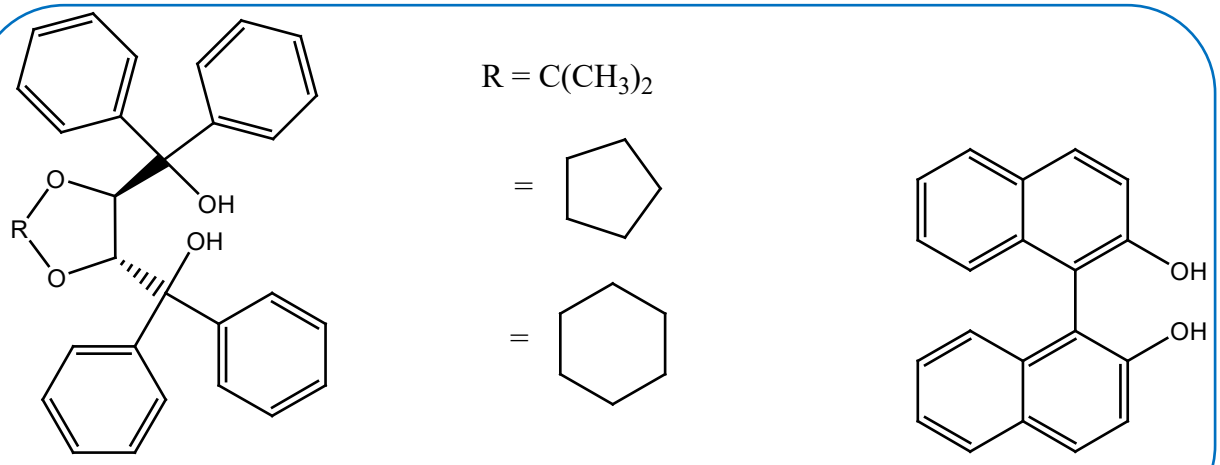


**1.22** **1.23**

In 2003 Sakurai *et al*.[44] demonstrated the resolution of the racemic *cis*-1-amino-2-indanol (**1.24**) by diastereomeric salt formation with (*S*)-2-phenylpropanoic acid (**1.25**). **1.24** in its enantiopure form is a chiral ligand and an auxiliary for asymmetric synthesis and the (1*S*,2*R*)-enantiomer is the main intermediate for the preparation of an HIV protease supressor, indinavir (**1.26**).

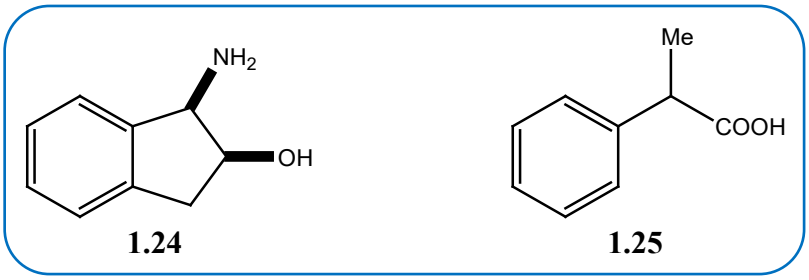


**1.24** **1.25**

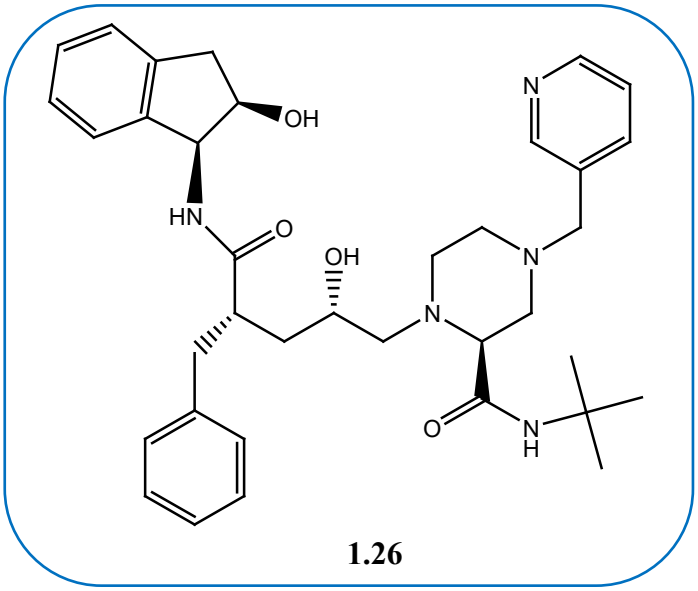


**1.26**

The O-substituted tartaric acids, dibenzoyl-D-tartaric acid (**1.15**) and ditoluoyl-D-tartaric acid (**1.12**) were used as the resolving agents for **1.24** which gave poor results. This led the authors to use other resolving agents, (*S*)-mandelic acid (**1.27**), (*R*)-2-methoxyphenylacetic acid (**1.28**) and **1.25**. These resolving agents are used in industrial scale productions. With **1.25** as a

resolving agent the highest diastereomeric excess and resolution efficiency (99%, 69%), of (+)-(1*R*,2*S*)-**1.25** was achieved.[44]

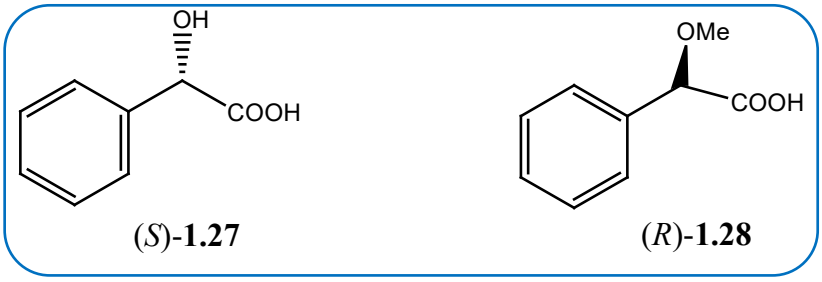


(*S*)-**1.27** (*R*)-**1.28**

The α-amino-ε-caprolactam (**1.29**) is used as an intermediate in the synthesis of pharmaceutical compounds and as the main intermediate for the preparation of enantiopure lysine. (*S*)-lysine is produced on an industrial scale from the (*S*)-**1.29** and various methods have been devised to resolve the racemic **1.29** to obtain the (*S*)-(**1.29**).

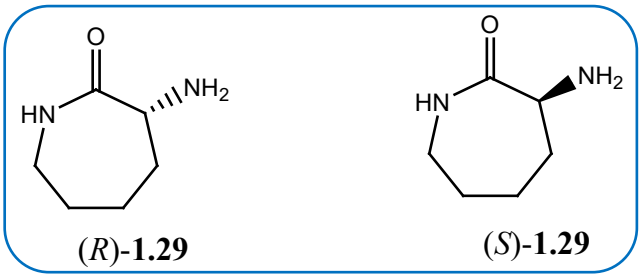


(*R*)-**1.29** (*S*)-**1.29**

Sakai *et al*. tried to resolve (*R,S*)-**1.29** using the commercially available resolving agents, L-tartaric acid (L-**1.14**), D-**1.12**, D-**1.15**, *N*-tosyl-(*S*)-phenylalanine (**1.30**), *N*-tosyl-(*S*)-alanine (**1.31**), (*S*)-**1.27** and (*S*)-**1.28**, using different solvents in the crystallisation process.[45]

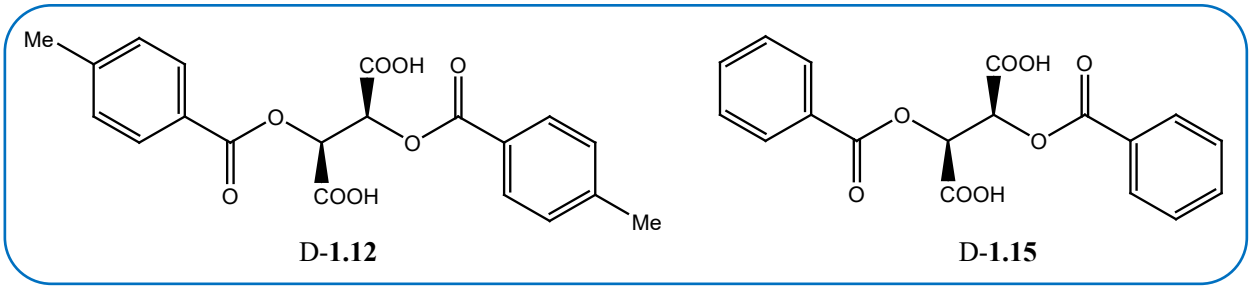


D-**1.12** D-**1.15**

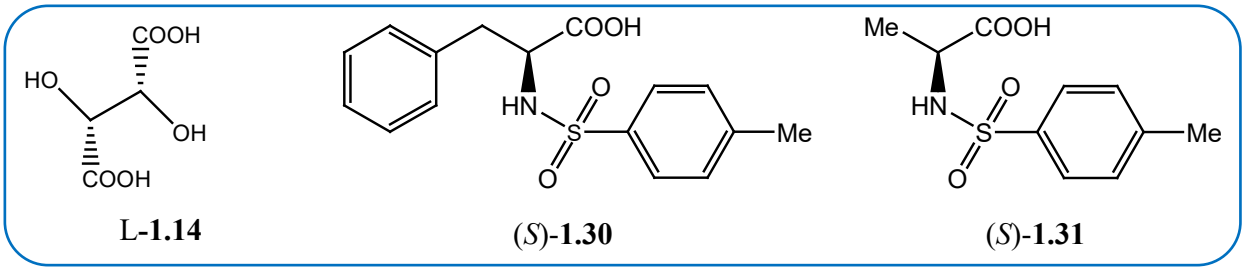


L-**1.14** (*S*)-**1.30** (*S*)-**1.31**

The resolving agent that showed the greatest resolution effectiveness of 56% was (*S*)-**1.31**, with a diastereomeric excess(de) of 93% for the (*S*)-enantiomer and resolution efficiency of 75%, de 92% for the (*R*)-enantiomer.

## 1.5. Optical resolution methods

The first spontaneous resolution was discovered by Louis Pasteur in 1848. This led him to investigate optical activity as a property of molecules.[46] Pasteur treated different samples of equal masses of racemic tartaric acid with soda and ammonia, mixed the two solutions and allowed them to spontaneously evaporate. The resultant product was a salt, that was an equimolar mixture of sodium ammonium (+)-tartrate and sodium ammonium (-)-tartrate that were hemihedral crystals.[46] He then separated the two crystals manually, which happened to be mirror images of each other. By this action he accomplished the first resolution, which laid the foundation for the field of stereochemistry, the study of the spatial arrangement of atoms in molecules. The historical background of chirality which resulted from Pasteur's discovery is well summarized by Kauffman and Myers.[46]

His discovery led him to the introduction of some terms and nomenclature for the new science of molecular and crystal chirality. The term dissymmetry in French was used to indicate disruption or absence of symmetry, or to differentiate between two objects regarding their appearance. Pasteur used the term in the latter connotation, with no reference to handedness.[46] After discovering molecular chirality he noticed the need to designate the phenomenon of handedness in chemistry and crystallography, and he used the term dissymmetry and dissymmetric for that purpose. The background related to this term as is generally used now in chemistry was well illustrated by Gal.[47]

Optical resolution is an operation designed to separate a racemic mixture, totally or partially, into its components. A lot of recorded resolutions have been performed by treating a racemate with one of the enantiomers of a chiral substance (the resolving agent) to form a mixture of diastereomers. Diastereomer pairs that are obtained due to resolutions may be ionic (diastereomeric salts), covalent, charge transfer complexes or inclusion compounds. The resolutions mediated by diastereomers, particularly salt mixtures, have been based on solubility differences of the resulting solids. The first classic resolution was described by Pasteur in 1853 and is outlined in Fig 1.17, (Jacques *et al*. cited by Eliel *et al*.[48]). This describes the preparation of a mixture of diastereomeric salts whose discrimination depends on the solubility differences of the *n*-Salt (substrate and resolving agent of unlike sign) and the *p*-Salt (substrate and resolving agent of like sign).

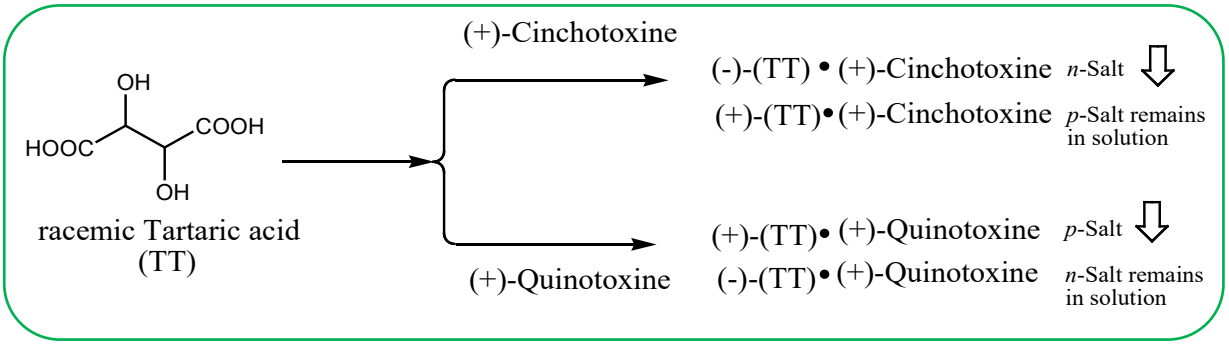


Figure 1.17 The first resolution *via* diastereomers. Tartaric acid resolution with cinchotoxine and quinotoxine as resolving agents (Pasteur, 1853).[48]

The first kinetic resolution was accomplished by Louis Pasteur in 1848 by digesting the racemic tartaric acid with the mold *Penicillium glaucum* and noticed that the unnatural (*S*,*S*)-tartaric acid remained unchanged. He also realized the first resolution by diastereomeric salt formation where he produced the (*R*,*R*)-enantiomer from the racemate through its salt with the (*R*,*R*)-quinotoxine resolving agent, (*R*,*R*-**1.32**), which is a resultant product of the acid catalyzed isomerization of quinine (**1.33**).

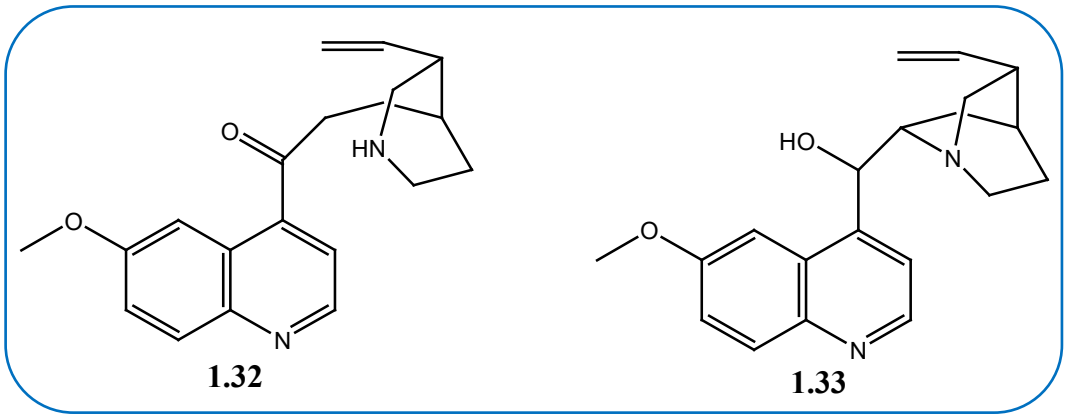


In 1899 Marckwald and MacKenzie discovered the non-enzymatic kinetic resolution, and Pope and Peachy illustrated the half equivalent resolution method, which is one of the more economic methods of resolution.[49]

Resolution is a function of the partial or total break-up of a racemic mixture into its constituents. It may serve the following purposes:[49]

(a) Structural studies- The resolution experiments of Pasteur led to the revelation of the tetrahedral configuration of the valencies of carbon (van't Hoff and Le Bel, 1874).
(b) Mechanistic studies- In biochemistry the stereochemistry of reactions can be elucidated by using the optically active compounds.
(c) The investigation of the biological activity of the enantiomers from chiral molecules.

(d) The isolation of harmful enantiomers (active and inactive) of drugs and pesticides in pharmaceutical industries. Currently it is difficult to register chiral drugs in their racemic forms. The FDA has approved > 80% chiral drugs as single enantiomers.

The separation and purification of enantiomers is necessary to achieve the pharmaceutical goals. In 2006 Fogassy *et al*.[49] presented the most often used modern methods,

(a) Uninhibited resolution, induced crystallization.
(b) Resolution by the preparation of diastereomers, (i) Resolution by the preparation of non-covalent diastereomers (resolution by diastereomeric salt preparation, eg resolution of racemic bases and resolution of racemic acids, isolation of enantiomers by diastereomeric complex preparation, 'half equivalent' methods of resolution, separation of enantiomers with mixtures of specific resolving agents (the family approach), resolution by employing a derivative of the earmarked molecule, enantioselective chromatography and enantioselective phase transfer), and (ii) resolution by preparation of covalent diastereomers.
(c) Isolation of enantiomers by substrate selective chemical reactions, (i) kinetic resolution without enzymes, (ii) kinetic resolution by enzyme catalysis and (iii) kinetic and thermodynamic control.
(d) Isolation of enantiomers combined with 2$^{nd}$ order asymmetric transformations. The formation of racemates and deracemization.
(e) Enrichment of partially resolved mixtures.
(f) Effect of the solvent and solvent properties, and procedures of development in the isolation of diastereomers.
(g) Non-linear effects.

Advanced technology utilizes preparative high performance liquid chromatography (HPLC) for separation of enantiomers. HPLC uses the chiral discriminator in chiral stationary phases (CSPs) or uses it in the mobile phase which is called chiral mobile phase additives (CMPA).[50] Indirect HPLC methods engage the derivatization of samples with a chiral derivatization agent, a pure single enantiomer, that will form two diastereomers that can be isolated by a simple reversed-phase column.[51] The CSPs cannot separate all of the different types of racemic compounds, therefore the choice of a suitable column for the enantioseparation is difficult. The main solution to the problem is the understanding of the recognition mechanisms of chiral discriminators with enantiomers. The chiral discriminators interact with enantiomers, forming temporary complexes that have different bonding energies. The two enantiomers can be collected separately due to the different elution times by the mobile phase. Chiral HPLC is also

affected by mobile phase composition (solvent nature, electrolytes, pH), column size and length, and temperature.

Simulated moving bed (SMB) chromatography, was used in the resolution of binaphthol enantiomers.[52] An asymmetric synthesis was developed using chiral catalysts in order to prevent racemization *in situ* during chiral drug formation.[53]

Perhexiline, an antianginal agent has been separated by the indirect HPLC method.[54] Direct chiral separations using CSPs are simple and rapid, and have been used to resolve amino acids,[55] metoprolol enantiomers (β-blockers),[56] donepezil enantiomers (anti-acetylcholinesterase for treating Alzheimer disease),[57] tetrahydropalmatine enantiomers (antiarrhythmic and antihypertensive),[58] and propranolol. [59]

## 1.6. Problem statement

Chirality in drugs is a major focus area in the discovery, design and marketing of modern drugs. In the past, racemates dominated the pharmacopoeia, but recently interest has shifted due to the synthesis of pure enantiomeric drugs in great quantities and the impact of stereochemistry on drug effectiveness.[60] Generally, an enantiomer has different effects compared to its partner.

When one enantiomer is active for a particular role, its partner could be inactive, be a competitor of the active one or have a different effect that could be beneficial or toxic to a patient.[35] There are lots of benefits in employing stereochemically pure drugs, corresponding to a reduction of the administered dose, improved therapeutic window and accurate estimation of dose-response relationships.[34]

In the pharmaceutical industry two types of techniques are employed for chiral resolution: the classic procedures and new technologies. In the classic approach, resolution by diastereomeric salt formation, an acid-base reaction is involved between a racemic drug and a chiral resolving agent. This results in two diastereomeric salts that can be isolated by crystallization depending on their solubilities in the chosen solvent. The salt is decomposed by treating it with an acid or a base to obtain the pure enantiomer.[61] The classic approach is one of the oldest techniques and is still widely used due to its simplicity.

The four *Cinchona* alkaloids, cinchonine (**CINC**), cinchonidine (**CIND**), quinine (**QUIN**) and quinidine (**QUID**) have been listed as the principal resolving agents of carboxylic acids.[62] They are also inexpensive and readily available. The use of these resolving agents with selected racemic acids would provide ideal systems to gain insight into the chiral separation process.

## 1.7. Research aim

The aim of the research is to investigate the chiral discrimination process by analyzing the resultant crystal structures of the diastereomeric salts. The dominant non-bonded interactions and crystal packing features which could contribute towards the crystallization of one diasteromeric salt over another will be studied. In addition, the effect of solvent on the chiral discrimination process will be investigated.

## 1.8. Research hypothesis

The hypothesis is that the *Cinchona* alkaloids will form distereomeric salts with the selected chiral acids. A solution of the chosen resolving agent and the racemic acid will result in one of the diastereomeric salts precipitating from solution. Analysis of the crystal structures of these salts will result in a better understanding of the mechanism of chiral resolution.

## 1.9. Delimitations

A series of five chiral acids were studied, although experiments were conducted on many others, suitable results were only obtained from the selected chiral acids. The scope of the study did not include treatment of the resultant diastereomeric salts with a base or acid to give rise to the pure enantiomeric acid.

## 1.10. References


1. (a) McMurry JE, *Organic Chemistry*, 8th Ed., Brooks/Cole, **2008**. (b) Barron LD. Molecular light scattering and optical activity, 2nd Ed., Cambridge University Press, Cambridge, **2004**. (c) Le Grel P, Asprogenidi A, Huez P, Le Grel B, Salaün A, Roinsel T, Potel M, Rasti E and Hocquet A. Stereodynamics of Nitrogen chiral centres in aza-$\beta^3$-cyclodipeptides. *Chirality*, **2013**, 25, 341-349. (d) Qiu S, Li G, Lu S, Huang B, Feng Z and Li C. Chiral Sulfur compounds studied by Raman optical activity: *tert*-Butanesulfinamide and its precursor *tert*-Butyl *tert*-Butanethiosulfinate. *Chirality*, **2012**, 24, 731-740. (e) Cintas P. Chirality of living systems: A helping hand from crystals and oligopeptides. *Angew. Chem. Int. Ed*., **2002**, 41, 1139-1145. (f) Caglioti L, Micskei K and Páyli G. First molecules, biological chirality, origin(s) of life. *Chirality*, **2011**, 23, 65-68.
2. Eliel ET and Baslo F. In: *Elements of Stereochemistry*. John Wiley and Sons, New York, **1969**, 16.
3. Brocks DR and Jamali F. Stereochemical aspects of pharmacotherapy. *Pharmacotherapy*, **1995**, 15, 551-564.
4. Lee EJD and Williams KM. Chirality. Clinical pharmacokinetic and pharmacodynamic considerations. *Clin. Pharmacokinet*., **1990**,18, 339-345.
5. Martindale, *The Extra Pharmacopoeia*, 29th edition, The Pharmaceutical Press, London, UK, **1989**.
6. Gal J. Stereoisomerism and drug nomenclature. *Clin. Pharmacol. Ther*., **1988**, 44, 251-253.
7. Nguyen LA, He H and Pham-Huy C. Chiral drugs: An overview. *Int. J. Biomed. Sci*., **2006**, 2, 85-100.
8. Mitchell AG. Racemic Drugs: Racemic mixture, racemic compound, or pseudoracemate? *J. Pharm. Pharmaceut. Sci*., **1998**, 8-12.
9. Bettinetti C, Giordano F, Fronza C, Italia A, Pellegata R, Villa M and Ventura P. Sobrerol enantiomers and racemates: solid state spectroscopy, thermal behavior and phase diagrams. *J. Pharm. Sci*., **1990**, 79, 470-475.
10. Duddu SP Grant DJW. Formation of the racemic compound of ephedrine base from a physical mixture of its enantiomers in the solid, liquid, solution or vapour state. *Pharm. Res*., **1992**, 9, 1083-1091.
11. Romero AJ and Rhodes C. Stereochemical aspects of the molecular pharmaceutics of ibuprofen. *J. Pharm. Pharmacol*., **1993**, 45, 258-262.

12. Burger A, Rollinger JM and Bruggeller P. Binary system of (*R*)- and (*S*)-nitrendipine—Polymorphism and structure. *J. Pharm. Sci.,* **1997**, 86, 674-679.
13. Pitaluga Jr A, Prado LD, Seiceira R, Wardell JL and Wardell SMCV. Further study of (+/-)-mefloquinium chloride solvates. Crystal structures of the hemihydrate and monohydrate of (+/-)-mefloquinium chloride, from data collected at 120 K. *Int. J. Pharm*., **2010**, 398, 50-60.
14. Repta AJ, Baltezor MJ and Eansal PC. Utilization of art enantiomer as a solution to pharmaceutical problem: application to solubilization of 1,2-di (4-piperazine-2,6-dione) propane. *J. Pharm. Sci*., **1976**, 64, 238-242.
15. Liu ST and Hurwitz A. Effect of enantiomeric purity on solubility determination of dexclamol hydrochloride. *J. Pharm. Sci*., **1978**, 67, 636-638.
16. Dwivedi SK, Sattari S, Jamali F and Mitchell AG. Ibuprofen racemate and enantiomers: phase diagram, solubility and thermodynamic data. *Int. J. Pharm*., **1992**, 87, 95-104.
17. Qiao N, Li M, Schlindwein W, Malek N, Davies A and Trappitt G. Pharmaceutical co-crystals: An overview. *Int. J. of Pharm*., **2011**, 419, 1-11.
18. Aakeröy CB, Forbes S and Desper J. Using co-crystal to systematically modulate aqueous solubility and melting behaviour of an anticancer drug. *J. Am. Chem. Soc*., **2009**, 131, 17048-17049.
19. Cho E, Cho W, Cha K, Park J, Kim M-S, Park HJ and Hwang S-J. Enhanced dissolution of megestrol acetate microcrystals prepared by antisolvent precipitation process using hydrophilic additives. *Int. J. Pharm.,* **2010**, 396, 91-98.
20. Rasenack N, Hartenhauer H and Muller B W. Microcrystals for dissolution rate enhancement of poorly water soluble drugs. *Int. J. Pharm*., **2003**, 254, 137-145.
21. Umeda Y, Fukami T, Furuishi T, Suzuki T, Tanjoh K and Tomono K. Characterization of multicomponent crystal formed between indomethacin and lidocaine. *Drug Dev. Ind. Pharm*., **2009**, 35, 843-851.
22. Torchilin V. Micellar nanocarriers: pharmaceutical perspectives. *Pharm. Res*., **2007**, 24, 1-16.
23. Amin K, Dannenfelser, R-M, Zielinski J and Wang B. Lyophilization of polyethylene glycol mixtures. *J. Pharm. Sci*., **2004**, 93, 2244-2249.
24. Blagden N, de Matas M, Gavan PT and York P. Crystal engineering of active pharmaceutical ingredients to improve solubility and dissolution rates. *Adv. Drug Deliv. Rev.*, **2007**, 59, 617-630.

25. Almarsson Ö and Zaworotko MJ. Crystal engineering of the composition of pharmaceutical phases. Do pharmaceutical co-crystals represent a new path to improved medicines? *Chem. Commun.,* **2004**, 1889-1896.
26. Aakeröy CB, Fasulo M, Schulteiss N, Desper J and Moore C. Structural completion between hydrogen bonds and halogen bonds. *J. Am. Chem. Soc*., **2007**, 129, 13772-13773.
27. Desiraju GR. Supramolecular synthons in crystal engineering- a new organic synthesis. *Angew Chem., Int. Ed. Engl*., **1995**, 34, 2311-2327
28. Basavoju S, Bostrom D and Velaga S. Indomethacin-saccharin co-crystal design, synthesis and preliminary pharmaceutical characterization. *Pharm. Res*., **2008**, 25, 530-541.
29. Vishweshwar P, McMahon JA, Bis JA and Zaworotko MJ. Pharmaceutical co-crystals. *J. Pharm. Sci.*, **2006**, 95, 499-516.
30. (a) Groom CR, Bruno IJ, Lightfoot MP and Ward SC. The Cambridge Structural Database. A*cta Cryst*., **2016**, B72, 171-179. (b) Bis JA, Vishweshwar P, Weyna D and Zaworotko MJ. Hierachy of supramolecular synthons: persistent hydroxyl-pyridine hydrogen bonds in co-crystals that contain a cyano acceptor. *Mol. Pharm*., **2007**, 4, 401-416.
31. Weyna DR, Shattock T, Vishweshwar P and Zaworotko MJ. Synthesis and characterization of co-crystals and pharmaceutical co-crystals: mechanochemistry *vs* slow evaporation from solution. *Cryst. Growth Des.,* **2009**, 9, 1106-1123.
32. Steiner T. Competition of hydrogen-bond acceptors for the strong carboxyl donor. *Acta Crystallogr., Sect. B*, **2001**, 57, 103-106.
33. Basavoju S, Bostrom D and Velaga S. Indomethacin-saccharin co-crystal: design, synthesis and preliminary pharmaceutical characterization. *Pharm. Res.,* **2008**, 25, 530-541.
34. (a) Mellin GW and Katzentein M. The saga of thalidomide: neuropathy to embryopathy, with case reports and congenital anomalies. *N. Engl. J. Med*., **1962**, 1184-1244. (b) Gunzler V. Thalidomide in human immunodeficiency virus (HIV) patients. A review of safety considerations. *Drug Saf*., **1992**, 7, 116-134. (c) Knoche B and Blaschke G. Investigations on the *in vitro* racemization of thalidomide by high-performance liquid chromatography. *J. Chromatogr*., **1994**, 666, 235-240. (d) Eriksson T, Björkam S, Roth B, Fyge A and Höglund P. Stereospecific determination, chiral inversion *in vitro* and pharmacokinetics in humans of the enantiomers of thalidomide. *Chirality*, **1995**, 7, 44-52. (e) Agranat I, Caner H and Caldwell J. Putting

chirality to work: the strategy of chiral switches. *Nat. Rev. Drug Discov. 1*, **2002**, 753-768. (f) Miller MT, Ventura L and Strömland K. Thalidomide and misoprostol: Ophthalmologic manifestations and associations both expected and unexpected. *Birth Defects Research (Part A),* **2009**, 85, 667-676.

35. Caner H, Groner E and Levy L. Trends in the development of chiral drugs. *Drug Discov. Today*, **2004**, 9, 105-110.
36. Mansfield P, Henry D and Tonkin A. Single-enantiomer drugs, elegant science, disappointing effects. *Clin. Pharmacokinet*., **2004**, 43, 287-290.
37. Kozma D, Madarasz Z, Kassai C and Fogassy E. Optical resolution of *N*-methylamphetamine *via* diastereomeric salt formation with 2*R*,3*R*-*O*,*O*'-Di-*p*-toluoyltartaric acid. *Chirality*, **1999**, 11, 373-375.
38. Kozma D, Madarasz Z, Acs M and Fogassy E. Study of mechanism of an optical resolution *via* diastereoisomeric salt formation by Pope-Peachy method. *Tetrahedron: Asymmetry*, **1994**, 5, 193–194.
39. Kozma D, Novak Cs, Pokol G and Fogassy E. Study of the mechanism of optical resolutions *via* diastereoisomeric salt formation. Part 5. Thermoanalytical investigation of the optical resolution of the *N*-methylamphetamine by tartaric acid. *J. Therm. Anal*., **1996**, 47, 727–735.
40. Jacques J, Collet A and Wilen SH. *Enantiomers, Racemates and Resolutions*, John Wiley and Sons, **1981**, 306-312.
41. Kim SK, Sack JS, Tokarski JS, Qian N, Chao ST, Leith L, Kelly YF, Misra RN, Hunt JT, Kimball SD, Humphreys WG, Wautlet BS, Mulheron JG and Webster KR. Thio- and Oxoflavopiridols, Cyclin-dependent Kinase (CDK) 1-Selective Inhibitors: Synthesis and Biological effects. *J. Med. Chem*., **2000**, 43, 4126-4134.
42. Deng J, Chi Y, Fu F, Cui X, Yu K, Zhu J and Jiang Y. Resolution of omeprazole by inclusion complexation with a chiral host BINOL. *Tetrahedron: Asymmetry*, **2000**, 11, 1729-1732.
43. von Unge S, Langer V and Sjolin L. Stereochemical assignment of the enantiomers of omeprazole from X-ray analysis of a fenchyloxymethyl derivative of (+)-(*R*)-omeprazole. *Tetrahedron: Asymmetry*, **1997**, 8, 1967-1970.
44. Sakurai R and Sakai K. Resolution of racemic *cis*-1-amino-2-indanol by diastereomeric salt formation with (*S*)-2-phenylpropionic acid. *Tetrahedron: Asymmetry*, **2003**, 14, 411-413.

45. Sakai K, Sakurai R, Yuzawa A and Hiramaya N. Practical continuous resolution of α-amino-ε-caprolactam by diastereomeric salt formation using a single resolving agent with a solvent switch method. *Tetrahedron: Asymmetry*, **2003**, 14, 3713-3718.
46. Kauffman GB and Myers RD. The resolution of racemic acid. A classic stereochemical experiment for the undergraduate laboratory. *J. Chem. Ed*., **1975**, 777-781.
47. Gal J. Louis Pasteur, language, and molecular chirality. I. Background and *dissymmetry*. *Chirality*, **2011**, 23, 1-16.
48. Eliel EL, Wilen SH and Mander LN. *Stereochemistry of Organic Compounds*, John Wiley and Sons, **1994**, p322.
49. Fogassy E, Nógrádi M, Kozma D, Egri G, Pálovics E and Kiss V. Optical resolution methods. *Org. Biomol. Chem*., **2006**, 3011-3030.
50. Anderson S and Allenmark SG. Preparative chiral chromatographic resolution of enantiomers in drug discovery. *J. Biomed. Biophys. Methods*, **2002**, 54, 11-23.
51. Toyo'oka T. Resolution of chiral drugs by liquid chromatography based upon diastereomer formation with chiral derivatization reagents. *J. Biomed. Biophys*. *Methods*, **2002**, 54, 25-56.
52. Johannsen M, Peper S and Depta A. Simulated moving bed chromatography with supercritical fluids for the resolution of binaphthol enantiomers and phytol isomers. *J. Biomed. Biophys. Methods*, **2002**, 54, 85-102.
53. Borman S. Asymmetric catalysis wins. Chemistry nobel honors Knowles, Noyori, Sharpless for chiral synthesis. *ChemEngNews*, **2001**, 79, 5-6.
54. Davies BJ, Herbert MK, Culbert JA, Pyke SM, Coller JK, Somogyi AA, Milne RW and Sallustio BD. Enantioselective assay for the determination of perhexiline enantiomers in human plasma by liquid chromatography. *J. Chromatogr. B*, **2006**, 832, 114-120.
55. Staroverov SM, Kuznetsov MA, Nesterenko ON, Vasiarov GG, Katrukha GS and Fedorova GB. New chiral stationary phase with macroscyclic glycopeptide antibiotic eremomycin chemically bonded to silica. *J. Chromatogr. A*, **2006,** 1108, 263-267.
56. Boralli VB, Coelho EB, Cerqueira PM and Lanchote VL. Stereoselective analysis of metoprolol and its metabolites in rat plasma with application to oxidative metabolism. *J. Chromatogr. B*, **2005,** 823, 195-202.
57. Radwan MA, Abdine HH, Al-Quadeb BT, Aboul-Enein HY and Nakashima K. Stereoselective HPLC assay of donepezil enantiomers with uv detection and its application to pharmacokinetics in rats. *J. Chromatogr. B*, **2006,** 830, 114-119.

58. Hong ZY, Fan GR, Chai YF, Yin XP, Wen J and Wu YT. Chiral liquid chromatography resolution and stereoselective pharmacokinetic study of tetrahydropalmatine enantiomers in dogs. *J. Chromatogr. B*, **2005,** 826, 108-113.
59. Pham-Huy C, Radenen B, Sahui-Gnassi A and Claude JR. High performance liquid chromatographic determination of (*S*)- and (*R*)-propranolol in human plasma and urine with a chiral β-cyclodextrin bonded phase. *J. Chromatogr. B*, **1995,** 665, 125-132.
60. Caldwell J. Through the looking glass in chiral drug development. *Modern Drug Discov*., **1999**, 2, 51-60.
61. Burke D and Henderson DJ. Chirality: a blueprint for the future. *British J. Anaesthesia*, **2002**, 88, 563-576.
62. Wilen SH, Collet A and Jacques J. Strategies in Optical Resolution. *Tetrahedron,* **1977**, 33, 2725-2736.

# Chapter 2

## Resolving agents

A resolving agent, or a chiral resolving agent, also known as a chiral derivatizing agent, is an auxiliary that is utilized in the conversion of a mixture of enantiomers into diastereomers to analyze the quantities of each of the enantiomers in the mixture. The analysis can be performed using spectroscopic or chromatographic methods. A resolving agent can also be used for the chiral resolution, which is the actual physical separation of the enantiomers. It is an important tool in obtaining optically active drugs. This process is also termed as optical resolution and mechanical resolution. Below are the resolving agents that were employed in the study.

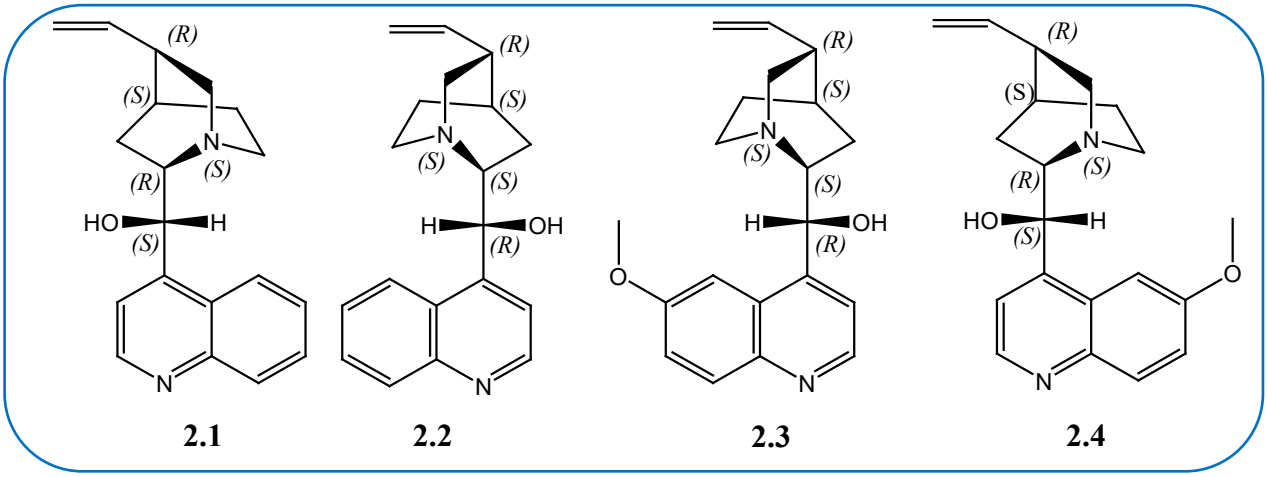


Common names: (i) Cinchonine (**CINC, 2.1**), (ii) Cinchonidine (**CIND, 2.2**), (iii) Quinine (**QUIN, 2.3)** and (iv) Quinidine (**QUID, 2.4)**.

Chemical names: (i) (*S*)-quinolin-4-yl[(1*S*,2*R*,4*S*,5*R*)-5-ethenylquinuclidinium-2-yl]methyl alcohol or (*S*)-[(2*R*,4*S*,5*R*)-5-vinyl-1-azabicyclo[2.2.2]octan-2-yl]-quinolin-4-ylmethyl alcohol.

(ii) (*R*)-quinolin-4-yl[(1*S*,2*S*,4*S*,5*R*)-5-ethenylquinuclidinium-2-yl]methyl alcohol or (*R*)-[(2*S*,4*S*,5*R*)-5-vinyl-1-azabicyclo[2.2.2]octan-2-yl]-quinolin-4-ylmethyl alcohol.

(iii) (*R*)-(6-methoxyquinolin-4-yl)-[(1*S*,2*S*,4*S*,5*R*)-5-ethenylquinuclidinium-2-yl]methyl alcohol or (*R*)-[(2*S*,4*S*,5*R*)-5-vinyl-1-azabicyclo[2.2.2]octan-2-yl]-(6-methoxyquinolin-4-yl)methyl alcohol.

(iv) (*S*)-(6-methoxyquinolin-4-yl)-[(1*S*,2*R*,4*S*,5*R*)-5-ethenylquinuclidinium-2-yl]methyl alcohol or (*S*)-[(2*R*,4*S*,5*R*)-5-vinyl-1-azabicyclo[2.2.2]octan-2-yl]-(6-methoxyquinolin-4-yl)methyl alcohol.

The physical properties of the resolving agents studied are listed in Table 2.1.

Table 2.1 Physical properties of the resolving agents studied.

| Resolving agents | Structure number | Configuration at C9 | Formula | $M_r$ g/mol | Mp °C |
|---|---|---|---|---|---|
| Cinchonine | **2.1** | *S* -(+) | $C_{19}H_{22}N_2O$ | 294.40 | 265 |
| Cinchonidine | **2.2** | *R*-(-) | $C_{19}H_{22}N_2O$ | 294.40 | 210 |
| Quinine | **2.3** | *R*-(-) | $C_{20}H_{24}N_2O_2$ | 324.42 | 170 |
| Quinidine | **2.4** | *S*-(+) | $C_{20}H_{24}N_2O_2$ | 324.42 | 176 |

## 2.1. Historical Perspective

The *Cinchona* bark is the dried bark from the plant stem of species *Cinchona* (*Rubiaceae*),[1] with the following species varying in alkaloid content, *Cinchona calisaya*, *Cinchon*a *ledgeriana* and *Cinchona succinubra*.[1] The selected resolving agents are the main alkaloids in *Cinchona* bark, with **2.3** and **2.4** as diastereoisomers as are **2.1** and **2.2**, altogether accounting for roughly 28-61% of the total alkaloid content.[1] These alkaloids were used to treat fever before 1599 by the Peruvian native Indians, and used as a remedy for malaria in Europe.[2] In the late 1920s the *Cinchona ledgeriana* from the Dutch plantations in the Indonasian island of Java, provided the majority of the world's production. The allied forces were cut off from the *Cinchona* trees in Java in the advent of World War 2 and an interest then developed for the synthesis of quinine.[2]

In 2001 Stork *et al*. illustrated the first entirely stereoselective overall preparation of (-)-quinine.[3] They synthesized it by the oxidation of deoxyquinine plus oxygen in *tert*-butanol-dimethylsulphoxide (DMSO) in addition to potassium *tert*-butoxide. A higher selectivity resulted by accomplishing the oxidation in the presence of sodium hydride in anhydrous DMSO, and the yield was 78%. The high resolution mass, proton and carbon NMR spectra were similar to the ones of an original sample from Sigma-Aldrich.[3] Over the past 160 years a considerable amount of effort has been made to establish the stereoselective preparation of quinine. This was due to the supply problem that was as a result of the political vagaries of the countries that produced quinine, and this initiated the foundation for much of current organic chemistry.[4] In 2012 Carroll *et al*. reported the separation and structure determination of cinchonine and quinine from *Cinchona calisaya.*[5] Cinchonine was isolated by acid-base extraction that was followed by selective crystallization, and quinine was isolated by flash chromatography.[5]

The *Cinchona* alkaloids are a versatile class of natural products, medicinally **2.3** is used to treat malaria and leg cramps, **2.4** is used as an anti-arrhythmic agent, and **2.1** and **2.2** as catalysts and ligands for asymmetric synthesis.[6]

## 2.2. Structural information on the *Cinchona* alkaloids

These alkaloids differ regarding their stereochemistry and their substituents on the quinoline ring. Their structures demonstrate the stereochemical relationship between **2.1** and **2.2** (as well as **2.3** and **2.4** with methoxy groups at C19) (Figure 2.1). Quinine and quinidine are diastereomers whereby **QUIN** is a levorotatory isomer (-) and **QUID** a dextrorotatory isomer (+). The vinyl group appears at position 3 of the quinuclidine ring (bicyclic system) that creates two centres of chirality, and the two bases are mirror images as they have opposite chiralities at C8 and C9. It could be predicted that they would form quasidiastereomeric salts, the (*R*)-A salt of **2.1** would be similar to the (*S*)-A salt of **2.2** and *vice versa*.[7]

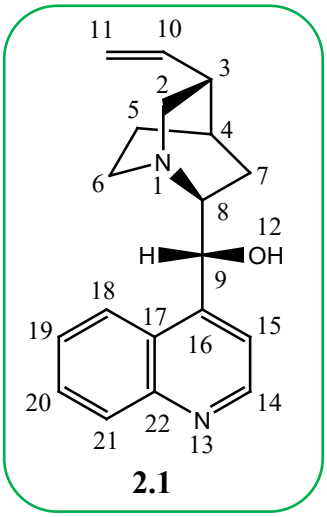


**2.1**

Figure 2.1 Atomic numbering of the resolving agents.

The general structure of these resolving agents is characterized by the presence of an aromatic quinoline ring system that is linked to an aliphatic quinuclidine bicyclic system through a —CH(OH)— linkage. The latter structural framework generates a β-hydroxyamine (secondary amino-alcohol) functionality next to the aromatic ring. The resolving agents have five stereogenic centres: N1, C3, C4, C8 and C9. In the four *Cinchona* alkaloids the absolute configurations are N1 (*S*), C3 (*R*), and C4 (*S*). The differences occur at positions 8 and 9. The total number of stereoisomers of these compounds is 16, not 32 ($2^5$), this is because the absolute configurations at the bridgehead atoms N1 and C4 of the quinuclidine bicyclic system are inter-

dependent. The quinine molecule (1*S*, 3*R*, 4*S*, 8*S*, 9*R*) and the quinidine molecule (1*S*, 3*R*, 4*S*, 8*R*, 9*S)* are diastereomers.[8] They are, however *quasi*-enantiomeric at the β-hydroxyamine functionality.[9] Caner *et al*. have explored systematically the conformational spaces of the *Cinchona* alkaloids by employing a semi-empirical methodology. They explored the intramolecular hydrogen bond N1···H···O12 in the conformers of the *Cinchona* alkaloids. Their results revealed the *quasi*-enantiomeric character between the *Cinchona* alkaloid molecules.[8] The complexity of these resolving agents involves five areas that are susceptible to the rotation around a single bond in each of the molecules:

(i) The most essential rotations are around the C16—C9 and C9—C8 single bonds, these link the two spatial rings of the reagents (the backbone rotations). The main conformations of the *Cinchona* alkaloids are illustrated by the rotations around these two bonds.[10]

(ii) C9—O12 rotation is significant due to the likelihood of an intramolecular hydrogen bond between the N1 bicyclic nitrogen atom and the C9 OH group.

(iii) The other rotations are due to the vinyl and methoxy substituents around C3—C10 and C19 attached to the methoxy group. There is another rotation at the methoxy substituent between the oxygen and the carbon bond of the methoxy substituent.[8]

The role of the *Cinchona* alkaloids was secured with the discovery of their ability as resolving agents by Pasteur in the year 1853, which resulted in a period where research focusing on racemic resolutions were achieved by the formation of crystals of diastereomeric salts.[11] The derivatives of quinine and cinchonine, quinicine and cinchonicine were used to carry out the first resolution, and by the 1990s 25% of all resolutions involved *Cinchona* alkaloids.[12] In the literature many examples are given where the *Cinchona* alkaloids have been utilized as chiral resolving agents.[13] In the late 1970s and early 1980s Wynberg *et al*.'s work began a period of research in asymmetric catalysis utilizing *Cinchona* alkaloids.[14] They employed the *Cinchona* alkaloids as chiral Lewis base/nucleophilic catalysts for a wide spectrum of enantioselective changes, and subsequently the use of the *Cinchona* derivatives increased considerably. In the mid 1990s Sharpless *et al*. developed the osmium-catalyzed asymmetric dihydroxylation of olefins,[15] which had a huge effect on synthetic chemistry.

The Cinchona alkaloids have structural features related to their several conformations and self-assembly phenomena. The information on the chiral effect and selecting ability of these alkaloids can be provided by the knowledge of their "real structure" in solution. In the late 1980s the conformational action of the alkaloids was established by Dijkstra *et al*. by using NMR spectroscopic methods and molecular mechanics calculations.[16] Their results enabled

them to recognize that the bonds between C8—C9 and C16—C9 were the most important bonds in the determination of the universal conformation. They identified four low-energy conformers as *syn*-closed, *syn*-open, *anti*-closed and *anti*-open conformers. Molecular mechanics calculations revealed that the parent alkaloids prefer the anti-open conformation in non-polar solvents.[16] Calculations that were conducted at a later stage showed that the anti-open conformation is the more stable in apolar solvents.[12]

## 2.3. Active sites in the resolving agents

The above resolving agents are molecules that possess functional groups that can hydrogen bond to both donors and acceptors. All have a nitrogen atom N1 at the quinuclidine ring that can accept a proton, to form a salt resulting in a charge assisted hydrogen bond. They also have a hydroxyl group at C9 that can donate a hydrogen atom in a hydrogen bond, and **2.3** and **2.4** have an electron donating group in the form of a methoxy group at position 19, while the quinoline ring can be involved in π-bonding.

The four alkaloids are readily available and inexpensive, possessing chiral structures which are readily adjustable for various kinds of chemical reactions. They are powerful ligands for a vast number of metal-catalyzed chemical reactions due to the quinuclidinic base functionality, and an example of this is the use of osmium in the asymmetric dihydroxylation of olefins.[12] In the enantioselective heterogeneous asymmetric hydrogenation of α-ketoesters the quinuclidine N allowed the alkaloids to be used as metal surface modifiers, showing their metal binding properties. The two reactions fall under the class of ligand-accelerated catalyses.[17]

More than one of the Cinchona alkaloids active sites may interact with the reacting species at the same time and in some instances the aromatic quinoline system facilitates π—π interactions or is a steric hinderance.[18-21]

## 2.4. Biological involvement

These compounds have been used to treat malaria, bacterial infections and heart related problems.[22] There are several factors that impact the biological activity of these molecules, and the mechanism of action is not thoroughly understood. The activity appears to be associated with the stereochemistry of the chiral centres at adjacent positions 8 and 9.[23] The amino and OH groups at positions 8 and 9 can form intermolecular hydrogen bonds with the receptors, which is considered important for biological activity. This ability is lost when these groups are involved in intramolecular hydrogen bonds.

## 2.5. Cinchonine

Cinchonine is one of the alkaloids that have been employed as a resolving agent for carboxylic acids. A recent Cambridge Structural Database search (version 5.41, November 2019) conducted with ConQuest yielded only 21 structures with cinchonine and 29 structures with cinchoninium fragments (Appendix B).

The tertiary diphosphines and monophosphines are the chiral organophosphorous compounds that are used in the field of asymmetric catalysis and as chiral ligands.[24] The use of enantiopure phosphine ligands that are in possession of a chiral centre at the phosphorous atom is growing in the field of asymmetric reactions catalyzed by transition metals.[25,26] The *tert*-butylphenylphosphinous acid-borane (**2.5**) was resolved by using ephedrine (**2.6**) and cinchonine (Scheme 2.1).[27] The resolution of the racemic phosphonic acid mono-ester was achieved with cinchonine in methanol *via* diastereomeric salt formation. The results demonstrated that phosphonic mono-ester enantiomers could be distinguished by proton NMR due to their strong hydrogen bonding properties.[28]

Racemic **2.5** and a (1*R*,2*S*)-**2.6** solution mixed with DCM and hexane resulted in the precipitation of a crystalline salt which was recrystallized to form the ephedrine salt (**2.7**). The treatment of **2.7** with aqueous HCl resulted in (*S*)-**2.5.** Treatment of the mother liquor enriched with (*R*)-**2.5** with cinchonine afforded the diastereomerically pure **2.8**, which was confirmed by the use of $H^1$ NMR. The treatment of **2.8** with acid provided the enantiomerically pure (*R*)-**2.5** in 31.9% overall yield.[27]

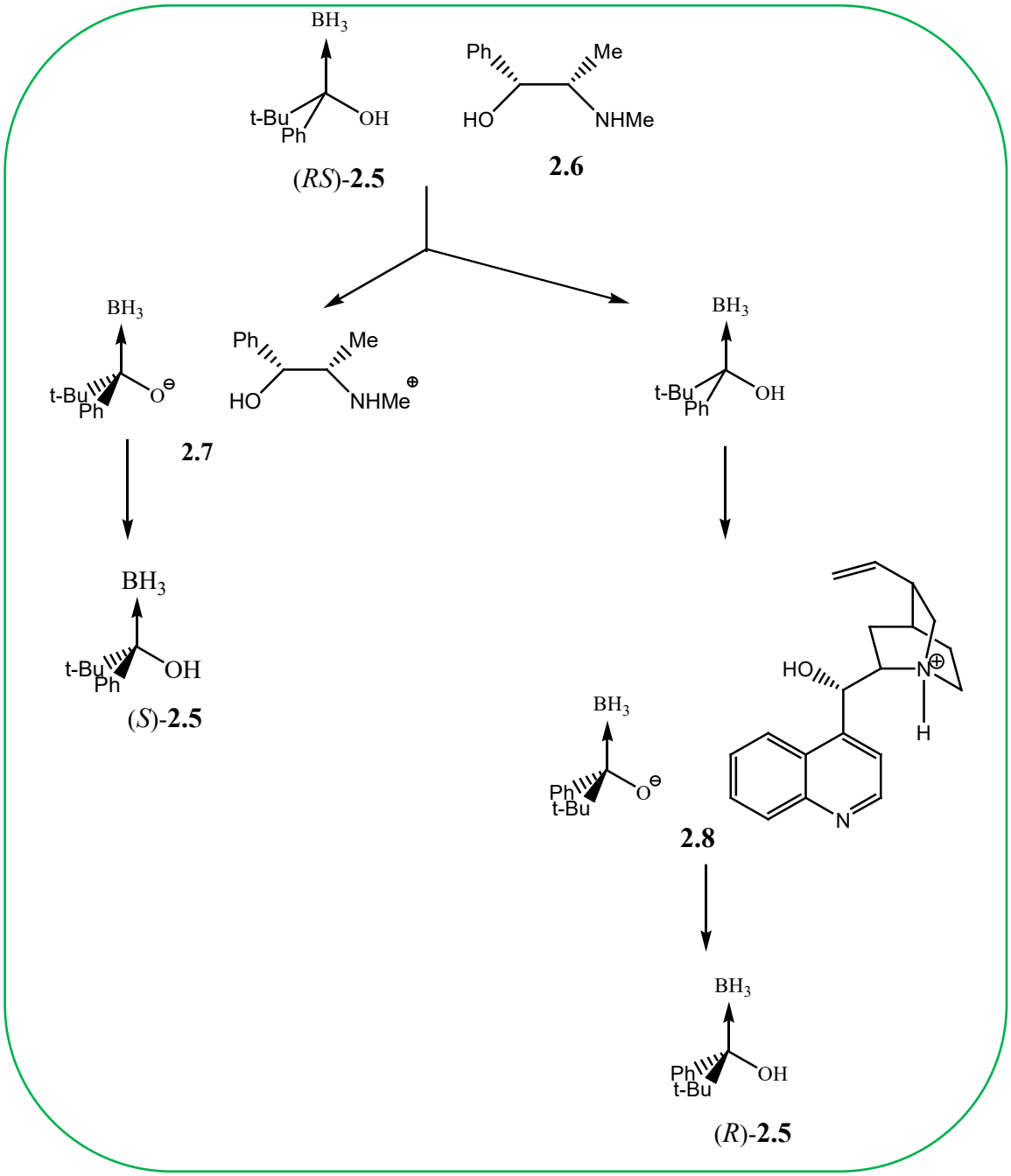


Scheme 2.1 The resolution of **2.5** with **2.6** and **2.1**.[27]

In 1899 McKenzie resolved racemic mandelic acid (**(+/-)-2.9**) by reacting it with cinchonine in water. He found that the (*S*)-mandelate salt formed was more stable than the counterpart (*R*)-mandelate salt. In 1993 Larsen *et al*. found that the resultant diastereomeric salts of cinchonine and mandelic acid from the solvent ethyl acetate was different from McKenzie's resultant salts. Larsen *et al*. found that the (*R*)-mandelate was the less soluble salt.[29]

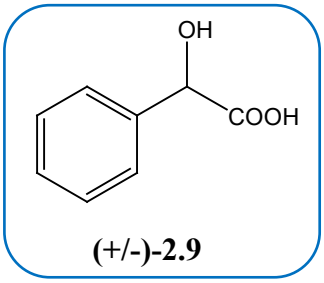


**(+/-)-2.9**

In 1994 Kozma *et al*. investigated the function of the solvent by performing the optical resolution of mandelic acid (**MA**) with cinchonine in various solvents, and the reaction products are shown in Table 2.2.[30]

Table 2.2 Experimental results in the resolution of **MA**.[30]

| | Solvent (ml) | Precipitating salt | | | S | Solvate |
|---|---|---|---|---|---|---|
| | | Config of MA | Yield % | Optical purity % | | |
| 1 | Water 50 | *S*-(+) | 100 | 28 | 0.28 | Water |
| 2 | 4:1 (v/v) Water:ethanol 25 | *S*-(+) | 55 | 13 | 0.07 | Water |
| 3 | 2:1 (v/v) Water:ethanol 15 | *R*-(-) | 88 | 9 | 0.08 | No solvate |
| 4 | Water free ethyl acetate 110 | *R*-(-) | 82 | 36 | 0.30 | Ethylacetate |
| 5 | Water saturated ethyl acetate 30 | *R*-(-) | 73 | 61 | 0.45 | Ethylacetate |

The most efficient resolution was achieved in water saturated ethyl acetate. The resultant salts differed in configuration of the **MA** and in the included solvent. The 4:1 water:ethanol mixture gave the (*S*)-(+)- enantiomer and a hydrate whereas the 2:1 water:ethanol mixture reversed the chirality of **MA** and no solvent co-crystallized. Water was included in the crystal structures when it was in abundance and the unsolvated crystals had the lowest optical purity.[30]

Enantiomeric (*S*)-(+)- and (*R*)-(-)-binaphthyl phosphoric acids (**BNP**) (**2.10**) are useful resolving agents that give rise to well crystallized and easily separated salts with a variety of amines. They have been used in preparing the enantiomers of 7-phenylquinolizidine,[31] a biologically and therapeutically active compound.[31] **BNP** acid has been used for the resolution of underivatized *o*-tyrosine.[32] In 1971 Jacques *et al*.[33] were able to resolve the racemic **BNP** using cinchonine as a resolving agent, where they obtained the (+)-**BNP** enantiomer.

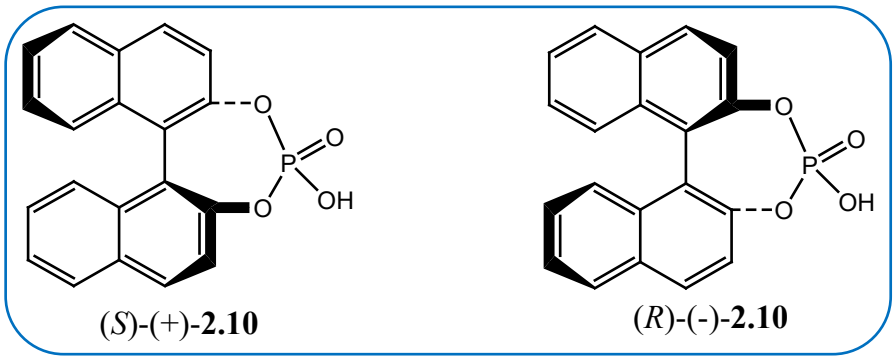


(*S*)-(+)-**2.10** (*R*)-(-)-**2.10**

A modification of the above resolution was performed by Kyba *et al*. who also obtained the (+)-**BNP** acid *via* the cinchonine salt but they isolated the (-)-enantiomer from the more soluble salt without the use of cinchonine.[34] In 1989 Jacques *et al*. resolved the **BNP** acid using cinchonine and they avoided the purifications that were performed by Kyba *et al*. The (*S*)-(+)-**BNP** acid yield due to the presence of the enantiomer in the racemate was 56%, and the (*R*)-(-)-**BNP** acid yield was 49%.[35]

The optically active 1,1'-bi-2-naphthyl alcohol (**BINOL**) (**2.11)** and its counterparts are applied in chiral ligands of catalysts for asymmetric chemical reactions,[36] as hosts for molecular recognition and enantiomer isolation,[37] and as intermediates in the synthesis of chiral molecules.[37] Wang *et al*. resolved **BINOL** through molecular complexation of **BINOL** with a cinchonine derivative, *N*-benzylcinchoninium chloride (**2.12**), an epimer of **2.13**.[38]

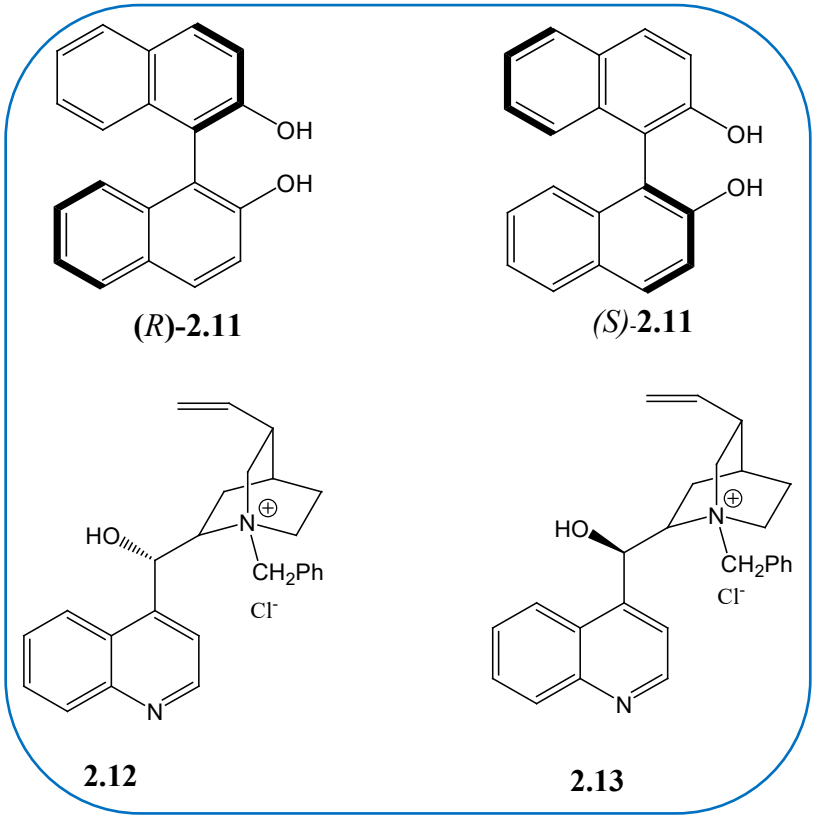


**(*R*)-2.11** *(S)*-**2.11**

**2.12** **2.13**

**2.1** (3*R*,4*S*,8*R*,9*S*) owes its physiological action to the stereochemistry of its chiral atoms, *viz* the amino group attached at position 8 and the hydroxyl group at position 9.[39] When **2.1** was

treated with one mole of tartaric acid, the product was cinchoninium-bitartrate tetrahydrate.[40] On altering the stereochemistry of the alkaloid, as in **2.2** (3*R*,4*S*,8*S*,9*R*), the reaction produced the diammonium tartrate (**2.14**), as a dihydrate, compared to the tetrahydrate (**2.15**).

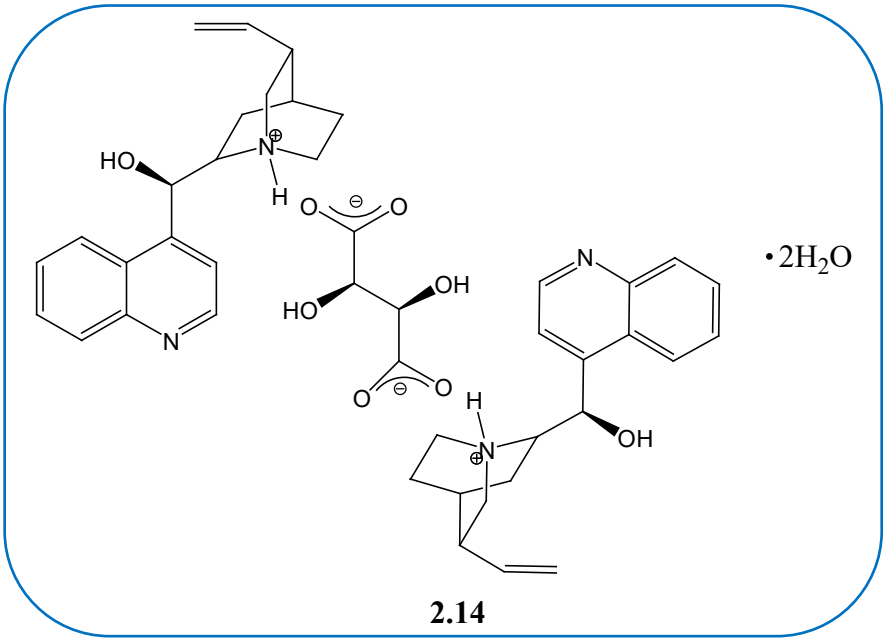


**2.14**

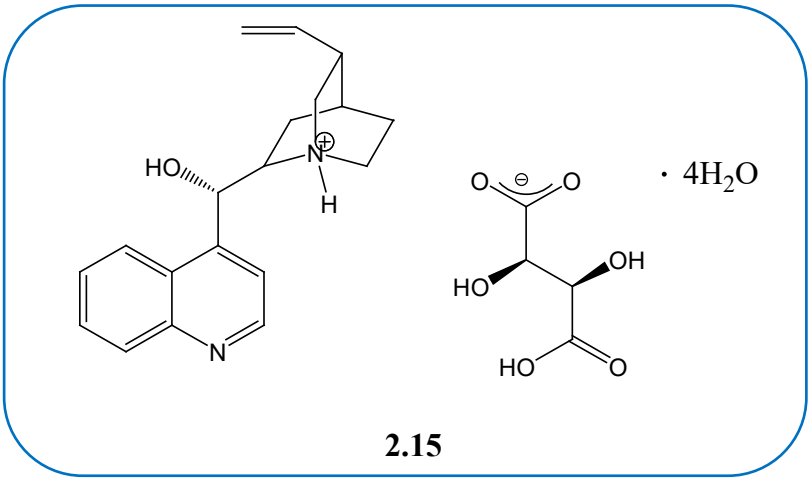


**2.15**

Cinchonine has also been used to resolve racemic **2.11** *via* the cyclic borate ester **2.10a**, which was produced from the reaction of the racemic 1,1'-binaphthoborane with cinchonine in THF, and one diastereomer was more soluble, while the other one was less soluble and precipitated from solution. The precipitated salt was treated with 2N HCl and recrystallized from diethyl ether to produce (*R*)-(+)-**2.13** in 70% yield and 100% ee.[41(a),(b)]

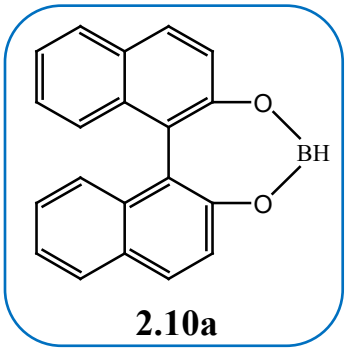


**2.10a**

## 2.6. Cinchonidine

Cinchonidine has also been used as a resolving agent though only a few publications describe the structural results. A CSD (version 5.41, November 2019) search revealed only 26 cinchonidine and 38 cinchonidinium structures (Appendix B).

The $C_2$-symmetric 2,2'-dihydroxy-1,1'-binaphthalene-4,4'-dicarboxylic acid (**2.16**) was used as a ligand in the development of 2-dimensional and 3-dimensional homochiral metal-organic structures.[42,43] Tanaka *et al*. resolved this compound by complexing it with cinchonidine.[44]

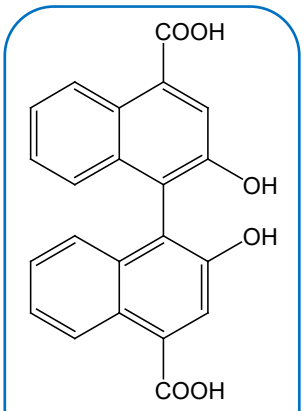


**2.16**

Citronellic acid, 3,7-dimethyl-6-octenoic acid (**2.17**), is obtained from camphor oil in a racemic form. This acid has been successfully resolved by treating it with **CIND** as a resolving agent to form the salt cinchonidinium-(*S*)-citronellate monohydrate.[45] Citronellic acid has antibacterial and antifungal properties,[46] and can be synthesized *via* the oxidation of citronellal.[47] Detailed information regarding the salt is given in Chapter 7.

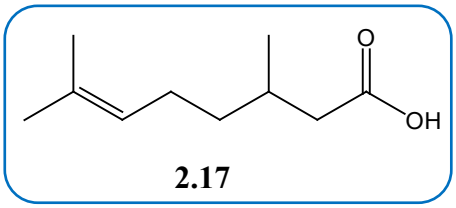


**2.17**

Cai *et al*. reported a straightforward and effective resolution of **BINOL** using a derivative of **CIND**.[48(a)] They managed to obtain both enantiomers of **BINOL** in > 95% yield (*R*) and > 99%

(*S*) ee. Their procedure in which they used acetonitrile as a solvent represented a much better resolution for **BINOL** than the previously reported methods.[48(b)] The procedure could also be applied to binaphthyl alcohol equivalents such as 6,6'-dibromo-1,1'-bi-2-naphthyl alcohol (**2.20**) or 6,6'-dimethyl-1,1'-bi-2-naphthyl alcohol (**2.21**) with similar results.[49]

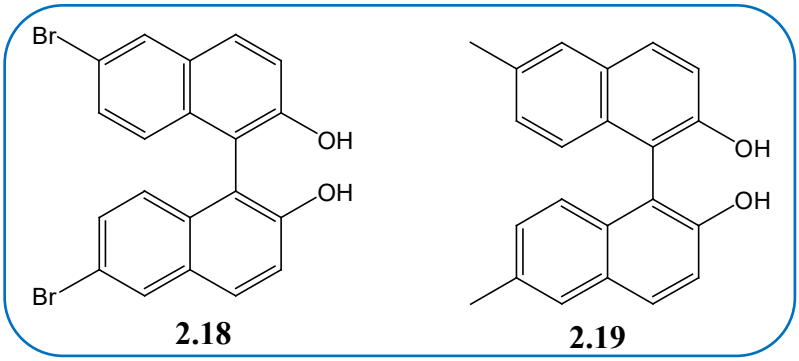


**2.18** **2.19**

Tanaka *et al.* have noted the effective chiral discrimination in the formation of inclusion complexes of **CIND** derivatives **2.13** and **2.20** with $C_2$-symmetrical chiral biaryldiol derivatives **2.11**, **2.18** and **2.21**. The behaviour of the **CIND** derivatives was completely different from that of **CIND** itself, which did not form inclusion complexes with **2.11**, **2.18** and **2.21**.[50]

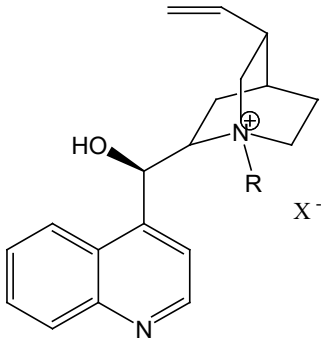


**2.13** : R = $PhCH_2$; X = Cl

**2.20**: R = nBu; X = Br

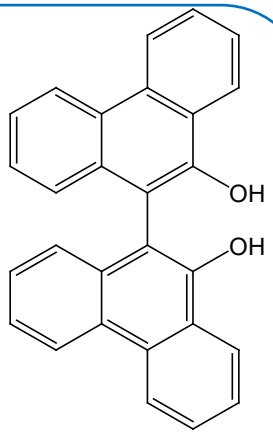


**2.21**

They found that commercially available **2.13** was effective in the resolution of **2.11** to form 1:1 inclusion crystals of **2.13** and (+)-**2.11** (72% yield, mp 240 - 244 °C) and an inclusion complex of **2.13** and (-)-**2.18** (89% yield, mp 229-232 °C). The separation of **2.21** was achieved by using *N*-butylcinchonidinium bromide (**2.20**) forming a 1:1 inclusion compound of **2.20** and (+)-**2.21** (83% yield, mp 168-169 °C). The salt **2.20** did not form inclusion compounds with **2.11** and **2.18**. This showed that the inclusion behaviour of the derivatives **2.13** and **2.20** varied according to the alkyl substituent at the bridgehead nitrogen atom of these molecules. They then concluded that the results might have been as a result of the type of molecular discrimination in the inclusion complex.

The **CIND** derivatives were therefore very important in the selection of the enantiomers of biaryldiols, and the **CIND** itself did not separate the enantiomers of the diols.[48(a)] However, **QUIN** itself separated the enantiomers by forming inclusion complexes with the 7,7'-*bis*(benzyloxy)derivatives of **2.11**.[51]

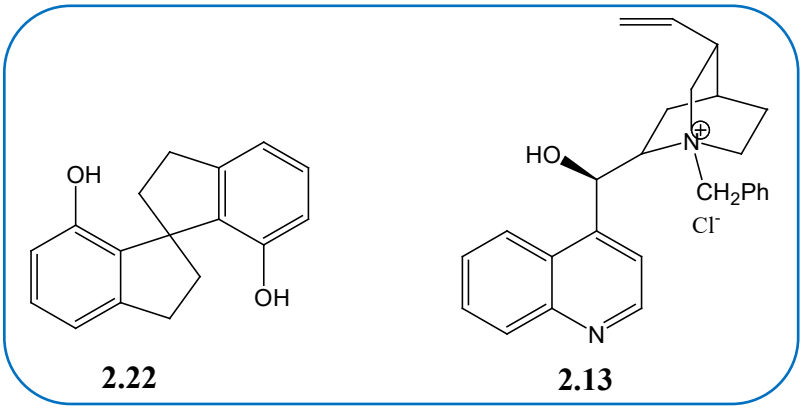


**2.22** **2.13**

A spirobiindane analogue, 1,1'-spirobiindane-7,7'-diol (**SPINLO**) (**2.22**), has a structure that provides a potential combination of chemical strength and conformational rigidity, and the two hydroxyl groups at C7 and C7' are available for chelation. A modified **CIND (2.13)** was used to resolve **2.22** by inclusion complexation.[52]

Growth promoting auxins, eg indole-3-succinic acid (**ISA**) **2.23**, have been synthesized as the racemate[53,54] and Armstrong *et al*. have been able to resolve it to its enantiomers using **CIND**.[55] The resultant ee values of (*S*)-**ISA** and (*R*)-**ISA** were found to be 97-99% and 93-95% respectively, by enantioselective HPLC determination.

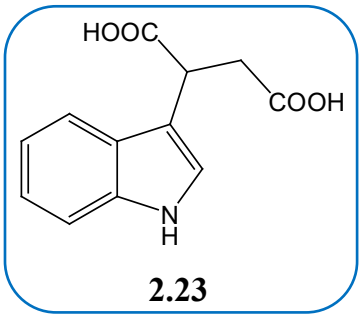


**2.23**

The optically active isoxazoline intermediate was synthetically prepared from the acid **2.24** through resolution by the fractional crystallization of the diastereomeric cinchonidine salts of **2.24**, from acetone. The resultant asymmetric unit consisted of an ion pair and an acetone solvate of crystallization in general positions. From the known **CIND** stereochemistry, the isoxazoline stereochemistry was determined to be the (*S*)-configuration. In the crystal lattice, it was observed that the anion firmly hydrogen-bonded to the hydroxyl and the amine groups of the cation.[56]

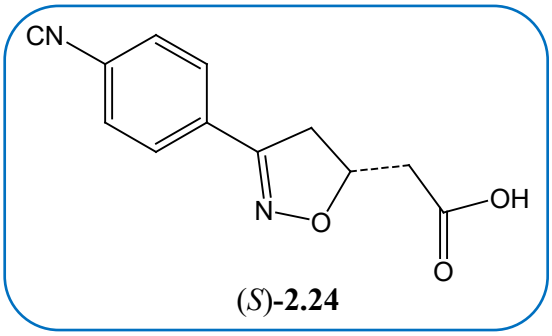


(*S*)-**2.24**

Enantiopure anions of $D_3$ symmetry could be employed in many of the chemistry fields that incorporate chiral or prostereogenic cation moieties. The optically pure or enriched phosphate(V) ions that have a hexa-coordinated phosphorous centre do not have chemical stability with regard to acids and oxidants, therefore they cannot be used. An immediately accessible, configurationally stable anion, with a hexa-coordinated phosphorous atom, was synthesized and their enantiomers resolved using **CIND**.[57]

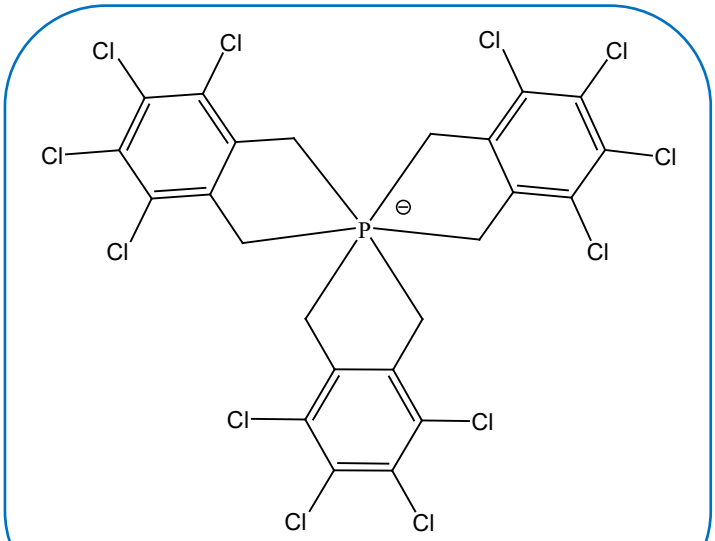


**2.25**

Efficient resolution of **2.25** by crystallization of the mixtures of **CIND**-(*P*)-**2.25** and **CIND**-(*M*)-**2.25** in EtOAc/acetone (3/1) gave rise to pure **CIND**-(*P*)-**2.25** after filtration. The solid had a molecule of ethyl acetate in 47-51% yield, ($[\alpha]_D^{20}$ = -375, c = 0.111 in ETOH). The (*P*)-configuration was confirmed by X-ray structure analysis.[57] In the early 1960s **CIND** and **QUIN** were employed in the resolution of the arsenic(V)-catechol complex, and they gave rise to the *d*(+)-anion of the complex.[58]

## 2.7. Quinine

Quinine is the alkaloid that has been mostly employed in chiral resolutions compared to the other three resolving agents, as per the CSD (version 5.41, November 2019) search which gave 47 quinine fragments and 38 quininium fragments (Appendix B).

In 1963 quinine was employed in the resolution of (+/-)-*trans*-1,2-cyclohexanedicarboxylic acid in 95% EtOH. The resultant diastereomer gave rise to (+)-*trans*-1,2-cyclohexanedicarboxylic acid with high optical purity.[59] This di-acid was used in the preparation of an optically active silver *trans*-1,2-cyclohexanedicarboxylate that was brominatively decarboxylated to give rise to an optically active *trans*-1,2-dibromocyclohexane.[59]

The resolution of a racemate was performed *via* its derivative to produce both of the enantiomers in high yield and enantiomeric excess.[41(b)] Racemic **2.11** was resolved *via* the cyclic borate ester **2.10a** using **QUIN** in tetrahydrofuran (THF). Due to the easy method of forming or cleaving the boron-oxygen bonds, Shan *et al*. studied the resolution of **2.11** by first converting it to the borate ester **2.10a**. THF was found to be the best solvent to obtain both diastereomers of the 1,1'-bi-2-naphtholborane quinine derivative. The resultant precipitate derivative and the filtrate were separated. These were then acidified and purified to give rise to (*R*)-**2.11** and (*S*)-**2.11** in about 80% yield and 100% ee respectively. The procedure was advantageous because it was very easy to carry out, the preparation period was short and it resulted in both enantiomers in high optical purity. The cyclic borate ester approach was the most successful method to resolve the racemic **2.11**.[41(b)]

The racemic 1,1'-binaphthyl-2,2'-dicarboxylic acid (**BNDA**) has been used to prepare chiral binaphthyl based molecules like crown ethers and catalysts.[60,61] Brucine was used by Kanoh *et al*. to resolve the dicarboxylic acid,[62] Seki *et al.* used (*R*)-(-)-1-cyclohexylethylamine[63] and Imai *et al*. used (1*R*,2*R*)-diphenylethylenediamine.[64] Jacobs *et al.* have resolved **BNDA** by employing **QUIN**, (*R*)-(6-methoxyquinolinium-4-yl)-[(1*S*,2*S*,4*S*,5*R*)-5-ethenylquinuclidinium-2-yl]methanol[65] to give the more stable salt, quininium (*S*)-1,1'-binaphthyl-2,2'-dicarboxylate dihydrate which was determined using single crystal X-ray diffraction.

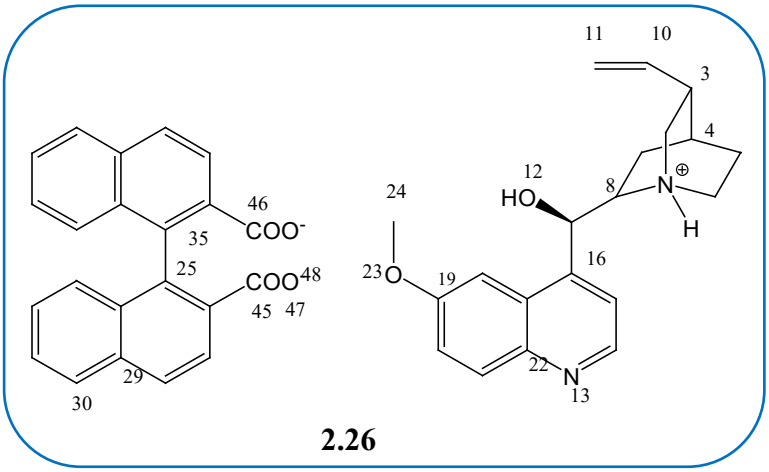


**2.26**

The **2.26** salt crystallized in the orthorhombic space group $P2_12_12_1$ with a dicarboxylate anion, plus two quininium cations and two water molecules of crystallization in the asymmetric unit. The dicarboxylate had an *S* configuration and C9 of the **QUIN** is known to be *R*.

Malic acid exists as the *L*-(+) molecule and the *D*-(-) molecule in its racemic form **2.27**. Resolution of the racemic form was attempted by exposing it to *R*-phenylethylamine.[66] Bàthori *et al*. have studied the partial discrimination of quininium malates *via* diastereomeric salt formation where they treated quinine with the racemic (*DL*) malic acid.[67]

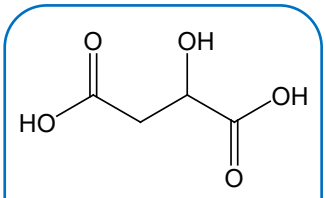


**2.27**

**QUIN** partially resolved the racemic malic acid giving rise to a salt of 2(**QUIN**$^{+}$)·(*D*-MA$^{2-}$)·2$H_2O$. The crystal structure was solved in the space group *C*2 with Z = 2. **QUIN** was further crystallized with pure *L*- and *D*-malic acids and the resultant structures were discussed.

Sesquiterpenoids are isolated from fungi and can be synthesized from hydroazulenes.[68] The resolution of a hydroazulenone (+/-) **2.28** was achieved by first converting it to a monoacid (+/-) **2.29** by treating it with NaOH and dichloromethane. The monoacid was then treated with **QUIN** in MeOH to give rise to a salt. The configuration of the acid moiety was demonstrated by X-ray diffraction analysis to be (3a*R*,4*S*,8a*R*)-(+)-**2.29**.

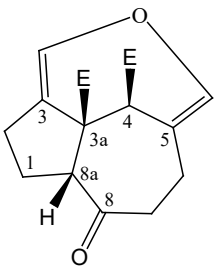


**(+/-) 2.28**

E = $COOCH_3$

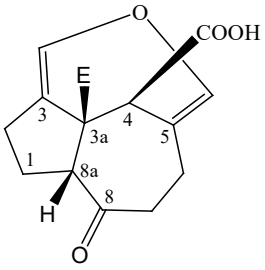


**(+/-) 2.29**

E = $COOCH_3$

Esterification of (+)-**2.29** with diazomethane produced (-)-**2.28** in 96% yield.[68] The resolved hydroazulenones would then be accessible for the synthesis of enantiomerically pure sesquiterpenoids on a preparative laboratory scale.

Proton NMR studies of the associations between the optically active **QUIN** and the enantiomerically pure 2,2',7,7'-tetrahydroxy-1,1'-binaphthyl analogues **2.30 a-d** were undertaken by Castro *et al.*[51]

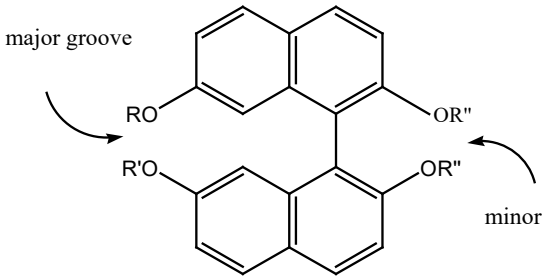


**2.30**

| **2.30** | R | R' | R" |
|---|---|---|---|
| a | $PhCH_2$ | $PhCH_2$ | H |
| b | $PhCH_2$ | $PhCH_2$ | $CH_3$ |
| c | H | H | $CH_3$ |
| d | H | $PhCH_2$ | $CH_3$ |

The resolution of these derivatives resulted in the formation of complexes with 1:1 stoichiometry that was established in binding titrations at a temperature of 293 K in which the resonances of the binaphthyl analogue, which was chosen at a constant concentration, were observed and the progress checked as a function of increasing **QUIN** concentration. With **2.30a,** a fairly strong complexation of **QUIN** as well as a meaningful differential stability of the diastereomeric complex was noticed. The (*R*)-**2.30a-QUIN** complex that was the first to precipitate in the optical resolution was the most stable, less soluble one. The alkylation of the hydroxyl groups in **b** led to the removal of measurable binding interactions. That was proof for the relevance of hydrogen bonding for the discrimination process.[69,70] The difference in stability between the complexes of (*R*)-**2.30d** was high, approximately 1 kcal $mol^{-1}$.

In another case where the solvent played a determinant function in the configuration of the resolved acid was reported by Wilen *et al.*[71] There are cases where the salt crystallizes only if they are solvated by a certain solvent, and where crystallization does not take place (neither of

one nor the other isomer) in the absence of solvating compounds. In other instances, only one isomer crystallizes. It is rare to find both of the diastereomeric salts crystallizing when only one is solvated. Dimethyl-3-phenylpentanoic acid on treatment with **QUIN** in EtOH and EtOH/$H_2O$ gave rise to diastereomeric salts of different configuration (Scheme 2.2).[71]

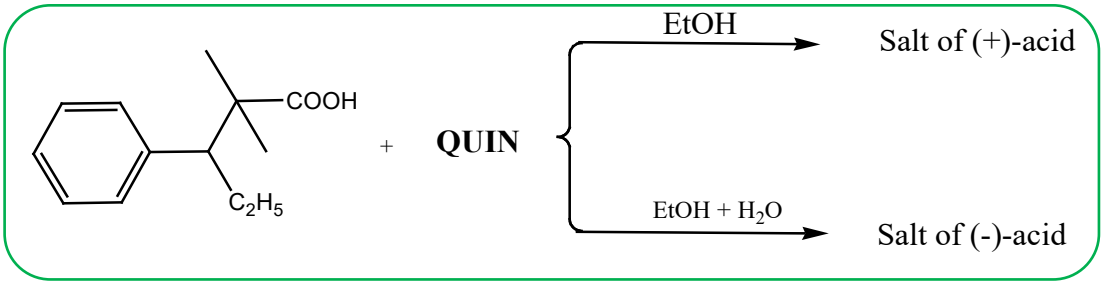


Scheme 2.2 The effect of solvent on the relative solubility of diastereomeric salts.[71]

Chromatographic techniques have been utilized in the resolution of racemic amino acids with thin layer chromatography (TLC) providing advantages over other chromatographic techniques.[72-76]

In 2001, Bhushan *et al*. resolved the enantiomers of *DL*-amino acids on thin silica gel plates that were impregnated with an optically pure resolving agent, (-)-quinine as a chiral selector.[77] Different solvents and mixtures were used to influence the resolution of *DL*-amino acids.

The solvent mixtures that were successful in the resolution were, butyl alcohol:chloroform:acetic acid (3:7:5) for *DL*-methionine, 6:8:4 for alanine, 10:1:4 for threonine, and ethylacetate:carbontetrachloride:propanoic acid (10.5:6.5:3.5) for valine and 10.5:4:7 for both leucine and isoleucine. Table 2.3 shows the $hR_F$ values regarding the resolved isomers, pure isomers and their solvent compositions.

Table 2.3 The *h*$R_F$ values ($R_F$ x 100) of the resolved *DL*-amino acids on silica gel plates impregnated with (-)-quinine (0.1%).[77]

| | | | | *h*$R_F$ values | | |
|---|---|---|---|---|---|---|
| Sample no | *DL*-amino acids | Solvent system | Ratio v/v | Pure *L* | Racemic mix *D* | Racemic mix *L* |
| 1 | Methionine | $S_1$ | 3:7:5 | 50 | 25 | 50 |
| 2 | Alanine | $S_1$ | 6:8:4 | 16 | 7 | 16 |
| 3 | Threonine | $S_1$ | 10:1:4 | 11 | 5.5 | 11 |
| 4 | Valine | $S_2$ | 10.5:6.5:3.5 | 19.3 | 11.8 | 19.3 |
| 5 | Leucine | $S_2$ | 10.5:4:7 | 13.8 | 6.4 | 13.8 |
| 6 | Isoleucine | $S_2$ | 10.5:4:7 | 12.9 | 6.4 | 12.9 |
| Time, 45 mins; solvent front, 10 cm; detection, ninhydrin solution; temperature, 25+/- 2 °C. The temperature for valine was 18+/- 2 °C<br>$S_1$ n-Butanol-chloroform-acetic acid. $S_2$ ethyl acetate-carbon tetrachloride-propionic acid. | | | | | | |

The best resolution was at 0.1% of (-)-quinine for all the racemic amino acids, and no resolution occurred at 0.05% - 0.07%, poor resolution occurred at an increased concentration to 0.15%, and no resolution on increasing the concentration to 0.2%. The temperature of the system affected the chiral interaction during the resolution between the chiral discriminator and the analyte, and their best resolutions were obtained at 25+/- 2 °C. There was no resolution at 15, 30 and 35 °C, but the *DL*-valine resolution occurred at 18 +/- 2 °C.[82] It was observed that (-)-quinine demonstrated the best enantioselective behaviour.[77]

The enantiodiscriminating capabilities of **QUIN** derivatives were studied by Uccello-Barretta *et al*. to indicate how derivatization can be used in the improvement of enantioselectivity.

H NMR spectroscopy was used to compare the enantiodiscriminating efficiencies of 9-O-acetyl**QUIN (2.31)**, 9-O-(3,5-dimethoxyphenylcarbamate)**QUIN (2.32)**, and *N*-benzylquininium chloride (**2.33)** concerning the multifunctional chiral analyte 2-(3',5'-dinitrobenzamido)-1-hydroxy-1-phenylethane (**2.34).**[83]

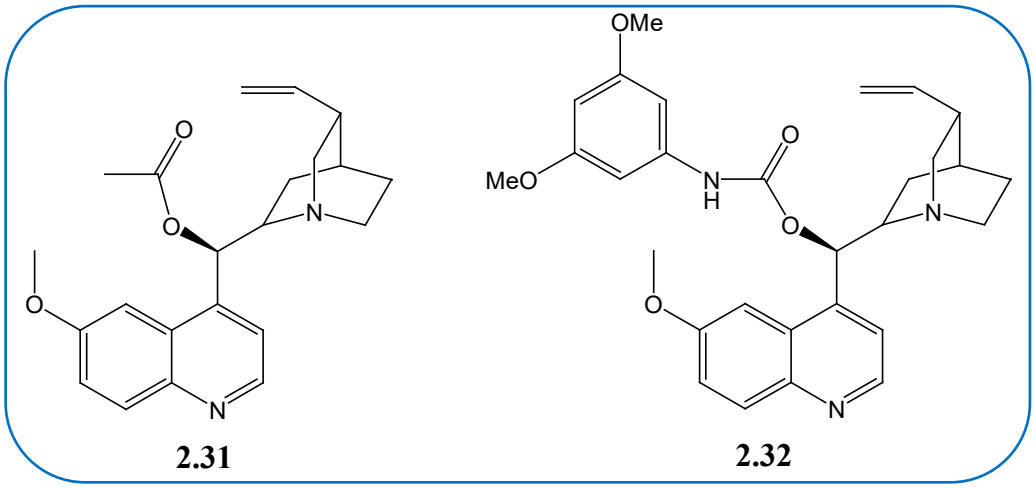


**2.31** **2.32**

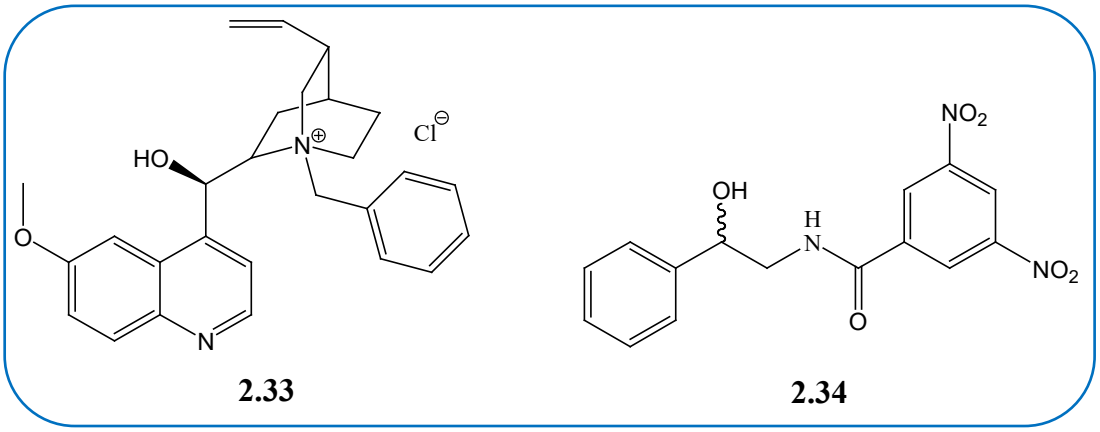


**2.33** **2.34**

## 2.8. Quinidine

Quinidine has the least number of quinidinium fragments deposited in the CSD, as per the CSD (version 5.41, November 2019) search results with 28 quinidine fragments and only 13 quinidinium fragments, indicating the few structural results that have been published (Appendix B).

In order to have a good understanding of the interaction mode between the *Cinchona* alkaloids and biphenyl 2,2'-dicarboxylic acid analogues, Kubicki *et al.*[80] executed X-ray analysis of a range of 2:1 salts. They were able to present the outcomes of the crystal structure elucidation of the salt of **QUID-2.35** (biphenyl-5,5'-dinitro-2,2'-dicarboxylic acid).

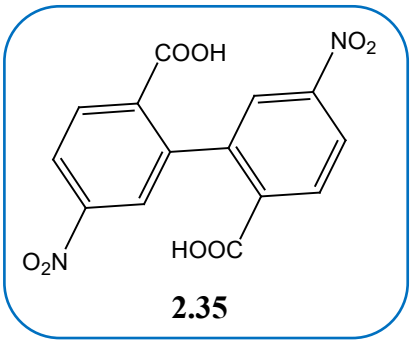


**2.35**

The salt fragment consisted of two **QUID** cations and one 5,5'-dinitrodiphenic anion ((*R*)-**2.35**). The salt crystallized with four acetonitrile molecules per unit cell. As a result of the large thermal parameters of the ethenyl groups and the acetonitrile molecules, the precision of the bond lengths and bond angles was poor. Both of the **QUID** cations were protonated at the nitrogen atoms N(1) and N(1'). Each COOH group of 5,5'-dinitrophenic acid was hydrogen bonded to the two **QUID** cations. The same pattern of interlocking hydrogen bonds had been found in the salt of **QUIN** with diphenic acid.[81]

In an earlier resolution of racemic **2.35** with **QUIN**, the (*S*)-**2.35** was selected from the racemate.[81] The analyzed crystals were formed after the diffusion of methylethyl ether vapour into the **QUIN**-(*S*)-**2.35** salt solution in chloroform, yet with the **QUID** resolution the crystals were obtained from an acetonitrile solution.

The authors concluded that the chirality of the salt was governed by the absolute configuration of the *Cinchona* alkaloid fragment as confirmed by their results.[80]

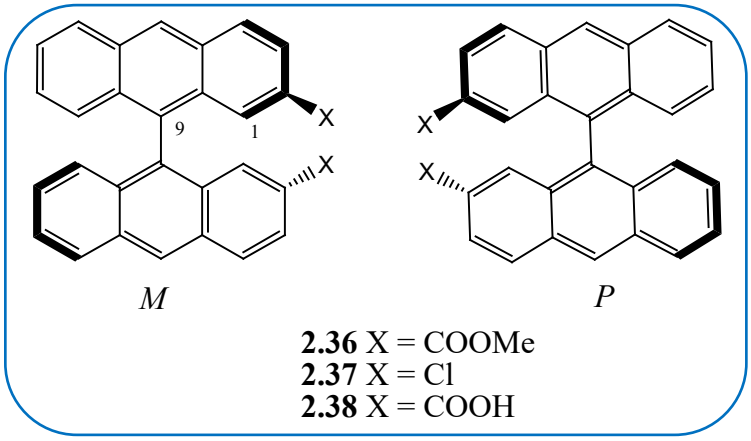


**2.36** X = COOMe
**2.37** X = Cl
**2.38** X = COOH

The 9,9'-bianthryls are popular in the formation of inclusion compounds with different types of guest molecules.[82,83] Therefore, knowledge of their stereochemistry is very important in applying the enantiopure hosts to host-guest chemistry. The racemic diacid (+/-)-**2.38** was synthesized from **2.37** and the acid was resolved by treating it with **QUID** in acetone. The reaction of the readily crystallized salt **2.39** with an acid produced the levorotatory diacid **2.38**. The treatment of (-)-**2.38** with diazomethane resulted in the corresponding dimethylester (-)-**2.36** whose specific rotation was $[\alpha]_D^{25}$ = -123. The racemic dichloride has been reported to participate in the formation of inclusion compounds with small organic fragments.[84,85] Toyota *et al*. prepared the enantiopure form of the host molecule from (-)-**2.41** using Barton's method.[86,87]

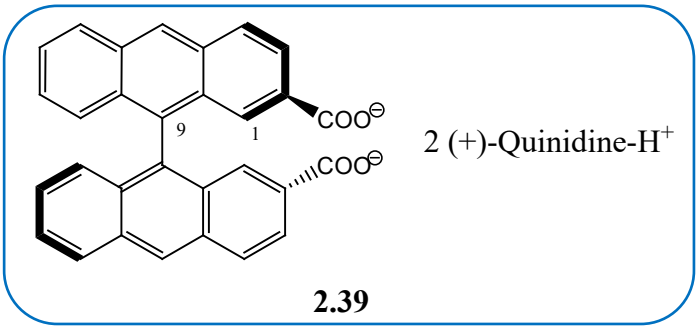


**2.39**

The structure of **2.39** was solved and the **QUID** species had the known absolute configurations, which was utilized as the internal reference. The dihedral angle between the two anthryl groups was -68.9(8)°, which showed that the absolute stereochemistry about the C9—C9' axis was *M*. As a result, the absolute stereochemistry of **2.38** was (*M*)-(-), and **2.36** and **2.37** had a similar stereochemical relationship.

A unique pair of enantiomeric unnatural *Cinchona* alkaloid derivatives (+/-)-**2.40** that had a similar configuration on both stereogenic centres in the methyl alcohol bridge and the adjacent bicyclic system carbon atom as in quinine and quinidine was formed by attaching a spirobifluorene unit *via* its C-2 to the quinuclidine-2-methanol moiety.[88] The optical resolution of racemic **2.40** was performed by HPLC on a chiral stationary phase that was prepared by a covalent binding of quinine through a thiol spacer to a silica-gel surface. **QUIN** and **QUID** prefer an open conformation where the bicyclic system nitrogen atom points away from the quinoline ring, and the alkaloid analogues preferred the "closed" conformation, where the nitrogen atom points into the 9,9'-spirobifluorene cleft.

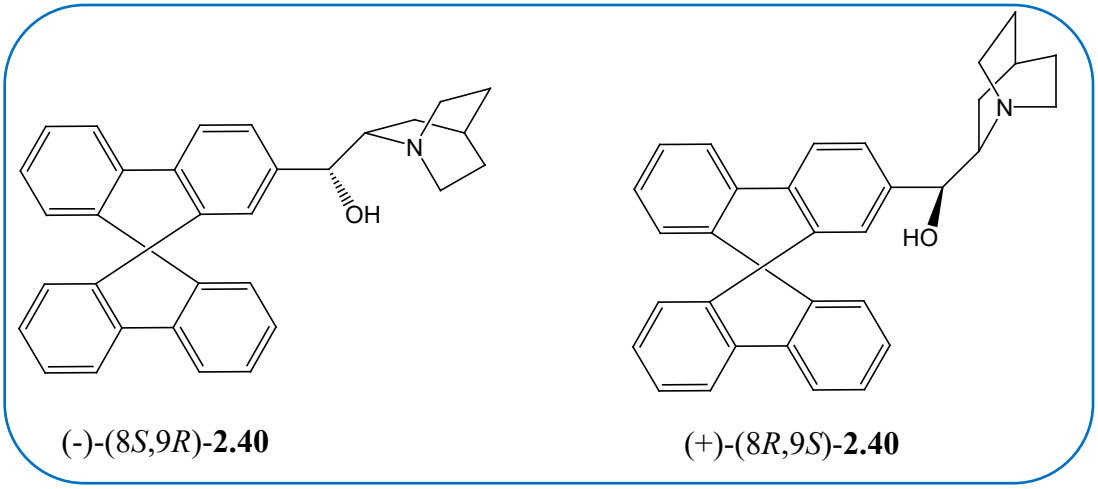


(-)-(8*S*,9*R*)-**2.40** (+)-(8*R*,9*S*)-**2.40**

Complexes of these with **QUIN** were analyzed experimentally and computationally. The results revealed (+)-(8*R*,9*S*)-**2.40** as the more stable complex, compared to the other one. The "closed" conformation was preferred over the "open" conformation, the bicyclic system nitrogen atom in (+)-**2.40** and (-)-**2.40** was unaccessible sterically for hydrogen bonding, which provided the new chiral shapes with lesser molecular discrimination characteristics in comparison to **QUIN**

or **QUID**.[88] The results therefore demonstrated that (+)-**2.40** and (-)-**2.40** differed greatly in their conformational inclination from their natural equivalents, **QUIN** and **QUID**.[89]

The four *Cinchona* alkaloids, cinchonine, cinchonidine, quinine, and quinidine have been reported in the resolution of anionic metal complexes. Their cations are soluble in water and bear a hydrophobic character, making them candidates for ion-pairing compounds in the reversed-phase ion pair chromatography technique.[90] The cations of these resolving agents as the ion-pairing compounds with the reversed-phase ion-pair chromatography have been employed in the resolution of various anionic complexes of the kind *cis*-(N)-$[Co(N)_2(O)_4]^-$.[91] The optical resolution was successful for $[Co(EDTA)]^-$, *cis*-$[Co(IDA)_2]^-$, $[Co(CYDTA)]^-$, $[Co(Ox)_2(en)]^-$ and $[Co(EDDA)]^-$ by three of the alkaloids except by cinchonine.[91] EDTA = ethylenediaminetetraacetate, IDA = iminodiacetate, CYDTA = *trans*-1,2-cyclohexanediaminetetraacetate, Ox = oxalate, en = ethylenediamine, and EDDA = *N*,*N*'-ethylenediaminediacetate.[91]

For many decades, attempts have been made to understand the chiral selection mechanism, and to establish a fast and simple method to screen optimal resolving agents for a certain earmarked racemate. A methodology was proposed to select resolving agents based on thermal analysis of the diastereomeric salts.[92-94] A good resolving agent would be the one forming a pair of diastereomeric salts exhibiting a huge difference in the melting point and in the heat of fusion. The problem with this method is it requires many experiments to record basic physicochemical information before administering the compounds to the target for resolution, and the procedure needs pure enantiomers, thereby limiting its application.[95]

Some researchers have quantitatively compared the resolution effectiveness to the lattice energy difference between the resultant diastereomeric salts.[96,97] The method was reported to involve calculation of the lattice energy difference between the two diastereomeric salts. It was noted that it was difficult to accurately calculate the lattice energies as the anticipated energy difference is susceptible to the balance between the intra- and the intermolecular forces as the ions are flexible in three-dimensional orientation.[95] This problem makes the method applicable to limited systems.

Resolution *via* diastereomeric salt formation involves an enantiopure resolving agent that reacts with the molecule to be resolved in the formation of the diastereomeric salts. The difference in the solubilities between the pair of the resultant salts provides an enantio-separation by crystallization of the more stable salt. After the recovery of the resolving fragment the expected enantiomer can be isolated. The choice of a resolving agent is crucial and relies on an

experimental approach, a procedure that involves a lot of time to produce suitable results or crystals.

The resolving agents for the study were chosen on ease of availability.

## 2.9. Comparative resolutions

The drug 2-(*N*-benzyl-*N*-methylamino)ethyl methyl 2,6-dimethyl-4-(*m*-nitrophenyl)-1,4-dihydropyridine-3,5-dicarboxylate hydrochloride (YC-93), has been predicted to be a future vasodilator among a vast number of tested 1,4-dihydropyridine derivatives that are soluble in water.[98] The drug is a racemic compound with an asymmetric position at carbon 4 of the dihydropyridine ring, and its optical isomers were characterized regarding their vasodilating activity. The resolution of the free base of the drug did not yield results from a variety of resolving agents. The optically pure (+)- and (-)-2-(*N*-benzyl-*N*-methylamino)ethyl methyl 2,6-dimethyl-4-(3-nitrophenyl)-1,4-dihydropyridine-3,5-dicarboxylate (**2.41**) was prepared from the resolved 1-ethoxymethyl-5-methoxycarbonyl-2,6-dimethyl-4-(3-nitrophenyl)-1,4-dihydropyridine)-3-carboxylic acid (**2.42**).

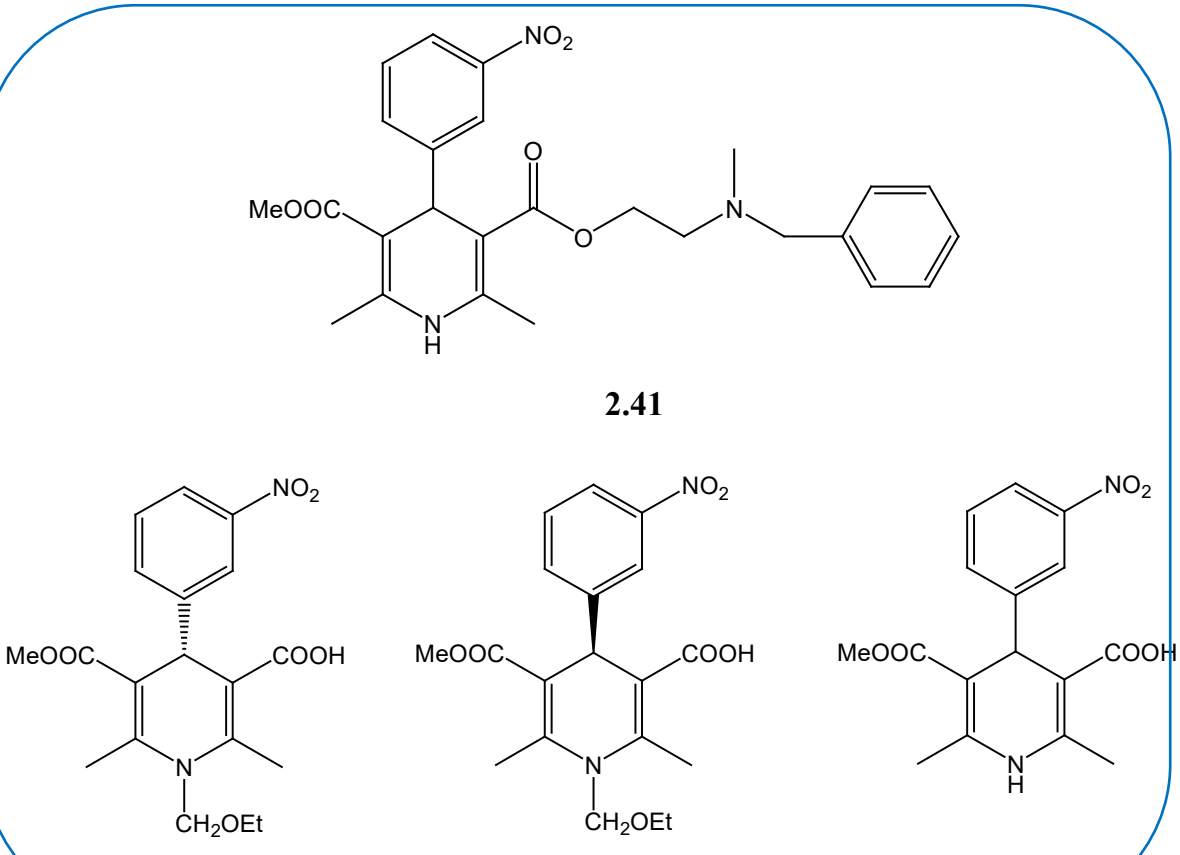


The resolution of **2.42** was achieved by treating it with **CIND** and **CINC** in MeOH. The enantiopure (-)-**2.42** was obtained from the **CIND** salt, and (+)-**2.42** was obtained from the

**CINC** salt. On treating (-)-**2.42** with 1N HCl, (-)-5-methoxycarbonyl-2,6-dimethyl-4-(3-nitrophenyl)-1,4-dihydropyridine-3-carboxylic acid ((-)-**2.43**) was achieved.[99] The resolution of **2.42** occurred with the NH position protected. The formation of an enantiopure **2.43** was achieved by the removal of the NH-protecting group. Zhang *et al*.[100] resolved the unprotected **2.43** using **CIND** and **QUID**. In their resolution the solvent played a significant role and that was shown by the inefficiency of the resolution and the poor ee value (entries 1 and 2 in Table 2.4). Changing of the solvent and the addition of water to the solvent improved the crystallization of **2.43**, in one aspect the yield was low (entry 3). The solvents used were EtOH, Acetone, DMF, and a mixture of DMF with water in different ratios. The outcomes of their resolutions are tabled below (Table 2.4).

Table 2.4 The resolution results of **2.43**.[100]

| Entry | RA | Solvent | Yield/% | Ee/% | AC |
|---|---|---|---|---|---|
| 1 | **CIND** | EtOH | 52 | 63.4 | *S*-**2.43** |
| 2 | **CIND** | Acetone | 49 | 72.1 | *S*-**2.43** |
| 3 | **CIND** | DMF | 26 | 99.3 | *S*-**2.43** |
| 4 | **CIND** | DMF-$H_2O$ (8:2) | 32 | 99.5 | *S*-**2.43** |
| 5 | **CIND** | DMF-$H_2O$ (8:5) | 41 | >99.5 | *S*-**2.43** |
| 6 | **CIND** | DMF-$H_2O$ (8:8) | 44 | 97.8 | *S*-**2.43** |
| 7 | **CIND** | DMF-$H_2O$ (8:11) | 46 | 95.0 | *S*-**2.43** |
| 8 | **QUID** | DMF-$H_2O$ (8:5) | 43 | >99.5 | *R*-**2.43** |
| 9 | **QUID** | DMF-$H_2O$ (8:8) | 46 | 96.6 | *R*-**2.43** |

In earlier investigations it was established that the absolute configurations and optical rotation signs at position 4 of **2.43** were (*S*)-(+)-**2.43** and (*R*)-(-)-**2.43**.[99,101,102] **CIND** selected the (*S*)-**2.43** enantiomer in all the different solvents and **QUID** selected the (*R*)-**2.43** enantiomer in both solvent mixtures.

Shibanuma *et al*. showed that **CIND** isolated (*R*)-**2.42**, whereas Zhang *et al*. found that **CIND** isolated (*S*)-**2.43**. The **CIND** absolute configuration is (*R*)- in C9 and in the two resolutions it isolated two different enantiomers. The differences in the two results are the substituent at the N atom in **2.42** compared to **2.43**, and the different solvents used in the resolution, MeOH in the resolution of **2.42** and the four solvents in the resolution of **2.43** (Table 2.4).

The results demonstrate the importance of the type of solvent employed in the resolution, which affected the enantiomeric excess percentage. The absolute configuration of the resolving agent also played a role in the selection of the enantiomer from the racemate. In this study the resultant

enantiomers had an absolute configuration opposite to that of the resolving agents irrespective of the solvents used.[100]

## 2.10. Modified resolving agents

The modified resolving agents play a major role in resolution, some give enantiomeric discrimination whereas others lessened enantiomeric discrimination, as highlighted in Chapter 4, regarding factors playing a role in the mechanism of enantiomeric resolution.

The *pseudo*-enantiomeric pairs, **CINC/CIND** and **QUIN/QUID** and their derivatives have shown high potential as chiral directing molecules in a broad range of asymmetric chemical reactions, including hydrogenation,[103] the addition of dialkyl zinc species to aldehydes,[104] and the dihydroxylation of alkenes.[105] These compounds have also been used as catalysts in enantioselective synthesis.

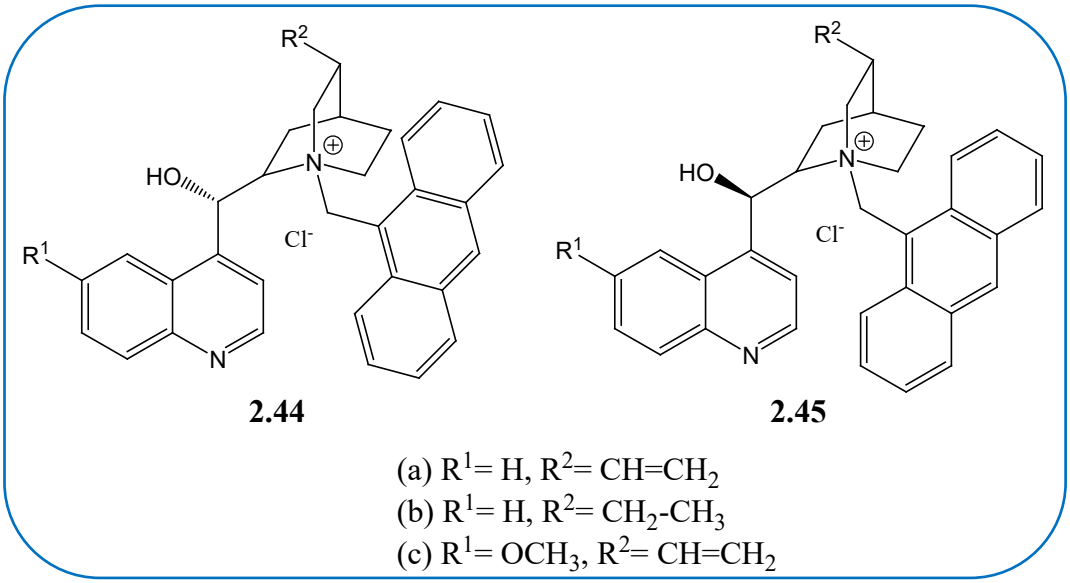


The efficiency of the alkaloid constituent on the reaction selectivity was investigated using catalysts that were derived from the following *Cinchona* alkaloids: cinchonine (**2.44a**), cinchonidine (**2.45a**), dihydrocinchonine (**2.44b**), dihydrocinchonidine (**2.45b**), quinidine (**2.44c**) and quinine (**2.45c**).[106]

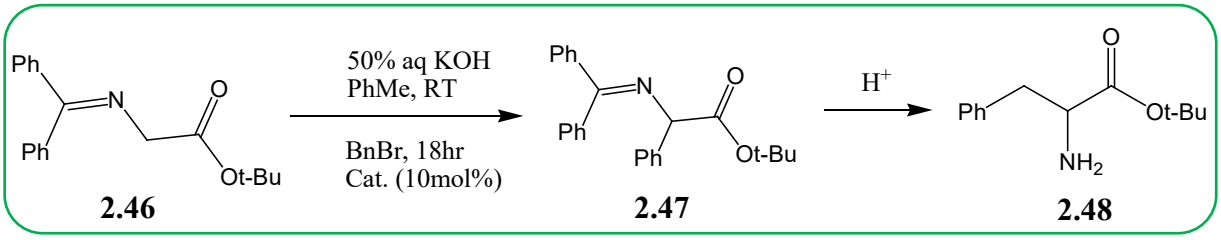


Scheme 2.3 The general reaction pathway in the alkylation of **2.46** to produce **2.48**.[106]

The results of the asymmetric phase transfer alkylation reaction of imine (**2.46**) to the product **2.48** are shown in Scheme 2.3 and in Table 2.5.

Table 2.5 Results for the alkylation of **2.46** to **2.48**.[106]

| Cat. | % ee of **2.50** (major isomer) | Overall yield of **2.52** |
|---|---|---|
| **2.44a** | 89 (*R*) | 63% |
| **2.44b** | 86 (*R*) | 77% |
| **2.44c** | 78 (*R*) | 56% |
| **2.45a** | 91 (*S*) | 68% |
| **2.45b** | 94 (*S*) | 85% |
| **2.45c** | 83 (*S*) | 58% |

As anticipated, the *pseudo*-enantiomeric pairs **2.44** and **2.45** gave relatively similar results, which were of opposite enantioselectivity, in the alkylation reaction of **2.46**. The catalysts **2.44c** and **2.45c** were the least effective, and they gave rise to lower selectivity and very low overall yields. The catalyst **2.45b** gave the best selectivity of 94% ee, higher than the catalyst it was derived from, **2.45a**, which had a selectivity of 91% ee.[106] Subsequently, success was also achieved in the development of another class of asymmetric phase-transfer catalysts that showed high enantioselectivity in the preparation of amino acids.

In another study the *Cinchona* alkaloids were employed in the enantioselective synthesis of the two enantiomeric isomers of methyl dihydrojasmonate (**2.49**). This compound was obtained by treating pentyl enone (**2.50)** with dimethyl malonate additional to a base at -20 °C. The product of the reaction, **2.51,** was then demethoxycarbonylated to give rise to **2.49,** as shown in the reaction pathway, Scheme 2.4.[107]

The catalysts that were employed were, **2.45a**, **2.52**, **2.44c**, **2.45c**, and **2.53**, and the results are tabulated in Table 2.6.

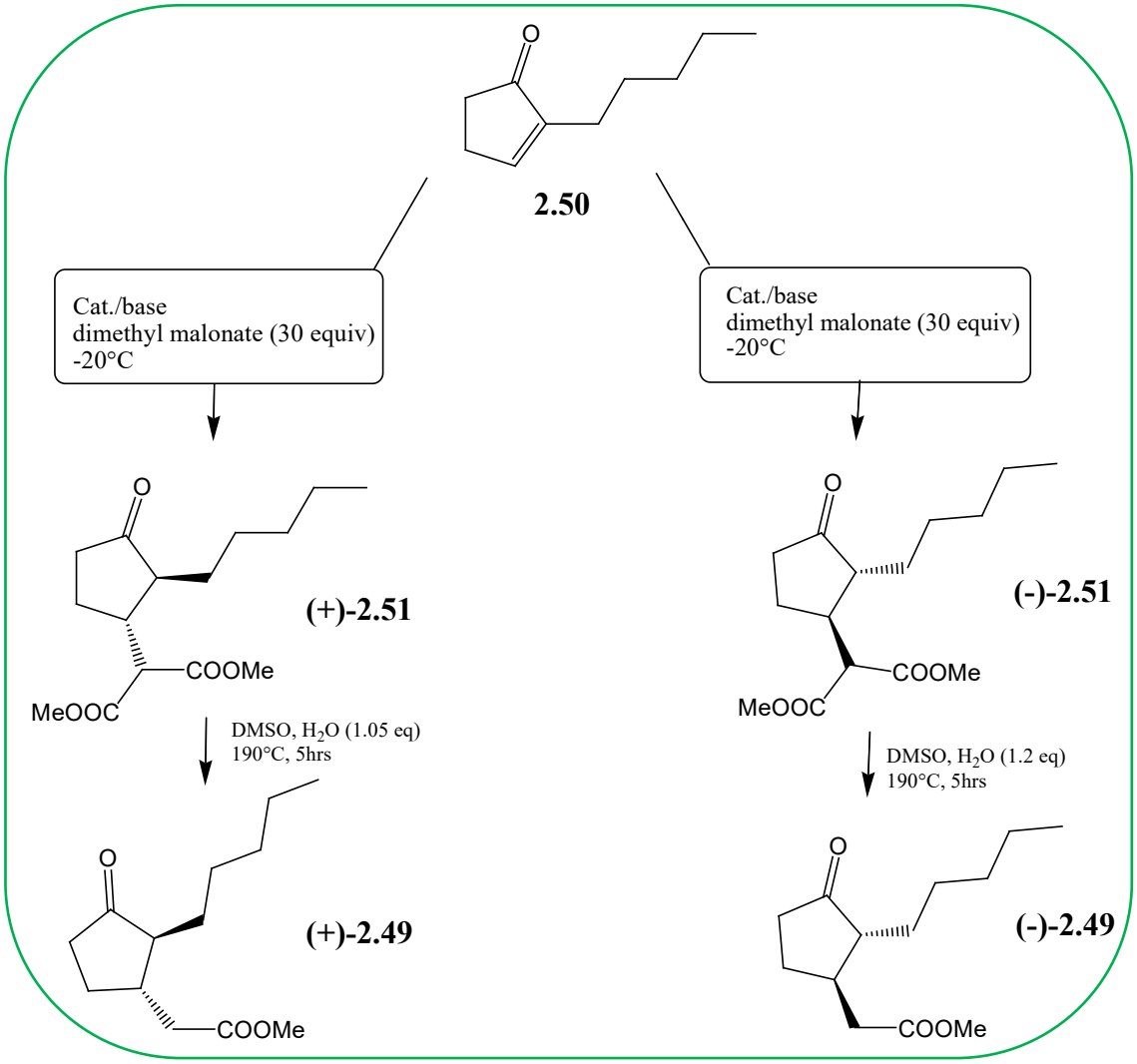


Scheme 2.4 The formation of the enantiomers of **2.49** from **2.50**.[107]

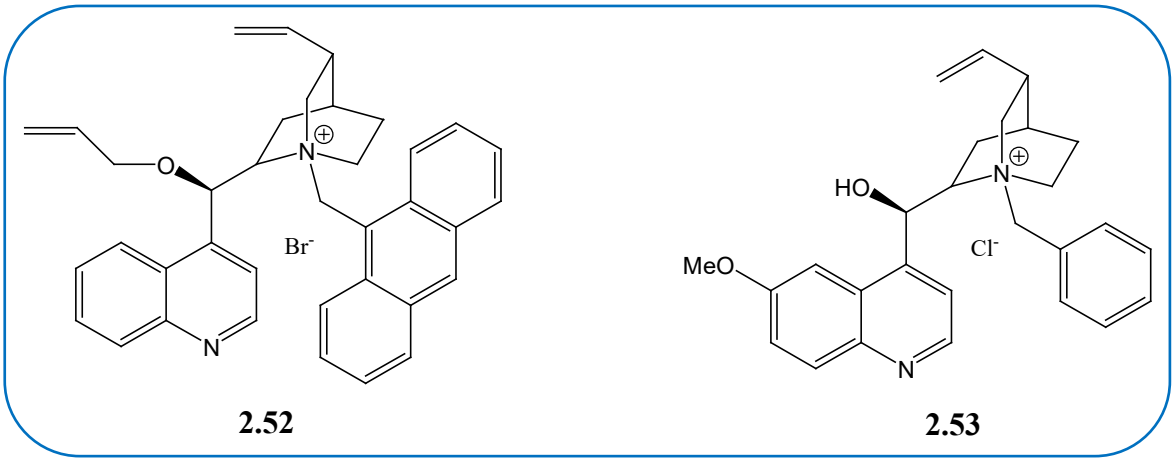

Table 2.6 Results of the formation of **2.51** from **2.50**.[107]

| Entry | Cat(equiv) | (+)-**2.51** ee (yield, [a] %) | (-)-**2.51** ee (yield, [a] %) |
|---|---|---|---|
| 1 | **2.45a** | 54 (75) | |
| 2 | **2.52** | No reaction | |
| 3 | **2.44c** | | 80 (60) |
| 4 | **2.45c** | 90 (91) | |
| 5 | **2.53** | 67 (21) | |
| [a] ee was established by NMR in the presence of $Pr(hfc)_3$ and confirmation was by chiral HPLC. The absolute configuration of stereogenic centres was established by chemical correlation after non racemic demethoxycarbonylation and the resultant yields quoted after purification by flash-chromatography. | | | |

The results demonstrated that the benzyl group in **2.53** was less effective than the N-9-methylanthracenyl group and that **2.45a** was less selective than the quinine derivative, **2.45c**. The *pseudo*-enantiomeric effect was noted with the N-alkylated **QUID** catalyst **2.44c** in the chemical reaction, in comparison to the stereoselectivity of the N-alkylated **QUIN** catalyst **2.45c**, the yield and the ee were less. In catalyst **2.52** the protection of the oxygen atom with an allyl group, gave rise to no reaction. The result led them to believe that a free OH group on the alkaloid was directly responsible for the reactivity of the catalytic moiety.[107]

In the demethoxycarbonylation step there was no racemization noted, and chemical correlation granted the assignment of the absolute configuration of the stereogenic centres of the enantiomers (+)-**2.51** and (-)-**2.51**. The solid-liquid asymmetric phase-transfer catalytic chemical reaction constituted another and effective method for access to the two enantiomers of compound **2.49,** Scheme 2.4.[107]

In 1998 Corey *et al*. employed the catalyst derived from cinchoninidine, **2.52**, in the synthesis of α-alkylated glycines by the reaction below, Scheme 2.5.

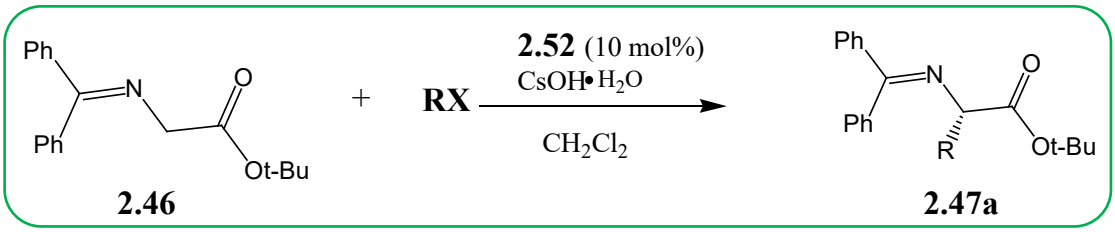


Scheme 2.5 The general reaction pathway in the formation of **2.47a** from **2.46.**[108]

The enantioselection from the above reactions was between 400:1 and 60:1 for the following halides, *n*-alkyl, cyclopropylcarbinyl, allyl, benzyl, propargyl, and aromatics. The enantioselective preparation of a wide range of α-amino acid derivatives was then possible and practical through the employment of the chiral phase transfer catalyst **2.52**.[108]

Arai *et al*. have explored the cinchonine and quinidine derivatives in the catalytic asymmetric epoxidation of enones. In experimentation on the effect of solvent and the phase transfer catalysts (PTC), **2.56** – **2.60,** they treated 2-methylnaphthoquinone (**2.54**) with the catalysts to obtain the desired epoxide **2.55,** Scheme 2.6.[109]

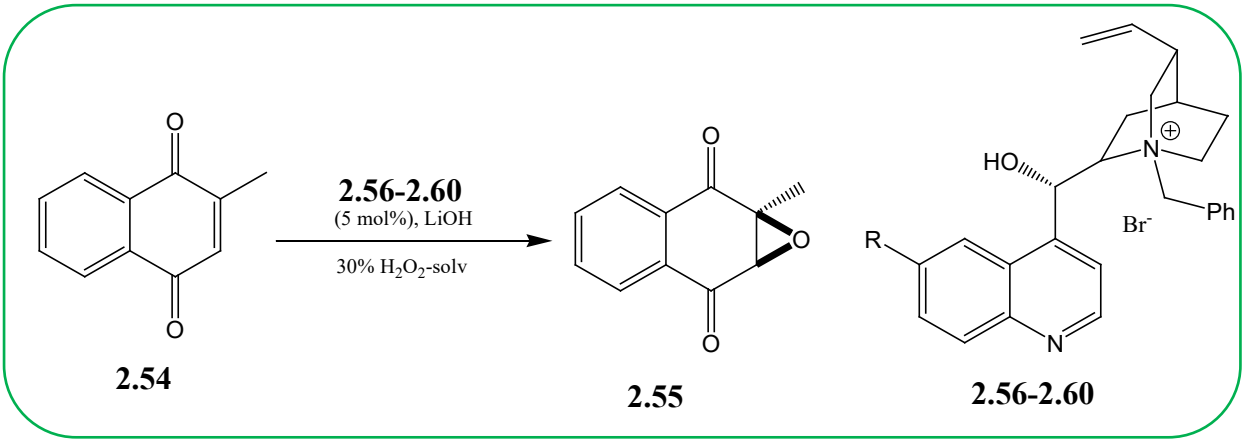


Scheme 2.6 Epoxide formation from **2.54** using different solvents and catalysts.[109]

Table 2.7 Effect of solvent and the PTC.[109]

| | Cat | R | Solvent | Temp | Time (hr) | Yield (%) | Ee (%) |
|---|---|---|---|---|---|---|---|
| 1 | **2.56** Ph = 4-I-$C_6H_4$ | H | *n*-$Bu_2O$ | Rt | 1 | 72 | 1 |
| 2 | **2.56** Ph = 4-I-$C_6H_4$ | H | Toluene | Rt | 4 | 72 | 4 |
| 3 | **2.56** Ph = 4-I-$C_6H_4$ | H | $CHCl_3$ | Rt | 1 | 94 | 10 |
| 4 | **2.57** Ph = 4-$CF_3$- $C_6H_4$ | H | $CHCl_3$ | Rt | 4 | 76 | 11 |
| 5 | **2.58** Ph = 2,4-$Me_2$- $C_6H_3$ | OMe | $CHCl_3$ | Rt | 1 | 93 | 26 |
| 6 | **2.59** Ph = α-naphthyl | OMe | $CHCl_3$ | Rt | 1 | 82 | 31 |
| 7 | **2.60** Ph = 9-anthracenyl | OMe | $CHCl_3$ | Rt | 1 | 91 | 28 |
| 8 | **2.59** Ph = α-naphthyl | OMe | $CHCl_3$ | -10 | 1 | 86 | 34 |

The reaction results (Table 2.7) gave rise to the desired epoxide in high yields in all the solvents, but the enantioselectivities were lower. The catalysts gave rise to better results, and the catalysts **2.58**, **2.59** and **2.60** were better in the epoxidation that produced **2.55** with approximately 30% ee. The reaction that was at very low temperatures, entry 8, gave rise to the best results.[109] The overall results exhibited the efficient asymmetric epoxidation of enones by employing the chiral quaternary salts derived from cinchonine and quinidine.

A lot of work was performed by Berkessel *et al*. on the epoxidation of **2.54**, employing the *Cinchona* alkaloids' derivatives, modified at carbon 9, at the quinuclidinic N atom, and at the position 19 of the quinoline ring, using different oxidants, and reaction conditions.[110] The employment of the oxidant, aqueous sodium hypochlorite, catalyst **2.61** that contained an OH group at carbon 19 of the quinoline ring and the hydrogenated vinyl group, resulted in an improved enantioselectivity by up to 85% ee, and the yield was 73%. The resultant epoxide was (2*R*,3*S*)-**2.55**, at a catalyst loading of about 2.5 mol% which happened to be the best enantioselectivity that was reported at that time.[110]

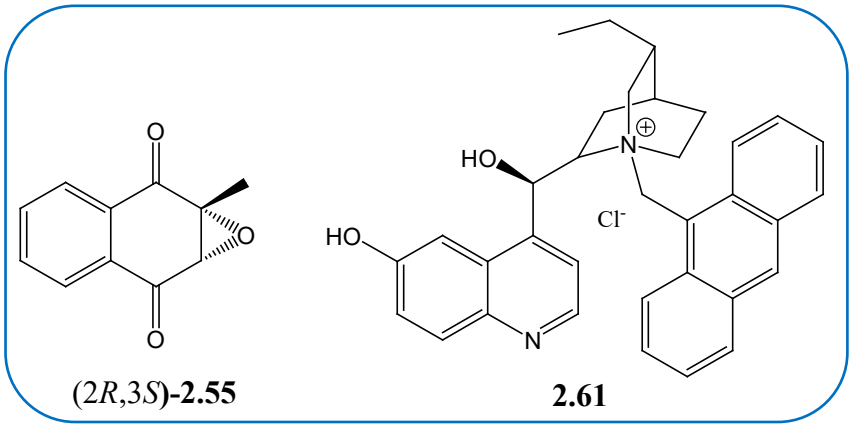


(2*R*,3*S*)**-2.55** **2.61**

The results of the asymmetric synthesis reactions shed some light on what to expect in the resolutions carried out in the research and the mechanism of enantiomeric resolution.

## 2.11. Conclusion

A summary of the chiral resolution studies involving the *Cinchona* alkaloids discussed in this chapter is given below in Tables 2.8-2.12.

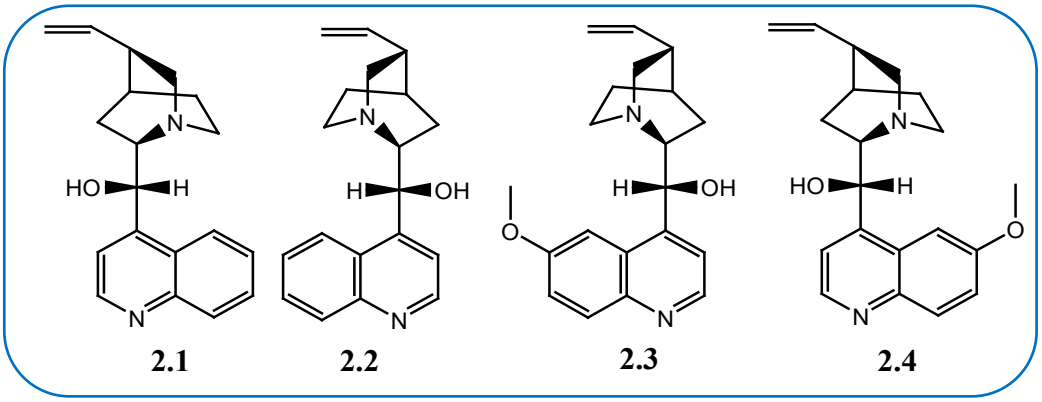


**2.1** **2.2** **2.3** **2.4**

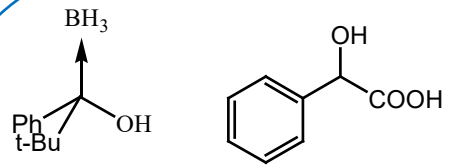


**2.5**




**2.9**

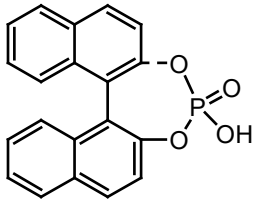


**2.10**

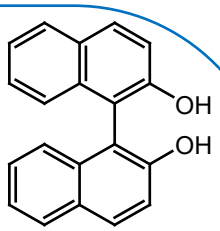


**2.11**

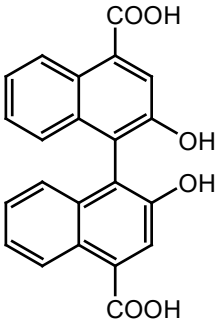


**2.16**

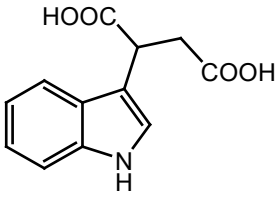


**2.23**

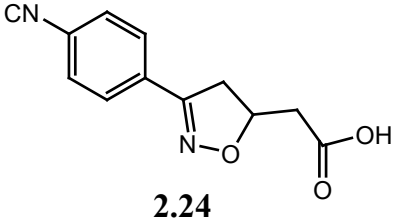


**2.24**

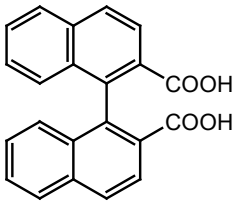


**BNDA**

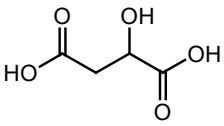


**2.27**

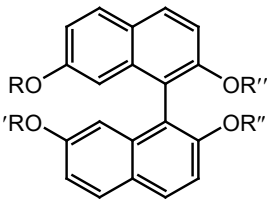


**2.30**

**2.30** **R** **R′** **R′′**
a PhCH2 PhCH2 H
d H PhCH2 CH3

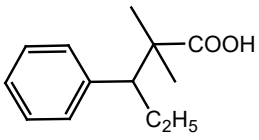


**DMPPA**

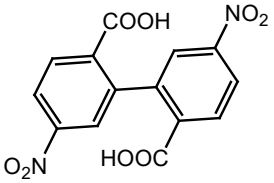


**2.35**

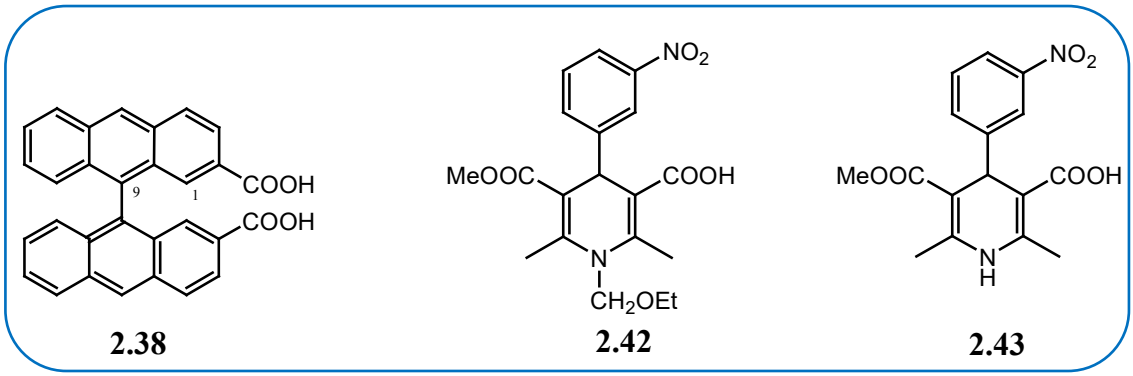


**2.38** **2.42** **2.43**

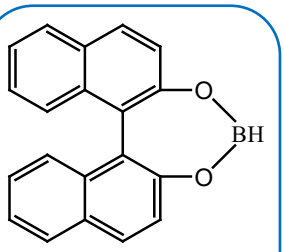


**2.10a**

Table 2.8 The resolution results of **CINC**.

| Entry | Solvent | Compound | AC | Solvate | Yield (%) | S | Ref |
|---|---|---|---|---|---|---|---|
| 1 | MeOH | **2.5** | (*R*) | - | 32 | - | 27 |
| 2 | $H_2O$ | **2.9** | (*S*) | - | - | - | 29 |
| 3 | $H_2O$ | **2.9** | (*S*) | $H_2O$ | 100 | 0.28 | 30 |
| 4 | $H_2O$:EtOH (4:1) | **2.9** | (*S*) | $H_2O$ | 55 | 0.07 | 30 |
| 5 | $H_2O$:EtOH (2:1) | **2.9** | (*R*) | - | 88 | 0.08 | 30 |
| 6 | EtOAc ($H_2O$ free) | **2.9** | (*R*) | EtOAc | 82 | 0.30 | 30 |
| 7 | EtOAc ($H_2O$ saturated) | **2.9** | (*R*) | EtOAc | 73 | 0.45 | 30 |
| 8 | MeOH | **2.10** | (*S*) | - | 56 | - | 33 |
| 9 | Toluene | **2.11** *via* **2.10a** | (*R*) | - | 70 | - | 41(a) |
| 10 | MeOH | **2.42** | (*S*) | - | - | - | 99 |

Table 2.9 The resolution results of **CIND**.

| Entry | Solvent | Compound | AC | Solvate | Yield (%) | S | Ref |
|---|---|---|---|---|---|---|---|
| 1 | MeOH | **2.16** | (*R*) | MeOH | - | - | 44 |
| 2 | Acetone | **2.24** | (*S*) | Acetone | 29 | - | 56 |
| 3 | EtOH | **2.23** | (*S*) | - | 13.1 | - | 55 |
| 4 | DMF:$H_2O$ (8:8) | **2.43** | (*S*) | - | 44 | - | 100 |
| 5 | MeOH | **2.42** | (*R*) | - | - | - | 99 |

Table 2.10 The resolution results of **QUIN**.

| Entry | Solvent | Compound | AC | Solvate | Yield (%) | S | Ref |
|---|---|---|---|---|---|---|---|
| 1 | THF | **2.11** *via* **2.10a** | (*S*) | - | 80 | - | 41(b) |
| 2 | $H_2O$ | **BNDA** | (*S*) | $2H_2O$ | - | - | 65 |
| 3 | $H_2O$ | **2.27** | (*D*) | $2H_2O$ | - | - | 69 |
| 4 | EtOH | **2.30a** | (*R*) | - | 76 | - | 51 |
| 5 | EtOH | **2.30d** | (*R*) | - | - | - | 51 |
| 6 | EtOH | **DMPPA** | (+) | - | - | - | 71 |
| 7 | EtOH:$H_2O$ | **DMPPA** | (-) | - | - | - | 71 |
| 8 | Ether/Chloroform | **2.35** | (*S*) | $H_2O$ | - | - | 81 |

Table 2.11 The resolution results of **QUID**.

| Entry | Solvent | Compound | AC | Solvate | Yield (%) | S | Ref |
|---|---|---|---|---|---|---|---|
| 1 | Acetonitrile | **2.35** | (*R*) | MeCN | - | - | 80 |
| 2 | Acetone | **2.38** | *M* | - | - | - | 85 |
| 3 | DMF:$H_2O$ (8:8) | **2.43** | (*R*) | - | 46 | - | 100 |

In the above tables, AC = absolute configuration, S = resolution efficiency, and Ref = references.

Table 2.12 The resolution results of a racemate using different resolving agents.

| Entry | RA | Solvent | Racemate | AC | Ref |
|---|---|---|---|---|---|
| 1 | **CINC** | MeOH | **2.10** | (*S*) | 33 |
| 2 | **CIND** | MeOH | **2.10** | (*R*) | 33 |
| 3 | **CINC** | Toluene | **2.11** *via* **2.10a** | (*R*) | 41(a) |
| 4 | **QUIN** | THF | **2.11** *via* **2.10a** | (*S*) | 41(b) |
| 5 | **QUID** | Acetonitrilre | **2.35** | (*R*) | 80 |
| 6 | **QUIN** | Ether/Chloroform | **2.35** | (*S*) | 81 |
| 7 | **CINC** | MeOH | **2.42** | (*S*) | 99 |
| 8 | **CIND** | MeOH | **2.42** | (*R*) | 99 |
| 9 | **CIND** | DMF:$H_2O$ (8:8) | **2.43** | (*S*) | 100 |
| 10 | **QUID** | DMF:$H_2O$ (8:8) | **2.43** | (*R*) | 100 |

RA = resolving agent, AC = absolute configuration, Ref = references.

The results show that the most important site for the formation of a hydrogen bond in the resolving agents is the quinuclidine N atom and the OH group, where the quinuclidine joins the quinoline ring. Tables 2.7-2.10 show the resolution results of the four resolving agents. All the resolving agents have the ability to select the (*S*)- or (*R*)-enantiomers for the different racemates, in different types of solvents. Some of the structures are solvated, others are unsolvated.

There was no correlation between the length and structure of the racemates and the resolving agents. In order to achieve good resolution results, one of the aspects to consider is the resolving agent. It has been reported that a high quality resolution is produced by using a resolving agent that is structurally related to the molecule to be resolved.[111] Sakai *et al*. reported that the best quality resolution can be achieved by employing a resolving agent and the molecule to be resolved with the same molecular length, the authors defined molecular length as the distance from the α atom to the end of the molecule.[112] Szeleczky *et al*.[113] examined the role played by the molecular lengths of the resolving agent and the molecule to be resolved in 49 individual resolutions. Their results revealed that a higher enantiomeric purity is possible by employing resolving agents and molecules to be resolved with a molecular length difference of 4 – 6 carbon atoms, compared to results where the reactants are of the same length. Regarding resolvability, molecular length differences of 3 - 6 showed more resolving ability compared to reactants of the same length.

It was concluded that the absolute length difference offered the best resolutions. The recommended molecule length difference is zero or 3-6.[113]

It has been reported that a solvate contributes to the stability of the diastereomeric salt formed in resolution. The above results show the presence (38%) and the absence of solvates in the resolutions. The solvents also dictated the outcome of the absolute configurations in some of the resolutions.

Absolute configuration of the resultant enantiomers has been reported to rely on the absolute configuration of the resolving agent. Generally, an (*R*-) or (*S*)-resolving agent isolates the (*R*-) or (*S)*-enantiomer. In the above results, about 50% followed the trend. The most noticeable effect of the solvent was the change in the configuration of the enantiomer when a different solvent was used for the same reaction. Table 2.7, entries 2-7, the stereochemistry of **2.9** changed on using a different solvent with the same resolving agent. Table 2.9, entries 4 and 5 show the resolution of **2.30a** and **2.30d**, with the same structural framework, using the same resolving agent **QUIN** in the same solvent, and the selected enantiomers are of the same absolute configuration, (*R*)-**2.30a** and (*R*)-**2.30d**. In entries 6 and 7, the change in solvent from EtOH to EtOH:$H_2O$ changed the absolute configuration using **QUIN**, from (+)-**DMPPA** to (-)-**DMPPA**, respectively. It has been shown that the dielectric constant of solvents also play a role in resolution as described in Chapter 4.

The modified resolving agents showed an improvement in resolution of compounds that were not resolved by their counterparts and were also used as catalysts in some chemical reactions to generate enantiopure compounds.

The molecular length of the reactants seems not to have played a role in these *Cinchona* alkaloid resolutions. Hydrogen bond formation occurred at the quinuclidine N atom and at the hydroxyl O atom. The absolute configuration of the resolving agent together with the chosen solvent contributed towards the selection of an enantiomer. Modification of these resolving agents at the quinuclidine N atom and at the hydroxyl O atoms enhanced the resolving ability of these agents, in some cases. This also depends on the type of substituent at these positions.

In 2002 the list of acidic compounds resolved by the four resolving agents was published, ie compounds resolved prior to 2002. It was reported that **CINC** resolved 95 racemates, **CIND** 233, **QUIN** 352, and **QUID** 35.[114] From the reported database, **QUID** resolved less or was the least capable of resolving racemates, compared to the others, and **QUIN** resolved more than the other agents. Comparing this report with the number of hits containing these resolving agents in the current CSD (**CINC** = 50, **CIND** = 64, **QUIN** = 85, and **QUID** = 41, salts, clathrates or inclusion compounds) shows that not all the structural results have been deposited in the CSD or are available. The common solvents used in the resolutions were: MeOH, EtOH, EtOAc, $H_2O$ and acetone. Solvent mixtures were also used with the most commonly used combinations: EtOH: $H_2O$, acetone:$H_2O$, MeOH:EtOAc and acetone:trichloroethane, in several ratios per combination. Other solvents that were used but to a lesser extent were: trichloromethane, benzene, isopropanol, petroleum ether, diethyl ether, carbon tetrachloride, hexane, acetonitrile and methyl ethyl ketone.[114]

## 2.12. References


1. British Pharmacopoeia 2012 (Ph. Eur. Monograph 0174) http://www.pharmacopoeia 2012.co.uk
2. Bruce-Chwatt LJ. Three hundred and fifty years of the Peruvian bark. *BMJ*, **1988**, 296, 1486-1487.
3. Stork G, Niu D, Fujimoto A, Koft ER, Balkovec JM, Tata JR and Dake GR. The first stereoselective total synthesis of quinine. *J. Am. Chem. Soc*., **2001**, 123, 3239-3242.
4. Carroll A-M, Kavanagh DJ, McGovern FP, Reilly JW and Walsh JJ. Nature's chiral catalyst and anti-malarial agent: Isolation and structure elucidation of cinchonine and quinine from *Cinchona calisaya*. *J. Chem. Educ*., **2012**, 89, 1578-1581.
5. Kaufman T and Rúveda EA. The quest for quinine: Those who won the battle and those who won the war. *Angew. Chem. Int. Ed*., **2005**, 44, 854-885.
6. Raheem IT, Goodman SN and Jacobsen EN. Catalytic asymmetric total synthesis of quinine and quinidine. *J. Am. Chem. Soc*., **2004**, 126, 706-707.
7. Gjerlov A and Larsen S. A study of diastereomeric mandelate salts of cinchonidine and the relation to their quasidiastereomeric analogues. *Acta Cryst*., **1997**, B53, 708-718.
8. Caner H, Biedermann PU and Agranat I. Conformational spaces of *Cinchona* Alkaloids. *Chirality*, **2003**, 15, 637-645.
9. Eliel EL, Wilen SH, and Mander LN. *Stereochemistry of Organic Compounds*. New York, John Wiley and Sons, **1994**, 866.
10. Aune M, Googall A and Matsson O. Solvent dependence of enantioselectivity for a base catalysed 1,3-hydrogen transfer-reaction- a kinetic isotope effect and NMR spectroscopic study. *J. Org. Chem*., **1995**, 60, 1356-1364.
11. Kauffma GB and Myers RD. The resolution of racemic acid. A classic stereochemical experiment for the undergraduate laboratory. *J. Chem. Ed.*, **1975**, 52, 777-781.
12. Dijkstra GH, Kellogg RM and Wynberg H. Conformational study of *Cinchona* alkaloids. A combined NMR and molecular orbital approach. *J. Org. Chem*., **1990**, 55, 6121-6131.
13. Jacques J, Collet A and Wilen SH. *Enantiomers, Racemates and Resolutions*. **1981**, John Wiley and Sons, Inc., New York, 254-257.
14. Wynberg H. Asymmetric catalysis by alkaloids. *Top. Stereochem*., **1986**, 16, 87-129.

15. Kolb HC, Van Nieuwenhze MS and Sharpless KB. Catalytic asymmetric dihydroxylation. *Chem. Rev*., **1994**, 94, 2483-2547.
16. Dijkstra GDH, Kellogg RM and Wynberg H, Svendsen JS, Marko I and Sharpless KB. Conformational study of *Cinchona* alkaloids, a combined NMR, molecular mechanics and X-ray approach. *J. Am. Chem. Soc*., **1989**, 111, 8069-8076.
17. Berrisford DJ, Bolm C and Sharpless KB. Ligand accelerated catalysis. *Angew. Chem. Int*. *Ed*., **1995**, 37, 487-487.
18. Hashimoto T and Maruoka K. Recent development and application of chiral phase-transfer catalysts. *Chem. Rev*., **2007**, 107, 5656-5682.
19. Doyle AG and Jacobsen EN. Small molecule H-bond donors in asymmetric catalysis. *Chem. Rev*., **2007**, 107, 5713-5743.
20. Mukherjee S, Yang JW, Hoffmann S and List B. Asymmetric enamine catalysis. *Chem. Rev*., **2007**, 107, 5471-5569.
21. Erkkilä A, Majander I and Pihko PM. Iminiumcatalysis. *Chem. Rev*., **2007,** 107, 5416-5470.
22. Oleksyn BJ and Serda P. Salt-bridge formation by *Cinchona* alkaloids: quininium salicylate monohydrate. *Acta Cryst*., **1993**, B49, 530-534.
23. Karle JM and Karle IL. Structure of 9-epiquinine hydrochloride dihydrate *versus* antimalarial activity. *Acta Cryst*., **1992**, C48, 1975-1980.
24. Lagasse F and Kagan HB. Chiral monophosphines as ligands for asymmetric organometallic catalysis. *Chem. Pharm. Bull*., **2000**, 48, 315-324.
25. Chen W, Mbafor W, Roberts SM and Whitehall J. A very simple, highly stereoselective and modular synthesis of ferrocene-based P-chiral phosphine ligands. *J. Am. Chem. Soc*., **2006**, 128, 3922-3923.
26. Imamoto T, Itoh T, Yamanoi Y, Narui I and Yoshida K. Highly enantioselective hydrosilylation of simple ketones catalysed by Rhodium complexes of P-chiral diphosphine ligands bearing *tert*-butylmethylphosphino groups. *Tertahedron: Asymmetry*, **2006**, 17, 560-565.
27. Stankevic M and Pietrusiewicz M. Resolution and stereochemistry of *tert*-butylphenylphosphinous acid-borane. *J. Org. Chem*., **2007**, 72, 816-822.
28. Mauger C, Masson S, Vazeux M, Saint-Clair J-F, Midura WH, Drabowicz J and Mikolajczyk M. Synthesis, characterization and resolution of racemic (2-methylsulfinyl)phenylphosphonic acid methyl ester *via* its cinchoninium salts. *Tetrahedron: Asymmetry*, **2001**, 12, 167-174.

29. Larsen S, de Diego HL and Kozma D. Optical resolution through diastereomeric salt formation: the crystal structures of cinchoninium (*S*)-mandelate and cinchoninium (*S*)-mandelate at low temperature. *Acta Cryst*., **1993**, B49, 310-316.
30. Kozma D, Nyéki Á, Ács M and Fogassy E. Optical resolution of mandelic acid by cinchonine in different solvents. *Tetrahedron: Asymmetry*, **1994**, 5, 315-316.
31. Imhof R, Kyburz E, and Daly JJ. Design, synthesis and X-ray data of novel potential antipsychotic agents. Substituted 7-phenylquinolizidines: stereospecific neuroleptic and antinociceptive properties. *J. Med. Chem.,* **1984**, 27, 165-175.
32. Garnier-Suillerot A, Albertini JP, Collet A, Faury L, Pastor JM and Tosi L. Spectrophotometric studies of the copper(II)-D-*o*-tyrosine complex. Assignment of the 330-nm dichroic band in copper (II) and iron (III) transferrins. *J. Chem. Soc. Dalton Trans.,* **1981**, 2544-2549.
33. Jacques J, Fouquey C and Viterbo R. Enantiomeric cyclic binaphthyl phosphoric acids as resolving agents. *Tetrahedron Letters,* **1971**, 48, 4617-4620.
34. Kyba EP, Gokel GW, de Jong F, Koga K, Sousa LR, Siegel MG, Kaplan L, Sogah GDY and Cram DJ. Host-guest complexation. 7. The binaphthyl structural unit in host compounds. *J. Org. Chem.,* **1977**, 42, 4173-4184.
35. Jacques J and Fouquey C. Enantiomeric (*S*)-(+)- and (*R*)-(-)-1,1'-Binaphthyl-2,2'-diylhydrogen phosphate. *Org. Synth.,* **1993**, 8, 50-55.
36. Pu L. 1,1'-Binaphthyl dimers, oligomers and polymers: Molecular recognition, asymmetric catalysis and new materials. *Chem. Rev*., **1998**, 98, 2405-2494.
37. Zhang M and Schuster GB. Chirochromism-photochromism by epimerisation: Search for a liquid crystal phototrigger. *J. Am. Chem. Soc*., **1994**, 116, 4852-4857.
38. Wang Y, Sun J and Ding K. Practical method and novel mechanism for optical resolution of BINOL by molecular complexation with *N*-benzylcinchoninium chloride. *Tetrahedron*, **2000**, 56, 4447-445.
39. Zhang H, Lin Z-Y, Zhou Z-H and Ng SW. *Bis*(cinchonidium) L-tartrate dihydrate. *Acta Cryst*., **2003**, E59, o183-o185.
40. Puliti R, Mattia CA, De Fazio A, Ghiara MR and Mazzarella L. Cinchoninium L-tatrate tetrahydrate. *Acta Cryst*., **2001**, C57, 1447-1449.
41. (a) Shan Z, Cheng F, Huang S, Zhao D and Jing Z. An improved approach to (*R*)-(+)-1,1'-bi-2-naphthol of 100% enantiomeric excess *via* a cyclic borate ester. *Tetrahedron: asymmetry*, **1997**, 8, 1175-1177. (b) Shan Z, Wang G, Duan B and Zhao D. Preparation of enantiomerically pure 1,1'-bi-2-naphthol *via* a cyclic borate ester. *Tetrahedron: asymmetry*, **1996**, 7, 2847-2850.

42. Tanaka K, Takanao H and Urbanczyk-Lipkowska ZJ. Novel host compounds 1,1'-binaphthyl-2,2'-dihydroxy-5,5'- and 6,6'-dicarboxylic acid, which trap guest molecules tightly in their inclusion crystals. *J. Inclusion. Phenom. Macr. Chem*., **2006**, 56, 281-285.
43. Imai Y, Murata K, Kamon K, Kinuta T, Sato T, Kuroda R and Matsubara Y. Formation and crystal structure of two-component host system having helical chirality and comprising 9,10-dihydro-9,10-ethanoanthracene-11,12-diamine 1,1'-binaphthyl-2,2'-dicarboxylic acid. *Cryst. Growth Des*., **2009**, 9, 602-605.
44. Tanaka K, Oda S, Nishihote S, Hiramaya D and Urbanczyk-Lipkowska Z. Efficient resolution of 2,2'-dihydroxy-1,1'-binaphthalene-4,4'- and 6,6'-dicarboxylic acid by complexation with cinchonine and brucine. *Tetrahedron: Asymmetry*, **2009**, 20, 2612-2615.
45. Báthori NB, Jacobs A, Mei MN and Nassimbeni LR. Resolution of (+/-)-Citronellic acid with (-)-Cinchonidine: The crystal structure of the cinchonidinium-(*S*)-citronellate diastereomeric salt. *J. Chem. Cryst*., **2013**, 43, 373-376.
46. Oh J, Bowling JJ, Carroll JF, Demirci B, Baser KHC, Leininger TD, Bernier UR and Haman MT. Natural product studies of US endangered plants: Volatile components of Lindera melissifolia (*Lauracae*) repel mosquitoes and ticks. *Phytochemistry*, **2012**, 80, 28-36
47. Martin A, Armbruster U, Decker D, Gedig T and Kockritz A. Oxidation of citronellal to citronellic acid by molecular oxidation using supported gold catalyst. *ChemSusChem*, **2008**, 1, 242-248.
48. (a) Cai D, Hughes DL, Verhoeven TR and Reider PJ. Simple and efficient resolution of 1,1'-bi-2-naphthol. *Tetrahedron Letters*, **1995**, 36, 7991-7994. (b) Oleksyn BJ. The alkaloid cinchonidine. *Acta Cryst*., **1982**, B38, 1832-1834.
49. Pirkle WH and Schreiner JL. Chiral HPLC (High Performance Liquid Chromatography) stationary phases. 4. Separation of the enantiomers of bi-beta. naphthols and analogs. *J. Org. Chem*., **1981**, 46, 4988-4991.
50. Tanaka K, Okada T and Toda F. Separation of the enantiomers of 2,2'-dihydroxy-1,1'-binaphthyl and 10,10'-dihydroxy-9,9'-biphenanthryl by complexation with N-alkylcinchonidinium halides. *Angew. Chem. Int. Ed. Engl*., **1993**, 32, 1147-1148.
51. Castro PP, Geogiadis TM and Diederich F. Chiral recognition in clefts and cyclophane cavities shaped by the 1,1'-binaphthyl major groove. *J. Org. Chem*., **1989**, 54, 5835-5838.

52. Zang J-H, Liao J, Cui X, Yu K-B, Zhu J, Deng J-G, Zhu S-F, Wang L-X, Zhou Q-L, Chung LW and Ye T. Highly efficient and practical resolution of 1,1'-spirobiindane-7,7'-diol by inclusion crystallization with *N*-benzylcinchonidinium chloride. *Tetrahedron: Asymmetry*, **2002**, 13, 1363-1366.
53. Noland W, Hammer CF. A new synthesis of indolesuccinic acid. *J. Org. Chem*., **1958**, 23, 320-322.
54. Noland W, Hammer CF. A novel rearrangement involving indole dimers. *J. Org. Chem*., **1960**, 25, 1536-1542.
55. Armstrong DW, Liu A-S, He L, Ekborg-Ott KH, Barnes CL and Hammer CF. Potent enantioselective auxin: Indole-3-succinic acid. *J. Agric. Food Chem*., **2002**, 50, 473-476.
56. Wityak J, Sielecki TM, Pinto DJ, Emmett G, Sze JY, Liu J, Ewa Tobin A, Wang S, Jiang B, Ma P, Mousa SA, Wexler RR and Olson RE. Discovery of potent glycoprotein IIb/IIIa receptor antagonists. *J. Med. Chem*., **1997**, 40, 50-60.
57. Lacour J, Ginglinger C, Grivet C and Bernadinelli G. Synthesis and resolution of the configurationally stable *tris*(tetra-chlorobenzenediolato)phosphate (V) ion. *Angew Chem. Int. Ed. Engl*., **1997**, 36, 608-610.
58. Craddock JH and Jones MM. The hydrolysis of octahedral complexes of Arsenic (V): The kinetics of hydrolysis of the octahedral complex. *J. Am. Chem. Soc*., **1961**, 83, 2839.
59. Applequist DE and Werner ND. The brominative decarboxylation of optically active Silver *trans*-1,2-cyclohexanedicarboxylate. *J. Org. Chem*., **1963**, 28, 48-54.
60. Tang D-H, Chen X-M and Fan Q-H. A convenient route to dendritic binaphthyl-containing chiral crown ethers. *J. Chem. Res*., **2004**, 10, 702-703.
61. Chen Y, Yekta S and Yudin AK. Modified BINOL ligands in asymmetric catalysis. *Chem. Rev*., **2003**, 103, 3155-3211.
62. Kanoh S, Hongoh Y, Motoi M and Suda H. Convenient optical resolution of axially chiral 1,1'-binaphthyl-2,2'-dicarboxylic acid. *Bull. Chem. Soc., Jpn*., **1988**, 61, 1032-1034.
63. Seki M, Yamada T, Kuroda T and Shimizu T. Practical synthesis of $C_2$-Symmetric chiral binaphthyl ketone catalyst. *Synthesis*, **2000**, 1677-1680.
64. Imai Y, Takeshita M, Sato T and Kuroda R. Successive optical resolution of two compounds by one enantiopure compound. *Chem. Commun*., **2006**, 10, 1070-1072.
65. Jacobs A, Nassimbeni LR, Sayed A and Weber E. Resolution of 1,1'-binaphthyl-2,2'-dicarboxylic acid with quinine: Structure of the intermediated (*S*)- 1,1'-binaphthyl-

2,2'-dicarboxylate dihydrate diastereomeric salt. *J. Chem. Crystallogr*., **2011**, 41, 854-857.

66. Turkington DE, Ferguson G, Lough AJ and Glidewell C. Supramolecular structures of three configurational isomers of 1-phenylethanaminiummalate(1-). *Acta Cryst*., **2004**, C60, o617-o622.
67. Báthori NB, Jacobs A, Nassimbeni LR and Sebogisi BK. Quininium malates: Partial discrimination *via* diastereomeric salt formation. *S. Afr. J. Chem*., **2014**, 67, 160-166.
68. Tochtermann W, Panitzsch T, Petroll M, Habeck T, Schlenger A, Wolff C, Peters E-M, Peters K and von Schnering HG. Selective reactions, resolution and absolute configuration of bridged hydroazulenes. *Eur. J. Org. Chem*., **1998**, 2651-2657.
69. Askew B, Ballester P, Buhr C, Jeong KS, Jones S, Parris K, and Rebek J Jr. Molecular recognition with convergent functional groups VI. Synthetic and structural studies with a model receptor for nucleic acid components. *J. Am. Chem. Soc.*, **1989**, 111, 1082-1090.
70. Kelly TR, Bilodeau MT, Bridger GJ and Zhao C. Receptors for uric acids. 2. A cautionary observation. *Tetrahedron Lett.,* **1989**, 30, 2485-2488.
71. Wilen SH, Collet A and Jacques J. Strategies in Optical Resolution. *Tetrahedron,* **1977**, 33, 2725-2736.
72. Bhushan R and Thiongo GT. Direct enantioseparation of some β-adrenergic blocking agents using impregnated thin layer chromatography. *J. Chrom. B*, **1998**, 708, 330-334.
73. Armstrong DW and Zhou Y. Use of a macrocyclic antibiotic as a chiral selector for enantiomeric separations by TLC. *J. Liquid Chrom.,* **1994**, 17, 1695-1707.
74. Bushan R and Martens J. Separation of amino acids, their derivatives and enantiomers by impregnated TLC. *Biomed. Chrom*., 2001, 15, 155-165.
75. Lepri L, Coas V, Desideri PG and Santianni D. Reversed phase planar chromatography of dansyl DL amino acids with bovine serum albumin in the mobile phase. *Chromatographi*a, **1993**, 36, 297-301.
76. Bhushan R and Ali I. TLC resolution of enantiomeric mixtures of amino acids. *Chromatographia*, **1987**, 23, 141-142.
77. Bhushan R and Arora M. Resolution of enantiomers of DL-amino acids on silica gel plates impregnated with optically pure (-)-quinine. *Biomed. Chrom*., **2001**, 15, 433-436.

78. Bhatt PM, Ravindra NV, Banerjee R and Desiraju GR. Saccharin as a salt former. Enhanced solubilities of saccharinates of active pharmaceutical ingredients. *Chem. Commun*., **2005**, 1073-1075.
79. Uccello-Barretta G, Balzano F, Quintavalli C and Salvadori P. Different enantioselective interaction pathways induced by derivatized quinines. *J. Org. Chem.,* **2000**, 65, 3596-3602.
80. Kubicki M, Borowiak T and Gawron M. Structure and molecular chirality of the acetonitrile adduct of the 2:1 salt of quinidine with biphenyl 5,5'-dinitro-2,2'-dicarboxylic acid (5,5'-dinitrophenic acid). *J. Cryst. Spectr. Res*., **1992**, 22, 205-211.
81. Kubicki M, Borowiak T, Gawron M, Giel M and Gawroński J. Structure and molecular chirality of the 2:1 salt of quinine with biphenyl 2,2'-dicarboxylic acid (diphenic acid). *J. Cryst. Spectr. Res*., **1990**, 20, 447-455.
82. Weber E, AhrendtJ, Czugler M and Csöregh I. Selective inclusion and separation of isomeric and homologous hydrocarbons by hydrocarbon host lattices. *Angew. Chem. Int. Ed. Engl.,* **1986**, 25, 746-748.
83. Toda F, Tanaka K and Fujiwara T. Isolation of conformational isomers of α- and β-lonones by inclusion complex formation. *Angew. Chem. Int. Ed. Engl*., **1990**, 29, 662-664.
84. Czarniecki S. optical activity of molecular dimers: Theoretical analysis of vibronic circular dichroism in model biaryls. *J. Mol. Struct*., **1978**, 47, 365-370.
85. Toyota S, Shimasaki T, Tanifuji N and Wakamutsu K. Experimental and theoretical investigation of absolute stereochemistry and chiroptical properties of enantiopure 2,2'-substituted 9,9'-bianthryls. *Tetrahedron: Asymmetry*, **2003**, 14, 1623-1629.
86. Barton DHR, Lacher B and Zard SZ. The invention of radical reactions: Part XVI. Radical decarboxylative bromination and iodination of aromatic compounds. *Tetrahedron*, **1987**, 43, 4321-4328.
87. Barton DHR and Ferreira J. N-hydroxypyridine-2(1H)-thione derivatives of carboxylic acids as activated esters. Part I. The synthesis of carboxamides. *Tetrahedron*, **1996**, 52, 9347-9366.
88. Uccello-Barretta G, Pini D, Rosini C and Salvadori P. Stereochemical features of the stereoselective interaction between (*R*)- or (*S*)-7,7'-*bis*(1-propen-3-oxy)-2,2'-dihydroxy-1,1"-binaphthyl and quinine. *J. Chromatogr., A*, **1994**, 666, 541-548.
89. Winter-Werner B, Diederich F and Gramlich V. Analogs of *Cinchona* alkaloids incorporating a 9,9'-spirobifluorene moiety. *Helv. Chim. Acta*, **1996**, 79, 1338-1360.

90. Bidlingmeyer BA. Separation of ionic compounds by reversed-phase liquid chromatography an update of ion-pairing techniques. *J. Chromatogr. Sci*., **1980**, 8, 525-539.

91. Izumoto S, Sakaguchi U and Yoneda H. Stereochemical aspects of the optical resolution of *cis*-(N)-$[Co(N)_2(O)_4]^-$ complexes by reversed-phase ion-pair chromatography with *Cinchona* alkaloid cations as the ion-pairing reagents. *Bull. Chem. Soc. Jpn*., **1983**, 56, 1646-1651.

92. Dyer UC, Henderson DA and Mitchell MB. Application of automation and thermal analysis to resolving agent selection. *Org. Process Res. Dev*., **1999**, 3, 161-165.

93. Borghese A, Libert V, Zhang T and Alt CA. Efficient fast screening methodology for optical resolution agents: Solvent effects are used to affect the efficiency of the resolution process. *Org. Process Res. Dev*., **2004**, 8, 532-534.

94. Ebber E, Ariaans A, Zwaneburg B and Bruggink A. Controlled design of resolution. Prediction of efficiency of resolution based on samples of arbitrary composition. *Tetrahedron: Asymmetry,* **1998**, 9, 2745-2753.

95. He Q, Rohani S, Zhu J and Gomaa H. Resolution of sertraline with (*R*)-mandelic acid: Chiral discrimination mechanism study. *Chirality,* **2012**, 24, 119-128.

96. Leusen FJJ. Crystal structure prediction of diastereomeric salts: a step toward rationalization of racemate resolution. *Cryst. Growth Des*., **2003**, 3, 189-192.

97. Karamertzanis PG and Price SL. Challenges of crystal structure prediction of diastereomeric salt pairs. *J. Phys. Chem. B,* **2005**, 109, 17134-17150.

98. Iwanami M, Shibanuma T, Fujimoto M, Kawai R, Tamazawa K, Takenaka T, Takahashi K and Murakami M. Synthesis of new water soluble dihydropyridine vasodilators. *Chem. Pharm. Bull*., **1979**, 27, 1426-1440.

99. Shibanuma T, Iwanani M, Okuda K, Takenaka T and Murakami M. Synthesis of optically active 2-(*N*-benzyl-*N*-methylamino)ethyl methyl 2,6-dimethyl-4-(*m*-nitrophenyl)-1,4-dihydropyridine-3,5-dicarboxylate (Nicardipine). *Chem. Pharm. Bull*., **1980**, 28, 2809-2812.

100. Zhang B, He W, Shi X, Huan M, Huang Q and Zhou S. Synthesis and biological activity of the calcium modulator (*R*) and (*S*)-3-methyl 5-pentyl 2,6-dimethyl-4-(3-nitrophenyl)-1,4-dihydropyridine-3,5-dicarboxylate. *Bioorg. Med. Chem. Lett*., **2010**, 20, 805-808.

101. Ashimori A, Uchida D, Ohtaki Y, Tanaka M, Ohe K, Fukaya C, Watanabe M, Kagitani M and Yokoyama K. Synthesis and pharmacological effects of optically active 2-[4-(4-benzhydryl-1-piperazinyl)phenyl] ethyl methyl 1,4-dihydro2,6-

dimethyl-4-(3-nitrophenyl)-3,5-pyridinedicarboxylate hydrochloride. *Chem. Pharm. Bull.*, **1991**, 39, 108-111.

102. Tamazawa T, Arima H, Kojima T, Isomura Y, Okada M, Fujita S, Furuya T, Takenaka T, Inagaki O and Terai M. Stereoselectivity of a potent calcium antagonist, 1-benzyl-3-pyrrolodinyl methyl 2,6-dimethyl-4-(*m*-nitrophenyl)-1,4-dihydropyridine-3,5-dicarboxylate. *J. Med. Chem*., **1986**, 29, 2504-2511.
103. Simons KE, Ibbotson A, Johnston P, Plum H and Wells PB. Enantioselective hydrogenation III. Methyl pyruvate hydrogenation catalysed alkaloid-modified Iridium. *J. Cat*., **1994**, 150, 321-328.
104. Smaardijk AA and Wynberg H. Stereoselective addition diethylzinc to aldehydes, catalyzed by *Cinchona* alkaloids. *J. Org. Chem*., **1987**, 52, 135-137.
105. Sharpless KB, Amberg W, Bennani L, Crispino GA, Hartung J, Jeong KS, Kwong HL, Morikawa K, Wang ZM, Xu D and Zhang L. The Osmium-catalyzed asymmetric dihydroxylation: a new ligand class and a process improvement. *J. Org*. *Chem.,* **1992**, 57, 2768-2771.
106. Lygo B and Wainwright PG. A new class of asymmetric phase-transfer catalysts derived from *Cinchona* alkaloids – Application in the enantioselective synthesis of α-amino acids. *Tetrahedron Lett*., **1997**, 38, 8595-8598.
107. Perrard T, Plaquevent J-C, Desmurs J-R and Hébrault. Enantioselective synthesis of both enantiomers of methyl dihydrojasmonate using solid-liquid asymmetric phase transfer catalysis. *Org. Lett*., **2000**, 2, 2959-2962.
108. Corey EJ, Noe MC and Xu F. Highly enantioselective synthesis of cyclic and functionalized α-amino acids by means of a chiral phase transfer catalyst. *Tetrahedron Lett*., **1998**, 39, 5347-5350.
109. Arai S, Tsuge H, Oku M, Miura M and Shioiri T. Catalytic asymmetric epoxidation of enones under phase-transfer catalysed conditions. *Tetrahedron*, **2002**, 58, 1623-1630.
110. Berkessel A, Guixà M, Schmidt F, Neudörfl JM and Lex J. Highly eantioselective epoxidation of 2-methylnaphthoquinone (Vitamin $K_3$) mediated by new *Cinchona* alkaloid phase-transfer catalysts. *Chem. Eur. J*., **2007**, 13, 4483-4498.
111. Pálovics E, Schindler J, Faigl F and Fogassy E. The influence of molecular structure and crystallization time on efficiency of diastereomeric salt forming resolutions. *Tetrahedron: Asymmetry*, **2010**, 19, 2429-2434.
112. Sakai K, Sakurai I and Nohira H. New resolution technologies controlled by chiral discrimination mechanisms. *Novel Optical resolution technologies*, **2007**, 199-231.

113. Szeleczky Z, Semsey S, Bagi P, Fodi B, Faigl F, Pálovics E and Fogassy E. An aspect of selecting resolving agents: The role of differences in molecule length in diastereomeric salt resolutions. *Separation Science Technology*, **2016**, 51, 727-732.
114. Kozma D. *Optical resolutions via diastereomeric salt formation*. CRC Press, London, **2002**, 278-420.

# Chapter 3

## Racemic substrates

A racemate is a compound that has equal amounts of the constituent enantiomers and shows zero optical activity due to the cancellation of the opposite optical rotations. The chemical name or the formula of a racemate is distinguishable by the prefix (±)- or *rac*- (or *racem*-) or by the symbols *RS*- or *SR*-. The prefix racemic pertains to a racemate.[1] In some sectors of chemistry the prefix *dl* (for sugars the prefix *DL*-) is used to denote a racemate, but IUPAC firmly discourages the use of *d* and *l* as prefixes.[1] The usage of 'racemic mixture' is also strongly discouraged by IUPAC as the term has been used as a synonym for the two names, racemate and racemic conglomerate.[1] Below are the structures of the racemic substrates used in the study, and their physical properties are listed in Table 3.1.

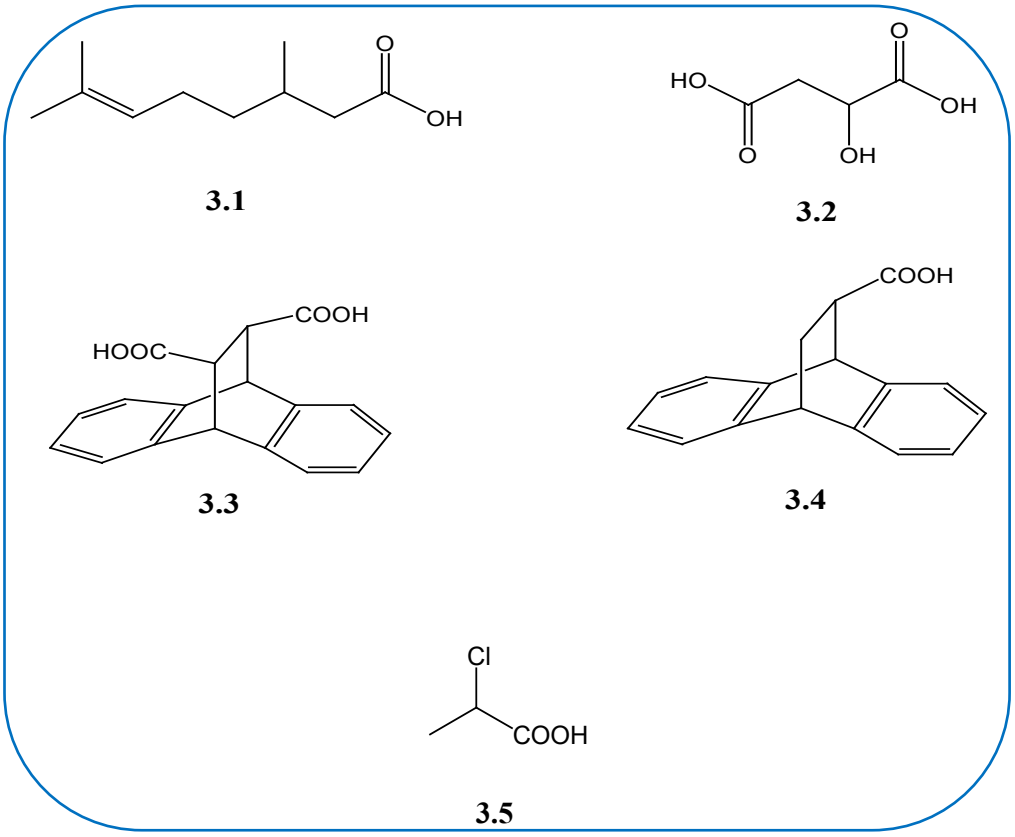


**3.1** **3.2** **3.3** **3.4** **3.5**

Citronellic acid (3,7-dimethyloct-6-enoic acid) (**3.1**), malic acid (2-hydroxybutanedioic acid) (**3.2**), *trans*-9,10-dihydro-9,10-ethanoanthracene-11,12-dicarboxylic acid (**3.3**), 9,10-dihydro-9,10-ethanoanthracene-11-carboxylic acid (**3.4**) and 2-chloropropanoic acid (**3.5**), are the racemic compounds used in this study.

All these compounds have the carboxylic acid (-COOH) functional group that can act as a proton donor and as a proton acceptor. The proton donated to a base can then form a salt which

results in a charge assisted hydrogen bond, or it can form a bond in a neutral compound where no proton transfer occurs.

Table 3.1 The physical properties of the racemic substrates studied.[2]

| Racemates | Formula | $M_r$ g/mol | Density g/ml | Bp °C | Mp °C |
|---|---|---|---|---|---|
| **3.1** | $C_{10}H_{18}O_2$ | 170.3 | 0.923 | 121-122 | - |
| **3.2** | $C_4H_6O_5$ | 134.09 | 1.609 | - | 131-132 |
| **3.3** | $C_{18}H_{14}O_4$ | 294 | 1.33 | - | 261 |
| **3.4** | $C_{17}H_{14}O_2$ | 250 | - | - | 193 |
| **3.5** | $C_3H_5ClO_2$ | 108.52 | 1.18 | 170-190 | - |

## 3.1. Citronellic acid (3,7-dimethyl-6-octenoic acid) (**3.1**)

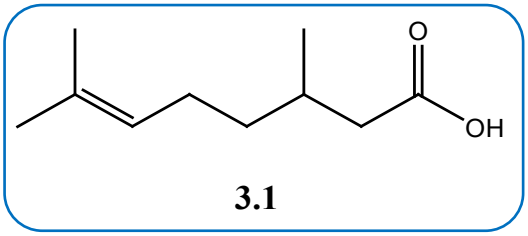


**3.1**

The only structure involving this compound in the CSD is the one that was submitted by my research group in 2013. Citronellic acid is the main constituent of two *Pelagornium* plant species, Geraniaceae and 'Sweet Rosina'. It is obtained from the leaf oils of the two species by steam distillation and solvent extraction using the solvents hexane and petroleum spirit. These were noticed to have citronellic acid in the range of 27.9 to 89.3%.[3] It is used in concoctions for repelling mosquitoes and managing termites. Its antibacterial and antifungal properties make it useful in cosmetics.[4-6] Chemically it is produced by the oxidation of citronellal,[7] and the same reaction was used to determine the *R/S* ratios of citronellal. Citronellic acid has been characterized using NMR spectroscopy in the presence of a chiral europium shift chemical reagent, and by high pressure liquid chromatography of diastereomeric amides.[8]

Enzymatic resolutions catalyzed by *Candida rugosa* Lipase (**CRL**) have been broadly employed in the formation of esters from the corresponding acids in non-polar solvents.[9,10] This strategy was employed in the resolution of citronellic acid. It was treated at a steady water activity ($a_w$ = 8) in cyclohexane with hexadecan-1-ol in the presence of the catalyst, **CRL** (Scheme 3.1).[11]

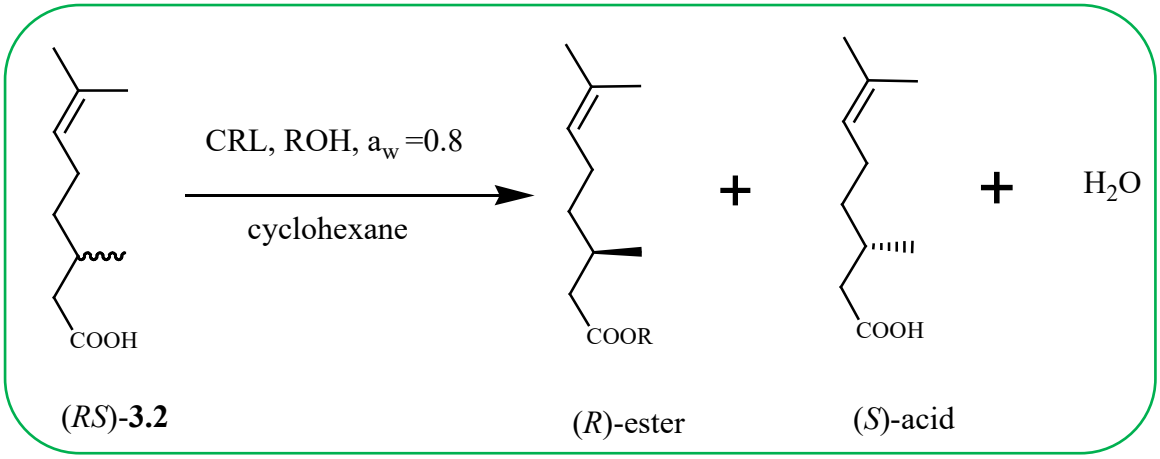


Scheme 3.1 The resolution of racemic citronellic acid in the formation of esters with a long chain alcohol in cyclohexane using an immobilized chiral catalyst, the *Candida rugosa* lipase. ROH = hexadecan-1-ol.[11]

The citronellic acid gave rise to the product (*R*)-ester with 90% ee and the remaining substrate with 29.9% ee. The resolution of the acid was slow, and it took 6 days to reach 25% conversion. The *S*-enantiomer did not fit into the active site tunnel of **CRL.** The (*R*)-citronellic acid might have reacted through another productive mode, which is similar to the case of 2-methyldecanoic acid ester.[12] The slow reaction rate was also thought to be as the result of conformational changes that are required in order to make it imitate a 2*S*-substrate. Similar variations ought to demand more energy for the 3*S*-enantiomer than for the 3*R*-enantiomer.[11]

## 3.2. Malic acid (2-hydroxybutanedioic acid) (**3.2**).

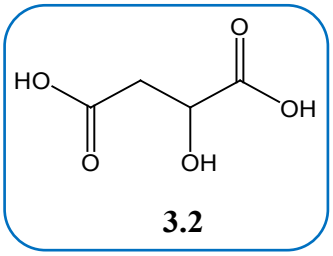


**3.2**

Malic acid is naturally found in the *L*-form and is a constituent of apples and other fruits and plants.[2] Its racemic form was earlier resolved by McKenzie *et al.* with quinine as a resolving agent.[13] A number of investigations regarding the chiral resolution of malic acid have been conducted using chromatography, and one of the most commonly used techniques is HPLC.[14] Direct chiral resolution by ligand exchange electrophoresis employing copper(II)-*L*-tartrate has been reported.[15]

The structures of *L*-malic acid with *L*-tartaric acid were reported by Aakeröy *et al.*[16] and Eddleston *et al.*[17] The latter's milling results showed that *L*-tartaric acid was a suitable molecule for the chiral resolution of racemic malic acid *via* co-crystallization.[17]

In the late 1800s and early 1900s indirect methods were used for obtaining *d*-malic acid, and these were listed by Dakin in 1923 as, (i) the reduction of *d*-tartaric acid by hydriotic acid, (ii) the action of nitrous acid on *d*-asparagine, (iii) nitric acid in the oxidation of *d*-α-hydroxybutyrolactone, (iv) *d*-chloro- and *d*-bromosuccinic acids in the reactions with silver oxide and water, and (v) *d*-malic acid resulted after the monoacetylation of *d*-tartaric acid with thionyl chloride and pyridine had given an acetyl derivative, after-which it was hydrolysed and reduced.[13] Dakin was successful in resolving malic acid with cinchonine in methanol, which resulted into the separation of the *l*-malate.[13]

In synthetic chemistry the malic acid enantiomers play a major role as reactive synthons for different compounds, such as for β-lactam precursors of antibiotics and for the carnitine enantiomers.[18] (*R*)-Carnitine is a substance that resembles a vitamin and it plays a role in the conversion of stored body fat into body energy.

Various methods have been used to resolve malic acid, including enzymes, and some enzymes have been used in the preparation of malic acid enantiomers from other acids. An industrial process that has been used for the synthesis of (*S*)-2-hydroxybutanedioic acid is the fumarase-catalyzed hydration of fumaric acid.[19]

The alkaloid brucine is a well-known resolving agent for the resolution of chiral compounds from enantiomeric mixtures of several organic molecule types, including α-hydroxy acids. It was overlooked as a potential resolving agent for other analogues such as glyceric acid, 2-hydroxybutanedioic acid and 2,3-dihydroxybutanedioic acid.[20(a)] In 2005 Bialonska *et al*.[21] demonstrated the resolution of racemic glyceric acid to its *L*-form, and determined the brucinium salt. That led to Smith *et al*. [20(a)] attempting similar resolutions with malic acid (2-hydroxybutanedioic acid) and 2,3-dihydroxybutanedioic acid. They refluxed brucine with *DL*-malic acid in a 50% mixture of ethanol and water.

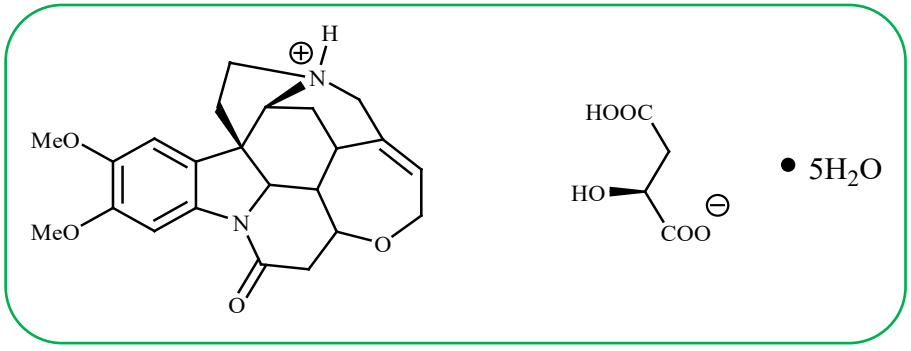


Figure 3.1 Brucinium (2,3-dimethoxy-10-oxostrychnidinium) salt of the α-hydroxy acid, *L*-malic acid.[20(a)]

The structure determination confirmed the presence of two independent brucinium cations, two hydrogen *L*-malate anions and ten water molecules of crystallization in the asymmetric unit (Figure 3.1), and it formed a complex hydrogen-bonded three dimensional framework structure.[20(a)] The use of brucine is not popular because it is poisonous.[20(b),(c)]

## 3.3. *Trans*-9,10-dihydro-9,10-ethanoanthracene-11,12-dicarboxylic acid (**3.3**)

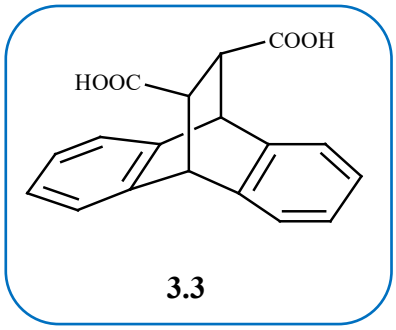


**3.3**

There are 26 crystal structures involving the compound *trans*-9,10-dihydro-9,10-ethanoanthracene-11,12-dicarboxylic acid (**3.3**) in the CSD. The majority of these are clathrates (20 crystal structures), 2 co-crystals, 1 apohost structure and 3 organometallic structures. A search of the carboxylate fragment gave 10 hits, with 7 of these involving metals.

Weber *et al*.[22,23] have demonstrated that racemic *trans*-9,10-dihydro-9,10-ethanoanthracene-11,12-dicarboxylic acid (**3.3**) is a flexible clathrate host which produces a 1:1 (host:guest) inclusion compound with acetic acid in its racemic form. Its space filling characteristics and the presence of the COOH functional groups coupled with special molecular symmetry provides some beneficial possibilities. It also has a roof shaped molecular framework. The compound under study, **3.3**, as a coordinantoclathrate host, shows the following structural features,

-a bulky molecular skeleton which gives rise to voids in the crystal lattice

-appended carboxylic acid (sensor) groups, which provide hydrogen bonding sites to guests or to other **3.3** molecules.

Hosts that can recognize and bind to suitable guests play a major role in analytical applications and also in the development of carriers, reagents and effective catalysts.[24] The roof shaped molecule demonstrates versatile host properties, that is it allows stoichiometric, selective inclusions of a large number of different polar organic guests, most of which are able to form hydrogen bonds. **3.3** forms homologous clathrates with acetic acid and propanoic acid under ambient conditions.[25]

A mixture of isomers (+/-)-1,2; 5,6-dibenzo-9,10-dihydro-9,10-ethanoanthracene-11,12-*trans*-dicarboxylic acids was produced from the *cis*-ester[26] by hydrolysis with KOH. The conversion

from the *cis*-di-ester to two *trans*-di-acids was generally observed.[27] The conversion of the *trans*-di-ester to two *trans*-di-acids was achievable by base catalyzed hydrolysis and this was noticed in the conversion of (+)-*trans*-di-ester ((+)-**3.6**) to (+/-)-*trans*-di-acid ((+/-)-**3.3**, Scheme 3.2.[24]

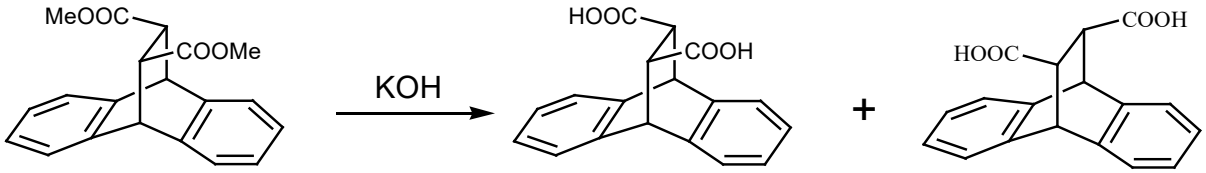


(+)-**3.6** (+/-)-**3.3**

Scheme 3.2 The conversion of a (+)-di-ester to (+/-)-diacid.[24]

Recrystallization of **3.3** resulted in the production of inclusion compounds with various solvents.[28] Small molecules such as MeOH, EtOH or acetonitrile did not act as applicable guests for the host lattices produced by **3.3**. Higher alcohols, normal or branched were chosen over the lower candidates. Dimethylformamide (DMF) was favoured over butanol, but acetic acid was preferred over DMF and ethylene glycol was favoured over acetic acid. The unique shape of the host molecule, the hydrogen bond donor/acceptor functionality, and the two-fold molecular symmetry facilitated the formation of new clathrates.[29(a),(b)]

In 1988 Weber *et al*. used an array of clathrate hosts distinguishable by a roof-shaped molecular framework and selected functional groups, including **3.3**, to study their inclusion behaviour, in 68 different inclusion complexes.[22]

The chiral synthons appropriate for transformation into discriminators for liquid chromatography separation of enantiomers, catalytic asymmetric chemical reactions and synthesis of $C_2$-symmetric dicarboxylic acids derivatives are of importance as they can be produced on a huge scale from readily accessible starting compounds. Many chiral *trans*-dicarboxylic acids can be formed *via* Diels-Alder chemical reactions with fumaric acid as a dienophile and from metallation/carbonation reactions that have appropriate double bonds.[30] **3.3** was used in the preparation of these two selector types, **3.7** and **3.8**, and their enantiomer-discriminating ability, which was showed by induced chemical shift differences in the NMR, was reported.[31]

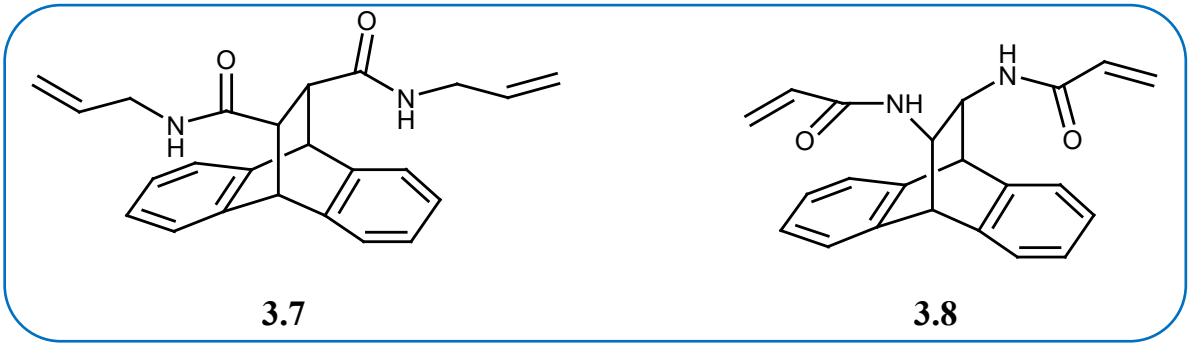

**3.7** **3.8**

The chiral resolution of racemic **3.3** has also been explored using the amino acid (*S*)-proline (**3.9**). Amino acids are produced naturally or by the resolution of racemates.[31] The racemic proline was resolved by employing an optically active 2,3-dihydroxybatanedioic acid as a resolving agent.[32] Periasamy *et al*. have described the use of (*S*)-proline in the resolution of some racemic molecules through the equivalent diastereomeric complex formation.[33] Ramanathan *et al*.[34] have resolved the racemic-**3.3** to form the corresponding (*S,S*)-isomer in 95.9% ee and the (*R,R*)-isomer in 96.8% ee by way of complexation with (*S*)-proline in hydroxymethane, with low yield.

Racemic **3.3** and (*S*)-**3.9** in MeOH solution were heated, and a precipitate was obtained after 4 hrs (Scheme 3.3). (11*S*,12*S*)-(-)-**3.3** was isolated (25%, 96% ee) after filtration and decomposition of the precipitate with an ether and water mixture. The residue formed after evaporation of the fraction of the complex that contained the (+)-isomer gave rise to crystals upon recrystallization from fresh MeOH. On the decomposition of the crystalline complex with an ether and water mixture, (11*R*,12*R*)-(+)-**3.3** resulted (18.9% yield, 96.8% ee). The same results were produced by concentrating the filtrate, and crystallization resulted.[34]

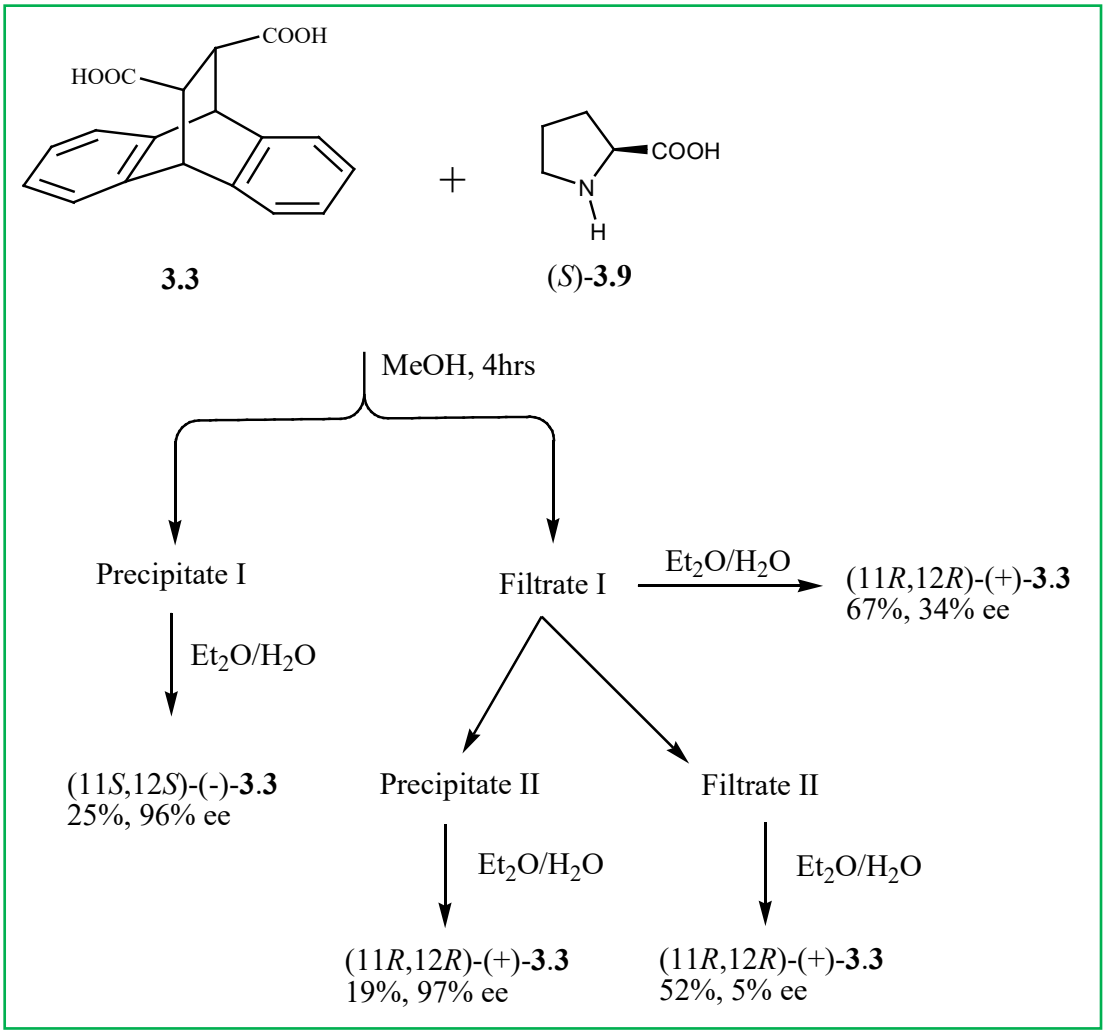


Scheme 3.3 Resolution of **3.3**.[36]

The compound formed from (-)-**3.3** and **3.9** was not appropriate for crystal structure analysis.[34]

The chiral dicarboxylic acid **3.3** has been employed in the synthesis of chiral compounds of phosphines and chiral diols for applications in reactions that are catalyzed by palladium and titanium.[35,36]

In another study the asymmetric cycloaddition pathways to the two enantiomers of **3.3** were reported.[37] Fumarates that were prepared from a set of optically active alcohols were used as dienophiles in Lewis acid catalyzed asymmetric cycloaddition to the anthracene. The reactions gave large yields and de's of the di-ester cycloaddition products and acid hydrolysis could be accomplished under reaction conditions yielding only about 9,9 % racemization. The chemical reactions formed an important synthetic route to the two enantiomers of **3.3**. The di-(-)-menthyl fumarate gave rise to the (-)-(*S,S*)-**3.3** isomer and the di-(+)-iso-menthyl fumarate gave rise to the (+)-(*R,R*)-**3.3** isomer of the acid, Scheme 3.4. The other fumarates that were produced from (-)-borneol, (+)-fenchol and (-)-isopulegol, all gave rise to the (-)-(*S,S*)-**3.3** isomer of the diacid.[35]

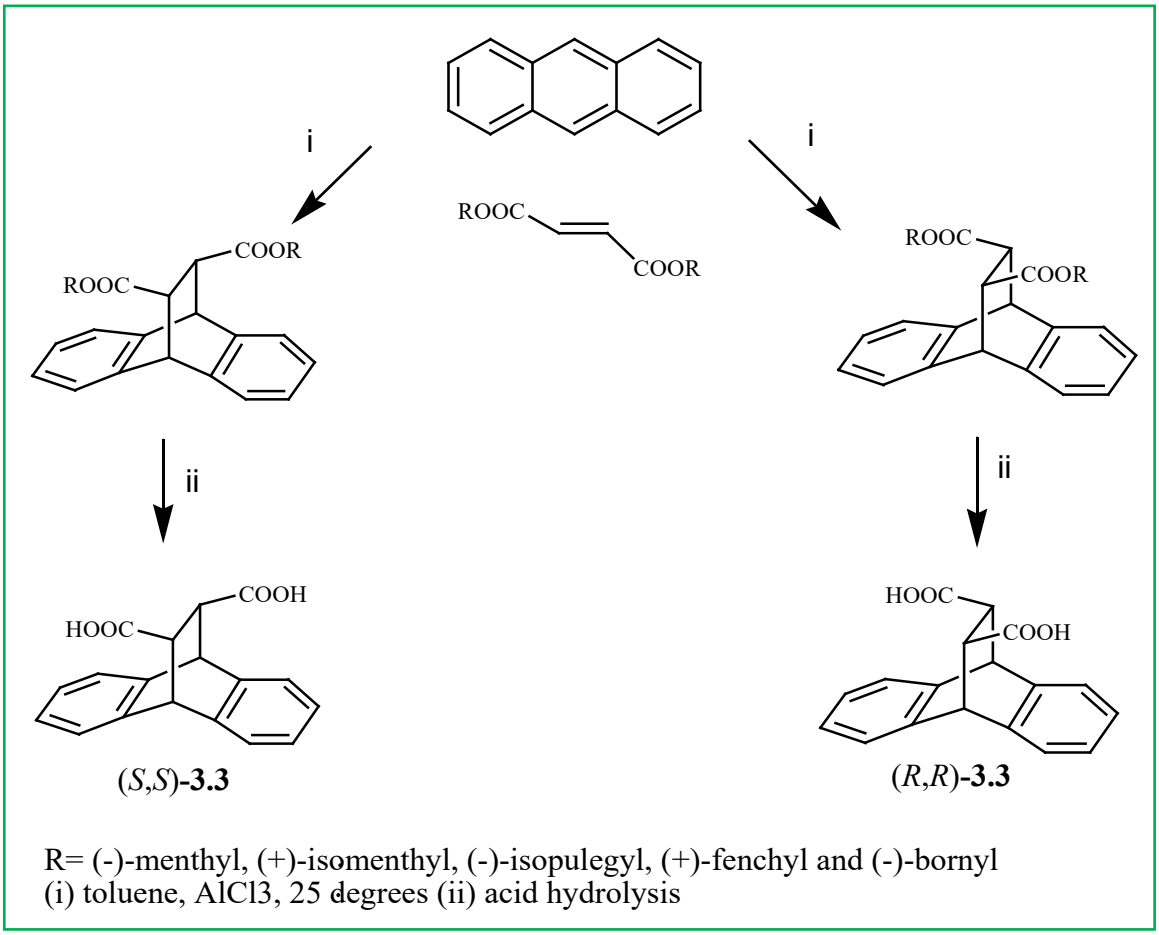


Scheme 3.4 Cycloaddition reactions to both enantiomers of **3.3**.[37]

The absolute stereochemistry of the resultant compounds was demonstrated *via* a single crystal X-ray crystallographic structure analysis of the brucine diastereomeric salt of the (-)-(*S,S*)-**3.3**.[37] Prior to this the chiral resolution of racemic **3.3** using brucine[38] was reported.

## 3.4. 9,10-Dihydro-9,10-ethanoanthracene-11-carboxylic acid (**3.4**)

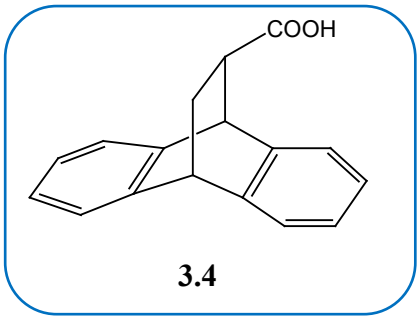


**3.4**

The CSD search results revealed one clathrate of **3.4** with **DMSO** (VEVMEO).[39]

The others were **3.4** ethyl esters[40] with different types of substituents at position 12; (6-chloropyridin-2-yl) (WEDFIW), (6-(4-methoxyphenyl)pyridine-2-yl) (WEDFOC), (6-phenylpyridin-2-yl) (WEDFUI), (6-(2,4,6-trimethoxyphenyl)pyridine-2-yl) (WEDGAP), (6-(anthracen-9-yl)pyridine-2-yl) (WEDGIX) and (4-chloropyridin-2-yl) (WEDGOD).

**3.4** is able to identify and bind to particular molecules and therefore is valuable for analytical applications and to develop more effective catalysts, reagents and carriers.[41,42]

A significant number of clathrate hosts similar to **3.4** with the characteristic roof-shaped molecular framework and particularly attached functional groups were prepared by Weber *et al*.[22] and studied with respect to their inclusion behaviour. It was found that the selectivities, stoichiometries and formation of the clathrates depended on the structural characteristics of the hosts, eg the flexibility and the number, geometries, natures of the functional groups.[22]

These roof-shaped compounds find some applications in various fields ranging from material science to medicinal chemistry.[43,44] Jain *et al*. reported the preparation and resolution of the roof shaped alcohols and the use of the roof-shaped chiral enantiopure alcohols as another auxiliary for asymmetric preparation of α-halo acid analogues.[45,46] The optically pure roof-shaped alcohols were further modified to the corresponding amines as chiral solvating fragments for the selection of the signals of some optically active molecules in NMR spectroscopy studies.[46] Gupta *et al*. prepared and investigated the optically active roof-shaped amines as chiral solvating fragments in the study of molecular discrimination of acids by NMR determinations.[47]

Csöregh *et al*.[48] have studied the crystal structures of four dimethyl sulphoxide (DMSO) inclusion crystals with various carboxylic acid host compounds (including **3.4**) by single crystal X-ray analysis.

In the last few decades there has been an interest in organotin(IV) carboxylates which was associated with their significant biological activities as anticancer and antiviral agents, wood preservatives and pesticides. In 2009 Wu *et al*. synthesized and studied the crystal structures and biological properties of the two unusual organotin(IV) complexes prepared from a derivative of **3.4**, 12-(4-methylbenzoyl)-9,10-dihydro-9,10-ethanoanthracene-11-carboxylic acid**, (3.10).** The two complexes, $[(n\text{-}Bu_2Sn)_4(\mathbf{3.10})_2O_2(OC_2H_5)_2]$ and $[(C_6H_5)_3Sn(\mathbf{3.10})]$ showed good antibacterial and antitumor properties for potential drug use.[49]

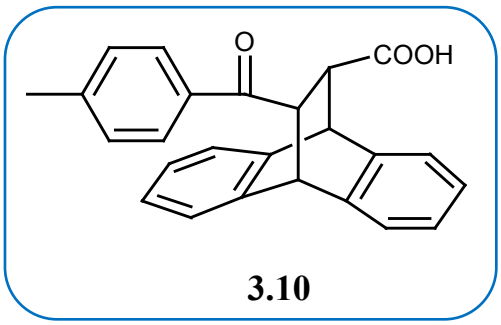


**3.10**

In the development of organo-catalytic asymmetric synthesis, Sasaoka *et al*. have synthesized roof-shaped anthracene-fused chiral prolines as organocatalysts for the asymmetric Mannich chemical reactions.[50]

## 3.5. 2-Chloropropanoic acid (**3.5**)

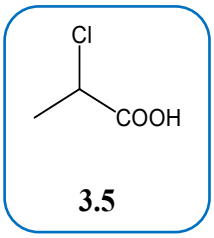


**3.5**

A CSD search gave one nickel salt (LAKRIZ) of 2-chloropropionic acid (**3.5**). A metal complex, *bis*-(2-chloropropionic acid)-*tris*(tetraphenylimidodiphosphinato)-praseodymium (ZAXSOG) and an ester with an (*R*)-**3.5** fragment were the only other hits found in the CSD.[51,52]

(*S*)-**3.5** is a building block in the preparation of aryloxyphenoxypropanoic acid, the (*R*)-enantiomer has herbicidal activity.[53] Industrially (*S*)-**3.5** is obtained by the resolution of the racemate in which the (*R*)-**3.5** isomer is selectively degraded by using (*R*)-2-haloacid dehalogenase enzyme.[54] Kurata *et al*.[55] have established a process in which (*S*)-**3.5** was enzymatically produced by asymmetric reduction of the alkene portion in 2-chloroacrylic acid (**3.11**), Scheme 3.5.

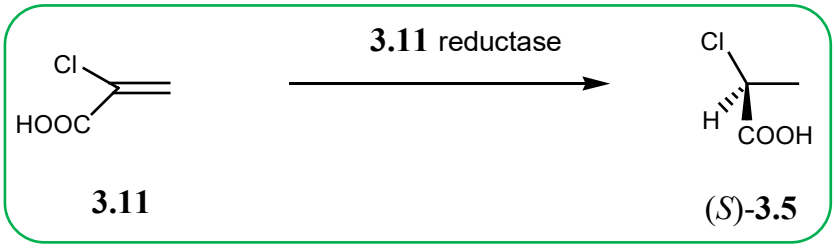


**3.11** (*S*)-**3.5**

Scheme 3.5 Putative pathway of **3.11** reduction.[55]

Racemic **3.5** is employed as a chemical intermediate in the pharmaceutical, chemical and agrochemical industries and earlier investigations focused on **3.5** as a neurotoxic molecule.[55] This compound has been reported to cause degeneration of granule cells in the cerebellum of adult rats[56] and further affects other sections of the brain.[57] Aam *et al*. have studied the effect of **3.5** on reactive oxygen species formation in human neutrophil granulocytes *in vitro*, and they observed an increased formation of the reactive oxygen species (ROS) after exposure to **3.5**. Their results also implied that **3.5** may be immunotoxic.[55]

The kinetic resolution of **3.5** by enzyme catalyzed formation of esters in various organic solvents had been investigated by Bodnár *et al*.[58] Lipase is among the most valuable enzymes used as a chiral catalyst, because it does not need a co-factor regeneration and is stable and

available commercially. The studied reaction was the enantioselective esterification of **3.5** using a suspended enzyme, lipase, from *Candida cylindracea* as a catalyst. The general reaction is shown in Scheme 3.6.

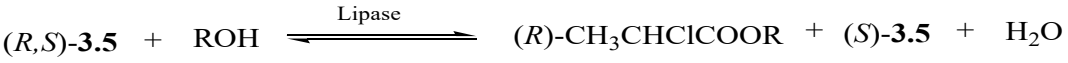


Scheme 3.6 The resolution of **3.5** *via* esterification.[58]

The enzyme esterification occurred on the (*R*)-isomer of the acid. The enantioselectivity and reactivity of the enzyme firmly depended on the physical properties of the solvent and the circulation of water between the enzyme as a heterogeneous catalyst and the organic solvents. A suitable amount of water was crucial for the enzyme's catalytic activity, and the water that was generated in the reaction retarded the activity.

Another method of synthesizing the (*S*)-enantiomer of **3.5** was related to the method reported by Fu *et al*.[59] where (*S*)-alanine was reacted with sodium nitrite in acidic medium**.**

## 3.6. Conclusion

The CSD searches indicated that there are few crystal structures involving the racemic carboxylic acid compounds (**3.1** – **3.5**) used in this study. Furthermore, not much work has been done regarding the chiral resolution of these acids with malic acid being studied more compared to the others. Analysis of the available crystal structures showed the importance of the carboxylic acid group in the formation of hydrogen bonds via heterosynthons due to it being a strong hydrogen bond donor and acceptor group.

## 3.7. References


1. Moss GP. Basic terminology of stereochemistry. *Pure and Appl. Chem*., **1996**, 68, 2193-2222.
2. Windholz M. Ed. The Merck Index: An Encyclopaedia for Chemicals and drugs, Merck and Co. Inc., New Jersey, **1976**.
3. Lis-Balchin M and Roth G. Citronellic acid: a major component in two Pelargonium species (Geraniaceae). *J. Essent. Oil Res*., **1999**, 11, 83-85.
4. Oh J, Bowling JJ, Carroll JFP, Demirci B, Baser KHC, Leininger TD, Bernier UR and Hamann MT. Natural product studies of US endangered plants: Volatile components of *Lindera melissifolia* (Lauraceae) repel mosquitoes and ticks. *Phytochemistry*, **2012**, 80, 28-36.
5. Choi SY. Inhibitory effects of geranic acid derivatives on melanin biosynthesis. *J. Cosmetic Sc.,* **2012**, 63, 351-358.
6. Regnier T and Combrinck S. *In vitro* and *in vivo* screening of essential oils for the control of wet bubble disease of *Agaricus bisporus*. *S.Afr. J. Bot*., **2010**, 76, 681-685.
7. Martin A, Armbruster U, Decker D, Gedig T and Kockritz A. Oxidation of Citronellal to Citronellic acid by molecular oxygen using supported gold catalyst. *ChemSusChem*., **2008**, 1, 242-248.
8. Valentine D Jr, Chan KK, Scott GG, Johnson KK, Toth K and Saucy G. Direct determinations of *R*/*S* enantiomer ratios of citronellic acid and related substances by nuclear magnetic resonance spectroscopy and high pressure liqid chromatography. *J. Org. Chem*., **1976**, 41, 62-65.
9. Berglund P, Vörde C and Högberg H-E. Esterification of 2-methylakanoic acids catalysed by lipase from *Candida rugosa*: Enantioselectivity as a function of water activity and alcohol chain length. *Biocatalysis*, **1994**, 9, 123-130.
10. Edlund H, Berglund P, Jensen M, Hendeström E and Högberg H-E. Resolution of 2-methylalkanoic acids. Enantioselectivity esterification with long chain alcohols catalysed by *Candida rugosa* lipase. *Acta Chem. Scand*., **1996**, 50, 666-671.
11. Nguyen B-V and Hedenström E. *Candida rugosa* lipase as an enantioselective catalyst in the esterification of methyl branched carboxylic acids: resolution of *rac*-3,7-dimethyl-6-octenoic acid (citronellic acid). *Tetrahedron: Asymmetry*, **1999**, 10, 1821-1826.

12. Holmquist M, Haeffner F, Norin T and Hult K. A structural basis for enantioselective inhibition of *Candida rugosa* lipase by long chain aliphatic alcohols. *Protein Sci*., **1996**, 5, 83-88.
13. Dakin HD. The resolution of inactive malic acid into optically active forms. *J. Biol. Chem*., **1924**, 59, 7-12.
14. Doner LW and Cavender PJ. Chiral liquid chromatography for resolving malic acid enantiomers in adulterated apple juice. *J. Food Sci*., **1988**, 53, 1898-1899.
15. Kodama S, Yamamoto A, Matsunaga A, Soga T and Hayakawa K. Direct chiral resolution of malic acid in apple juice by ligand-exchange capillary electrophoresis using Copper(II)-L-tartaric acid as a chiral selector. *Electrophoresis*, **2001**, 22(15), 3286-3290.
16. Aakeröy CB, Cooke TI and Niewenhuyzen M. The crystal structure of the molecular cocrystal L-malic acid L-tartaric acid (1/1). *Supramol. Chem*., **1996**, 7, 153-156.
17. Eddleston MD, Arhangelskis M, Friscic T and Jones W. Solid state grinding as a tool to aid enantiomeric resolution by co-crystallization. *Chem. Commun*., **2012**, 48, 11340-11342.
18. Bellamy FD, Bondoux M and Dodey P. A new, short and efficient synthesis of both enantiomers of carnitine. *Tetrahedron Lett*., **1990**, 31, 7323-7326.
19. Marletta MA, Cheung Y-A and Walsh C. Stereochemical studies on the hydration of monofluorofumarate and 2,3-difluorofumarate by fumarase. *Biochemistry,* **1982**, 21, 2637-2644.
20. (a) Smith G, Wermuth UD and White JM. Brucine salts of *L-alpha*-hydroxy acids: brucinium hydrogen (*S*)-malate pentahydrate and unhydrous brucinium hydrogen (2*R*,3*R*)-tartrate at 130K. *Acta Cryst.,* **2006**, C62, o353-o357. (b) Achappa B, Madi D, Babu YPR and Mahalingam S. Rituals can kill- a fatal case of brucine poisoning. *Australasian Med. J*., **2012**, 5, 421-423. (c) Shu G, Mi X, Cai J, Zhang X, Yin W, Yang X, Li Y, Chen L and Deng X. Brucine, an alkaloid from Strychnos nux-vomica Linn., represses hepatocellular carcinoma cell migration and metastasis: the role of hypoxia inducible factor 1 pathway. *Toxicol. Lett*., **2013**, 222, 91-101.
21. Białońska A, Ciunik Z, Popek T and Lis T. Cyclic water pentamers in triclinic crystals of brucinium L-glycerate. *Acta Cryst.,* **2005**, C61, o88-o91.
22. Weber E, Csöregh I, Ahrendt J, Finge S and Czugler M. Design of roof-shaped clathrates hosts. Inclusion properties and X-ray crystal structures of a free host and of inclusion compounds with 1-butenol and DMF. *J. Org. Chem*., **1988**, 53, 5831-5839.

23. Weber E. Molecular recognition: designed crystalline inclusion complexes of carboxylic hosts. *J. Mol. Graphics*, **1989**, 7, 12-27.
24. Hagishita S and Kuriyama K. Optical activity of $C_2$ symmetrical 9,10-dihydro-9,10-anthracenes. *Tetrahedron*, **1972**, 28, 1435-1467.
25. Atwood JL, Davies JAD and MacNicol DD. *Inclusion Compounds*, Oxford: University Press, **1991**.
26. Bachmann WE and Kloetzel MC. The reaction between maleic anhydride and polycyclic hydrocarbons. *J. Am. Chem. Soc*., **1938**, 60, 481-481.
27. Takeda K, Hagishita S, Sugiura M, Kitahonoki K, Ban I, Miyazaki S and Kuriyama K. Diels-Alder reaction-IX: The reaction of 1,7-, 2,7-, 2,6- and 1,6-dihydroxynaphthalene and 6-bromo-2-naphthol with maleic anhydride and the resolution of some derivatives of the adducts. *Tetrahedron*, **1970**, 26, 1435-1451.
28. Davies JED, Kemula W, Powell HM and Smith NO. Inclusion compounds- Past, present and future. *J. Incl. Phenom*., **1983**, 1, 3-44.
29. (a) Czugler M, Weber E and Ahrendt J. Selective clathrate formation with the new host systems *cis*- and *trans*-9,10-dihydro-9,10-ethanoanthracene-11,12-dicarboxylic acid: Inclusion properties and X-ray structure of an encapsulated acetic acid dimer. *J. Chem. Soc., Chem. Commun*., **1984**, 1632-1634. (b) Davies JED, Kemula W, Powell HM and Smith NO. Inclusion compounds- Past, present and future. *J. Incl. Phenom*., **1983**, 1, 3-44.
30. Allenmark S, Skogsberg U and Thunberg L. Chiral selectors based on C2-symmetric dicarboxylic acids. *Tetrahedron: Asymmetry*, **2000**, 11, 3527-3534.
31. Eliel EL, Wilen SH and Mander LN. *Stereochemistry of Organic Compounds*, John Wiley and Sons, **1994**, 336.
32. Yamada S, Hongo C and Chibata I. Optical resolution of DL-proline by forming a new diastereomeric solid complex with L-tartaric acid. *Agri. Biol. Chem*., **1977**, 41, 2413-2416.
33. Periasamy M, Prasad ASB, Kanth JVB and Reddy CH. A simple convenient method for the resolution of racemic 2,2'-dihydroxy-1,1'-binaphthyl using (*S*)-proline. *Tetrahedron: Asymmetry*, **1995**, 6, 341-344.
34. Ramanathan CR and Periasamy M. Resolution of C2-symmetric 9,10-dihydro-9,10-ethanoanthracene-11,12-dicarboxylic acid and 2,3-diphenylsuccinic acid using (*S*)-proline. *Tetrahedron: Asymmetry*, **1998**, 9, 2651-2656.
35. Trost BM. Designing a receptor for molecular recognition in a catalytic synthetic reaction: Allylic alkylation. *Acc. Chem. Res*., **1996**, 29, 355-364.

36. Giffels G, Dreisbach C, Kragl U, Weigerding M, Waldman H and Wandrey C. Chiral Titanium alkoxides as catalysts for the enantioselective reduction of ketones with boranes. *Angew. Chem., Int. Ed. Engl*., **1995**, 34, 2005-2006.
37. Thunberg L and Allenmark S. Asymmetric cycloaddition routes to both enantiomers of *trans*-9,10-dihydro-9,10-ethanoanthracene-11,12-dicarboxylic acid. *Tetrahedron: Asymmetry*, **2003**, 14, 1317-1322.
38. Brienen M.-J. Jacques J. *Bull. Soc. Chim. Fr*. 1973, 190.
39. Csöregh I, Gallardo O, Weber E, Finge S and Reutel C. The unusual structure of the crystalline inclusion compound between (11*S*,12*S*)-(-)-9,10-dihydro-9,10-ethanoanthracene-11,12-dicarboxylic acid and acetic acid. *Tetrahedron: Asymmetry*, **1992**, 3, 1555-1562.
40. Gnanamani E, Someshwar N and Ramanathan CR. Conformationally rigid chiral pyridine N-oxides as organocatalyst: Asymmetric allylation of aldehydes. *Adv. Synth. Catal*., **2012**, 354, 2101-2106.
41. Van Binst G: *Design and synthesis of organic molecules based on molecular recognition*. Springer Verlag, New York, **1986**.
42. Weber E, Csöregh I, Stensland B and Czugler M. A novel clathrate design: selective inclusion of uncharged molecules *via* the binaphthyl hinge and appended co-ordinating groups. X-ray crystal structures and binding modes of 1,1'-binaphthyl-2,2'-dicarboxylic acid host/hydroxylic guest inclusions. *J. Am. Chem. Soc*., **1984**, 106, 3297-3306.
43. Alibert S, Santelli-Rouvier C, Pradines B, Houdoin C, Parzy D, Karolak-Wojciechowska J and Barbe J. Synthesis and effects on chloroquine susceptibility in Plasmodium falciparum of a series of new dihydroanthracene derivatives. *J. Med. Chem*., **2002**, 45, 3195-3209.
44. Wang B, Feng X, Huang Y, Liu H, Cui X and Jiang Y. A highly enantioselective hetero-Diels-Alder reaction of aldehydes with Danishefsky's diene catalysed by chiral Titanium(IV) 5,5', 6,6', 7,7', 8,8'-octahydro-1,1'-bi-2-naphthol complexes. *J. Org. Chem*., **2002**, 67, 2175-2182.
45. Jain N and Bedekar AV. Roof shape chiral alcohol: Auxilliary for asymmetric synthesis of α-halo acid derivatives. *Tetrahedron Letters*, **2016**, 57, 692-695.
46. Jain N, Mandal MB and Bedekar AV. Roof shape amines: Synthesis and application as NMR chiral solvating agents for discrimination of α-functionalised acids. *Tetrahedron*, **2014**, 70, 4343-4354.

47. Gupta R, Gonnade RG and Bedekar AV. Application of roof shape amines as chiral solvating agents for discrimination of optically active acids by NMR spectroscopy: Study of match-mismatch effect and crystal structure of the diastereomeric salt. *J. Org. Chem*., **2016**, 81, 7384-7392.

48. Csöregh I, Czugler M, Ertan A, Weber E and Ahrendt J. Solid-state binding of dimethylsulphoxide involving carboxylic acid host molecules. X-ray crystal structures of four inclusion species. *J. Incl. Phenom. Mol. Rec. Chem*., **1990**, 8, 275-287.

49. Wu X, Kang W, Zhu D, Zhu C and Liu S. Synthesis, crystal structure and biological activities of two novel organotin(IV) complexes constructed from 12-(4-methylbenzoyl)-9,10-dihydro-9,10-ethanoanthracene-11-carboxylic acid. *J. Organometallic Chem*., **2009**, 694, 2981-2986.

50. Sasaoka A, Uddin MI, Shimomoto A, Ichikawa Y, Shiro M and Kotsuki H. A novel design of roof-shaped anthracene-fused chiral prolines as organocatalysts for asymmetric Mannich reactions. *Tetrahedron: Asymmetry*, **2006**, 17, 2963-2969.

51. Platzer N, Rudler H, Barkaoul L, Denise B, Goasdouė N, Rager M-N, Alvarez C, Vaissermann J and Daran J-C. Praseodymium NMR-Shift reagents for carboxylic acids and their carboxylates: Synthesis, X-ray structure and applications. *Bull. Soc. Chim. Fr.*, **1995**, 132, 95-113.

52. Jain N and Bedekar AV. Lipase catalysed desymmetrization of roof shape *cis*-11,12-*bis*(hydroxymethyl)-9,10-dihydro-9,10-ethanoanthracene. *RSC Adv*., **2015**, 5, 62678-62685.

53. Kurata A, Kurihara T, Kamachi H and Esaki N. Asymmetric reduction of 2-chloroacrylic acid to (*S*)-2-chloropropionic acid by a novel reductase from *Burkholderia sp. WS*. *Tetrahedron: Asymmetry*, **2004**, 15, 2837-2839.

*54.* Breuer M, Ditrich K, Habicher T, Hauer B, Keβeler M, Stürmer R and Zelinski T. Industrial methods for the production of optically active intermediates. *Angew. Chem., Int. Ed.,* **2004***,* 43, 788-824.

55. Aam BB and Fonnum F. (+/-)-2-Chloropropanoic acid elevates reactive oxygen species formation in human neutrophil granulocytes. *Toxicology*, **2006**, 228, 124-134.

56. Simpson MG, Wyatt I, Jones HB, Gyte AJ, Widdowson PS and Lock EA. Neuropathological changes in rat brain following oral administration of 2-chloropropanoic acid. *Neurotoxicology*, **1996**, 17(2), 471-480.

57. Lock EA, Gyte A, Duffell S and Wyatt I. The effect of postnasal age on *L*-2-chloropropanoic acid-induced cerebellar granule cell necrosis in the rat. *Arch. Toxicol*., **2001**, 74, 783-788.
58. Bodnár J, Gubicza L and Szabó L-P. Enantiomeric separation of 2-chloropropanoic acid by enzymatic esterification in organic solvents. *J. Mol. Cat*., **1990**, 61, 353-361.
59. Fu S-CJ, Birnbaum SM and Greenstein JP. Influence of optically active acyl groups on the enzymatic hydrolysis of *N*-acetylated-*L*-amino acids. *J. Am. Chem. Soc*., **1954**, 76, 6054-6058.

# Chapter 4

## Factors playing a role in the resolution of racemates

Resolution, the separation of a racemic modification (racemate) into enantiomers, often results in the formation of salts, co-crystals, hydrates, solvates and/or polymorphs.

Up to this day the problems encountered during optical resolution have remained unsolved, despite the decades that have passed since Pasteur discovered this technique. Regardless of the practical significance of the resolution technique, the effect of kinetic and thermodynamic factors together with the structural basis of resolution, during optical resolution *via* diastereomeric salt formation are not known, including the mechanism involved in the resolution of racemates.[1]

Crystalline materials acquire their principal physical characteristics from the molecular positioning within the solid; and changing the orientation and/or hydrogen bond patterns between these molecules can have a direct effect on the properties of the specific solid. The chemical and physical solid-state characteristics of active pharmaceutical ingredients (APIs) can be altered by the formation of hydrates, polymorphs, salts, solvates and co-crystals.[2]

In the crystalline solid-state the difference between a salt and a co-crystal is subtle, reliant on the unambiguous position of a hydrogen atom and the involvement/non-involvement of charges, as depicted in Figure 4.1. In addition, the relative lengths of the two C-O distances are important, being approximately the same in the salt and significantly different in the co-crystal.

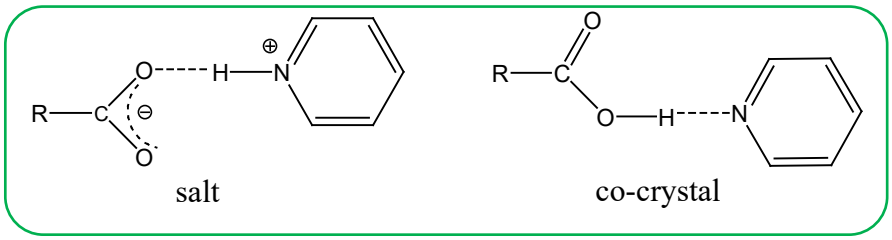


Figure 4.1 Salt *vs* co-crystal formation.

Salt generation is one of the main solid-state methods utilized to change the physical characteristics of APIs in the pharmaceutical industry, and it is estimated that more than half of the medicines on the market are sold as salts.[2] For salt formation the API must possess appropriate basic or acidic groups. Co-crystallization of an API with a suitable co-former provides an alternative route for improving physicochemical properties of drugs. Pharmaceutical co-crystals offer a lot of opportunities in the modification of the chemical or physical characteristics of an API without the formation or destruction of covalent bonds.[2]

## 4.1. Co-crystals and salts

There has been much debate in the literature about what constitutes a co-crystal. Pharmaceutical co-crystals are crystals that have an API as one of the molecular species in the multicomponent crystal. According to the literature there are several definitions of co-crystals,[3-6] including the following, "a molecular complex that contains two or more different molecules in the same crystal lattice"[7] and "crystalline material made up of two or more components, usually in a stoichiometric ratio, each component being an atom, ionic compound, or molecule".[8] A more current definition of a co-crystal is, "cocrystals are solids that are crystalline single phase materials composed of two or more different molecular and/or ionic compounds generally in a stoichiometric ratio".[9]

Several factors are important in the design of multicomponent crystals. These include the number of hydrogen bond donors and acceptors, and the differences in p$K_a$'s of the reacting molecules.[10,11] A CSD analysis by Fábián showed that molecular polarity and size affect co-crystallization.[12]

On using a carboxylic acid as a co-former or when a neutral hydrogen bond (O—H···N) is formed between an acid and a base, IR spectroscopy can be a very powerful tool in detecting co-crystal formation. The differences in IR spectra can be used to interpret results as to whether a neutral carboxylic acid moiety or a carboxylate anion is formed. A neutral COOH group is represented by a strong C=O stretching frequency around 1700 $cm^{-1}$ and a weaker C—O stretching frequency around 1200 $cm^{-1}$. The carboxylate anion ($-COO^-$), as a result of resonance, is represented by a single C—O stretching frequency in the fingerprint region of 1000 – 1400 $cm^{-1}$. If a neutral intermolecular O—H···N hydrogen bond has resulted between the components, two broad stretching frequencies are noticeable around 2450 and 1950 $cm^{-1}$. The nature of the carboxylic acid system can also be verified by measuring the C—O and C=O bond distances from the X-ray diffraction results. A classic C=O bond length is about 1.2 Å and the C—O bond length is approximately 1.3 Å, loss of a proton gives rise to the resonance stabilized C—O bond distances being of the same length.[13]

These various characterization techniques can be used to help differentiate between a co-crystal and a salt, in some cases differentiation between the two may be challenging.[14]

Schultheiss and Newman[2] have highlighted instances where the physicochemical characteristics of an API have been fine-tuned *via* the formation of API-based co-crystals, with reference to the melting point (mp), stability, solubility, dissolution and bio-availability. They found that mp's are altered for some of the co-crystals, roughly 50.7% resulting in a mp between

those of the API and co-former and 38.8% resulting in a lower mp. In a few instances improved stability of the co-crystal inhibits the formation of hydrates. Poorly soluble compounds' solubility was improved by using co-crystals, and in other publications it has been demonstrated that salt formation is a common method used to improve solubility.[15] Co-crystals on the other hand can offer higher and lower dissolution rates in comparison to the API.

"To date, predicting whether or not a co-crystallization reaction will be successful is not yet possible".[16] Therefore, chemical reactions need to be carried out experimentally under various reaction conditions with various techniques to obtain suitable co-crystals.[2]

## 4.2. Polymorphs

Polymorphs are the different crystalline forms resulting from the same substance. Some scientists consider solvation or hydration by-products as a type of polymorph (sometimes known as pseudopolymorphs).[9] However the term 'pseudopolymorph' is discouraged and should be replaced by 'solvate'.[17,18] This was also debated against, with some preferring to retain the term, 'pseudopolymorph'.[19,20]

## 4.3. Are crystal structures predictable?

Gavezzotti[21] posed the question, "Are crystal structures predictable?" in 1994, and his immediate answer was "No". He based this on questions he posed in his study. One of the questions was, "Will this compound crystallize at all?" According to thermodynamics every pure compound will crystallize provided the temperature is low, or the pressure is high enough. However organic chemistry occurs under mild temperature-pressure conditions where kinetics plays a role. Gavezzotti also noted that crystal growth from solution is problematic while dissolution always works in certain solvents, and a crystal is more easily destroyed than constructed.[21] Solidification, crystal growth and crystal morphology are difficult to control due to kinetic factors.[22]

Gavezzotti further concluded that the melting temperature was one of the most problematic crystal characteristics to predict, the total lattice energy carried no data on the geometrical framework of the crystal. Furthermore, he stated it was impossible to predict the entire structure of any organic crystal including the atomic positions, cell parameters and space group.[23]

Therefore, a co-operation between statistical investigations, energetic studies on the basis of crystal kinetics and thermodynamics, and static and dynamic computational techniques will presumably guide theoretical chemists in crystal structure prediction.

In 2003 Dunitz[24] supported Gavezzotti in his publication, stating that the question regarding the formation of crystals was more difficult, very little was known and it was much more problematic to make realistic calculations computationally.

Finding a resolving agent for a specific racemate requires the strenuous experimental screening of numerous candidate resolving agents. A predictive system for racemate resolution would be preferable, even to reduce a lengthy list of possible chiral resolving agents to the most promising candidates. Leusen reported that intrinsic thermodynamics showed that the resolution efficiency of a suitable resolving agent was related to the lattice energy difference between the global energy minima found for both diastereomeric salts in a pair. The accuracy of his calculations on lattice energy were insufficient to reliably predict the stability order of potential diastereomeric salts. Improvement in computer speed, the efficacy of search algorithms for versatile compounds, analysis tools and the accuracy of lattice energy calculations were needed to improve the prediction of crystal formation.[25]

With the advancement of research on crystal structure prediction (CSP), Dunitz and Gavezzotti described the CSP as an exercise in which unknown crystal structures of organic fragments are to be guessed (deduced) from the information provided by molecular connectivity.[26] In 2005, Karamertzanis and Price[27] studied the challenges of CSP of diastereomeric salt pairs, where they provided a notable advance over traditional search algorithms and empirical force fields in illustrating the structures and relative stabilities of diastereomeric salt pairs. In 2014, Price concluded that the primary use of CSP investigations was to find the range of various packings that are credible structures, thermodynamically. A systematic CSP investigation can reduce or expand the time required for experimental work to determine the total complexity of the solid state landscape of a molecule by either verifying that all practically possible polymorphs are known, or suggesting additional structures that should be searched for.[28]

CSP has evolved since the 1999 collaborative workshop that was held at the Cambridge Crystallographic Data Centre. The workshop was to test the performance of accessible methods of crystal structure prediction on organic compounds.[29] Crystal structures of organic compounds were predicted from their molecular structures, and the results offered more information regarding the possibilities and limitations, and hope in crystal structure prediction. The latest outcomes revealed the applicability of the state of the art CSP calculations in a broad range of products, in salts, hydrates and in more flexible and large organic compounds.[30-34]

## 4.4. The role played by the p$K_a$

In 2008 Gilli *et al*.[35] emphasized the role played by the p$K_a$ equalization, by using an instrument called the p$K_a$ slide rule. This is a bar chart that reports in various scales the p$K_a$'s of the D—H proton donors and :A proton acceptors most regularly involved in D—H···:A bond formation. D—H are termed hydrogen bond donors (acids) with a dissociation constant $K_a = K_{AH}$, and the :A hydrogen bond acceptors (bases) with a dissociation constant $K_a = K_{BH^+}$. The equation describing the change in p$K_a$ takes the form $\Delta pK_a(D—H\cdots:A) = pK_{AH}(D—H) - pK_{BH^+}(A—H^+)$, and is negative or positive depending on whether or not the $D:^-\cdots H—A^+$ proton transfer occurred. Their study was to establish a practical tool for estimating hydrogen bond strengths from the acid-base parameters of the interacting molecules and they verified those predictions by comparing the experimental values.[35]

According to their study the p$K_a$ equalization concept states that the strength of the D—H···:A bond increases with the decreasing $\Delta pK_a = pK_a(D—H) - pK_a(A—H^+)$, and the strength gets to a maximum when $\Delta pK_a$ approaches zero.

Cruz-Cabeza[36] calculated the differences in the aqueous p$K_a$ values ($\Delta pK_a$) for 6465 crystalline complexes comprising ionized and non-ionized acid-base pairs reported in the CSD where the possibility of proton transfer between acid-base pairs had been derived for crystalline complexes with $\Delta pK_a$ between -1 and 4, and the p$K_a$ rule was validated and quantified.

The p$K_a$ rule is used to predict the formation of salts, where it is accepted that when the p$K_a$ difference between a co-crystallizing acid and base is greater than 2 or 3 [$\Delta pK_a = pK_a$(protonated base) – p$K_a$(acid) > 2 or 3], salt formation is expected. This rule of thumb had been exemplified by a finite number of investigations in the reported literature, on small datasets of multicomponent complexes.[37,38] Cruz-Cabeza concluded that for $\Delta pK_a$ less than -1, non-ionized species were observed, ionized acid-base pairs were found when $\Delta pK_a$ is greater than 4. For $\Delta pK_a$ between -1 and 4, every increase in the $\Delta pK_a$ difference increases the possibility of proton transfer between the proton donor and the proton acceptor.

Ramon *et al*.[39] crystallized a vast series of five substituted benzoic acids with ten substituted pyridines and quinolines, with their $\Delta pK_a$'s varying from -1.14 to 4.16 (base – acid), the uncertainty region for the formation of salt *vs* co-crystal.

Most of their results verified that structure formation of co-crystal *vs* salt crosses over at $\Delta pK_a = 2$. They also reported a structure that did not follow the general rule. The structure was obtained by combining 4-aminobenzoic acid and 6-aminoquinoline ($\Delta pK_a = 0.38$) and a salt

was formed. Based on the Cruz-Cabeza investigation, there is a 34% probability of the molecule being a salt at this value of $\Delta pK_a$, and their study revealed that secondary hydrogen bonds can influence the stabilization of the ionic structure.

## 4.5. Molecular lengths of compounds

The selection of an appropriate chiral resolving reagent for an earmarked racemic molecule is achieved predominantly by time consuming trial-and-error methods. The prediction or rational engineering of an appropriate resolving reagent is a matter of importance, especially in the pharmaceutical industry.

Mandelic acid (**MA**) (**4.1**) is one of the most frequently used resolving reagent.[40] Sakai *et al*. [41] found that enantiomerically pure **MA** could resolve 1-(3-methoxyphenyl)ethylamine as well as 1-phenylethylamine through the formation of a diastereomeric salt and the crystal structures of their most stable salts were very similar to each other. Therefore, an investigation regarding the resolution of the 1-arylalkylamines by **MA** would provide a way to engineer a more appropriate resolving reagent for these amines.

In 1996 Kinbara *et al*. undertook a study to design resolving agents for the 1-arylalkylamines by addressing the role played by a substituent in 1-arylalkylamines on the resolution effectiveness through the formation of a diastereomeric salt with **MA** (**4.1).** An equimolar mixture of (*R)*-**MA** and the racemic amines **4.2**-**4.10** led to the resolution of the amines at 38 °C,[42] with the summary of the results in Table 4.1.

Table 4.1 The resolution results of 1-Arylalkylamines **4.2**-**4.10** by *(R)*-**MA**.[42]

| Entry | Racemic amine | Solvent | Resolution efficiency |
|---|---|---|---|
| 1 | **4.2** | Water | 0.66 |
| 2 | **4.3** | Water | 0.75 |
| 3 | **4.4** | Water | 0.71 |
| 4 | **4.5** | Water | 0.56 |
| 5 | **4.6** | MeOH | 0.11 |
| 6 | **4.7** | MeOH | 0.62 |
| 7 | **4.8** | Water/MeOH | 0.65 |
| 8 | **4.9** | MeOH | 0.04 |
| 9 | **4.10** | MeOH | 0.03 |
| Resolution efficiency = yield (%) x diastereomeric excess (% de) x 2/100 | | | |

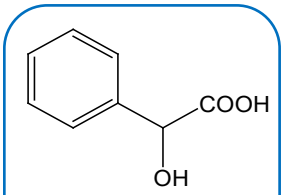


**4.1**

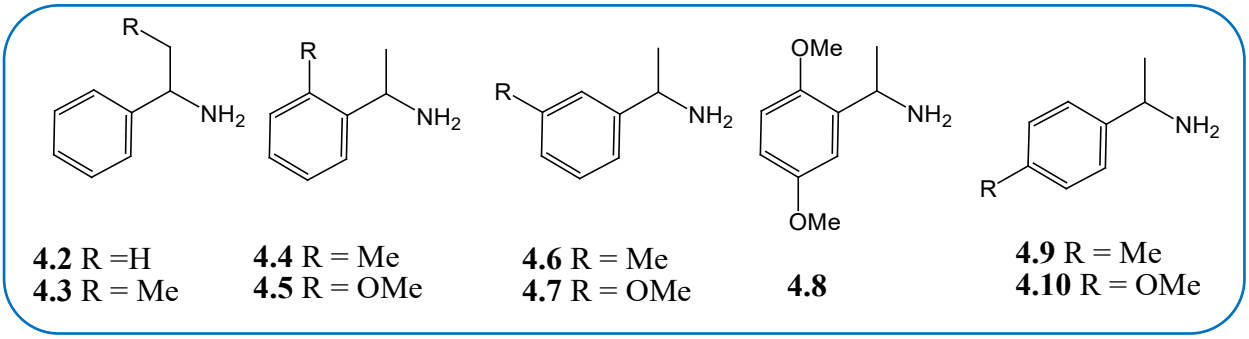


**4.2** R =H
**4.3** R = Me

**4.4** R = Me
**4.5** R = OMe

**4.6** R = Me
**4.7** R = OMe

**4.8**

**4.9** R = Me
**4.10** R = OMe

Their results (Table 4.1) showed a relationship between the location of the substituent on the racemic amines and the resolution efficacy. (*R)*-**MA** systematically resolved **4.2** - **4.5**, which had a substituent at the *o*-position on the aromatic ring. **4.9** and **4.10** were scarcely resolved and they had a substituent at the *p*-position of the aromatic ring. The results of the *m*-substituted amines **4.6-4.8** depended on the amines. The relationship was interpreted based on the molecular length of the amines. The molecular length of the *p*-substituted 1-arylalkylamines was longer than that of (*R*)-**4.1**, the *o*-substituted isomer had similar molecular length.

It was proposed that the amines which had similar molecular length to that of **4.1** could be efficiently resolved by **4.1**. On the other hand, the results indicated that the longer molecular length resolving agents would be efficient in resolving *m*- and/or *p*- substituted 1-arylalkylamines.

Kinbara *et al*.[42] then prepared the (*S*)-*p*-methyl**MA**, (*S*)-**4.11** and (*R*)-*p*-methoxymandelic acid, (*R*)-**4.12**, which had similar molecular lengths to **4.9,** and these were used to resolve **4.9** and **4.2** (Table 4.2).

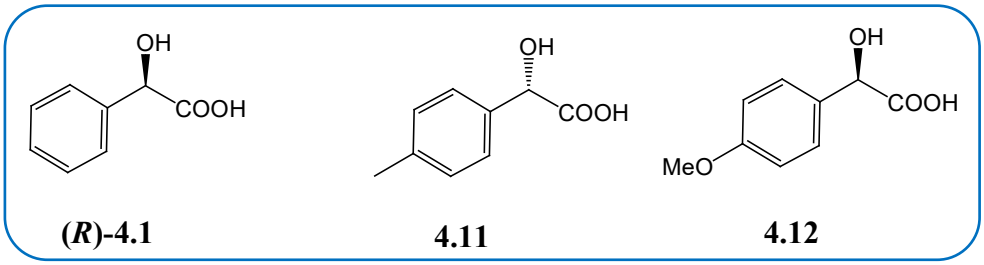


**(*R*)-4.1**

**4.11**

**4.12**

Table 4.2 The resolution results of **4.2**, **4.6**, **4.9** and **4.10** by **4.11** and **4.12**.[42]

| Entry | Racemic Amine | Resolving Reagent | solvent | Resolution efficiency |
|---|---|---|---|---|
| 1 | **4.2** | **4.11** | MeOH | 0.59 |
| 2 | **4.9** | **4.11** | MeOH | 0.54 |
| 3 | **4.2** | **4.12** | MeOH | 0.62 |
| 4 | **4.9** | **4.12** | MeOH | 0.61 |
| 5 | **4.6** | **4.12** | MeOH | 0.57 |
| 6 | **4.10** | **4.12** | MeOH | 0.29 |

The *p*-substituted **MA** compounds showed a higher resolving ability for **4.9**, which increased in the order (*R*)-**4.1** < (*S)*-**4.11** < (*R*)-**4.12**. (*R*)-**4.12** improving the resolution efficiency of **4.6** and **4.10**. The *p*-substituted **MA** compounds were efficient in resolving the 1-arylalkylamines that were scarcely resolved by (*R*)-**4.1**, and they had a higher resolving ability for **4.2** as did (*R*)-**4.1**. Therefore (*S*)-**4.11** and (*R*)-**4.12** would be able to resolve 1-arylalkylamines with shorter molecular lengths as well as those with similar molecular lengths.

The results suggested that the molecular length of the resolving agent and the molecule to be resolved play a specific function in the mechanism of resolution.

Later on, Kinbara *et al*.[43] undertook a crystallographic survey of their crystal structures of a pair of the diastereomeric salts to get a clarification on the mechanism of chiral selection. They studied the crystal structures of the most stable salts of **4.2** and **4.9** with (*R*)-**4.12**. The crystal structure of the more stable salts of (*R*)-**4.12**·(*R*)-**4.9** revealed that a hydrogen-bond network similar to those of the more stable salts (*R*)-**4.1**·(*R*)-**4.2**, (*R*)-**4.1**·(*S*)-**4.4** and (*R*)-**4.1**·(*R*)-**2.7** was also formed. Hydrogen bonded columns around a two-fold screw axis ($2_1$-columns) were formed between the $COO^-$ and the ammonium groups and a layered network was constructed by linkage of the $2_1$-columns. The failure of the resolution of **4.9** with (*R*)-**4.1** was ascribed to the projection of the *p*-substituent of the amine out of the hydrogen-bond layer consisting of $2_1$-columns. In the crystal structure of (*R*)-**4.12**·(*R*)-**4.9** both the methoxy group of (*R*)-**4.12** and the *p*-methyl group of **4.9** projected out of the layer making the boundary surfaces planar.

A similar hydrogen bond layer was obtained in the crystal of the more stable (*R*)-**4.12**·(*R*)-**4.2** that precipitated on crystallization. The planarity of the boundary surfaces was preserved regardless of the presence of a *p*-substituent on (*R*)-**4.12**. When the molecular length of the amine to be resolved is shorter than that of the resolving acid being employed, the carboxylate

molecules can alter their conformation to a certain extent to make the boundary surfaces of the layer planar, thereby maintaining the interlinking of $2_1$-columns.[43]

It was concluded that the formation of a hydrogen bond layer, consisting of $2_1$-columns and having planar boundary surfaces is mandatory for a well-organized resolution, and to form the hydrogen bond layer, the length of the molecule should be similar to or a little shorter than that of the resolving agent being employed.

Kinbara *et al*.[44(a)] later considered that the variabiity of the substituent at the *p*-position of the aromatic ring of the resolving reagent made the molecular length ambiguous, thereby reducing the resolution efficacy. They designed another resolving agent, (2-naphthyl)glycolic acid (2-**NGA**), **4.13**, that had a rigid skeleton and a suitable molecular length. The (*R*)- and (*S*)-**4.13** was used as a resolving agent for various *p*-substituted 1-arylethylamines, **4.14**.

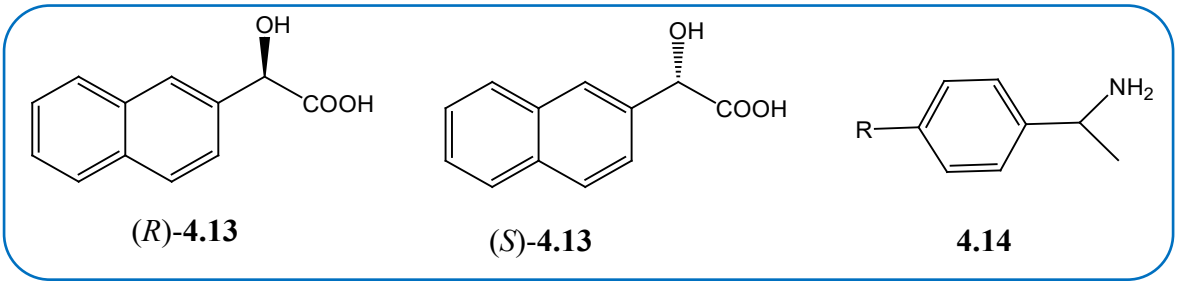


(*R*)-**4.13** (*S*)-**4.13** **4.14**

The results show an appreciable resolving ability of **4.13** over a wide range of **4.14** compounds (R = Me, Et, Pr, OMe, cyclohexane, Cl, Br, $NO_2$ and 1-naphthyl). The absolute configurations of the amines in the more stable salts agreed with that of 2-**NGA**, it suggested that a common chiral discrimination mechanism was responsible for the resolution of *p*-substituted 1-arylalkylamines.

## 4.6. Solvents, dielectrically controlled resolution (DCR)

The role of the solvent used in the process of chiral recognition has received much attention. The function of the solvent is to dissolve both the resolving agent and the earmarked racemate mixture, but it has been shown that the properties of the media have an influence on the molecular recognition. Sakai *et al*. undertook a vast number of experiments to investigate the effects of solvent on chiral resolution, which is a typical phenomenon of molecular discrimination.[45] In the course of their studies they discovered an example of an extreme effect of solvent on chiral resolution, where chiral recognition was governed by the dielectric properties of the solvents used. They then termed the phenomenon dielectrically controlled resolution (DCR).

4.6(a) (*R,S*)-α-Amino-ε-caprolactam:*N*-tosyl-(*S*)-phenylalanine system

During the resolution of (*R,S*)-α-amino-ε-caprolactam (**ACL**), (**4.15**) with *N*-tosyl-(*S*)-phenylalanine **4.16** high optical yields for (*R*)- and (*S*)-**ACL** could be obtained only by altering the dielectric constants (ε) of the solvents used.

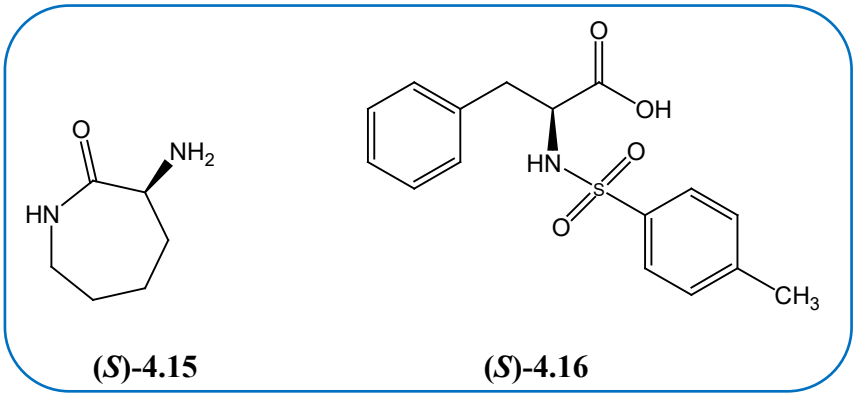


**(*S*)-4.15** **(*S*)-4.16**

The outcomes of a number of resolution experiments obtained for the (*R,S*)-**4.15**:(*S*)-**4.16** system in different alcohol-water solvent systems[46] showed that (*S*)-**4.15** was more favourably discriminated in the solvents with ε between 26 and 58. In the solvents with ε less than 26 and greater than 58, (*R*)-**4.15** was precipitated. In a solvent with a low dielectric constant the electrostatic contacts between polar groups of the molecules get stronger and they can approach close enough to interact. For this reason the (*R*)-**4.15**:(*S*)-**4.16** crystal was formed from the solvent system with a ε of 18. In solvent systems with moderate dielectric constants polar groups should be separated. Under such conditions a water molecule is required to retain the close packing of the hydrophilic layer. Thus (*S*)-**4.15** was preferentially discriminated. The (*S*)-**4.15**:(*S*)-**4.16** $H_2O$ crystal was formed from the solvent system with a ε of 34.[46]

The crystal structures of (*R*)-**4.15**:(*S*)-**4.16** and (*S*)-**4.15**:(*S*)-**4.16** $H_2O$ showed that the hydrophilic layers obtained in the crystals can accommodate the two isomers, (*R*)-**4.15** and (*S*)-**4.15**. The recognition of one of the enantiomers might be a matter of selecting the necessary intermolecular contacts between the chiral discriminator and the enantiomer to be recognized. The resultant data suggested that the modes of the intermolecular contacts could be governed by changing the dielectric property of the used solvent.[45]

4.6(b) (*R,S*)-2-Methylpyrrolidine: (*R,R*)-2,3-dihydroxybutanedioic acid system

In the earlier systems aromatic rings played prominent roles in molecular discrimination. Sakai *et al.*[45] studied the impact of dielectric attributes of the solvent on various resolution systems that did not have aromatic rings. Enantiomerically pure 2-methylpyrrolidine (**MPRD**), **4.17** is

an important key intermediate in the pharmaceutical industry for ABT-239 which is an accepted histamine $H_3$ receptor antagonist for Alzheimer disease.[47] Sakai *et al*. found that (*R,R*)-2,3-dihydroxybutanedioic acid, **4.18** was an appropriate chiral discriminator and they used it to show the DCR phenomenon.

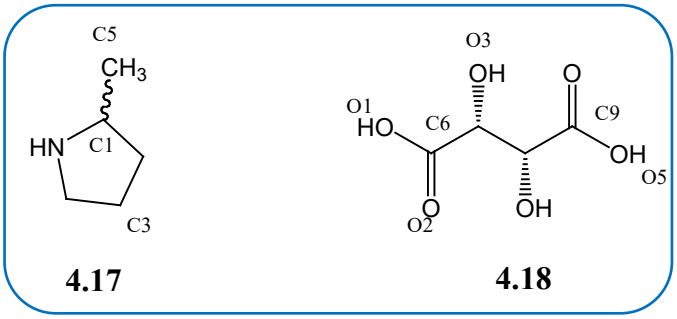


**4.17** **4.18**

The resultant outcomes of a vast number of resolution experiments achieved after the treatment of (*R,S*)-**4.17** and (*R,R*)-**4.18** system in EtOH/water mixed solvents[45] showed that the preferred enantiomer of **4.17** in the salt obtained by the resolution process depended on the dielectric constant of the solvent employed. The more stable diastereomeric salt of (*R*)-**4.17**:(*R,R*)-**4.18** resulted from the mixed solvents with dielectric constant equal to or greater than 24 and equal to or less than 29. (*S*)-**4.17**:(*R,R*)-**4.18** $H_2O$ resulted from solvents with the dielectric constants equal to or greater than 30 and equal to or less than 36. The latter salt contained a water molecule.[45,48]

The study signified that the DCR phenomenon also occurs in a resolution system that lacks aromatic rings. The chiral discriminator (*R,R*)-**4.18** formed chains linked by strengthened negative charge assisted hydrogen bonds [(-)CAHBs].[40] The theory is that in the solution the chains built layers, and between the layers a particular chiral space was generated and one of the enantiomers of **4.17** was selected into that space. The size and shape of the space depended on the dielectric constant of the solvent system. In solvents with a larger dielectric constant the hydrophilic layers are isolated and a bigger chiral space was obtained.[45]

4.6(c) (*R,S*)-Phenyl-2-*p*-Tolyl Ethanamine : (*S*)-2-Hydroxy-2-phenylethanoicic acid system

Phenyl-2-*p*-tolyl ethanamine (**PTE**) **4.19** was resolved by (*S*)-mandelic acid (**MA**) (2-Hydroxy-2-phenylethanoic acid) (*S*)-**4.1**). Sakai *et al*. undertook well-structured experiments to study the effects of dielectric properties of solvents on the resolution of racemates.[45]

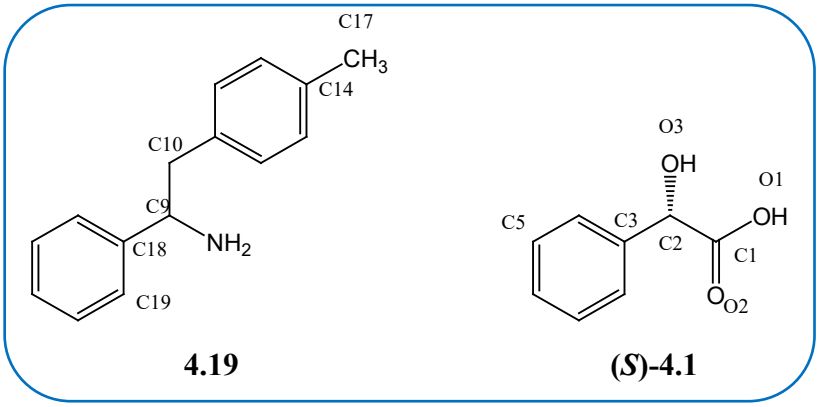


**4.19** **(*S*)-4.1**

The results showed that the DCR phenomenon occurred as predicted.[49] (*R*)- and *(S)*-**4.19** resulted with the highest efficacy when the absolute ethyl alcohol ε was equal to 24 and 74% EtOH (ε = 38) were used. In the two crystal structures (*R*)-**4.24**:(*S*)-**4.1** and (*S*)-**4.24**:(*S*)-**4.1**:$H_2O$ the (*S*)-**4.1** molecules are similarly packed and formed a chiral space where **4.19** molecules were recognized. The conformations of **4.24** molecules differed in the two crystals.

The geometrical differences indicated that the chiral discriminators and the target molecules would experience conformational adjustments to form crystals in which both enantiomers could be discriminated by the same resolving agent.[45]

In the solution, (*S*)-**4.1** likely aggregated to form columns interspersed with chiral spaces. In the smaller dielectric constant solvents, the columns were close together and formed small chiral spaces, and O2 formed hydrogen bond interactions with the ammonium ion. Only the (*R*)-**4.19** could be discriminated at the abovementioned chiral space. In the solvents with larger dielectric constants the separation between the columns was increased because of the reduced electrostatic contacts between them. The water molecules were then incorporated between the columns to preserve the crystal packing. In the larger chiral spaces only (*S*)-**4.19** was recognized. Therefore, both **4.19** and **4.1** had to experience some degree of conformational adjustments to realize the perfect discrimination.[45]

In 1994 Kozma *et al*. analyzed the DSC results of sixteen conglomerate forming diastereomeric salt pairs. The study was about the prediction of which diastereomeric salt precipitates during an optical resolution through diastereomeric salt formation. The sixteen conglomerates forming diastereomeric salt pairs belonged to successful resolutions. It was always the diastereomeric salt with the higher melting point that precipitated during the optical resolutions of a racemate by fractional crystallization. In their studies the solvated salt was the less soluble salt and it precipitated during the process of resolution.[49]

Kozma *et al*.[50] also studied the function of the solvents in the optical resolution of α-phenylethanamine (**4.2**) by 2*R*,3*R*-2,3-dihydroxybutanedioic acid (**4.18**). The optical resolution

of this amine was carried out in methanol in 1965, and it was an efficient resolution.[51] Kozma *et al*. accomplished the resolution in MeOH, water, EtOH, acetonitrile, and in two solvent mixtures [1:1 ratio (v/v) mixture of MeOH:acetonitrile and MeOH:water]. In the salts that precipitated from MeOH containing solvents, (*S*)-(-)-**4.2** was in abundance and in the other solvents the salts contained the (*R*)-(+)-**4.2** in abundance. The TGA and DSC measurements of the salts revealed the pure (*S*)-(-)-**4.2**•(2*R*,3*R*)-(+)-**4.18** salt did not contain any solvent. The salts that precipitated from MeOH and MeOH:acetonitrile mixture contained very small amounts of the solvent. The (*R*)-(+)-**4.2**•(2*R*,3*R*)-(+)-**4.18** salt and the precipitates from the other solvents contained substantial but different amounts of solvent that evaporated from the substance between 30 and 85 °C.[50] The results indicated that (*S*)-(-)-**4.2**•(2*R*,3*R*)-(+)-**4.18** precipitated if water was not present in the process.

In water, EtOH and acetonitrile, a reversed and less effective resolution could be achieved by precipitation of a hydrate. Langkilde et al. deduced that the relative stability of the salts was:

(*S*)-(-)-**4.2**•(2*R*,3*R*)-(+)-**4.18** > (*R*)-(+)-**4.2**•(2*R*,3*R*)-(+)-**4.18**•hydrate > (*R*)-(+)-**4.2**•(2*R*,3*R*)-(+)-**4.18**

Generally, the introduction of water molecules into a structure gives rise to many hydrogen bond interactions. Based on the Langkilde et al.'s literature results, the incorporation of water did not necessarily lead to the less soluble and more stable diastereomeric salt. Their results showed that the hydrated salts fell almost equally between the less and the more stable salts.[52]

The role played by a solvent in the resolution of racemates was also showed by He *et al*. in the resolution of racemic sertraline (*rac*-**4.20**), an antidepressant of the selective serotonin reuptake inhibitor class, with (*R*)-mandelic acid (**4.1**).[53]

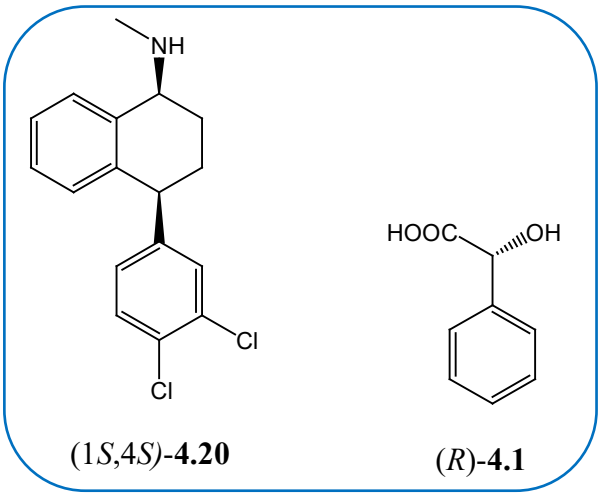


(1*S*,4*S*)-**4.20** (*R*)-**4.1**

In this example the solvent was not incorporated into the more stable salt but the less stable salt was solvated.[53] This result shows that the effect of solvent on the stability of diastereomeric salts is complex.

Solvents play other roles in the resolution rather than just being a dissolution medium. In general solvents are incorporated into crystal structures to provide more hydrogen bond sites or fill empty spaces which benefit the stability of the salts.[54-56] The solvent plays an important role in molecular recognition and in the racemic resolution process, Jacques *et al*. cited by Bialonska *et al*.[57] Borghese *et al*. demonstrated that a solvent can influence the effectiveness of the resolution process by redesigning the eutectic constitution.[58]

Solubility of a diastereomeric salt is one of the physical properties that needs to be considered as it governs resolution, or separation of the two salts from the solution. The solubility of a salt is directly related to the melting points and enthalpies of fusion. A resolution is easier when there is a large difference in the solubilities of the two possible diastereomeric salts.[40]

Kozma *et al*. reported that the diastereomeric salts with the higher melting points always precipitated during the optical resolutions of a racemate by fractional crystallization.[49] Other investigations reported the presence of a solvate to stabilize the less soluble salt compared to the unsolvated one, while in other studies the solvate was present in the more soluble salt.[39,42,44(a-c)] The dielectric constant of the solvent also dictates which diastereomeric salt will precipitate or will be less soluble in resolution.[45,46]

In another resolution study where the solvent played a determinant function in the solubility of the diastereomeric salts was determined by Wilen *et al*.[58(b)] Generally, a change in solvent impacts on the relative solubilities of the two diastereomeric salts to a slight extent. In some cases, the salt will only crystallize when solvated with a certain solvent.

2,2-Dimethyl-3-phenylpentanoic acid (**DMPPA**) on treatment with **QUIN** in EtOH and EtOH plus $H_2O$ gave rise to diastereomeric salts of different configurations (Scheme 4.1).[58(b)]


Scheme 4.1 The effect of solvent on the relative solubility of diastereomeric salts.[58(b)]

In EtOH the salt of the (+)-acid was less soluble and precipitated out of the solution, in EtOH + $H_2O$ the salt of the (-)-acid was less soluble. A change in solvent resulted in the precipitation of the opposite enantiomer. Solubility of the diastereomeric salt is one of the important factors in the resolution of racemates.

## 4.7. Aromatic CH/π interactions

The physical characteristics of a vast number of diastereomeric salts of the acids (**4.21** and **4.1**) and the base (**4.2**) have been demonstrated by Jacques *et al*. as cited by Suezawa *et al*.[59]

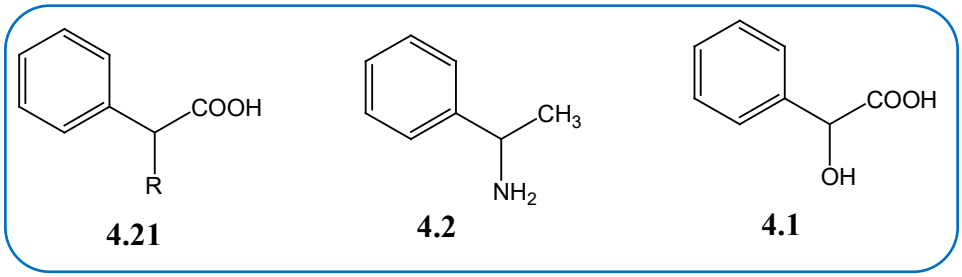


**4.21** **4.2** **4.1**

The more stable salt melted at a higher temperature than the less stable one in their elucidation of the mechanism of enantiomeric resolution. However, they could not explain the differences in solubility.[59]

Suezawa *et al*.[59] have carried out a methodical investigation to understand the concept underlying the process of chiral resolution using the CSD. They analyzed (in the context of the aromatic CH/π hydrogen bond) the crystal frameworks of fourteen pairs of diastereomeric salts that contained the mandelate anion and its analogues as the chiral acid constituent. They looked at the short aromatic CH/π attachments in the crystal frameworks of diastereomeric salts of hydroxyphenylethanoic acid and its derivatives. The C−H···π distance and the C−H···π plane access angle was smaller in the more stable salts than in the less stable salts.[59] It was concluded that the aromatic CH/π hydrogen bond plays a role in the mechanism of enantiomeric discrimination. Therefore, the contribution from the CH/π bonds should be taken into consideration in the analysis of enantiomeric resolution.

The anions and cations of (*S*)- and (*R)*-hydratropic acid (**4.21)** salts of (*S*)-1-phenylethanamine (**4.2**) were reported to possess a similar conformation in the various diastereomeric salts. The hydrogen-bond networks were similar and the only noticeable difference was the orientation of the phenyl rings of the acid and the base components of the salts. In the less soluble salt the phenyl rings were almost perpendicular to each other and in the more soluble salt the phenyl rings were nearly parallel to each other (Brianso cited by Suezawa *et al*.).[59]

Ogura *et al*. have demonstrated the significance of CH/π hydrogen bond interactions in the enantiomeric resolution, by (*R*)-arylglycyl-(*R*)-phenylglycine (**4.22**, where aryl referred to phenyl or naphthyl group), of the racemic mixtures of sulfoxides,[60,61] 1-arylethylamines[62] and

hydroxyl esters.[63] Tomori *et al*. have also resolved the racemic dibenzopyrazinoazepine by using the chiral 2,3-di-*O*-(arylcarbonyl)-2,3-dihydroxybutanedioic acids (**4.23**).[64]

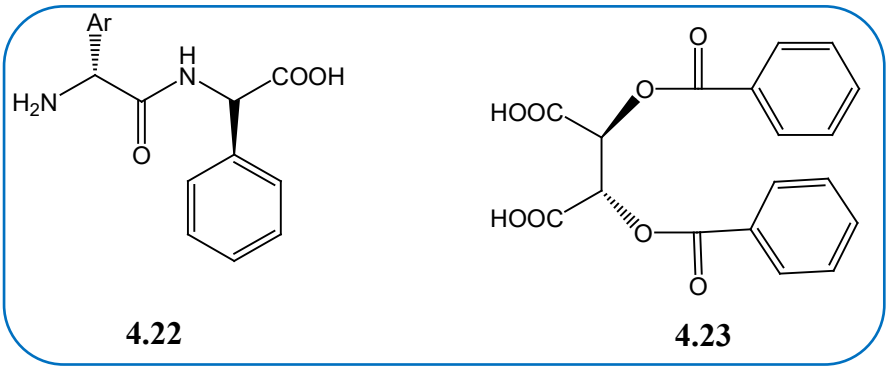


**4.22** **4.23**

The role of the CH/π hydrogen bond interaction in the resolution of *DL*-amino acids by the optically active 1,1'-binaphthalene-2,2'-diyl phosphate (**4.24**) was demonstrated by Fujii *et al*.[65] They indicated that the naphthalene moieties of **4.24** packed together in a special way *via* aromatic CH/π hydrogen bond interactions in the crystals.

In another study the crystal framework of the diastereomeric salts consisted of optically active 2-naphthylglycolic acid (**4.13**)[66] and 3'-4'-methylenedioxymandelic acid **(4.25**)[67] with a number of 1-phenylethanamine derivatives determined. The orientation of the aromatic system of **4.9** to that of **4.13** and **4.25** were different between the more stable and the less stable diastereomeric salts and a more condensed packing of the aromatic rings was found in the former salt compared to the latter. The results were argued in the framework of the CH/π hydrogen bond interaction, which suggested that the difference in solubility could be associated with the aromatic CH/π interaction and hydrogen bonding.

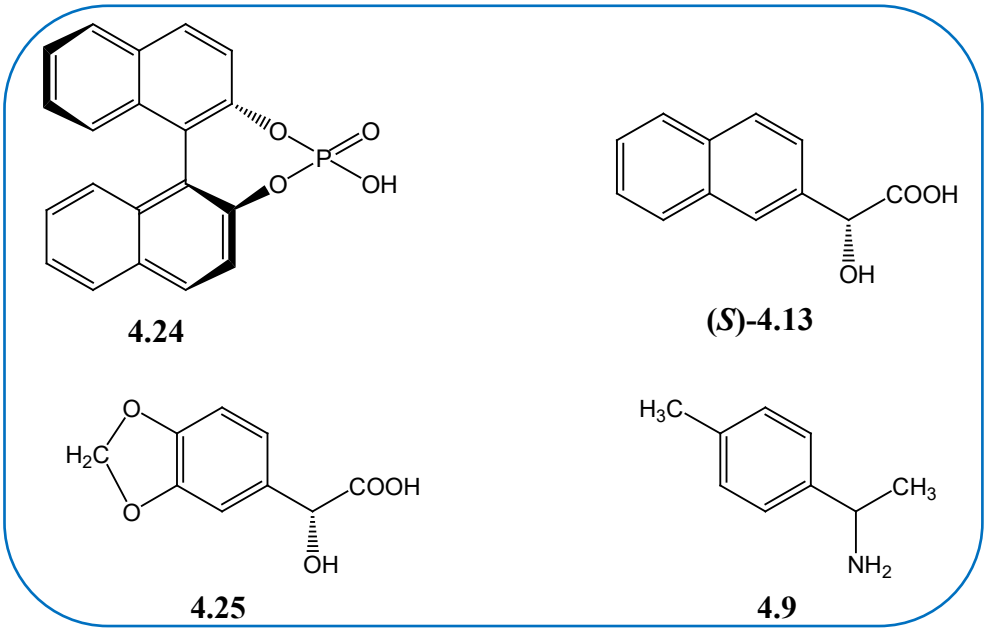


**4.24** **(*S*)-4.13**

**4.25** **4.9**

In 1999 Umezawa *et al*. completed a study using the CSD to investigate the role of the CH/π contact in the conformation of organic molecules. They noted a number of short intramolecular CH/π distances in the crystal framework of those molecules. The framework was investigated to determine whether the crystal conformation was as a result of the so called packing forces or whether the CH/π contact played a role. They concluded that the CH/π contact played a prominent role in governing the conformation of organic molecules.[68]

In 2007 Saigo and Kobayashi reported the role of CH/π interactions in the stabilization of the more stable diastereomeric salt crystals.[69] They performed an X-ray crystallographic determination of the diastereomeric salt crystals with **4.13** and with **4.26**, the results of which showed that efficient T-shaped CH/π interaction(s) were formed in the more stable diastereomeric salt crystals. The results suggested that enlarging the aromatic ring systems of the resolving agents was one of the logical designs for developing new efficient resolving agents. Periodic *ab initio* calculations to represent long range interactions, for the structures of *cis*-1-aminoben[f]indan-2-ol (**4.26**) and *cis*-aminoindan-2-ol (**4.27)** salt crystals demonstrated the co-operativity and hydrogen-bonding characteristics of the CH/π interaction in crystals.[69]

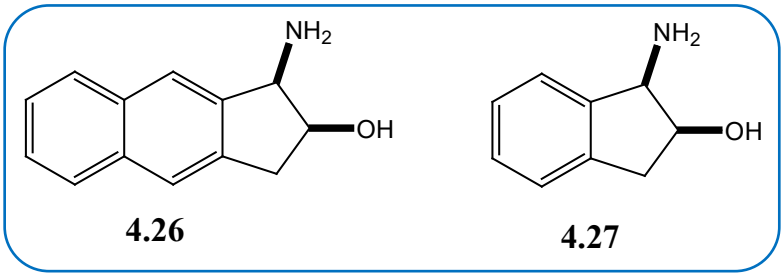


**4.26** **4.27**

## 4.8. Hydrogen bonding

A hydrogen bond is an interaction that is attractive and occurs between a hydrogen bond donor (DA) and the hydrogen bond acceptor (A) in the same molecule or between various compounds, represented by DH···A.[70] The strength of a hydrogen bond has been investigated which leads to the stabilization of molecular structures.[71,72] The description and importance of weak hydrogen bonds has been illustrated in several studies.[73-75]

In the formation of crystals, some atoms behave as hydrogen bond donors and others as hydrogen bond acceptors. Hydrogen bonds are either simple, where only one donor and one acceptor are involved, bifurcated (three-centre), or trifurcated (four centre), Figure 4.2, a few hydrogen bond donors and acceptors are listed in Table 4.3.

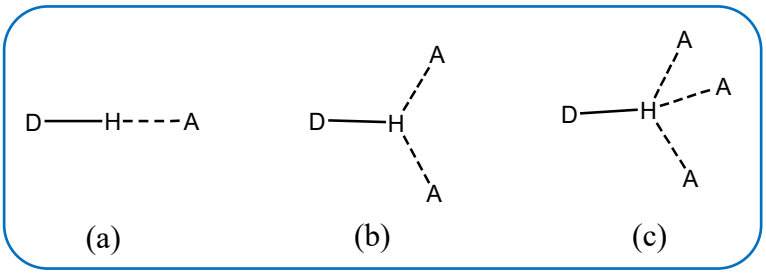


Figure 4.2 Common hydrogen bond arrangements, (a) simple, (b) bifurcated and (c) trifurcated.[76]

Table 4.3 Selcted hydrogen bond donors and acceptors.[76]

| Donors | Acceptors |
|---|---|
| C—H | C=C , C≡C , arenes |
| N—H | N |
| P—H | P |
| O—H | O |
| S—H | S |
| F—H | F |
| Cl—H | Cl |
| Br—H | Br |
| I—H | I |

In 2011, Arunan *et al*. gave the following definition of a hydrogen bond, after their discussion regarding the evolution of their understanding about hydrogen bonding,[77(a)]

"The hydrogen bond is an attractive interaction between a hydrogen atom from a molecule or a molecular fragment X—H in which X is more electronegative than H, and an atom or a group of atoms in the same or a different molecule, in which there is evidence of hydrogen bonding."[77(a)] One of the criteria used as evidence is based on the geometry and it points out that the three atoms X—H···Y tend toward linearity. X may be any element that has electronegativity greater than that of hydrogen such as F, N, O, C, P, S, Cl, Se, Br and I, and Y could be any of these elements and the pi-electrons. Typical weak hydrogen bonds include O—H···π, C—H···N and C—H···O interactions.[77(b)]

Hydrogen bonds play a vital role in the resolution of racemates by stabilising the crystal structures of the less soluble salts. Desiraju proposed that the C—H···O interaction, just like the O—H···O and N—H···O hydrogen bonds, is an electrostatic, attractive interaction with a range distance character. The bond's length is variable and it depends on the C—H bond acidity, and the angular approaches of the C—H and O—C groups that form the bond are predictable.[78] He suggested that chemists should consider all interactions, the weak ones (C—H···O,

O—H···C) and the strong ones (O—H···O, N—H···O), when attempting to understand hydrogen bond patterns and crystal packing.[78]

In many crystal structures weak hydrogen bonds are observed as secondary interactions compared to stronger hydrogen bonds. It has been revealed that these C—H···O interactions play an important role in structure stabilization.[79] They have also shown a conclusive impact on crystal packing in a vast number of cases,[80] and it was shown that they play a significant role in the recognition of host guest systems.[81] Hydrogen bonds have been reported to be the strongest interactions in crystal engineering, after the metal-coordination bonds, and are widely used since they are also directionally specific.[82]

The difference in the solubility between the pair of diastereomeric salts that are formed between a molecule to be resolved and a resolving agent contributes to the efficiency of resolution.[53] The solubility difference in turn is associated with the stabilities of the salts, which is determined by the crystal structures. Hydrogen bonds affect the packing of molecules in a crystal lattice, together with the other weaker intermolecular forces. As a result, the stability difference between the less soluble and the more soluble diastereomeric salts depends on the availability and magnitude of the intermolecular interactions in the crystal.[53]

The classical hydrogen bonds involving electronegative atoms are stronger than other intermolecular contacts and has been treated as the most valuable determinant that contributes to chiral discrimination and the stability of a crystal structure. There are common characteristics of the hydrogen bonding patterns of the more stable salts that have been identified in the high efficiency resolutions.[53] In successful resolutions the following characteristic hydrogen bonding networks have been identified: $2_1$ column, closed globular cluster and two-dimensional (2D) sheets.[43,83,84] These hydrogen bonding networks stabilized the less soluble salt which resulted in the favourable resolution outcome. The presence of a OH group in a resolving agent is believed to lead to the formation of extra hydrogen bonds to link $2_1$ hydrogen bonding columns, resulting in strengthened hydrogen-bonding patterns.[69]

## 4.9. Modification of the resolving agents

Modification of the resolving agent can also improve the resolution efficacy as in the resolution of 2-(2-chlorophenyl)-2-hydroxyethanoic acid (**4.28**) with (*R*)-(+)-*N*-(phenylmethyl)-1-phenylethanamine (**4.29**).[85]

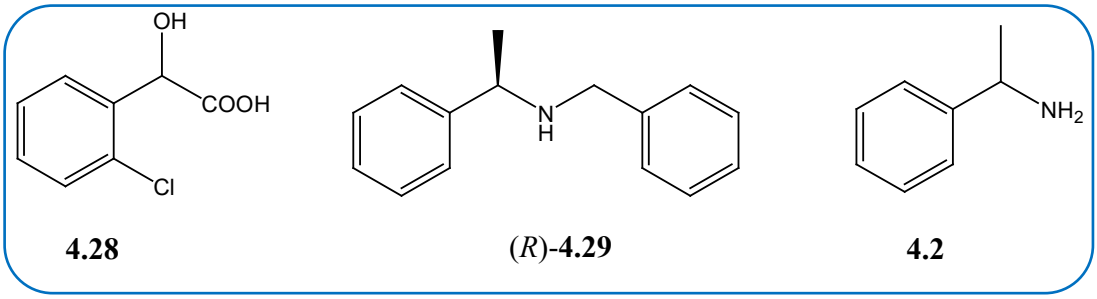


**4.28** (*R*)-**4.29** **4.2**

**4.2** is the most generally used basic resolving agent and it was employed to resolve **4.28** in seven different solvents, no crystals resulted, only an oily liquid phase resulted in six and in one solvent two liquid phases resulted. A benzyl group was introduced to **4.2** in order to increase the chiral discrimination ability to form **4.29**. **4.29** exhibited a much better resolving ability in five different solvents, 2-propanol, butyl acetate, isopropyl acetate, ethanol and toluene. The resolution efficiency was the highest in 2-propanol under their conditions. The more stable salt (*R*)-**4.28**·(*R*)-**4.29** provided a secondary amine and carboxylic acid salt framework that contained (*R*)-**4.29** ammonium cations and (*R*)-**4.28** carboxylate anions that were reinforced by van der Waals, electrostatic and hydrogen bond interactions.[85]

6-Methoxy-2-naphthylglycolic acid (**4.30**) was engineered as a simple acidic resolving reagent similar to 2-naphthylglycolic acid (**4.13**), and was synthesized from 2-bromo-6-methoxynaphthalene through four steps.[44(c)] The separation of a variety of the enantiomers of 1-arylethanamines with enantiopure **4.30** showed that **4.30** had a higher chiral discrimination capability compared to **4.13**.[44(c)] The methoxy group at position 6 of **4.30** played a prominent role in forming CH/π contacts between **4.30** and the earmarked amines.

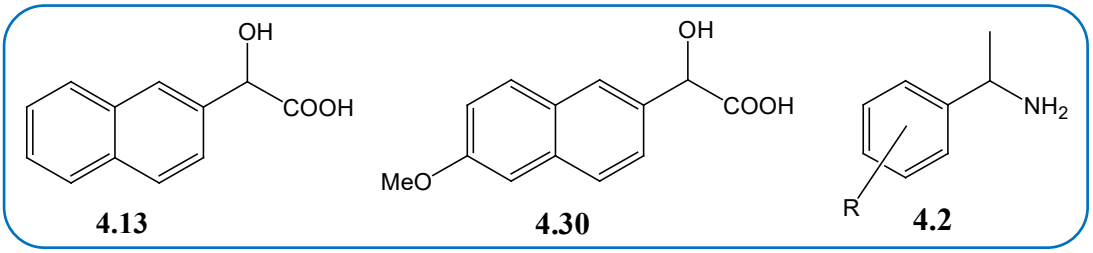


**4.13** **4.30** **4.2**

The chiral discrimination capability of **4.30** for the racemic **4.2** was determined by mixing the racemic **4.2** and **4.30** in an alcohol or aqueous solution in a molar ratio of 1:1. The ratio of water/alcohol and the quantity of the solvent were changed to control the outcome of the precipitated salt to be close to 50-90% (based on a half amount of the amine to be resolved). The substituents R in **4.2** were, H, *o*-Me, *o*-OMe, *m*-Me, *m*-OMe, *p*-Me, *p*-OMe, *p*-Cl and *p*-Ph.[44(c)]

The methoxy group, which is an electron donating group, reinforced the proton accepting ability of the naphthyl ring of (*R*)-**4.30** for the T-shaped CH/π contact in the more stable diastereomeric salts.[44(c)]

In another study Saigo *et al*.[69] designed **4.13** based on **4.1** and studied the chiral recognition of **4.2** derivatives by enantiopure **4.1**, **4.13** and **4.30**. The **4.2** derivatives were different in the R substituent, and their positions in the aromatic ring, R = (a) H, (b) o-Me, (c) o-OMe, (d) m-Me, (e) m-OMe, (f) p-Me, (g) p-OMe, (h) p-Et, (i) p-Pr (j) p-cyclohexyl (k) p-F, (l) p-Cl, (m) p-Br and (n) p-$NO_2$. The enantiopure **4.1** could not readily discriminate the chirality of the *p*-substituted **4.2** derivatives due to its molecular length. The research group then designed **4.13** to overcome the poor chiral discrimination capability of **4.1**. The naphthyl ring in **4.13** was to elongate the molecular length, to contribute to the effective packing of the supramolecular sheets, and to offer secondary interactions such as the π/π and CH/π contacts, due to the larger π surface compared to that of the phenyl group in **4.1**.

The enantioseparations of the racemic **4.2** derivatives with the enantiopure **4.13** showed a high chiral discrimination efficiency compared to **4.1**, except in the *o*-substituted **4.2** derivatives. They prepared another resolving agent in the model of **4.1**, which has an electron donating group in the form of a methoxy group at position 6, **4.30**. The enantiopure **4.30** showed an improved chiral discrimination efficiency for *o*-, *m*- and some *p*- substituted **4.2**. **4.30** also recognized the chirality of **4.2** (b) and (c) which was not recognized by **4.13**.[69]

In another case the chiral recognition ability of **4.27** was improved by modifying it to **4.26**. This was done by the enlargement of the aromatic ring of **4.27**. The chiral recognition ability of **4.27** and **4.26** was studied in the resolution of **4.31** derivatives, shown in Table 4.4.

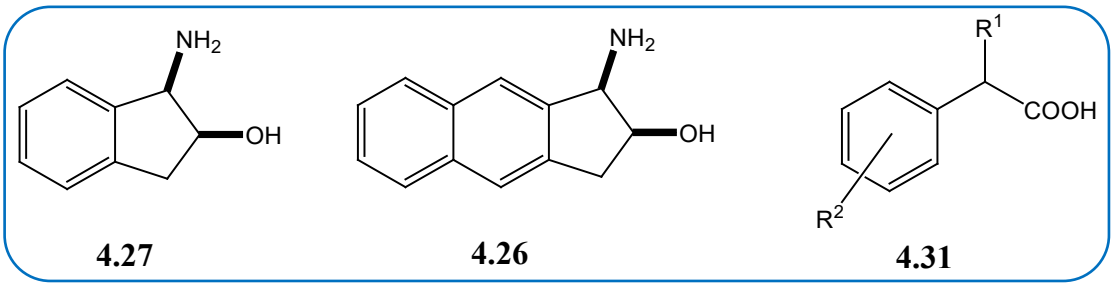


**4.27** **4.26** **4.31**

The chiral discrimination efficiency of **4.26** was greater than that of **4.27**, and the resolving abilities for **4.31** derivatives that had a substituent on the aromatic ring were improved by employing the enlarged resolving agent. The extended aromatic part played a role in the stabilization of the more stable diastereomeric **4.26** salt crystals.[69]

Table 4.4 **4.31** Derivatives and their resolution efficiencies with **4.27** and **4.26**.[69]

| | | | Efficiency | |
|---|---|---|---|---|
| **4.31** | $R^1$ | $R^2$ | **4.27** | **4.26** |
| (a) | Me | H | 0.62 | 0.56 |
| (b) | Me | *o*-Me | 0.21 | 0.58 |
| (c) | Me | *m*-Me | 0.54 | 0.56 |
| (d) | Me | *p*-Me | 0.20 | 0.53 |
| (e) | Me | *p*-Cl | - | 0.69 |
| (f) | Me | *p*-iBu | 0.06 | 0.48 |
| (g) | Et | H | 0.37 | 0.48 |
| (h) | Et | *p*-Me | 0.56 | 0.60 |
| (i) | $Pr^n$ | H | 0.35 | 0.28 |
| (j) | $Pr^i$ | H | 0.40 | 0.44 |

4.9(a) Cinchonine derivative

The reaction of cinchonine with phenylmethyl chloride in dimethylformamide gave rise to *N*-(phenylmethyl)cinchoninium chloride (**4.32**). This modified cinchonine was used in the resolution of 1,1'-bi-2-naphthol (**4.33**) in acetonitrile to yield (*R*)-**4.33**.[86] It was concluded that it was the electrostatic and hydrogen bonding interactions that predominated in the formation of the bridging link between **4.32**-**4.33** pairs. The CH/π interactions were the additional intermolecular non-bonding forces that played a role in the packing of **4.32**-**4.33** pairs in the crystal lattice.[86]

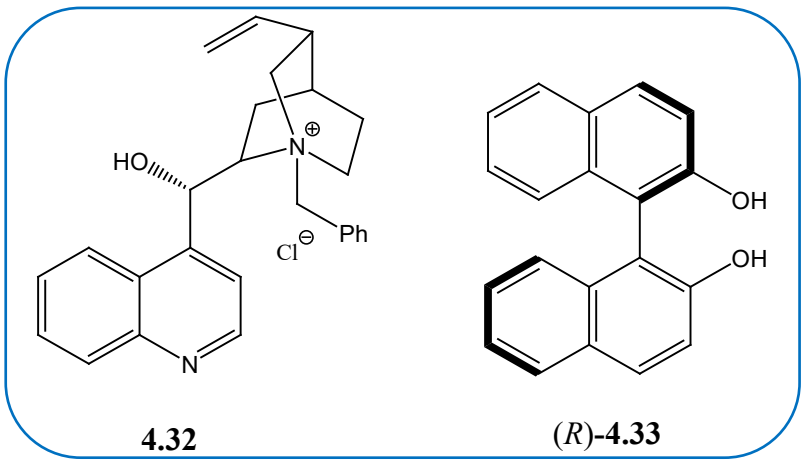


**4.32** (*R*)-**4.33**

4.9(b) Quinine derivatives

The enantiodiscriminating capabilities of quinine derivatives have been compared by proton NMR, in order to understand how derivatization could be employed to improve enantioselectivity, toward the multifunctional chiral compound, 2-(3',5'-dinitrobenzamido)-1-

phenylethanol (**4.34**). The derivatives used were of the quinine modified at the hydroxyl site, 9-*O*-acetylquinine (**4.35**), 9-*O*-(3.5-dimethoxyphenylcarbamate)quinine (**4.36**), and one modified at the quinuclidine nitrogen, *N*-benzylquininium chloride (**4.37**).[87]

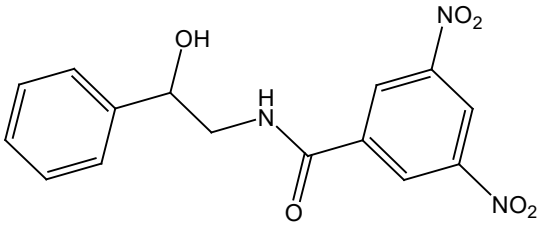


**4.34**

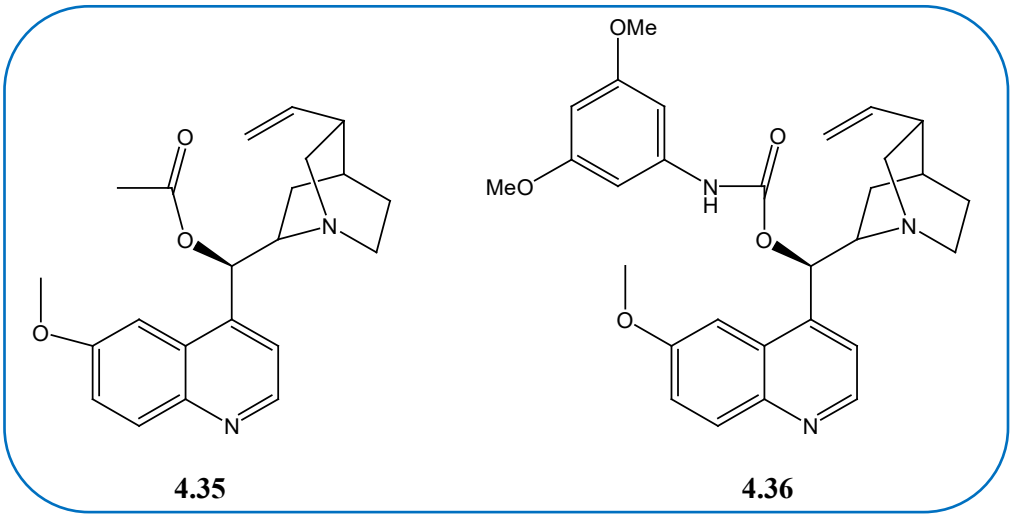


**4.35** **4.36**

The results showed that, quinine derivatives with a quinuclidine N available, **4.35** and **4.36**, resulted in the highest magnitude of enantiorecognition. The quaternization of the quinuclidine position, **4.37**, resulted in a completely dissimilar interaction with the chiral compound, and the degree of enantiodifferentiation was lowered.[87] Uccello-Barretta et al. further warned that, the hypothesis stating that the knowledge of the stereochemistry for the constituents of only one diastereomeric species, the less soluble one, can be assumed as a basis for extrapolating the stereochemistry of the most soluble diastereomer, is misleading. This is because totally dissimilar interaction pathways have been observed for the two enantiomers of **4.34** using the same chiral selectand.[87]

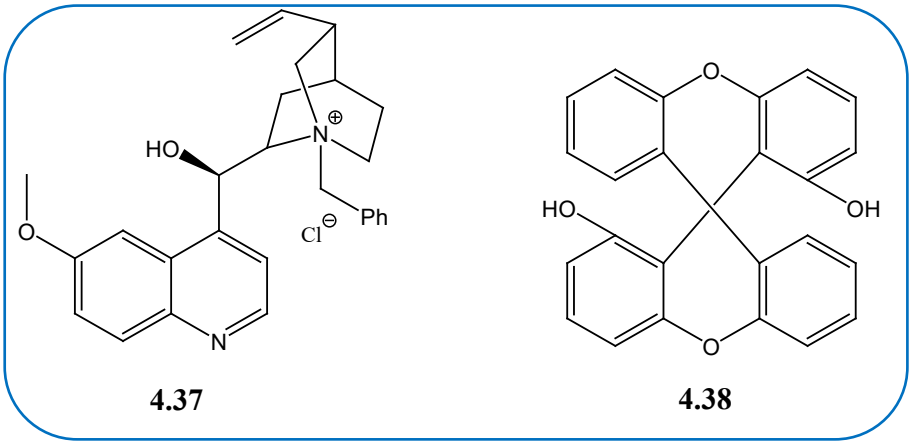


**4.37** **4.38**

In another study, **4.37** was used in the resolution of spirocyclic diol 9,9'-spirobixanthene-1,1'-diol (**4.38**) in acetonitrile, to give rise to the (*S*) enantiomer. The (*S*)- enantiomer was obtained from the mother solution by co-crystallization after separating the (*R*)-enantiomer using the most efficient resolving agent, *N*-benzylcinchonidinium chloride (**4.41**). The absolute configuration of **4.38** was assigned based on the crystal structure of **4.41**.[88]

4.9(c) Cinchonidine derivatives

Wu *et al*.[88] found **4.41** to be the most efficient reagent in the resolution of **4.38**. **4.41** precipitated as co-crystals with one enantiomer of **4.38** in acetonitrile. The results from the X-ray diffraction of a single crystal exhibited an efficiently packed molecular complex of **4.38** and **4.41** in a 1:1 molar ratio, and the absolute configuration of **4.38** was assigned as (*R*). The results contradicted those of Uccello-Barretta *et al*.'s[87] where the quaternization of the quinuclidine N atom lowered the enantiodifferentiation of the resolving agent. The behaviour of the resolving agent towards resolution therefore may be determined by the nature of the racemate involved.

The enhanced resolution ability of the resolving agents' derivatives was shown by Tanaka *et al*.[89] Cinchonidine does not form inclusion complexes with **4.33**, 6,6'-dibromo derivative (**4.39**) and the biphenanthryldiol (**4.40**). The behaviour of the cinchonidine is different from the behaviour of its derivatives towards the formation of complexes with the above-mentioned compounds.

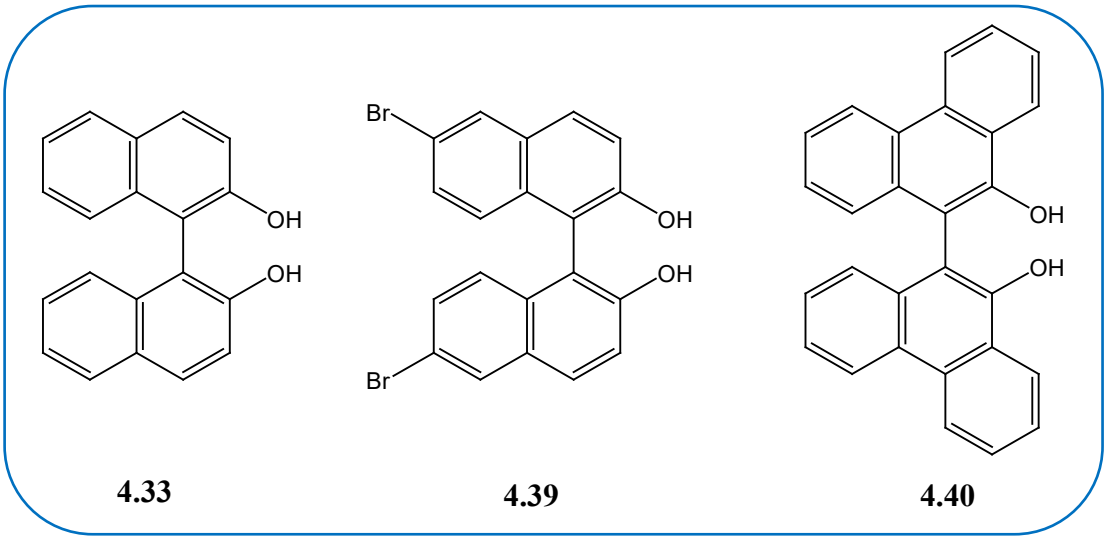


**4.33** **4.39** **4.40**

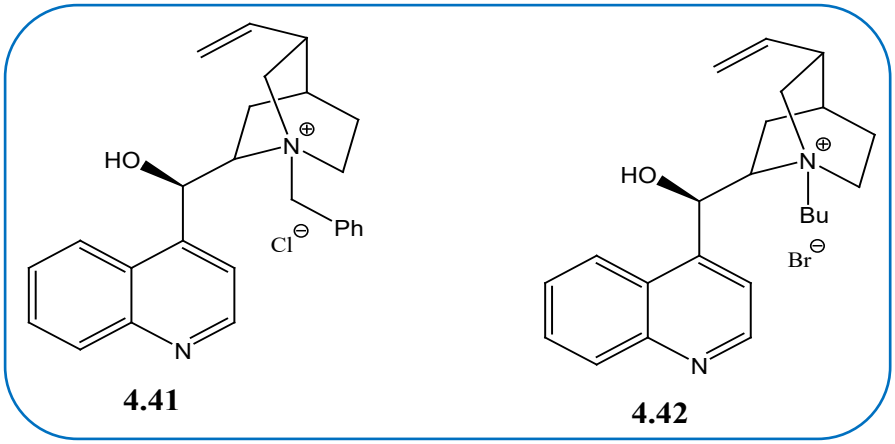


**4.41** **4.42**

*N*-benzylcinchonidinium chloride (**4.41**) was able to resolve **4.33** and **4.39**. **4.41** was unsuitable for the separation of **4.40**. **4.42** was able to separate the enantiomers of **4.40** but did not form complexes with **4.33** and **4.39**. Therefore, the discriminating ability of these derivatives varies depending on the alkyl substituent at the quinuclidine N atom. Hydrogen bonds were formed between the hydroxyl groups of **4.33**, **4.39** and **4.40** and the Cl and Br counter ions in the derivatives. The chiral recognition of the derivatives with the diol derivatives was very efficient.[89]

Toda *et al.*[90] suggested the fine-tuning of the cinchonidine resolving agent, by choosing an appropriate alkyl group, aryl group and counter ion, for the improvement of its resolution ability. More studies were carried out to resolve **4.33** to give rise to both of its enantiomers using modification of **4.41**.[91,92] Another resolution by **4.41** was developed which proved to be highly efficient and practical. 2-Amino-2'- hydroxyl-1,1'-binaphthyl (**4.43**) was resolved by molecular complexation with **4.41**, and this represented an early example of the optical resolution of an amino alcohol by a chiral ammonium salt as a resolving agent.[93]

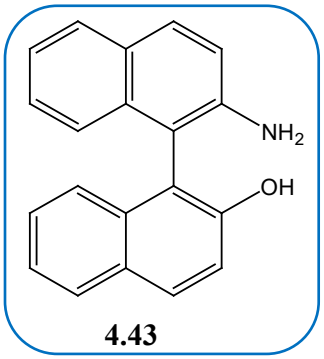


**4.43**

The racemic 2,2'-diamino-1,1'-bianthryl (**4.44**) was resolved by co-crystallizing it with **4.41** from acetonitrile, producing a 1:1 inclusion complex. The crystallographic data revealed that (*R*)-**4.44** resulted from the resolution.[94]

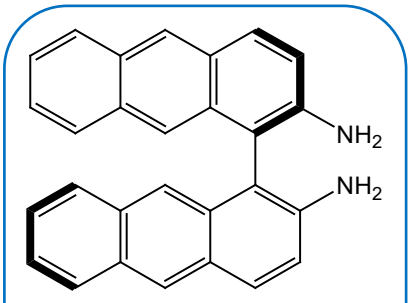


**4.44**

## 4.10. The Dutch Resolution

A predictable resolution technique is based on a hypothesis.[95] A group of scientists was motivated to develop a fast and reliable method to resolve racemic compounds after encountering problems in the resolution of racemates. Vries et al. considered a combinatorial approach, and the application of the method provided remarkable results.[95] The general technique in the resolution of racemates involves the addition of one chiral resolving agent to the molecule to be resolved, and observation of crystallization of one of the diastereomeric salts. Their combinatorial approach was based on the concurrent addition of multiple (two or three) resolving agents to decrease the time needed to form crystals. In such a case the general method of using one resolving agent at a time would be avoided in determining a suitable resolving agent.[95]

Vries et al. developed a principle of "families of resolving agents" where the resolving agents were similar structurally, and were homogeneous stereochemically, and they differed in the substitution pattern on the aromatic ring, some differed in the side chain. The addition of a family of resolving agents to a molecule to be resolved resulted in rapid crystallization of the diastereomeric salt in good to high enantiomeric purity and yield. In their cases the yields and enantiomeric excesses were superior to those obtained by using one resolving agent. The

diastereomeric salts constituted of more than one fragment of the resolving agents, and the nonstoichiometric compositions of the diastereomeric salts were retained after several crystallizations. Vries et al. resolved over 100 racemates, predominantly acids and bases. In their results only three racemates did not resolve by the family approach, due to the lack of salt formation.[95]

Table 4.5 Resolution with mixtures that contained racemic reagents, and reagents that had opposite configuration.[95]

| Row | Racemate | Acid | Acid | Ee (acid) [%] | Ee (amine) [%] | Ratio of acids |
|---|---|---|---|---|---|---|
| 1 | **4.45** | **4.1** (*S*) | **4.47** (*rac*) | 95 (*S*)-**4.47** | 90 | 4:3 |
| 2 | **4.45** | **4.1** (*rac*) | **4.47** (*S*) | 95 (*S*)**-4.1** | 99 | 3:4 |
| 3 | **4.46** | **4.1** (*R*) | **4.47** (*S*) | - | 90 | 1:6 |

Table 4.6 Resolution with mixtures of the related reagents, often referred to as the "family" approach.[95]

| Row | Substrate | Reagent mix | Solvent | Number of recryst (solvent) | Ee [%] | HPLC | Ragent ratio |
|---|---|---|---|---|---|---|---|
| 1 | **4.49** | **4.50** & **4.51** | Hexane | - | 82 | 3 | 1:1 |
| 2 | **4.52** | **4.47** | EtOH | - | 98 | 1 | 2:4:4 |
| 3 | **4.53** | **4.47** & **4.46** | EtOH | 1(EtOH) | 98 | 1 | 1:1:1 (amines) 1:1 (acids) |
| 4 | **4.53** | **4.47** & **4.54** | EtOH | 1 (EtOH/$H_2O$) | 98 | 1 | 1:1:1, contained both acids |
| 5 | **4.55** | **4.57** | EtOH | 2 (EtOH) | 96 | 2 | 0:2:1 |
| 6 | **4.56** | **4.58** | EtOH/$H_2O$ | - | 95 | 1 | 10:1:1 |

The published findings of the results were:[95]

(a) The addition of a family of reagents to a molecule to be resolved led to quick crystallization of a diastereomeric salt that contained various family members, in good to excellent yield, and the enantiomeric excess approached 100% in many cases.

(b) The method was efficient to investigate a resolution with a 1:1 or 1:1:1 mixture chosen from the family of resolving agents.

(c) It was possible to incorporate a racemic family member (Table 4.5, rows 1 and 2), and a family member of the opposite absolute configuration (row 3).

(d) The method was applicable to molecular complexation resolutions (Table 4.6 row 1).

(e) The mixtures of molecules could be resolved with a single resolving agent (row 2) or with many resolving agents (row 3 and 4).

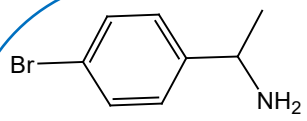


**4.45**

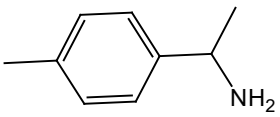


**4.46**

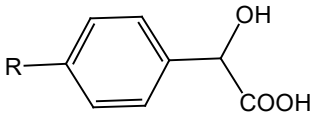


**4.1** R = H
**4.47** R = Me
**4.48** R = Br

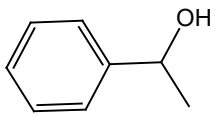


**4.49**

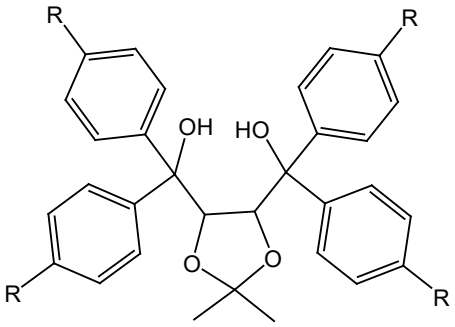


**4.50** R = H
**4.51** R = OMe

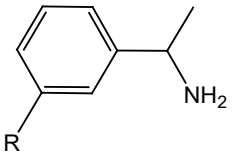


R = OMe, Cl, Br (1:1:1)

**4.52**

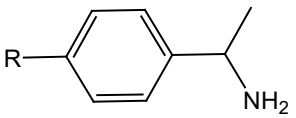


R = Cl, Me, Br (1:1:1)

**4.53**

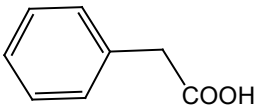


**4.54**

In other cases, the racemate was mixed with the mixture of resolving agents resulting in a high enantiomeric excess percentage, rows 5 and 6.

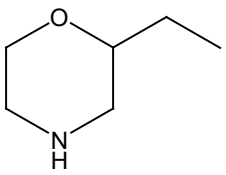


**4.55**

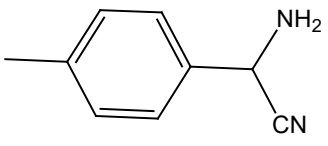


**4.56**

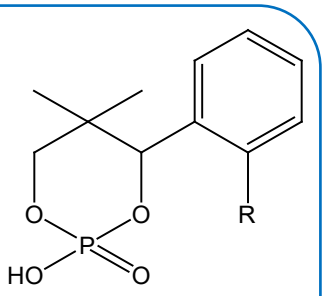


**4.57**

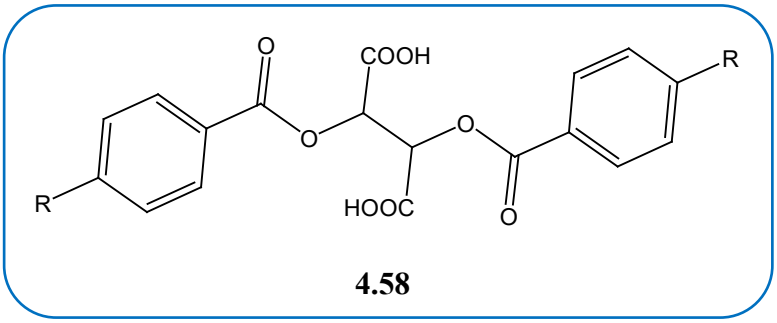


**4.58**

The results of Vries et al. regarding the use of a family of resolving agents, proved to have an effect in the trial and error method of the resolution of racemates.[95] The most significant feature of the approach in the resolution of molecules to be resolved was the high favourable outcome rate, that was defined in terms of yield and enantiomeric excess in an initial trial. This was an important modification of the classic technique. This method has also been referred to as the "Dutch Resolution".[96]

Nieuwenhuijzen *et al*. further studied the resolving agents that were repeatedly not incorporated, or which were incorporated to a smaller extent.[96] They had a perception that the resolutions did not proceed well in the absence of the unincorporated (or poorly incorporated) resolving fragments.

A model resolution was engineered with two resolving fragments, one the "parent" resolving agent, and the other the "additive" that was poorly incorporated or not incorporated at all. The solubility dissimilarities between the "parent" and the "additive" system were taken for granted to be minimal. The model involved the resolution of a racemic substrate, (2-chlorophenyl)ethylamine (**4.59**) with the "parent" resolving agent, 2-hydroxy-5,5-dimethyl-2-oxo-4-phenyl-1,3,2-dioxaphosphorinane (**4.60**), (1:1) (Table 4.7, row 1), the resolution of the racemic substrate with the "parent" resolving agent and the "additive" resolving agent, rows 2 and 3, 4-(2-chlorophenyl)-2-hydroxy-5,5-dimethyl-2-oxo-1,3,2-dioxaphosphorinane (**4.61**) and 2-hydroxy-4-(2-methoxyphenyl)-5,5-dimethyl-2-oxo-1,3,2-dioxaphosphorinane (**4.62**), (1:0.9:0.1). In 9 out of 10 systems there were profound improvements in the de value of the first salt, and the S factors were in the same range and in other instances even higher in the presence of an additive. In other instances, the improvements were dramatic, and in one resolution there was no significant improvement noticed. The results also involved nucleation inhibition, where the replacement of 10 mol% of the "parent" resolving reagent with the "additive" led to a shift in nucleation to a lower temperature.[96]

Table 4.7 The resolutions in the presence of 10% of a family member of the resolving agent.[96]

| Row | Substrate | Resolving agent | Additive | Conc | Yield [%] | Ee value [%] | S factor | HPLC |
|---|---|---|---|---|---|---|---|---|
| 1 | **4.59** | **4.60** | - | 0.20M EtOH | 23 | 68 | 0.31 | 2 |
| 2 | **4.59** | **4.60** | **4.61** | 0.20M EtOH | 29 | 86 | 0.50 | 2 |
| 3 | **4.59** | **4.60** | **4.62** | 0.20M EtOH | 30 | 88 | 0.53 | 2 |
| The S factor is, "S = kt, where k is the yield of the diastereomer salt taken as 1.00 if half the racemate has been separated in crystalline form, and t is the optical purity of the base derived from that salt, with its sign taken as positive if the enantiomer crystallizing out belongs to the D series."[97] | | | | | | | | |

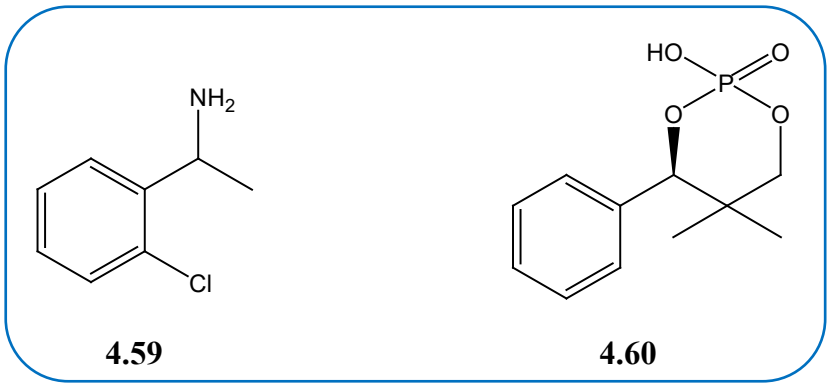


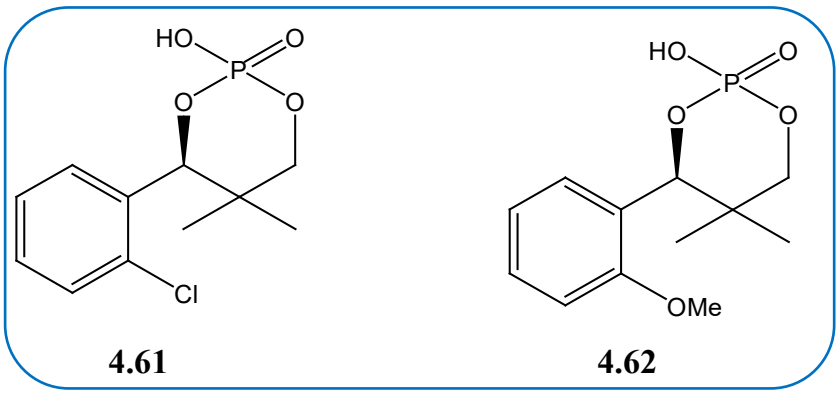


The addition of minute quantities of particular structurally related compounds led to the retardation of the crystallization rate of one of the enantiomers, which led to effective resolution. Their results led to a second generation of Dutch Resolution, the employment of minute quantities of a particular family member of the resolving agent as an additive.[96]

The three cyclic phosphoric acids were shown to be favourable resolving agents for various amines.[98] Therefore the structurally similar homo-chiral cyclic acids form a family. These were used as an example of the Dutch Resolution in the resolution of the thiamphenicol precursor (**4.63**). Each of the acids was used to resolve **4.63** and the enantiomeric excess with (-)-**4.60** and

(-)-**4.62** was acceptable (Table 4.8 rows 1-3), and the opposite enantiomers were obtained. The overall efficiency, the S-factor, varies between 0 (no resolution) and 1 (excellent resolution), the resultant yield of an excellent resolution can never be more than 50%.

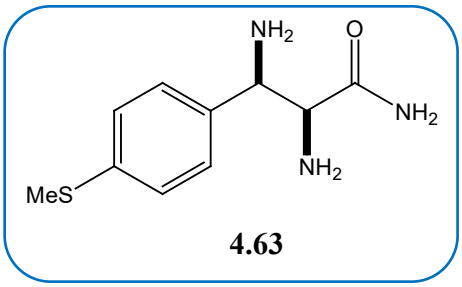


**4.63**

In the Dutch Resolution of **4.63** the enantiomeric excess was essentially perfect, yet the yield decreased (row 4).[99] The reduction in the yield is a generally noticed phenomenon in the Dutch Resolution. The achieved salt formed a mixed crystal where the cyclic phosphoric acids were present in nonstoichiometric ratio, also a general phenomenon in the Dutch Resolution.

Table 4.8 The Dutch resolution results of **4.63** with **4.60**, **4.61** and **4.62**.[99]

| Row | Resolving agent | Yield [%] | Ee [%] | S-factor | mix-ratio salt |
|---|---|---|---|---|---|
| 1 | (-)-**4.60** | 47 | 52 (2*R*,3*S*) | 0.49 | - |
| 2 | (-)-**4.61** | 55 | 17 (2*R*,3*S*) | 0.19 | - |
| 3 | (-)-**4.62** | 41 | 67 (2*S*,3*R*) | 0.55 | - |
| 4 | All three (1:1:1) | 25 | 99 (2*S*,3*R*) | 0.49 | **4.60**:**4.61**:**4.62** (12:35:53) |

The mechanism of the enantiomeric resolution of racemic 2-butanamine (**4.64**) by the chiral molecules (*R*,*R*)-(-)-*trans*-2,3-*bis*(hydroxydiphenylmethyl)-1,4-dioxaspiro(4.5)decane (**4.65**) and (*R*,*R*)-(-)-*trans*-4,5-*bis*(hydroxydiphenylmethyl)-2,2-dimethyl-1,3-dioxolane **4.66** was also investigated.[100] Báthori et al. further resolved **4.64** with two related molecules, (*R*,*R*)-(-)-*trans*-2,3-*bis*(hydroxydiphenylmethyl)-1,4-dioxaspiro(4.4)nonane (**4.67**) and (*S*,*S*)-(-)-*trans*-2,3-*bis*(hydroxydiphenylmethyl)-1,4-dioxaspiro(4.4)nonane (**4.68**), as well as the mixtures of the host compounds, **4.65** + **4.66**, **4.66** + **4.67**, **4.65** + **4.67**, and **4.65** + **4.68**. The host compounds were employed individually, mixed in a 1:1 ratio, and combined with the racemic amine **4.64** for crystallization. The combinatorial approach did not automatically improve the enantiomeric excess of **4.64** compared to that which resulted from individual host compounds. The results were attributed to the fixed packing networks of the structures.[100]

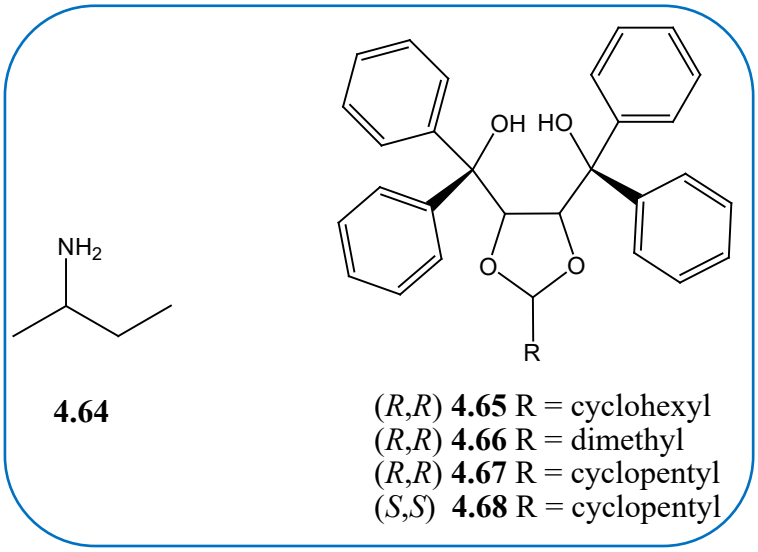


Scheme 4.2 shows some examples of compounds that were resolved using the Dutch Resolution method.[99]

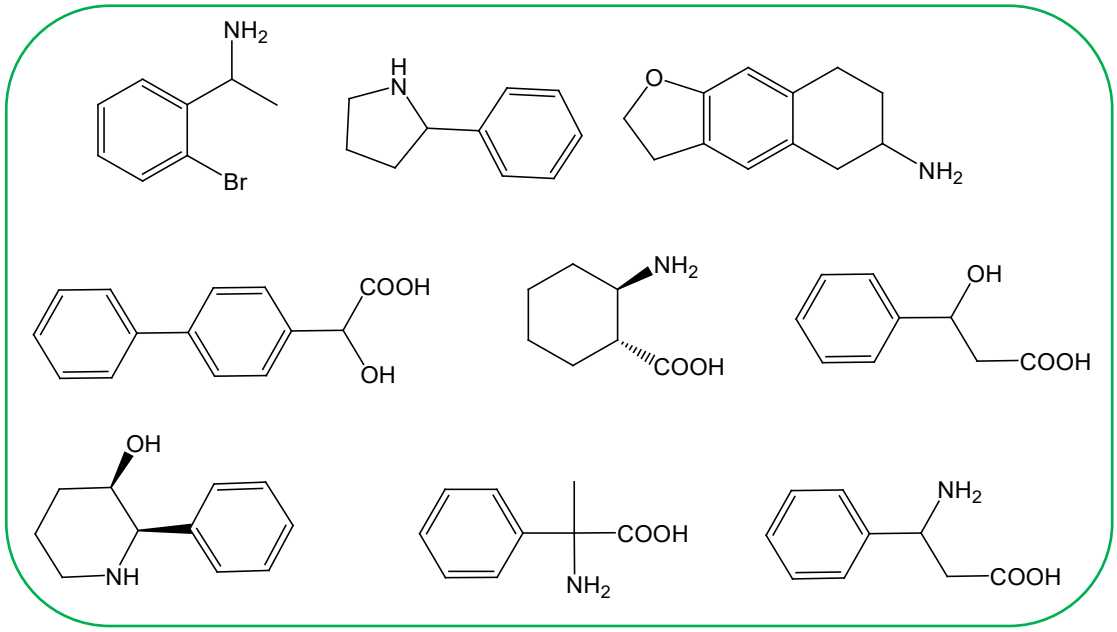


Scheme 4.2 A few examples of amines, carboxylic acids and amino acids that were resolved by the employment of the Dutch Resolution method.[99]

After the resolutions of thousands of new compounds by the Dutch Resolution method it was noted that:

-In the Dutch Resolution with acidic or basic families of resolving agents, formation of solid salts is quicker than in a resolution involving a single family member.

-The resultant salts consisted of mixed crystals that contained a nonstoichiometric ratio of resolving agents, they were solid solutions in the resolving agents.

-Single resolving agents produced salts with lower diastereomeric excesses compared to those from the Dutch Resolution method.[99]

## 4.11. Resolving agents

The resolving agent is required in resolutions to select one of the enantiomers from a racemate. The most difficult aspect is the selection of a good resolving agent for a particular racemic mixture. The easiest method of selecting a resolving agent is by consulting books and published materials, as they are usually covered in monographs and reviews.[40] These types of sources also indicate the racemates already resolved and the resolution conditions. Studies to select the appropriate resolving agent have been undertaken using solvent effects and differential scanning calorimetry (DSC).[58,101]

Similarities between the molecular structures of the resolving agent and the molecule to be resolved have a positive effect on resolution.[102] This was shown by Pálovics *et al*. in the resolution of racemic *N*-acyl amino acids with derivatives that are structurally similar to them, Table 4.9.[103] The *N*-acyl amino acids were, 2-acetamido-2-phenylacetic acid (**4.69**), 2-phenyl-2-(propionamido)acetic acid (**4.70**), 2-[(oxomethyl)amino]-3-phenylpropanoic acid (**4.71**), 3-phenyl-2-(propionamido)propanoic acid (**4.72**) and 2-acetamido-3-phenylpropanoic acid (**4.73**). The optically active methyl esters derived from the amino acids were methyl 2-amino-2-phenylacetate (**4.74**) and methyl-2-amino-3-phenylpropanoate (**4.75**). The results of the resolutions on the amino acids with their structurally similar derivatives are shown in Table 4.9.[103]

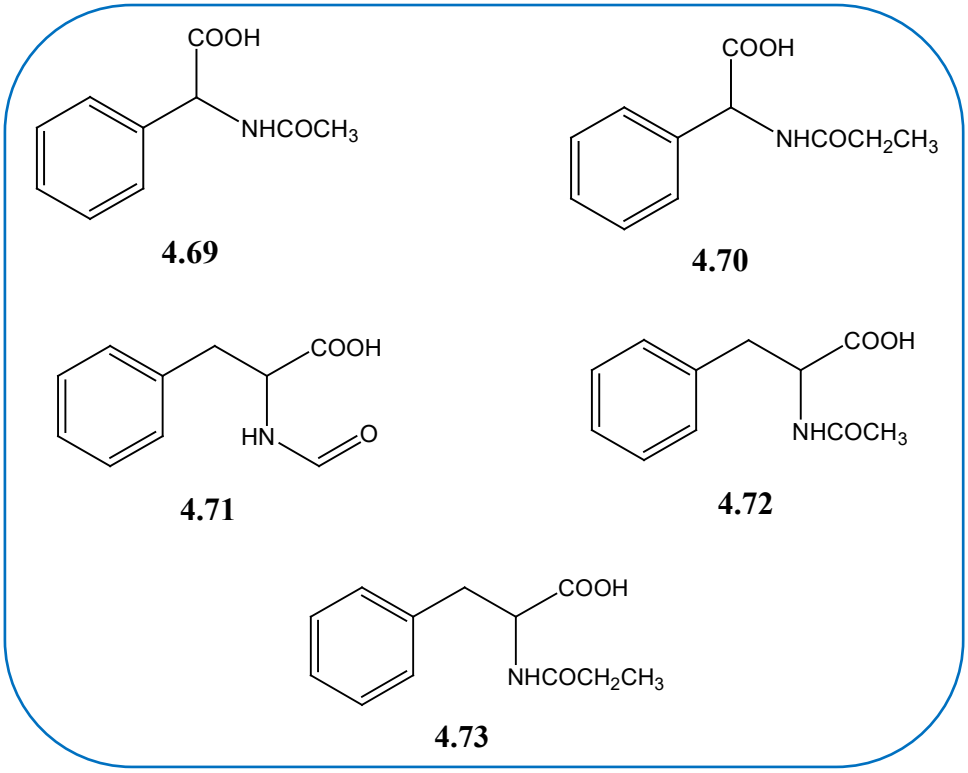

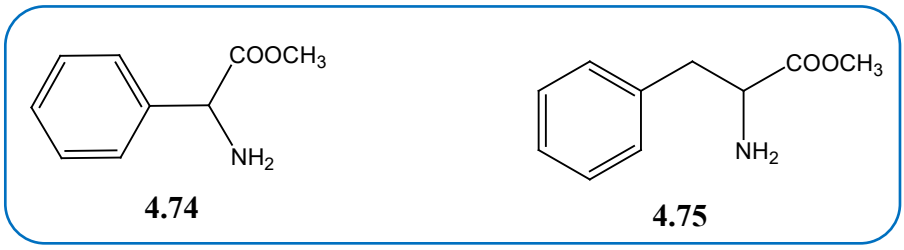


**4.74** **4.75**

Table 4.9 The resolution results of the racemic *N*-acyl amino acids with the structurally similar resolving agents, **4.74** and **4.75**.[103]

| Racemates | **4.74** | | | **4.75** | | |
|---|---|---|---|---|---|---|
| | oy[a] | Y[b] | F[c] | oy[a] | Y[b] | F[c] |
| **4.69** | 29.8 | 13.4 | 0.40 | 96.1 | 56.0 | 0.54 |
| **4.70** | 68.5 | 34.5 | 0.24 | | | |
| **4.71** | 71.9 | 54.0 | 0.39 | | | |
| **4.72** | 55.0 | 47.6 | 0.26 | 92.8 | 61.1 | 0.57 |
| **4.73** | 33.5 | 85.5 | 0.29 | | | |

[a] Optical yield: the maximum optical rotations of the *N*-acyl amino acids were known the optical yield was expected to be close to the enantiomeric excess (ee).
[b] Yield refers to one of the enantiomers in the racemate
[c] F = (oy x Y)/10000

The above results indicate that the optically active methyl esters of the amino acids **4.74** and **4.75** were suitable resolving fragments for the racemic compounds. **4.74** differentiated between the enantiomers of all the compounds and **4.75** differentiated between only two (**4.69** and **4.72**). The results show that the acids could be resolved with resolving agents that are structurally similar to them.

Faigl *et al*. suggested a way of selecting resolving agents by similarity between the molecules present in the racemic mixtures. The racemic mixtures of similar molecules should in theory be resolved using the same resolving agent. They termed this method as, "selection by structural analogy".[104] Gizur *et al*. resolved structurally similar compounds by doing trial experiments due to insufficiency of the targeted racemate. They did not have enough of racemic 1-(1,1'-biphenyl-4-yl0-3-[4-(4-fluorophenyl)-piperazin-1-yl]-1-propanol (**4.76**). They then chose a structurally similar compound, 1-[4-(4-chlorobenzyl)-phenyl]-3-(4-phenyl-1,2,3,6-tetrahydropyridin-1-yl)-1-propanol (**4.77**), to experiment on instead to find a suitable resolving agent for **4.76**. Several resolving agents were tried and (*R*,*R*)-di-(4-toluoyl)-tartaric acid ((*R*,*R*)-**4.79**) resolved **4.77** efficiently in methanol.[105]

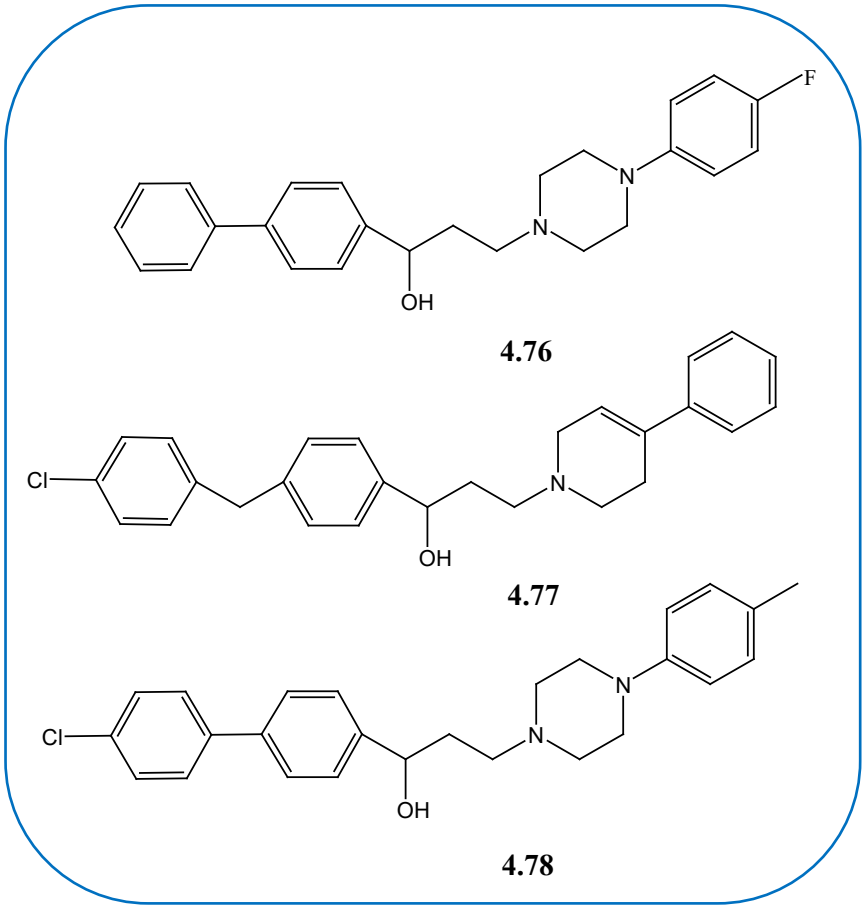


Using the same conditions **4.76** was resolved and the resolution efficiency was similar, S = 0.77 for **4.76** and S = 0.74 for **4.77**. Faigl *et al*. then suggested an analogue of (*R*,*R*)-**4.79**, ie (*R*,*R*)-**4.80** could be employed to resolve **4.78**. Their reasoning was that the orientation of the specific groups in **4.76** and **4.78** are similar, and the OH and N environments are identical in the two compounds.[104]

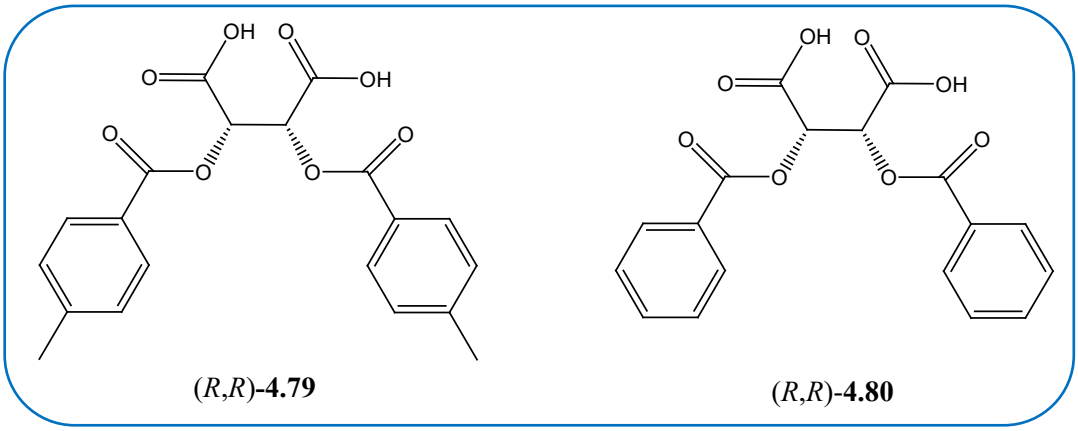


In another investigation 1,2-amino alcohols and a diamine were resolved by dehydroabietic acid (**4.81**). The resolved amino alcohols and a diamine were, 1-amino-3-phenyloxy-2-propanol (**4.82**), 2-amino-1-phenylethanol (**4.83**), 1-amino-2-propanol (**4.84**), 2-aminocyclohexanol (**4.85**) and 1,2-diaminocyclohexane (**4.86**).[106] The absolute configurations of **4.82** - **4.84** were inconsistent regardless of similar structures, and those of **4.85** and **4.86** were the same. The resolution ability of **4.81** was based on its rigid structure, the presence of the carboxyl group

and the two axial methyl groups, and finally its aromaticity as an extra interacting point especially for **4.82** and **4.83**. Faigl *et al.* indicated that a suitable resolving agent may be found by looking at the centre of chirality, which is the same in all the above racemates, and could explain why they were all resolved by the same resolving agent, **4.81**.[104]

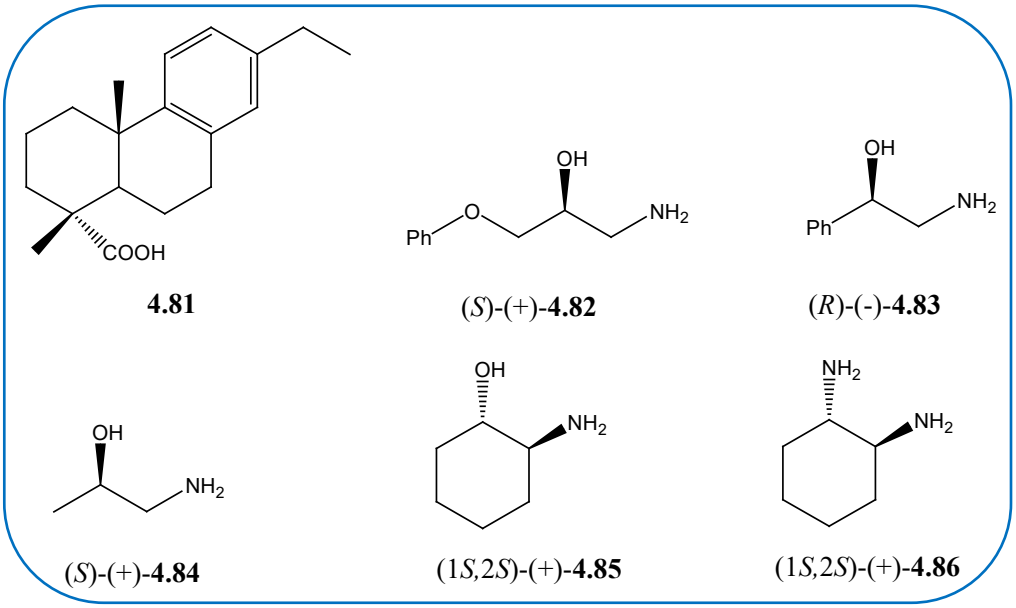


**4.81** (*S*)-(+)-**4.82** (*R*)-(-)-**4.83**

(*S*)-(+)-**4.84** (1*S*,2*S*)-(+)-**4.85** (1*S*,2*S*)-(+)-**4.86**

It is suspected that the chiral recognition process is reliant on the stereochemistry of the resolving agent and the earmarked racemate.[40] The notion that the chirality of the salt in a resolution is controlled by the chirality of the *Cinchona* alkaloid,[107] a resolving agent, does not hold for some resolutions, in terms of controlling which enantiomer is selected. It has been shown in several experiments that the same resolving agent can give rise to both enantiomers, depending on reaction conditions, eg dielectric constant of the solvent.[46,108] Racemic **4.83** was resolved using **4.81** in different solvents, Table 4.10.

Table 4.10 The resolution results of **4.83** with **4.81**.[108]

| Solvents | ε | Yield[a] (%) | Ee (%) | AC | F |
|---|---|---|---|---|---|
| EtOH | 24.0 | 8.4 | 34.8 | *R* | 0.06 |
| EtOH 65% | 43.0 | 22.6 | 15.1 | *R* | 0.07 |
| MeOH | 32.6 | 20.4 | 39.8 | *R* | 0.16 |
| MeOH 65% | 48.5 | 11.1 | 71.1 | *S* | 0.16 |
| MeOH 35% | 62.2 | 18.5 | 87.0 | *S* | 0.32 |
| i-PrOH 25% | 62.9 | 13.9 | 82.0 | *S* | 0.23 |
| [a] Based on whole amount of racemic **4.83**. ε = dielectric constant. Ee = enantiomeric excess. AC = absolute configuration, F = resolution efficiency | | | | | |

The efficiency was low in the production of the (*R*)-enantiomer and the optical purity was excellent in the production of the (*S*)-enantiomer. The difference was shown by the dielectric

constant of the solvents, less polar solvents with ε < 40 and > 20 giving rise to the (*R*)-enantiomer, and polar solvents with ε > 50 giving rise to the (*S*)-enantiomer. Both enantiomers were obtained with different yields and resolution efficiency.

Finding an appropriate resolving agent for a particular racemate is a daunting task that requires a lot of time to experiment. The resolving agents in this study were selected on ease of availability commercially, and as traditional resolving agents having been used in several resolution investigations.

## 4.12. Conclusion

The above literature survey shows the complexity of obtaining enantiomers *via* diastereomeric formation. There is no simple method of obtaining good crystals suitable for single crystal X-ray diffraction, some of the discussed factors gave contradictory results. The reaction conditions have to be well researched including the nature of the reacting species, the racemate, resolving agent and the solvent. In some examples, the change in the nature of the solvent, or its dielectric constant enhanced the effectiveness of the resolution, and in other results the absolute configuration of the enantiomer was affected. Inspection of the dielectric constant of a solvent on its own is insufficient in determining the outcome of a resolution experiment. This can be seen in Table 4.11 which shows variations in the ε values for selection of the (*R*) and (*S*) enantiomers of racemic compounds **4.15**, **4.17**, **4.19** and **4.83**.

Table 4.11 The absolute configuration (AC) results due to the dielectric constant range.

| | (*R*,*S*)-**4.15** | (*R*,*S*)-**4.17** | (*R*,*S*)-**4.19** | (*R*,*S*)-**4.83** |
|---|---|---|---|---|
| AC | ε | ε | ε | ε |
| (*R*) | $60 < \varepsilon < 25$ | $24 \leq \varepsilon < 29$ | $\varepsilon = 24$ | $23 < \varepsilon < 33$ |
| (*S*) | $25 < \varepsilon < 60$ | $30 \leq \varepsilon \leq 36$ | $27 < \varepsilon < 70$ | $33 < \varepsilon < 64$ |

The dielectric constant range for the determination of which enantiomer will be selected seems to depend on the racemate and the resolving agent. The above resolution results were conducted using EtOH and/or MeOH as solvents. This shows the importance of the solvent in enantiomer discrimination. Therefore, the solvent or the solvent mixtures contribute to the solubility difference of the diastereomeric salts, and further are involved in improving the enantiomeric purity and yield of the less soluble salt. The solvent may or may not be incorporated into the crystal structure to enhance crystal growth.

Additionally, the nature of the structures of the racemates and resolving agents also dictate the efficiency of resolution. It was reported that the difference in molecular length between the

resolving agent and the racemate influences the resolution outcome. The best resolutions were achieved when the effective molecular length difference was found to be zero or 3 - 6.[109] The p$K_a$ values, the Dutch Resolution methods, and the stereochemistry of the resolving agent assist in the planning and execution of resolution. Another factor scarcely reported is the temperature which is crucial in the crystallization of diastereomeric salts.[110] When the temperature of the hot solution is lowered, crystallization starts. Slow cooling is favoured for crystallization but the exact temperature at which crystals form is not generally noted. The pH of the medium has been reported to affect the outcome of resolution based on the configuration of the enantiomer, the yield and the enantiomeric excess of the enantiomer.[111,112]

## 4.13. References


1. Fogassy E, Ács M, Faigl F, Simon K, Rohonczy J and Ecsery Z. Pseudosymmetry and chiral discrimination in optical resolution *via* diastereomeric salt formation. The crystal structures of (*R*)- and (*S*)-*N*-Methylamphetamine Bitartrates (RMERTA and SMERTA). *J. Chem. Soc., Perkin Trans II*, **1986**, 1881-1886.
2. Schultheiss N and Newman A. Pharmaceutical co-crystals and their physicochemical properties. *Cryst. Growth Des.*, **2009**, 9, 2950-2967.
3. Aakeröy CB and Salmon DJ. Building co-crystals with molecular sense supramolecular sensibility. *Cryst. Eng. Comm*., **2005**, 7, 439-448.
4. Jones W, Motherwell WT and Trask A. Pharmaceutical co-crystals: An emerging approach to physical property enhancement. *MRS Bull*., **2006**, 341, 875-879.
5. Vishweshwar P, McMahon JA, Bis JA, and Zaworotko MJ. Pharmaceutical Co-crystals. *J. Pharm. Sci*., **2005**, 95, 499-516.
6. Bhogala BR and Nangia A. Ternary and quaternary co-crystals of 1,3-*cis*-, 5-*cis*-cyclohexanetricarboxylic acid and 4,4'-bipyridines. *New J. Chem*., **2008**, 32, 800-807.
7. Stahly GP. Diversity in single- and multiple-component systems. The search for and prevalence of polymorphs and co-crystals. *Cryst. Growth Des*., **2007**, 7, 1007-1026.
8. Childs SL and Hardcastle KI. Co-crystals of Piroxicam with carboxylic acids. *Cryst. Growth Des*., **2007**, 7, 1291-1304.
9. Aitipamula S, Banerjee R, Bansal AK, Biradha K, Cheney ML, Choudhury AR, Desiraju GR, Dikundwar AG, Dubey R, Duggirala N, Ghogale PP, Ghosh S, Goswami PK, Goud NR, Jetti RRKR, Karpinski P, Kaushik P, Kumar D, Kumar V, Moulton B, Mukherjee A, Mukherjee G, Myerson AS, Puri V, Ramanan A, Rajamannar T, Reddy CM, Rodriguez-Hornedo N, Rogers RD, Row TNG, Shan N, Shete G, Singh A, Sun CC, Swift JA, Thaimattam R, Thakur TS, Thaper RK, Thomas SP, Tothadi S, Vangala VR, Variankaval N, Vishweshwar P, Weyna DR and Zaworotko MJ. Polymorphs, salts, and cocrystals: What's in a name? *Cryst*. *Growth Des*., **2012**, 12, 2147-2152.
10. Aakeröy CB, Desper J and Urbina JF. Supramolecular reagents: versatile tools for noncovalent synthesis. *Chem. Commun*., **2005**, 2820-2822.
11. Etter MC. Hydrogen bonds as design elements in organic chemistry. *J. Chem. Phys*., **1991**, 95, 4601-4610.

12. Fábián L. Cambridge Structural Database analysis of molecular complementarity in co-crystals. *Cryst. Growth Des*., **2009**, 9, 1436-1443.
13. Aakeröy CB, Hussain I and Desper J. 2-Acetaminopyridine: A highly effective co-crystallizing agent. *Cryst. Growth Des*., **2006**, 6, 474-480.
14. Childs SL, Stahly GP and Park A. The salt-co-crystal continuum: The influence of crystal structure on ionization state. *Mol. Pharmaceutics,* **2007**, 4, 323-338.
15. Park C, Meghani NM, Shin Y, Oh E, Park J-B, Cui J-H, Cao Q-R, Tran TT-D, Tran PH-L and Lee B-J. Investigation of crystallization and salt formation of poorly soluble telmisartan for enhanced solubility. *Pharmaceutics*, **2019**, 11, 1-16.
16. Issa N, Karamertzanis PG, Welch GWA and Price SL. Can the formation of co-crystals be computationally predicted? I. Comparison of lattice energies. *Cryst. Growth Des.,* **2009**, 9, 442-453.
17. Seddon KR. *Pseudo*polymorph: A polemic. *Cryst. Growth Des*., **2004**, 4, 1087.
18. Bernstein J. …And another comment on *Pseudo*polymorphism. *Cryst. Growth Des*., **2005**, 5, 1661-1662.
19. Desiraju GR. Counterpoint: What's in a name? *Cryst. Growth Des*., **2004**, 4, 1089-1090.
20. Nangia A. Pseudopolymorph: Retain this widely accepted term. *Cryst. Growth Des*., **2006**, 6, 2-4.
21. Gavezzotti A. Are Crystal structures predictable? *Acc. Chem. Res*., **1994**, 27, 309-314.
22. Hulliger J. Chemistry and crystal growth. *Angew. Chem., Int. Ed. Engl*., **1994**, 33, 143-162.
23. Gavezzotti A and Filippini G. Crystal packing and lattice. *Synth. Met.,* **1991**, 40, 257-266.
24. Dunitz JD. Are Crystal stuctures predictable? *Chem. Commun*., **2003**, 545-548.
25. Leusen FJJ. Crystal structure prediction of diastereomeric salts: A step toward rationalization of racemic resolution. *Cryst. Growth Des.,* **2003**, 3, 189-192.
26. Dunitz JD and Gavezzotti A. How molecules stick together in organic crystals: weak intermolecular interactions. *Chem. Soc. Rev*., **2009**, 38, 2622-2633.
27. Karamertzanis PG and Price SL. Challenges of crystal structure prediction of diastereomeric salt pairs. *J. Phys. Chem. B*, **2005**, 109, 17134-17150.
28. Price SL. Predicting crystal structures of organic compounds. *Chem. Soc. Rev*., **2014**, 43, 2098-2111.

29. Lommerse JPM, Motherwell WDS, Ammon HL, Dunitz JD, Gavezzotti A, Hofmann DWM, Leusen FJJ, Mooij WTM, Price SL, Schweizer B, Schmidt MU, van Eijck BP, Verwer P and Williams DE. A test of crystal structure prediction of small organic molecules. *Acta Cryst*., **2000**, B56, 697-714.
30. Motherwell WDS, Ammon HL, Dunitz JD, Dzyabchenko A, Erk P, Gavezzotti A, Hofmann DWM, Leusen FJJ, Lommerse JPM, Mooij WTM, Price SL, Scheraga H, Schweizer B, Schmidt MU, van Eijck BP, Verwer P and Williams DE. Crystal structure prediction of small organic molecules: a second blind test. *Acta Cryst*., **2002**, B58, 647-661.
31. Day GM, Motherwell WDS, Ammon HL, Boerrigter SXM, Della Valle RG, Venuti E, Dzyabchenko A, Dunitz JD, Schweizer B, van Eijck BP, Erk P, Facelli JC, Bazterra VE, Ferraro MB, Hofmann DWM, Leusen FJJ, Liang C, Pantelides CC, Karamertzanis PG, Price SL, Lewis TC, Nowell H, Torrisi A, Scheraga HA, Arnautova, YA, Schmidt MU and Verwer P. A third blind test of crystal structure prediction. *Acta Cryst*., **2005**, B61, 511-527.
32. Day GM, Cooper TG, Cruz-Cabeza AJ, Hejczyk KE, Ammon HL, Boerrigter SXM, Tan JS, Della Valle RG, Venus E, Jose J, Gadre SR, Desiraju GR, Thakur TS, van Eijck BP, Facelli JC, Bazterra VE, Ferraro MB, Hofmann DWM, Neumann MA, Leusen FJJ, Kendrick J, Price SL, Misquitta AJ, Karamertzanis PG, Welch GWA, Scheraga HA, Arnautova YA, Schmidt MU, van de Streek J, Wolf AK and Schweizer B. Significant progress in predicting the crystal structures of small organic molecules – a report on the fourth blind test. *Acta Cryst*., **2009**, B65, 107-125.
33. Bardwell DA, Adjiman CS, Arnautova YA, Bartashevich E, Boerrigter SXM, Braun DE, Cruz-Cabeza AJ, Day GM, Della Valle RG, Desiraju GR, van Eijck BP, Facelli JC, Ferraro MB, Grillo D, Habgood M, Hofmann DWM, Hofmann F, Jose KVJ, Karamertzanis PG, Kazantsev AV, Kendrick J, Kuleshova LN, Leusen FJJ, Maleev AV, Misquitta AJ, Mohamed S, Needs RJ, Neumann MA, Nikylov D, Orendt AM, Pal R, Pantelides CC, Pickard CJ, Price LS, Price SL, Scheraga HA, van de Steek J, Thakur TS, Tiwari S, Venuti E and Zhitkov I. Towards crystal structure prediction of complex organic compounds – a report on the fifth blind test. *Acta Cryst*., **2011**, B67, 535-551.
34. Reilly AM, Cooper RI, Adjiman CS, Bhattacharya S, Boese AD, Bradenburg JG, Bygrave PJ, Bylsman R, Campbell JE, Car R, Case DH, Chadha R, Cole JC, Cosburn K, Cuppen HM, Curtis F, Day GM, DiStasio Jr RA, Dzyabchenko A, van Eijck BP, Elking DM, van den Ende JA, Facelli JC, Ferraro MB, Fushi-Molnar L, Gatsiou C-

A, Gee TS, de Gelder R, Ghiringhelli LM, Goto H, Grimme S, Guo R, Hofmann DWM, Hoja J, Hylton RK, Iuzzolino L, Jankiewicz W, de Jong DT, Kendrick J, de Klerk NJJ, Ko H-Y, Kuleshova LN, Li X, Lohani S, Leusen FJJ, Lund AM, Lv J, Ma Y, Marom N, Masunov AE, McCabe P, McMahon DP, Meekes H, Metz MP, Misquitta AJ, Mohamed S, Monserrat B, Needs RJ, Neumann MA, Nyman J, Obata S, Oberhofer H, Oganov AR, Orendt AM, Pagola GI, Pantelides CC, Pickard CJ, Podeszwa R, Price LS, Price SL, Pulido A, Read MG, Reuter K, Schneider E, Schober C, Shields GP, Singh P, Sugden IJ, Szalewicz K, Taylor CR, Tkatchenko A, Tuckerman ME, Vacarro F, Vasileiadis M, Vazquez-Mayagoitia A, Vogt L, Wang Y, Watson RE, de Wijs GA, Yang J, Zhu Q and Groom CR. Report on the sixth blind test of organic crystal structure prediction methods. *Acta Cryst*., **2016**, B72, 439-459.

35. Gilli P, Pretto L, Bertolasi V and Gilli G. Predicting Hydrogen-bond strengths from acid-base molecular properties. The p$K_a$ slide rule: Toward the solution of a long-lasting problem. *Acc. Chem. Res*., **2009**, 42, 33-44.
36. Cruz-Cubeza AJ. Acid-base crystalline complexes and the p$K_a$ rule. *CrystEngComm*, **2012**, 14, 6362-6365.
37. Johnson SL and Rumon KA. Infrared spectra of solid 1:1 pyridine-benzoic acid complexes, the nature of the hydrogen bond as a function of the acid-base levels in the complex. *J. Phys. Chem*., **1965**, 69, 74-86.
38. Tong WQT and Whitesell G. In situ salt screening- A useful technique for discovery support and preformulation studies. *Pharm. Dev. Technol*., **1998**, 3, 215-223.
39. Ramon G, Davies K and Nassimbeni LR. Structures of benzoic acids with substituted pyridines: salt *versus* co-crystal formation. *CrystEngComm.,* **2014**, 16, 5802-5810.
40. Jacques J, Collet A and Wilen SH. *Enantiomers, Racemates and Resolutions*, John Wiley & Sons, New York, **1981.**
41. Sakai K, Hashimoto Y, Kinbara K, Saigo K, Murakami H and Nohira H. Optical resolution of 1-(3-Methoxyphenyl)ethylamine with enantiomerically pure mandelic acid, and the crystal structure of less-soluble diastereomeric salt. *Bull. Chem. Soc., Jpn*., **1993**, 66, 3414-3418.
42. Kinbara K, Sakai K, Hashimoto Y, Nohira H and Saigo K. Design of resolving agents: *p*-Substituted Mandelic acids as resolving reagents for Arylalkylamines. *Tetrahedron: Asymmetry,* **1996,** 7, 1539-1542.
43. Kinbara K, Sakai K, Hashimoto Y, Nohira H and Saigo K. Chiral discrimination upon crystallization of the diastereomeric salts of 1-arylalkylamines with mandelic

acid or *p*-methoxymandelic acid: interpretation of the resolution efficiencies on the basis of the crystal structures. *J. Chem. Soc., Perkin Trans. 2*, **1996**, 2615-2622.

44. (a) Kinbara K, Harada Y and Saigo K. (2-Naphthyl)glycolic acid: a tailored resolving agent for *p*-substituted 1-arylalkylamines. *Tetrahedron: Asymmetry*, **1998,** 9, 2219-2222. (b) Kobayashi Y, Kurasawa T, Kinbara K and Saigo K. Rational design of CH/π interaction sites in a basic resolving agent. *J. Org. Chem*., **2004**, 69, 7436-7441. (c) Shimada T, Kobayashi Y and Saigo K. Synthesis of enantiopure 6-methoxy-2-naphthylglycolic acid and its application as a resolving agent. *Tetrahedron: Asymmetry*, **2005**, 16, 3807-3813.
45. Sakai K, Sakurai R and Hirayama N. Molecular mechanisms of dielectrically controlled resolutions. Novel optical resolution technologies. *Top. Curr. Chem*., **2007**, 269, 233-271.
46. Sakai K, Sakurai R, Yuzawa A and Hirayama N. Practical continuous resolution of α-amino-ε-caprolactam by diastereomeric salt formation using a single resolving agent with a solvent switch method. *Tetrahedron: Asymmetry*, **2003**, 14, 3713-3718.
47. Gfesser GA, Faghih R, Bennani YL, Curtis MP, Esbeshadev TA, Hancock AA and Cowart MD. Structure-activity relationships of arylbenzofuran $H_3$ receptor antagonists. *Bioorg*. *Med. Chem. Lett*., **2005**, 15, 2559-2563.
48. Gilli P, Bertolasi V, Ferretti V and Gilli G. Covalent nature of the strong homonuclear hydrogen bond. Study of the O−H•••O system by crystal structure correlation methods. *J. Am. Chem. Soc*., **1994**, 116, 909-915.
49. Kozma D, Ács M and Fogassy E. Predictions of which diastereomeric salt precipitates during an optical resolution *via* diastereomeric salt formation. *Tetrahedron,* **1994**, 50, 6907-6912.
50. Kozma D, Novák Cs, Tomor K, Pokol G and Fogassy E. Mechanism of optical resolutions *via* diastereomeric salt formation. Part 7 role of the solvents in the optical resolution of α-phenylethylamine by 2*R*,3*R*-tartaric acid. *J. Therm. Anal. Cal*., **2000**, 61, 45-50.
51. Ault A. Resolution of *D,L-alpha*-phenylethylamine: An introductory organic chemistry experiment. *J. Chem. Ed*., **1965**, 42, 269-269.
52. Langkilde A, Oddershede J and Larsen S. Diastereomeric salts of lactic acid and 1-phenylethylamine, their structures and relative stabilities. *Acta Cryst*., **2002**, B58, 1044-1050.
53. He Q, Rohani S, Zhu J and Gomaa H. Resolution of sertraline with (*R*)-mandelic acid: Chiral discrimination mechanism study. *Chirality,* **2012**, 24, 119-128.

54. Sakai K, Sakurai R and Nohira H. New resolution technologies controlled by chiral discrimination mechanisms. Novel optical resolution technologies. *Top. Curr. Chem.,* **2007**, 269, 199-231.
55. Białońska A and Ciunik Z. When in the presence of the strong hydrogen bonds, the weak hydrogen bonds gain an importance. *CrystEngComm,* **2006**, 8, 66-74.
56. Morimoto M, Yamakwa A, Katagiri H and Sakai K. Resolution of racemic 1-benzyl-5-oxo-3-pyrrolidinecarboxylic acid with enantiopure (*S*)-phenylalanine *N*-benzylamide *via* diastereomeric salt formation. *Tetrahedron: Asymmetry,* **2007**, 18, 2869-2875.
57. Białońska A and Ciunik Z. Brucine and two solvates. *Acta Cryst*., **2004**, C60, o853-o855.
58. (a) Borghese A, Libert V, Zhang T and Alt CA. Efficient fast screening methodology for optical resolution agents: Solvent effects are used to affect the efficiency of the resolution process. *Org. Process Res. Dev*., **2004**, 8, 532-534. (b) Wilen SH, Collet A and Jacques J. Strategies in optical resolution. *Tetrahedron*, **1977**, 33, 2725-2736.
59. Suezawa H, Ishihara S, Umezawa Y, Tsuboyama S and Nishio M. The aromatic CH/π hydrogen bond as an important factor in determining the relative stability of diastereomeric salts relevant to enantiomeric resolution – A crystallographic database study. *Eur. J. Org. Chem*., **2004**, 4816-4822.
60. Akazome M, Noguchi M, Tanaka O, Sumikawa A, Uchida T and Ogura K. Enantiomeric recognition of alkyl phenyl sulphoxides by crystalline (*R*)-phenylglycyl-(*R*)-phenylglycine. *Tetrahedron*, **1997**, 53, 8315-8322.
61. Ogura K, Uchida T, Noguchi M, Minoguchi M, Murata A, Fujita M and Ogata K. A new system for molecular recognition: Highly specific inclusion of (*S*)-isopropyl phenyl sulphoxide by solid (*R*)-phenylglycyl-(*R*)-phenylglycine. *Tetrahedron Lett*., **1990**, 31, 3331-3334.
62. Akazome M, Matsuno H and Ogura K. Asymmetric recognition of 1-arylethylamines by (*R*)-phenylglycyl-(*R*)-phenylglycine and its mechanism. *Tertahedron: Asymmetry*, **1997**, 8, 2331-2336.
63. Akazome M, Takahashi K and Ogura K. Enantiomeric inclusion of α-hydroxy esters by (*R*)-(1-naphthyl)glycyl-(*R*)-phenylglycine and the crystal structures of the inclusion cavities. *J. Org. Chem*., **1999**, 64, 2293-2300.
64. Tomori H, Yoshihara H and Ogura K. Dibenzopyrazinoazepine derivative and the nature of molecular recognition of amines by chiral 2,3-di-*O*-(arylcarbonyl)tartaric acids. *Bull. Chem. Soc. Jpn.,* **1996**, 69, 3581-3590.

65. Fujii I and Hiramaya N. Chiral space formed by (+)-(1*S*)-1,1'-binaphthalene-2,2'-diyl phosphate: Recognition of aliphatic L-α-amino acids. *Helv. Chim. Acta*, **2002**, 85, 2946-2960.
66. Kinbara K, Harada Y and Saigo K. A high performance, tailor-made resolving agent: Remarkable enhancement of resolution ability by introducing a naphthyl group into the fundamental skeleton. *J. Chem. Soc., Perkin Trans. 2*, **2000**, 1339.
67. Kinbara K, Oishi K, Harada Y and Saigo K. Effect of a substituent on an aromatic group in diastereomeric resolution. *Tetrahedron*, **2000**, 56, 6651-6655.
68. Umezawa Y, Tsuboyama S, Takahashi H, Uzawa J and Nishio M. CH/π interaction in the conformation of organic compounds. A database study. *Tetrahedron*, **1999**, 55, 10047-10057.
69. Saigo K and Kobayashi Y. The role of CH/π interaction in the stabilization of less-soluble diastereomeric salt crystals. *The Chemical Record*, **2007**, 7, 47-56.
70. Laurence C and Berthelot M. Observation of the strength of hydrogen bonding. *Perspective in drug Discovery and Design*, **2000**, 18, 39-60.
71. Jeffrey GA. An introduction to hydrogen bonding, Oxford University press: Oxford, **1997**.
72. Weber E, Franken S, Puff H and Ahrendt J. Enclave inclusion of nitromethane by a new crown host-X-ray crystal structure of the inclusion complex and host selectivity properties. *J. Chem. Soc., Chem. Commun*., **1986**, 467-469.
73. Desiraju GR. Hydrogen bridges in crystal engineering: Interactions without borders. *Acc. Chem. Res*., **2002**, 35, 565-573.
74. Etter MC, Urbanczyk Lipkowska Z, Jan DA and Frye JS. Solid state structural characrerisation of 1,3-cyclohexanedione-benzene cyclamer, a novel host-guest species. *J. Am. Chem. Soc*., **1986**, 108, 5871-5876.
75. Reddy DS, Goud BS, Panneerselvam K, Pilati T and Desiraju G. C—H···N mediated hexagonal network in the crystal structure of the 1:1 molecular complex 1,3,5-tri-cyanobenzene. *J. Chem. Soc., Chem Commun*., **1993**, 663-665.
76. Aakeröy CB and Seddon KR. The hydrogen bond and crystal engineering. *Chem. Soc. Rev*., **1993**, 397-407.
77. (a) Arunan E, Desiraju GR, Klein RA, Sadlej J, Scheiner S, Alkorta I, Clary DC, Crabtree RH, Dannenberg JJ, Hobza P, Kjaergaard HG, Legon AC, Mennucci B and Nesbitt DJ. Defining the hydrogen bond: An account (IUPAC technical report). *Pure Appl. Chem*., **2011**, 83, 1619-1636. (b) Desiraju GR and Steiner T. The weak hydrogen bond in structural chemistry and biology. *Acta Cryst*., **2000**, B56, 333-334.

78. Desiraju GR. The C—H···O hydrogen bond in crystals: What is it? *Acc. Chem. Res*., **1991**, 24, 290-296.
79. Steiner T. Unrolling the hydrogen bond properties of C—H•••O interactions. *Chem. Commun*., **1997**, 727-734.
80. Steiner T. C—H···O hydrogen bonding in crystals. *Cryst. Rev*., **2003**, 9, 177-228.
81. Aburaya K, Nakano K, Sada K, Yoswathananont N, Shigesato M, Hisaki I, Tohnai N and Miyata M. The importance of weak hydrogen bonds in the formation of cholamide inclusion crystals with aromatic guests. *Cryst. Growth Des*., **2008**, 8, 1013-1022.
82. Desiraju GR. Crystal engineering: A holistic view. *Angew. Chem. Int. Ed*., **2007**, 46, 8342-8356.
83. Kobayashi Y, Hiroaki H, Handa H, Maeda J and Saigo K. Factors determining the pattern of a hydrogen-bonding network in the diastereomeric salts of 1-arylethylamines with enantiopure P-chiral acids. *Chirality,* **2008**, 20, 577-584.
84. Molins E, Miravitlles C, Lopez-Calahora F, Castells J and Raventos J. Structure of (-)-1-phenylethylammonium hydrogen (+)-tartrate. *Acta Cryst*., **1989**, C45, 104-106.
85. Peng Y, He Q, Rohani S and Jenkins H. Resolution of 2-chloromandelic acid with (*R*)-(+)-*N*-benzyl-1-phenylethylamine: Chiral discrimination mechanism. *Chirality,* **2012**, 24, 349-355.
86. Wang Y, Sun J and Ding K. Practical method and novel mechanism for optical resolution of Binol by molecular complexation with *N*-benzylcinchoninium chloride. *Tetrahedron,* **2000**, 56, 4447-4451.
87. Uccello-Barretta G, Balzano F, Quintavalli C and Salvadori P. Different enantioselective pathways induced by derivatized quinines. *J. Org. Chem*., **2000**, 65, 3596-3602.
88. Wu S, Zhang W, Zhang Z and Zhang X. Synthesis of new monodentate spiro phosphoramidite ligand and its application in Rh-catalyzed asymmetric hydrogenation reactions. *Organic Letters,* **2004**, 6, 3565-3567.
89. Tanaka K, Okada T and Toda F. Separation of the enantiomers of 2,2'-dihydroxy-1,1'-binaphthyl and 10,10'-dihydroxy-9,9'-biphenanthryl by complexation with *N*-alkylcinchonidinium halides. *Angew. Chem. Int. Ed. Engl*., **1993**, 32, 1147-1148.
90. Toda F, Tanaka K, Stein Z and Goldberg I. Optical resolution of binaphthyl and biphenanthryl diols by inclusion crystallization with *N*-alkylcinchonidium halides. Structural characterisation of the resolved materials. *J. Org. Chem*., **1994**, 59, 5748-5751.

91. Hu Q, Vitharana D and Pu L. An efficient and practical resolution of racemic 1,1'-bi-2-naphthol to both of its pure enantiomers. *Tetrahedron: Asymmetry,* **1995**, 6, 2123-2126.
92. Cai D, Hughes DL, Verhoeven TR and Reider PJ. Simple and efficient resolution of 1,1'-bi-2-naphthol. *Tetrahedron Letters,* **1995**, 36, 7991-7994.
93. Ding K, Wang Y, Yun H, Liu J, Wu Y, Terada M, Okubo Y and Mikami K. Highly efficient and practical optical resolution of 2-Amino-2'- hydroxyl-1,1'-binaphthyl by molecular complexation with *N*-benzylcinchonidium chloride: A direct transformation to binaphthyl amino phosphine. *Chem. Eur. J*., **1999**, 5, 1734-1737.
94. Vyskočil S, Smrčina M, Lorenc M, Tislerová I, Brooks RD, Kulagowski JJ, Langer V, Farrigia LJ and Kočovský. Copper(II)-mediated oxidative coupling of 2-aminonaphthalene homologues. Competition between the straight dimerization and the formation of carbazoles. *J. Org. Chem*., **2001**, 66, 1359-1365.
95. Vries T, Wynberg H, van Echten E, Koek J, ten Hoeve W, Kellogg RM, Broxterman QB, Minaard A, Kaptein B, van der Sluis S, Hulshof L and Kooistra J. The family approach to the resolution of racemates. *Angew. Chem. Int. Ed*., **1998**, 37, 2349-2354.
96. Nieuwenhuijzen JW, Grimbergen RFP, Koopman C, Kellogg RM, Vries TR, Pouwer K, van Echten E, Kaptein B, Hulshof LA and Broxterman QB. The role of nucleation inhibition in optical resolutions with families of resolving agents. *Angew. Chem. Int. Ed.,* **2002**, 41, 4281-4286.
97. Fogassy E, Lopata A, Faigl F, Darvas F, Ács M and Tõke L. A quantitative approach to optical resolution. *Tetrahedron Lett*., **1980**, 21, 647-650.
98. Ten Hoeve W and Wynberg H. The design of resolving agents. Chiral cyclic phosphoric acids. *J. Org. Chem.,* **1985**, 50, 4508-4514.
99. Kellogg R, Kaptein B and Vries TR. Dutch Resolution of racemates and the roles of solid solution formation and nucleation. *Top. Curr. Chem*., **2007**, 269, 159-197.
100. Báthori NB and Nassimbeni LR. The Dutch Resolution Method: Attempted enhanced selectivity of 2-butylamine with mixed diol hosts. *Cryst. Growth Des*., **2012**, 12, 2501-2507.
101. Dyer UC, Henderson DA and Mitchell B. Application of automation and thermal analysis to resolving agent selection. *Org. Proc. Res. Dev.,* **1999**, 3, 161-165.
102. Pálovics E, Faigl F and Fogassy E. Separation of the mixtures of chiral compounds by crystallization. *Advances in Crystallization Process*, Mastai Y, Ed. Intech. **2012**.

103. Pálovics E, Schindler J, Faigl F and Fogassy E. The influence of molecular structure and crystallization time on the efficiency of diastereomeric salt forming resolutions. *Tetrahedron: Asymmetry*, **2010**, 21, 2429-2434.
104. Faigl F, Fogassy E, Nógrádi M, Pálovics E and Schindler J. Strategies in optical resolution: a practical guide. *Tetrahedron: Asymmetry*, **2008**, 19, 519-536.
105. Gizur T, Péter I, Harsányi K and Fogassy E. Resolution of racemic 1,3-disubstituted propanols by (*R*,*R*)-di-(4-toluoyl)-tartaric acid: Similar conditions for similar structures. *Tetrahedron: Asymmetry*, **1996**, 7, 1589-1590.
106. Guangyou Z, Yuquing L, Zhaohui W, Nohira H and Hirose T. Resolution of β-aminoalcohols and 1,2-diamines using fractional crystallization of diastereomeric salts of dehydroabietic acid. *Tetrahedron: Asymmetry*, **2003**, 14, 3297-3300.
107. Kubicki M, Borowiak T and Gawron M. Structure and molecular chirality of acetonitrile adduct of the 2:1 salt of quinidine with biphenyl 5,5'-dinitro-2,2'-dicarboxylic acid (5,5'-dinitrodiphenic acid). *J. Cryst. Spec. Res*., **1992**, 22, 205-211.
108. Taniguchi K, Aruga M, Yasutake M and Hirose T. Solvent control of optical resolution of 2-amino-1-phenylethanol using dehydroabietic acid. *Org. Biomol. Chem*., **2008**, 6, 458-463.
109. Szeleczky Z, Semsey A, Bagi P, Fődi B, Faigl F, Pálovivs E and Fogassy E. An aspect of selecting resolving agents: The role of differences in molecule length in diastereomeric salt resolutions. *Separation Science and Technology*, **2016**, 51, 727-732.
110. Fogassy E, Faigl F and Ács M. Diastereomeric interactions and selective reactions in solutions of enantiomers. *Tetrahedron,* **1985**, 41, 2841-2845.
111. Fogassy E, Faigl F, Ács M, Simon K, Kozsda É, Podányi B, Czugler M and Reck G. Structural studies on optical resolution *via* diastereomeric salt formation. Enantiomer separation for *cis*-permethrinic acid [*cis*-2,2-dimethyl-3-(2,2-dichlorovinylcyclopropanecarboxylic acid]. *J. Chem. Soc. Perkin Trans. 2*, **1988**, 1385-1392.
112. Simon K, Kozsda É, Faigl F, Fogassy E and Reck G. Structural studies on optical resolution *via* diastereomeric salt formation, part 2. The conformational flexibility of (*S*)-2-benzylaminobutan-1-ol in enantiomer separation for permethrinic acid. *J. Chem. Soc. Perkin Trans. 2*, **1990**, 1395-1400.

# Chapter 5

# Techniques

## 5.1 Materials

The chemicals and solvents used in the study were of analytical grade and were purchased from commercial sources and used without further purification. The two acids, **3.3** and **3.4** were obtained from Prof Weber, Technische Universität Bergakademie, Freiberg, Germany in limited amounts.

## 5.2 Differential scanning calorimetry (DSC)

Calorimetry involves the measurement of heat changes from chemical reactions or physical events. It therefore relies on the fact that all chemical reactions involve a change in energy, either the release of heat (exothermic reaction) or absorption of heat (endothermic reaction). Differential Scanning Calorimetry (DSC) is used to study these energy changes. It is a thermo-analytical technique in which the difference in the heat flow rate to a sample and a reference is measured as a function of temperature. In heat flux DSC the difference in power to the sample and reference is measured throughout the experiment with the temperature increasing linearly as a function of time. It is the most commonly used thermal analysis method because of its speed, simplicity and availability.

DSC is a technique used to monitor heat effects associated with phase transitions and chemical reactions as a function of temperature. The plotted graph shows a difference in the heat flow to the sample and a reference sample applied at the same temperature and is recorded as a function of temperature. The sample is sealed in an aluminium pan, and the reference is an empty pan. The temperature of the sample and reference is increased at a constant rate. The pressure is kept constant, and heat flow is equivalent to enthalpy changes depicted by the equation, $dq_p/dt = dH/dt$. The heat flow (dH/dt) measured in mW or mJ $s^{-1}$ gives a heat flow difference between the sample and the reference according to the equation: $\Delta dH/dt = (dH/dt)_{sample} - (dH/dt)_{reference}$

As the temperature rises during the analysis, positive and negative peaks of the heat flow will be generated and recorded. The resultant peaks will be indicative of the effect of heat associated with a certain process eg. oxidation, melting or a phase transition. The technique can be used to obtain the melting points and the temperature at which the compounds decompose or evaporate. Heating rate is an important consideration in thermal analysis as slower heating rates may more accurately indicate the onset temperature of a composition change. They also reduce chances of self-feeding reactions. Different transformations that have close temperature ranges

will be clearly observed as two separate peaks, compared to a faster heating rate where the two peaks maybe mistaken for a single peak. Peaks from slow heating rates are shorter and broader. Impurities broaden peaks and lower the onset temperature of compounds.[1-3]

The resultant DSC curves indicate thermal events like desolvation, phase transformation and melting. Generally, the thermal events are either endothermic (positive peaks) or exothermic (negative peaks).

The DSC technique has been widely used in the study of chiral systems. In optical resolution structural studies[4-10] DSC measurements of the precipitated salts gave information on the progress of resolution reactions.[11] DSC has also been used in thermo-analytical investigations of the optical resolution of racemic compounds.[12-14]

## 5.3 Thermogravimetric analysis (TGA)

Thermogravimetric analysis (TGA) is a technique that is used to measure changes in sample weight related to temperature changes. The obtained information helps in understanding the changes that occur in sample composition, the thermal stability of a sample, and also kinetic parameters for chemical reactions. The generated weight loss graph can be helpful to identify the temperature at which weight loss is apparent. The results of a TGA curve are displayed showing a mass or percent mass that is plotted against temperature or time. When a sample loses material or reacts with its surrounding atmosphere, mass change occurs.[1-3]

The TGA technique was employed to determine the solvents incorporated or absent in the final resolution products.

## 5.4 Single crystal X-ray diffraction

The most powerful instrument in the analysis of crystalline solids' structures is X-ray crystallography.[15] Modern technology and fast computers impacted on the speed of X-ray analysis, assisting in the speed and accurate data collection and processing of several large data sets within hours. Structure solution, refinement and tackling complicated problems is done in reasonable time periods due to fast computers. X-ray diffraction is a non-destructive technique in the determination of crystal structures and spacing of atoms. The technique is used to determine unit cell dimensions, bond lengths, bond angles and site-ordering details of crystal structures. The data obtained from the technique are refined and interpreted to determine crystal structures.[16]

The crystal itself is the most important feature in structure determination by X-ray crystallography. The crystal needs to have good periodicity, which is the packing of the

molecules to give a strong diffraction pattern. Heavier and well-ordered atoms in the lattice produce the best diffraction quality.[15] Generally organic supramolecular compounds consist of light elements in the crystal lattice, like carbon, hydrogen, nitrogen and oxygen.[15,17] To obtain good crystal data results the analyzed crystals must be stable. Crystals are very sensitive to the environment and fragile due to the weak intermolecular interactions holding together the supramolecular assemblies. The solvent plays a major role in crystal growth and in the crystal lattice construction. Some crystals are only stable when they are in the solvent they were crystallized from.[15] In X-ray crystallography, X-rays are diffracted by crystals, giving rise to accurate molecular structures.

The technique provides information regarding the stabilization of the less soluble salts in terms of intermolecular forces and the nature of the crystal structures.

## 5.5 Computing components

ConQuest: It is used in exploring the Cambridge Structural Database regarding information on deposited structural results related to the study.[18]

PovRay: Is used to obtain graphics for structures.[19]

LAYER: Exhibits simulated precession photographs of the reciprocal lattice levels and allows the investigation of the systematic absences which occur.[20]

LAZY PULVERIX: Software that is used in the calculation of the theoretical powder X-ray diffraction pattern of molecules from single crystal X-ray diffraction data.[21]

POVLabel: Is used in the editing of POV-RAY images.[22]

PLATON: The program provides a large variety of geometrical calculations.[23]

CCDC Mercury: The most important feature of Mercury is to import the chemical bond types from 2D connection tables and present them in the 3D form. It can build, locate, and display networks of intramolecular and intermolecular hydrogen bonds.[24]

CrystalExplorer: Is used to generate fingerprint plots.

In a crystal structure the molecular Hirshfeld surfaces are constructed based on the electron distribution that is calculated as the sum of spherical atom electron densities.[25,26] In a targeted crystal structure and the set of spherical atomic electron densities, the Hirshfeld surface is distinctive,[27] therefore this property suggests the probability of obtaining more information about the intermolecular interaction of molecular crystals. A molecule enclosed by the Hirshfeld surface is designated by points in which the contribution to the electron density from

the targeted molecule is equal to the contribution from all the other molecules. For each of the points two distances are designated, the distance from the point to the closest nucleus external to the surface, $d_e$, and the distance to the closest nucleus internal to the surface, $d_i$. The normalized contact distance, $d_{norm}$, is calculated relative to the two, $d_e$ and $d_i$, and the van der Waals radii of the atom. This normalized contact distance helps in identifying the regions of specific importance to the intermolecular interactions, and is given by the following equation[28]

$$d_{norm} = (d_i - r_i^{vdW}/r_i^{vdW}) + (d_e - r_e^{vaW}/r_e^{vdW})$$

The intermolecular contacts are related to the $d_{norm}$ value, negative when the contacts are shorter than the van der Waals separations, and positive when the contacts are longer than the van der Waals separations. A 2D fingerprint plot is generated *via* the combination of $d_e$ and $d_i$, and the plot offers a broad picture and a summary of the intermolecular contacts in the earmarked crystal.[28,29] It also provides the percentage contribution of contacts present in the crystal. The percentage contribution of the contacts also determines the stability of the crystal.[30]

Hirshfeld surface analysis is being adopted as an important modern approach towards the analysis of crystal packing and intermolecular contacts in crystals.[25] The approach of combining CrystalExplorer with quick computation of molecular wavefunctions, together with mechanical properties, has been reported to be an essential one.[31]

The 2D fingerprint plot of the Hirshfeld surface summarizes the vital information present in a molecular crystal framework, simplifying it into a single, specific full colour plot, providing a 'fingerprint' of the intermolecular interactions in the crystal. The 2D plots also summarize the frequency of each combination of $d_e$ and $d_i$ across the molecule's surface. They therefore indicate the different types of intermolecular interactions present in a crystal, providing a relative area of the surface corresponding to a particular kind of interaction. On the 2D fingerprint plot each point corresponds to a special pair ($d_e$, $d_i$). The area of contribution is indicated by a colour on the fingerprint plot. Points that do not have any contribution on the surface are not coloured, and those that contribute are coloured relative to the area of contribution.

"These plots are a novel visual representation of all the intermolecular interactions simultaneously and are unique for a given crystal structure and polymorph."[28] The 2D fingerprint plot generated from the Hirshfeld surface, comprise an essential resource for observing, learning, determining and quantifying the intermolecular contacts in molecular crystals with remarkable ease and speed.[25] The fingerprint plots can be decomposed to highlight specific close contacts. The decomposition separates the different contributions from various

contacts, which generally overlap in the full fingerprint. The decomposition also assists to quickly compare related molecules in different crystals or in the same crystal.[32] The fingerprint plots have been used in the characterization of structures in conjunction with other techniques.[33,34]

## 5.6 Infrared analysis

Infrared Spectroscopy:

Spectroscopy involves the interaction between matter and light or other electromagnetic radiation. It is utilized to characterize unknown molecular compounds by looking at their functional groups. Absorption spectroscopy is generally used to determine the structures of compounds. A schematic diagram of absorption spectroscopy is illustrated in Figure 5.1.[35]

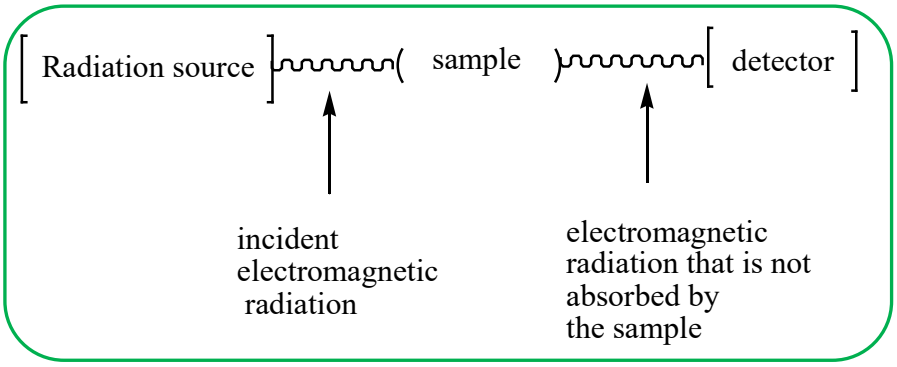


Figure 5.1 The rudiments of an absorption spectroscopy experiment.[35]

An IR spectrum is recorded as the light transmitted by the sample as a function of wavelength, and is measured using an infrared spectrophotometer. In the modern spectrometers, Fourier-transform infrared spectrometers (FT-IR) the IR spectrum is generated in a few seconds.

The molecular vibrations give rise to absorptions, which then give rise to peaks in the IR spectrum. Therefore, in the IR spectrum each peak corresponds to the energy absorbed as a result of the vibration of a specific bond or groups of bonds. The region between 400 and 1500 $cm^{-1}$ is referred to as the fingerprint region, and the absorptions in the region are not interpreted in detail. Absorption peaks are identified by their position and intensity on the spectrum. The position of a peak is controlled by the bonds' strength, masses of the atoms attached to the bond and the vibration type observed.

The functional groups have specific IR absorption bands that remain the same for all compounds. The IR region is divided into four parts:

The first region from 4000 to 2500 $cm^{-1}$ involves absorptions due to N—H, C—H and O—H stretching motions of single bonds. The second one is from 2500 to 2000 $cm^{-1}$ and this involves triple bond stretching vibrations. The double bonds absorb in the third region from 2000 to 1500

$cm^{-1}$.[36] The fourth region is the fingerprint region which occurs below 1500 $cm^{-1}$. A variety of C—C, C—O, C—N and C—X vibrations are found in this region.

Table 5.1 below lists the functional groups used in the study and their absorption ranges in the determination of the salts.[36-38]

Table 5.1 The characteristic absorptions of some functional groups.[36-38]

| Functional groups | Absorptions ($cm^{-1}$) |
|---|---|
| OH | 3650 – 3200 |
| COOH | 3400 – 2500 |
| C=O | 1780 – 1670 |
| $N^{+}$—H | 2500 – 1800<br>1670 – 1610 |
| $COO^{-}$ | 1610 – 1550<br>1420 – 1300 |
| C—O | 1300 – 1050 |

Infrared spectroscopy can be used to confirm the transfer of a proton from an acid to a base in the formation of a salt.[38] This can be done by the presence of medium to broad peaks between 2500 and 1800 $cm^{-1}$ plus the presence of a medium to weak amine salt peak at approximately 1600 $cm^{-1}$. Another confirmation is the presence of strong antisymmetric and symmetric carboxylate peaks at approximately 1570 and 1355 $cm^{-1}$. In addition, the absence of a strong carbonyl peak at approximately 1700 $cm^{-1}$ confirms the formation of a salt.[39] Therefore proton transfer salt formation is identified by the presence of $N^{+}$—H frequencies due to protonated tertiary amines, and the $COO^{-}$ frequencies due to the loss of a proton. IR spectroscopy has been used to confirm the presence of salts in complexes,[40-45] and to confirm the ionization or non-ionization of the carboxylic acid group.[46-53] The IR characteristics of α-amino acids which usually have the zwitterionic form, $N^{+}$—H and $COO^{-}$, are documented.[36]

In this study, the FT-IR technique was used to complement the single crystal X-ray diffraction results regarding the deprotonation of acids and the protonation of bases.

## 5.7 References


1. Brown ME. Introduction to Thermal Analysis, Techniques and Applications, Chapman and Hall, **1988**.
2. Speyer RF. Thermal analysis of Materials, Marcel Dekker, Inc, **1994**.
3. Gabbott P. Principles and applications of Thermal Analysis, Blackwell Pub, **2008.**
4. Wilen SH, Collet A and Jacques J. Strategies in optical resolution. *Tetrahedron*, **1977**, 33, 2725-2736.
5. Shimura Y and Tsutsui K. Optical resolution and ternary system solubility isotherms of Cobalt(III)complex salts. *Bull. Chem. Soc. Jpn.*, **1977**, 50, 145-149.
6. Fogassy E, Faigl F, Ács M, Simon K, Kozsda É, Podányi B, Czugler M and Reck G. Structural studies on optical resolution *via* diastereomeric salt formation. Enantiomer separation for *cis*-permethrinic acid [*cis*-2,2-dimethyl-3-(2,2-dichlorovinyl)cyclopropanecarboxylic acid]. *J. Chem. Soc., Perkin Trans. 2*, **1988**, 1385-1392.
7. Kozma D, Pokol G and Ács M. Calculation of the efficiency of optical resolutions on the basis of the binary phase diagram for the diastereomeric salts. *J. Chem. Soc., Perkin Trans. 2,* **1992**, 435-439.
8. Ács M, Novotny-Bregger E, Simon K and Argay G. Structural aspects of optical resolutions. Optical resolution of (*R*,*S*)-mandelic acid. DSC and X-ray studies of the diastereomeric salts. *J. Chem. Soc., Perkin Trans. 2,* **1992**, 2011-2017.
9. Kozma D, Ács M and Fogassy E. Predictions of which diastereomeric salt precipitates during an optical resolution *via* diastereomeric salt formation. *Tetrahedron*, **1994**, 50, 6907-6912.
10. Ebbers E, Ariaans GJA, Zwanenburg B and Briggink A. Controlled design of resolutions. Prediction of the efficiency of resolutions based on samples of arbitrary composition. *Tetrahedron: Asymmetry*, **1998**, 9, 2745-2753.
11. Kozma D, Novák C, Pokol G and Fogassy E. Study of the mechanism of optical resolutions *via* diastereomeric salt formation. V. Thermoanaltytical investigation of the optical resolution of the *N*-methylamphetamine by tartaric acid. *J. Therm. Anal*., **1996**, 47, 727-733.
12. Kozma D, Novák Cs, Tomor K, Pokol Gy and Fogassy E. Mechanism of optical resolutions *via* diastereomeric salt formation. Part 7. Role of the solvents in the optical resolution of α-phenylethylamine by 2*R*,3*R*-tartaric acid. *J. Therm. Anal. Cal*., **2000**, 61, 45-50.

13. Kozma D, Sztatisz J, Tomor K, Pokol G and Fogassy E. Mechanism of optical resolutions *via* diastereomeric salt formation. Part 6. Thermoanalytical investigation of the optical resolution of racemic mandelic acid with *S*-(+)-2-benzylamino-butanol. *J. Therm. Anal. Cal*., **2000**, 60, 409-415.
14. Grandeury A, Renou L, Dufour F, Petit S, Gouhier G and Coquerel G. Chiral resolution by crystallization of host-guest supramolecular complexes. A paradoxical situation with an efficient discrimination despite structural similarities. *J. Therm. Anal. Cal*., **2004**, 77, 377-390.
15. Rissanen K. X-ray crystallography. *Encyclopedia of supramolecular chemistry*. Ed: Atwood JL and Steed JW. Taylor and Francis, New York. **2004**, 2, 1596-1591.
16. Main P. Direct methods of crystal structure determination. *Crystal structure analysis: Principles and practice*. Oxford University Press, New York, **2009**, 133-147.
17. Rissanen K. Crystallography and crystal engineering. *Analytical methods in supramolecular chemistry*. Ed: Schalley CA. Wiley-VCH, Germany. **2004**, 1, 459-498.
18. ConQuest, 2018, A program to search the CSD, Version 5.39.
19. POV-RAY for windows. Persistence of Vision Pty. Ltd., Williamson, Victoria, Australia.2004.
20. Barbour LJ. *LAYER,* a computer program for the graphic display of intensity simulated precession photographs. *J. Appl. Cryst*., 32, **1999**, 351-352.
21. Yvon K, Jeitschko W and Parthe E. *LAZY PULVERIX,* a computer program calculating X-ray and neutron diffraction powder patterns. *J. Appl. Cryst*., **1977**, 10, 73-74.
22. Barbour LJ. *X-Seed*, A software tool for supramolecular crystallography. *J. Supramolecular Chem*., **2001**, 1, 189-191.
23. Spek AL. Structure validation in chemical crystallography. *Acta Cryst*., **2009**, D65, 148-155.
24. Allen FH and Lipscomb KJ. The Cambridge Structural Database, *Encyclopedia of supramolecular chemistry*. Ed. Atwood JL and Steed JL. Taylor and Francis, New York. **2004**, 1, 161-168.
25. Spackman MA and Jayatilaka D. Hirshfeld surface analysis. *CrystEngComm*, **2009**, 11, 19-32.
26. McKinnon JJ Mitchell AS and Spackman MA. Hirshfeld surfaces: A new tool for visualizing and exploring molecular crystals. *Chem.-Eur. J*., **1998**, 4, 2136-2141.
27. McKinnon JJ, Spackman MA and Mitchell AS. Novel tools for visualizing and exploring intermolecular interactions in molecular crystals. *Acta Cryst*., **2004**, B60, 627-668.

28. Spackman MA and McKinnon JJ. Fingerprinting intermolecular interactions in molecular crystals. *CrystEngComm*, **2002**, 4, 378-392.
29. Rohl AL, Moret M, Kaminsky W, Claborn K, McKinnon JJ and Kahr B. Hirshfeld surfaces identify inadequacies in computations of intermolecular interactions in crystals: Pentamorphic 1,8-dihydroxyanthaquinone. *Cryst Growth Des*., **2008**, 8, 4517-4525.
30. Grabowsky S, Dean PM, Skelton BW, Sobolev AN, Spackman MA and White AH. Crystal packing in the 2-R, 4-oxo-[1,3-*a*/*b*]-naphthodioxanes – Hirshfeld surface analysis and melting point correction. *CrystEngComm*, **2012,** 14, 1083-1093.
31. Spackman MA, McKinnon JJ and Jayatilaka D. Electrostatic potentials mapped on Hirshfeld surfaces provide direct insight into intermolecular interactions in crystals. *CrystEngComm*, **2008,** 10, 377-388.
32. McKinnon JJ, Jayatilaka D and Spackman MA. Towards quantitative analysis of intermolecular interactions with Hirshfeld surfaces. *Chem. Commun*., **2007**, 3814-3816.
33. Shelke A, Karade NN, Dutta PKr, Bahekar SP and Chandak HS. Crystal structure, DFT study, and Hirshfeld surface analysis of ethyl 5-(3,4-dimethoxyphenyl)-7-methyl-3-phenyl-5H-thiazol[3,2-a]pyrimidine-6-carboxylate. *J. Structural Chem.,* **2015**, 1246-1252.
34. Seth SK, Saha I, Estarellas C, Frontera A, Kar T and Mukhopadhyay S. Supramolecular self-assembly of M-IDA complexes involving lone-pair···π interactions: Crystal strucures, Hirshfeld surface analysis, and DFT calculations [$H_2$IDA = iminodiacetic acid, M = Cu(II), Ni(II)]. *Cryst. Growth Des.,* **2011,** 11, 3250-3265.
35. Loudon G. Organic Chemistry, 3rd Edition, The Benjamin/Cummings Publishing Company, Inc., **1988**, 535-556.
36. McMurry JE. Organic Chemistry, 8th Edition, Brooks/Cole Cengage learning, **2012**, 437-446.
37. Pavia DL, Lampman GM, Kriz GS and Vyvyan JR. Introduction to spectroscopy, 4th Edition, Brooks/Cole, **2009**, 15-83.
38. Williams DH and Fleming I. Spectroscopic Methods in Organic Chemistry, 5th Edition, McGraw Hill, London, **1995**, 28-62.
39. Lynch DE, Thomas LC, Smith G, Byriel KA and Kennard CHL. A new supramolecular synthon using *N*-methylaniline. The crystal structure of the 1:1 adduct of *N*-methylaniline with 5-nitrofuran-2-carboxylic acid. *Aust. J. Chem*., **1998**, 51, 867-869.
40. Byriel KA, Kennard CHL, Lynch DE, Smith G and Thompson JG. Molecular co-crystals of carboxylic acids. IX Carboxylic acid interactions with organic acid

heterocyclic bases. The crystal structures of the adducts of (2,4-dichlorophenoxy)acetic acid with 3-hydroxypyridine, 2,4,6-trinitrobenzoic acid with 2-aminopyrimidine, and 4-nitrobenzoic acid with 3-amino1,2,4-triazole. *Aust. J. Chem*., **1992**, 45, 969-981.

41. MacDonald JC, Dorrestein PC and Pilley MM. Design of supramolecular layers *via* self-assembly of imidazole and carboxylic acids. *Cryst. Growth Des*., **2001**, 1, 29-38.
42. Lynch DE, Smith G, Byriel KA, Kennard CHL and Whittaker AK. Molecular co-crystals of carboxylic acids. XIV The crystal structures of the adducts of pyrizine-2,3-dicarboxylic acid with 4-aminobenzoic acid, 3-hydroxypyridine and 3-amino-1,2,4-triazole. *Aust. J. Chem*., **1994**, 47, 309-319.
43. Smith G, Lynch DE, Byriel KA and Kennard CHL. The utility of 4-aminobenzoic acid in promotion of hydrogen bonding in crystallization processes: the structures of the co-crystals with halo and nitro substituted aromatic compounds, and the crystal structures of the adducts with 4-nitroaniline (1:1), 4-(4-nitrobenzyl)pyridine (1:2), and (4-nitrophenyl)acetic acid (1:1). *J. Chem. Crystallogr*., **1997**, 27, 307-317.
44. Smith G and White JM. Molecular co-crystals of carboxylic acids: the preparation of the 1:1 proton transfer compounds of creatinine with a series of aromatic acids and the crystal structure of that with pyrazine-2,3-dicarboxylic acid. *Aust. J. Chem*., **2001**, 54, 97-100.
45. Boopathi K and Ramasamy P. Synthesis, crystal growth and physical characterizations of organic nonlinear optical crystal: Ammonium hydrogen L-malate. *Spectrochimica Acta Part A: Molecular and biomolecular spectroscopy*, **2014**, 126, 7-13.
46. Bis JA and Zaworotko M. The 2-aminopyridinium-carboxylate supramolecular heterosynthon: A robust motif for generation of multiple-component crystals. *Cryst. Growth Des*., **2005**, 5, 1169-1179.
47. Aakerőy CB, Hussai I and Desper J. 2-Acetaminopyridine: a highly effective cocrystallizing agent. *Cryst. Growth Des*., **2006**, 6, 474-480.
48. Aakerőy CB, Salmon DJ, Smith MM and Desper J. Cyanophenyloximes: Reliable and versatile tools for hydrogen-bond directed supramolecular synthesis of cocrystals. *Cryst. Growth Des*., **2006**, 6, 1033-1042.
49. Schultheiss N and Newman A. Pharmaceutical cocrystals and their physicochemical properties. *Cryst. Growth Des*., **2009**, 9, 2950-2967.
50. Lee T and Wang Y. Screening, manufacturing, photoluminescence, and molecular recognition of co-crystals: Cytosine with dicarboxylic acids. *Cryst. Growth Des*., **2010**, 10, 1419-1434.

51. Childs SL, Stahly PG and Park A. The salt-cocrystal continuum: The influence of crystal structure on ionization state. *Mol. Pharmaceutics*, **2007**, 4, 323-338.
52. Odabaşoğlu M, Büyükgüngör O, Turgut G, Karadağ A, Bulak E and Lönnecke P. Crystal structure, spectral and thermal properties of 2-aminopyridinium adipate monoadipic acid dihydrate. *J. Mol. Struct*., **2003**, 648, 133-138.
53. De MatosGomes E, Rodrigues VH, Costa MMR, Belsley MS, Cardoso PJM, Gonçalves CF and Proença F. Unusual supramolecular assembly and nonlinear optical properties of *L*-histidinium hydrogen malate. *J. Solid State Chem*., **2006**, 179, 2521-2528.

# Chapter 6

## Experimental

In all the experiments, a racemate was mixed with each of the four resolving agents, in nineteen different solvents, and the successful resolution experiments are discussed below. The solvents used were: water, methanol, ethanol, propanol, propan-2-ol, butanol, hexanol, amyl alcohol, isoamyl alcohol, methyl ethyl ketone, dichloromethane, acetone, toluene, ethyl acetate, acetonitrile, acetonitrile:water, chloroform and diethyl ether, although the last two were not used extensively. In some experiments that did not yield results acetone:water was used as a solvent. The racemates that did not give rise to crystals suitable for analysis were; citronellal, citronellol, 2-phenylpropanoic acid, 2-phenylbutanoic acid, and Tröger's base. Attempts to resolve the racemates using the Dutch Resolution method, where a combination of the resolving agents (two, three and four per resolution in the different solvents) did not yield results. Only one such experiment yielded suitable crystals for analysis and gave results similar to the single resolving agent experiment (**P11**).

The following successful resolutions are described:

### 6.1 The resolution of racemic citronellic acid (*rac*-**3.1**)

(-)-Cinchonidine (**CIND**) (50 mg, 0.168 mmol) was dissolved in an aqueous hot solution of racemic citronellic acid (57.2 mg, 0.336 mmol) in a 2:1 ratio. The solution was filtered. Rod-shaped, colourless crystals were obtained after 12 days by the slow evaporation method, giving rise to product 1, **P1,** Scheme 6.1.

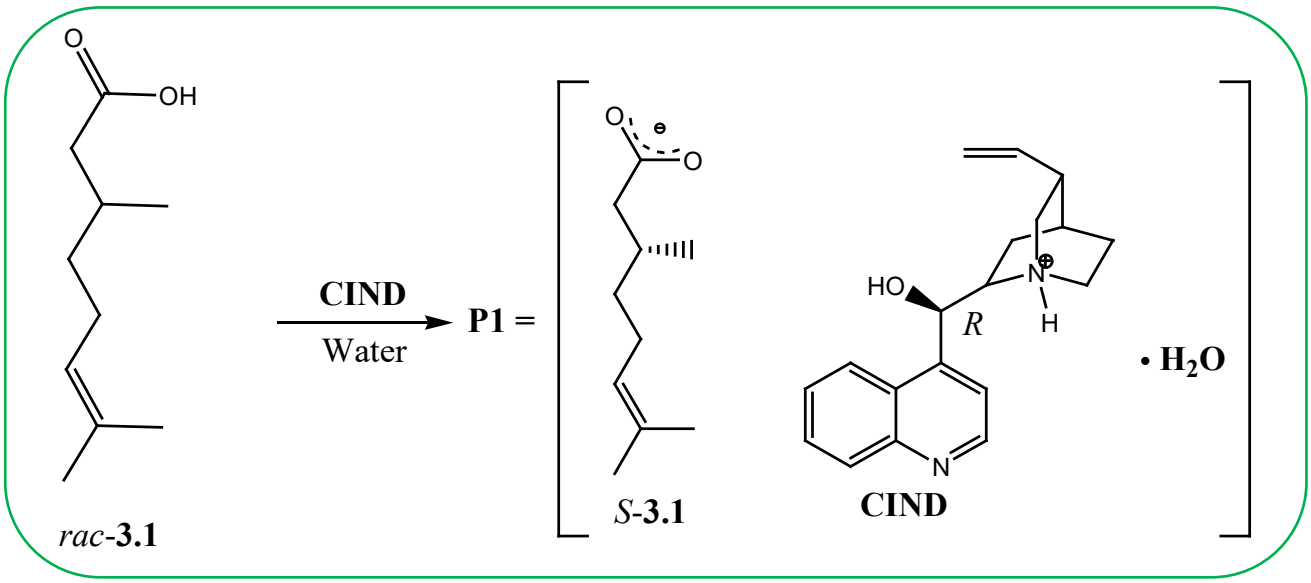


Scheme 6.1 The diastereomeric salt formation of **P1**.

## 6.2 The resolution of racemic malic acid (*rac*-**3.2**)

Salts **P2-P3a** were prepared by mixing cinchonine (**CINC**) or cinchonidine (**CIND**) (100 mg, 0.29 mmol) with the appropriate racemic modification (**3.2**) or the chiral *L*-malic acid (18 mg, 0.14 mmol) in the stoichiometric ratio of 2:1, using 96% ethanol as solvent. Needle-shaped crystals were obtained by slow evaporation after several weeks, providing **P2, P2a, P3** and **P3a**. In Scheme 6.2 only **P2** and **P3** are illustrated.

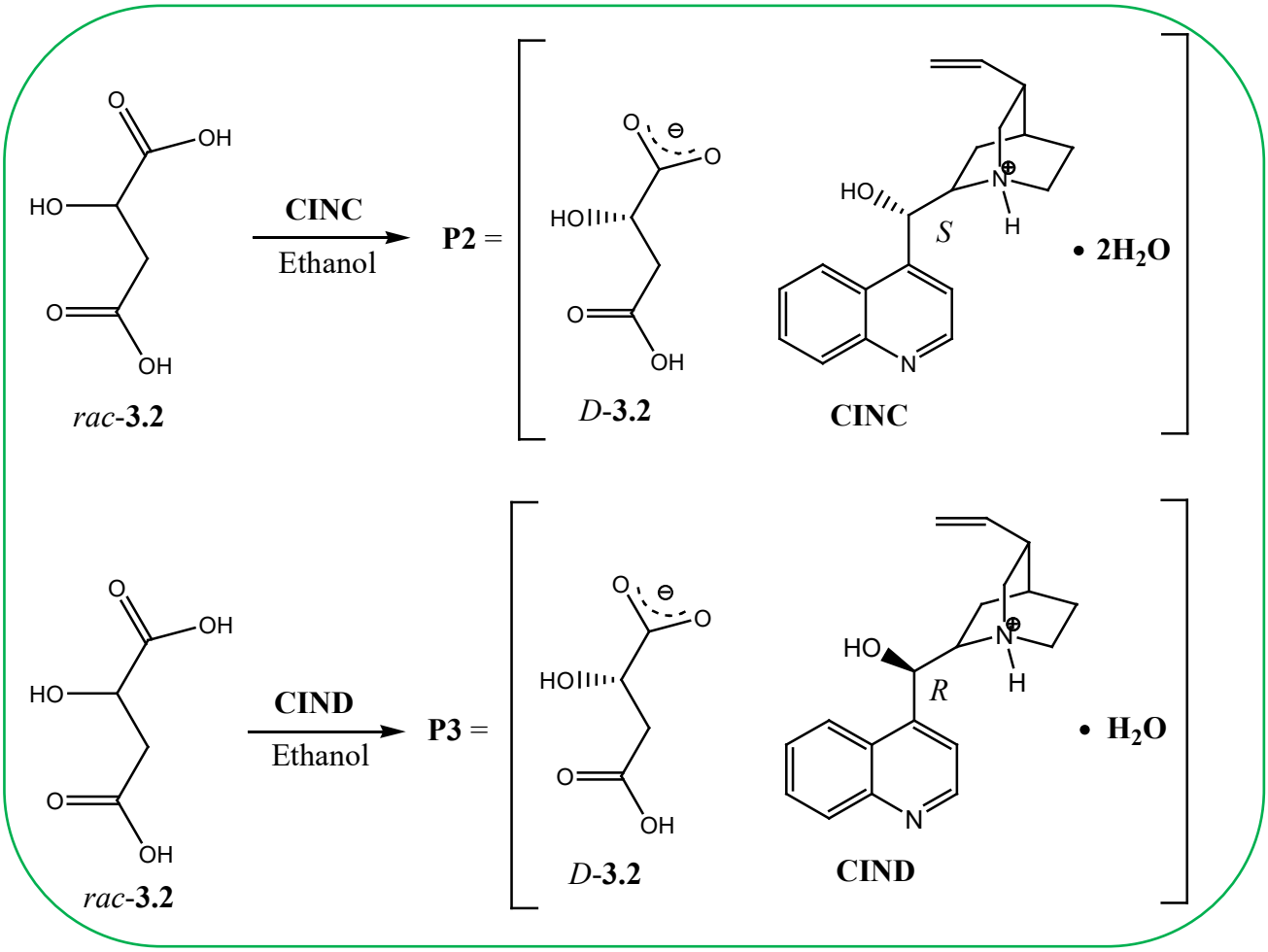


Scheme 6.2 The diastereomeric salt formation of **P2** and **P3**.

## 6.3 The resolution of racemic *trans*-9,10-dihydro-9,10-ethanoanthracene-11,12-dicarboxylic acid (*rac*-**3.3**)

The four alkaloids were individually employed to resolve *rac*-**3.3** in different solvents. The alkaloids **CINC**/**CIND** (1.47 g, 0.005 mol) or **QUIN**/**QUID** (quinine/quinidine) (1.6221 g, 0.005 mol) were mixed with the dicarboxylic acid (1.47 g, 0.005 mol) in a 1:1 mole ratio in the different solvents and heated to form solutions. The solutions were left to evaporate until crystals appeared.

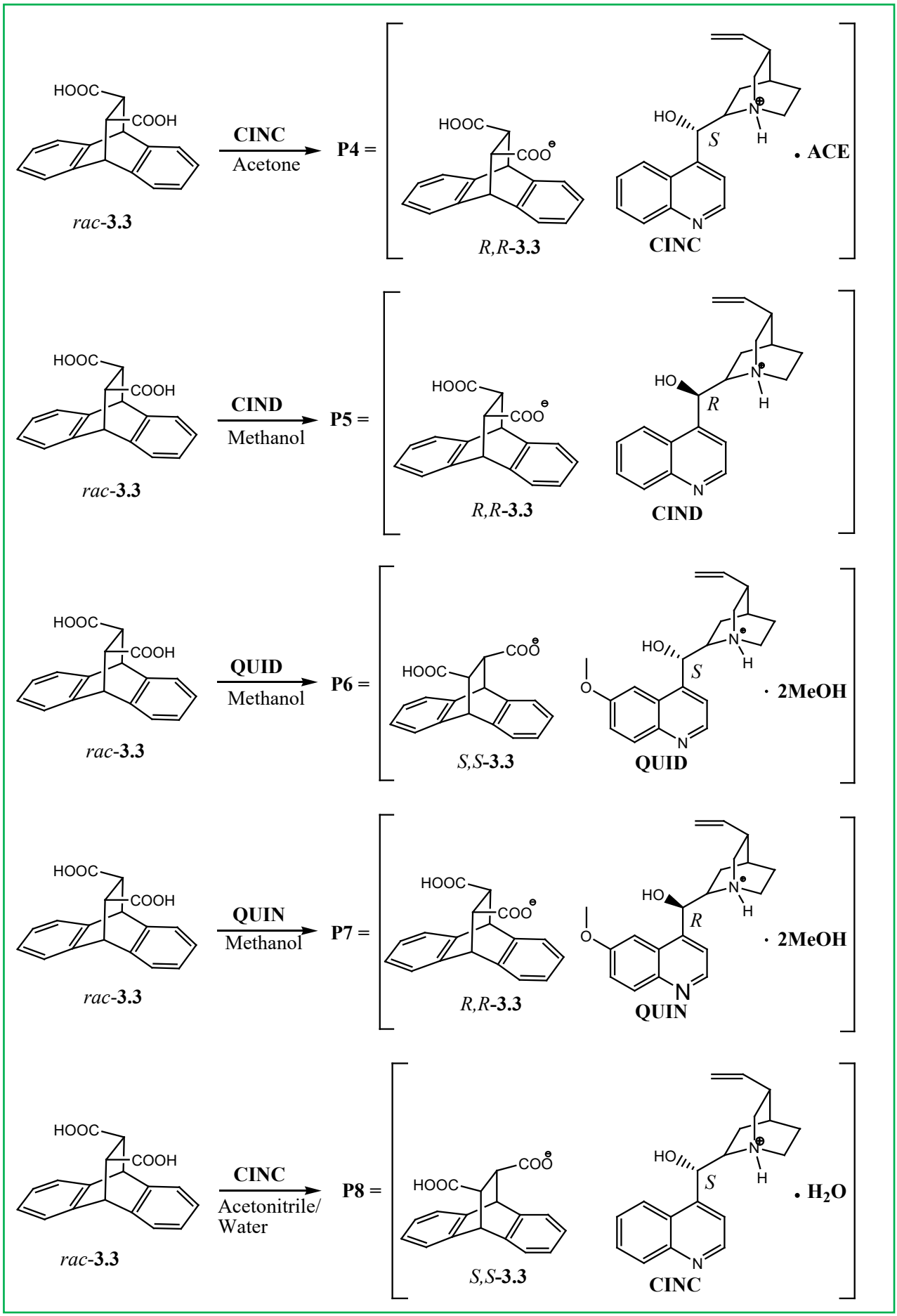


Scheme 6.3 The diastereomeric salt formation of **P4 – P8**.

The resultant salts of the experiments were from the combination of **CINC** and *rac*-**3.3** in acetone (**ACE**) (**P4**) and in acetonitrile and water (**P8**), **CIND** and *rac*-**3.3** in methanol (**P5**), **QUID** and *rac*-**3.3** in methanol (**P6**) and **QUIN** and *rac*-**3.3** in methanol (**P7**)**,** Scheme 6.3.

## 6.4 The resolution of racemic 9,10-dihydro-9,10-ethanoanthracene-11-carboxylic acid (*rac*-**3.4**)

The two alkaloids **QUIN** and **QUID** were individually employed to resolve racemic **3.4** in different solvents. The alkaloids **QUIN**/**QUID** (1.6221 g, 0.005 mol) were individually mixed with the carboxylic acid (1.25 g, 0.005 mol) in a 1:1 mole ratio in the different solvents and heated to form solutions. The solutions were left to evaporate until crystals appeared. The resultant salts of the experiments were from the combination of racemic **3.4** and **QUIN** in methanol (MeOH) (**P9**), and, racemic **3.4** and **QUID** in pentanol (PeOH) (**P10**), Scheme 6.4. In the reaction mixtures of racemic **3.4** with **QUIN** in PeOH and racemic **3.4** with **QUID** in MeOH no crystals were obtained.

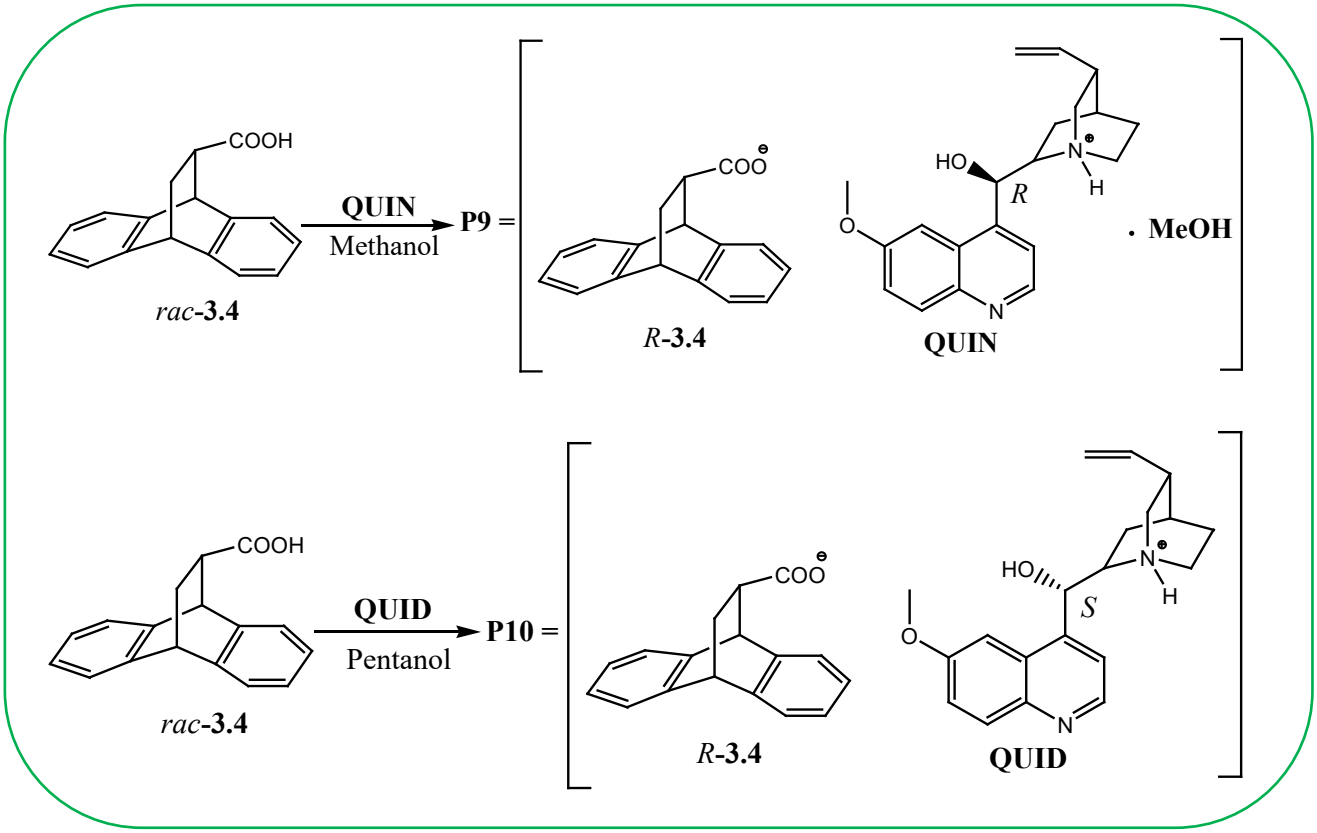


Scheme 6.4 The diastereomeric salt formation of **P9** and **P10**.

## 6.5 The resolution of racemic 2-chloropropanoic acid (2-**CPA**) (*rac*-**3.5**)

The alkaloids **CINC** and **CIND** (1.47 g, 0.005 mol), **QUIN** and **QUID** (1.6221 g, 0.005 mol) were mixed with 2-**CPA**/$H_2O$ and 2-**CPA**/MeOH (0.4598 ml, 0.005 mol) respectively in a 1:1 mole ratio in the various solvents and the mixtures were refluxed to form solutions which were evaporated until crystals formed. Suitable crystals for analysis were obtained from the following mixtures, **QUIN** + 2-**CPA**/$H_2O$ in water, **QUID** + 2-**CPA**/$H_2O$ in toluene, **CINC** + 2-**CPA**/MeOH in water, and **CIND** + 2-**CPA**/$H_2O$ in water, Scheme 6.5.

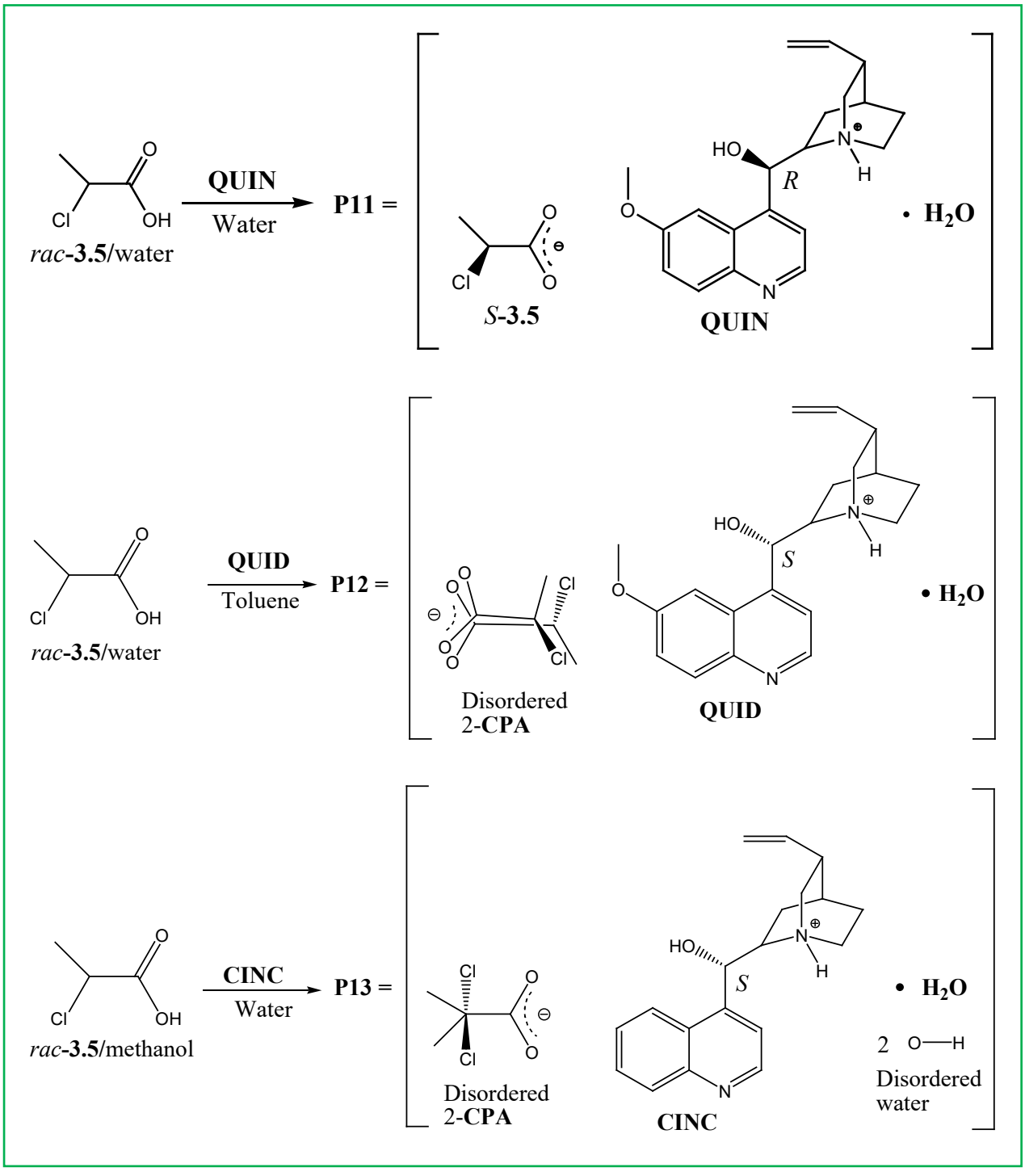

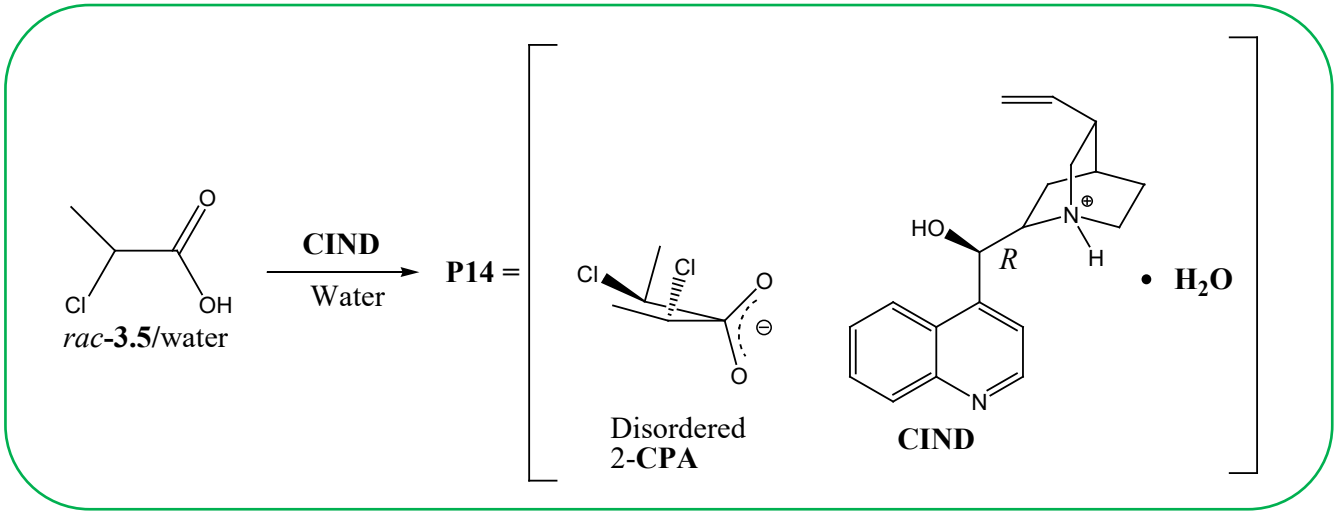


Scheme 6.5 The diastereomeric salt formation of **P11 – P14**.

## 6.6 Thermal analysis

The resultant salts were characterized using differential scanning calorimetry (DSC). A Perkin Elmer DSC 6000 system was used and the samples, weighing 3-5 mg, were purged with $N_2$ gas that flowed at 20 ml $min^{-1}$. The samples were placed in crimped and vented aluminium pans and the experiments were performed at temperatures ranging from 30 – 400 °C, with a scan rate of 10 °C $min^{-1}$.

The loss of solvent and the thermal degradation of the salts were determined using a TGA 4000 instrument. TGA thermograms were recorded at heating rates of 10 °C/min under a nitrogen purge of 20 ml/min. The sample masses analyzed were between 3-5 mg, weighed on an open standard crucible. Mass loss in percentages was calculated based on the original salt mass.

## 6.7 Structure analysis

Intensity data for the single crystals were collected on a Bruker DUO APEX II[1] diffractometer with graphite monochromated Mo-Kα radiation (λ = 0.71073 Å) at 173 K using an Oxford Cryostream 700. Cell refinement together with data reduction was performed using *SAINT*-Plus.[2] The space group was determined using XPREP.[3] *SHELXS*-97[4] was used to solve the structures and they were refined by using full matrix least squares methods in *SHELXL*-97[4] with the employment of the program X-*Seed*.[5] The H atoms on the C atoms were placed at idealized positions and refined as riding atoms with $U_{iso}$ (H) = 1.2 Ueq (Ar-H, $CH_2$) or 1.5 $U_{eq}$ ($CH_3$). The refinements of the OH group hydrogens and those of the N atoms were carried out by first locating them in the difference electron density map and imposing an appropriate bond length constraint. The crystal data are summarized in tables under results and discussion.

## 6.8 Hirshfeld surface analysis

The Hirshfeld surfaces and the 2D fingerprint plots of the salts or products were generated by using version 3.1 of CrystalExplorer.[6]

The molecular surfaces calculations were obtained from CrystalExplorer after entering the cif file of the salts into the CrystalExplorer program. All the bond lengths to the hydrogen were necessarily modified to the standard neutron values (C-H = 1.083 Å). The 2D fingerprint plots produced are plotted on a graph employing the standard 0.4 – 2.6 Å view having the $d_e$ and $d_i$ distance scales displayed on the *x* and *y* axes.[7-9]

## 6.9 Infrared analysis

The computer-interfaced FT-IR spectrometer operates in a single beam mode. The interferogram of the background was obtained, which consisted of the infrared active gases such as $CO_2$ and $H_2O$ vapour (oxygen and nitrogen gases are infrared inactive). The interferogram is then subjected to a Fourier transform, which then generates the spectrum of the background. The solid state spectra were recorded with a Fourier transformation infrared spectrometer. The samples were analyzed through a diamond window. The sample was placed in the beam and the gauge set at 20, and the spectra were obtained from the Fourier transform of the interferogram. The number of scans covered the 400 – 4000 $cm^{-1}$ spectral region. The spectra consisted of absorption peaks for the sample and the background. The computer software automatically subtracted the background spectrum from that of the sample.

## 6.10. References


1. *APEX 2*, Version 1.0-27, Bruker AXS Inc, Madison, Wisconsin, USA, **2005**.
2. *SAINT-Plus*, *Version 7.12*, Bruker AXS Inc., Madison, Wisconsin, USA, **2004**.
3. *XPREP*, Bruker AXS Inc., Madison, Wisconsin, USA, **2008**.
4. Sheldrick GM. SHELX-97: *Program for Crystal Structure Refinement*, Germany: University of Göttingen; **1997**.
5. Barbour LJ. X-Seed-A Software Tool for Supramolecular Crystallography. *J Supramol. Chem* **2001**; 1, 189-191.
6. Wolff SK, Grimwood DJ, McKinnon JJ, Turner MJ, Jayatilaka D, and Spackman MA, CrystalExplorer 3.1 (**2013**), University of Western Austalia, Crawley, Western Austalia, 2005-2013, http://hirshfeldsurface.net/CrystalExplorer.
7. Spackman MA and McKinnon JJ. Fingerprinting intermolecular interactions in molecular crystals. *CrystEngComm*, **2002**, 4, 378-392.
8. Spackman MA and Jayatilaka D. Hirshfeld surface analysis. *CrystEngComm*, **2009**, 11, 19-32.
9. Shamsuzzaman, Khanam H, Mashrai A, Asif M, Ali A, Barakat A and Mabkhot YN. Synthesis, crystal structure, Hirshfeld surfaces, and thermal, mechanical and dielectrical properties of choles-5-ene. *J. Taibah Univ. Sc*., **2017**, 11, 141-150.

# Chapter 7

## Results and discussions

### 7.1 The resolution of racemic citronellic acid (**3.1**) (published in the *Journal of Chemical Crystallography*, **2013**, 43, 373-376, DOI 10.1007/s10870-0430-1). Title: Resolution of (±)-Citronellic acid with (-)-Cinchonidine: The crystal structure of the cinchonidinium-(*S*)-citronellate diastereomeric salt. Authors: Nikoletta B. Báthori, Ayesha Jacobs, Mawonga Mei and Luigi R. Nassimbeni.

The resolution of racemic citronellic acid was attempted using the *Cinchona* alkaloids in various solvents. The Dutch Resolution method was also attempted and no successful results were obtained. A successful result was only obtained using **CIND** in the solvent, water. A resolution experiment resulted in a single crystal that was submitted for X-ray structure analysis, which exhibited the structure of a diastereomeric salt, **P1**, the crystal data and refinement details are shown in Table 7.1.

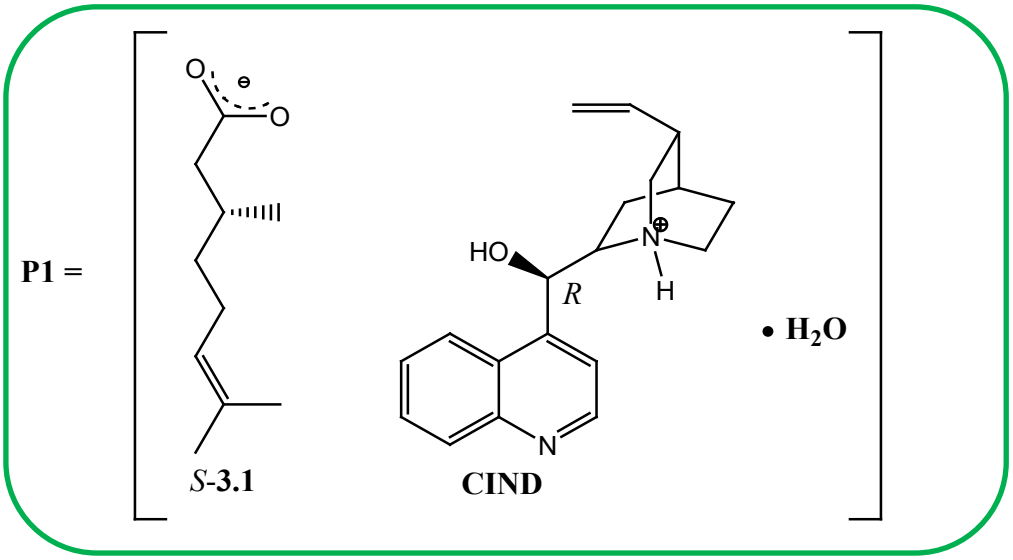

Table 7.1 Crystal data and refinement details of **P1**.

| Compound | **P1** **(*S*-3.1$^-$)(2.2$^+$)·H$_2$O** |
|---|---|
| Molecular formula | $C_{29}H_{42}N_2O_4$ |
| $M_r$ (g/mol) | 606.76 |
| Temperature (K) | 173(2) |
| Crystal size (mm) | 0.15 x 0.15 x 0.10 |
| Crystal system | Monoclinic |
| Space group | $P2_1$ |
| $a$ (Å) | 13.381(3) |
| $b$ (Å) | 6.7834(14) |
| $c$ (Å) | 15.129(3) |
| $\alpha$ (°) | 90 |
| $\beta$ (°) | 92.35(3) |
| $\gamma$ (°) | 90 |
| V (Å$^3$) | 1372.1(5) |
| $Z$ | 2 |
| $\rho$ (calcd) (g/cm$^3$) | 1.168 |
| μ (Mo-Kα) (mm$^{-1}$) | 0.077 |
| Theta range for data collection (°) | 1.52; 25.64 |
| Reflections collected | 5785 |
| No. unique data | 2768 |
| No. data with $I > 2\sigma(I)$ | 2341 |
| No. parameters | 323 |
| Final R ($I > 2\sigma(I)$)/wR$_2$ | 0.0524; 0.1515 |

The compound crystallized in the space group $P2_1$ with $Z$ = 2. Hydrogen transfer occurred between the carboxylic acid group and the quinuclidine nitrogen atom resulting in salt formation. The p$K_a$ value of citronellic acid is 5.19, and for the quinuclidine N in **CIND** it is 9.2,[1] giving rise to a p$K_a$ difference of 4.01. The p$K_a$ difference suggested the formation of a salt.[2]

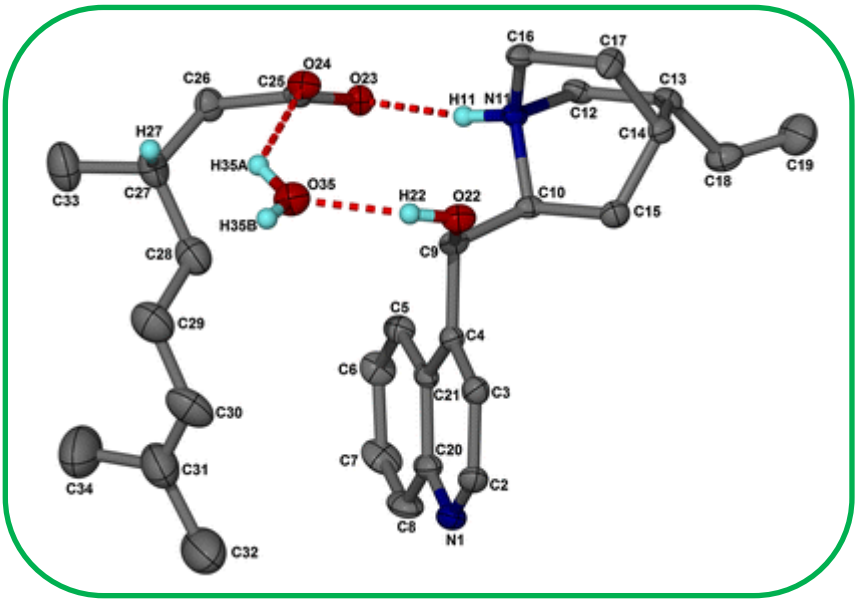


Figure 7.1 Thermal ellipsoid plot (50% probability) of the ion pair of cinchonidinium citronellate hydrate with hydrogen bonds (alkyl hydrogens, except H27 are omitted for clarity).

The C—O distances of the COO$^-$ group have nearly equal bond lengths (C25—O23 1.286(1)) and C25—O24 1.241(9) Å), suggesting a proton transfer occurred from the acid to the base.

The cinchonidinium citronellate ion pair with the water of crystallization is shown in Figure 7.1.

In the crystal structure of **P1**, the conformation of the citronellate anion is assigned (*S*), based on the known conformation of cinchonidine, and the crystal structure did not exhibit the presence of the other enantiomer. The hydrogen bonding network is represented by three interactions: (**CIND**$^+$)-N11—H···O23-(**CA**$^-$)—O24···H35—O35-(water)···H22—O22-(**CIND**$^+$) that can be described using a graph set notation[3] $R_3^3(11)$. The water molecule also forms hydrogen bonds between the ion pairs in the [010] direction. The hydrogen bonding metrics are listed in Table 7.2.

Table 7.2 Hydrogen bond metrics of **P1**.

| D—H···A | D—H (Å) | H···A (Å) | D···A (Å) | D—H···A (°) | Symmetry operator |
|---|---|---|---|---|---|
| **P1** | | | | | |
| N11—H11···O23 | 0.89 | 1.82 | 2.702(8) | 171 | |
| O22—H22···O35 | 0.84 | 1.90 | 2.715(3) | 164 | x, 1+y, z |
| O35—H35A···O24 | 0.85 | 2.24 | 2.762(9) | 120 | x, -1 + y, z |
| O35—H35B···O23 | 0.85 | 2.22 | 2.693(6) | 115 | |
| C3—H3···O22 | 0.95 | 2.46 | 2.791(1) | 100 | |
| C12—H12A···O24 | 0.99 | 2.34 | 3.219(2) | 148 | 1-x, $-^1/_2$ + y, -z |
| C12—H12B···O22 | 0.99 | 2.49 | 3.437(7) | 160 | x, -1 + y, z |
| C15—H15B···O22 | 0.99 | 2.39 | 2.859(9) | 108 | |
| C16—H16B···O22 | 0.99 | 2.47 | 3.076(6) | 119 | |

The crystal packing of the structure is characterized by short H···H contacts between the aliphatic tails of the citronellate anions, as well as a herringbone packing positioning between the quinoline aromatic groups, whose planes unite at an angle of 57.7° (Figures 7.2 and 7.3).

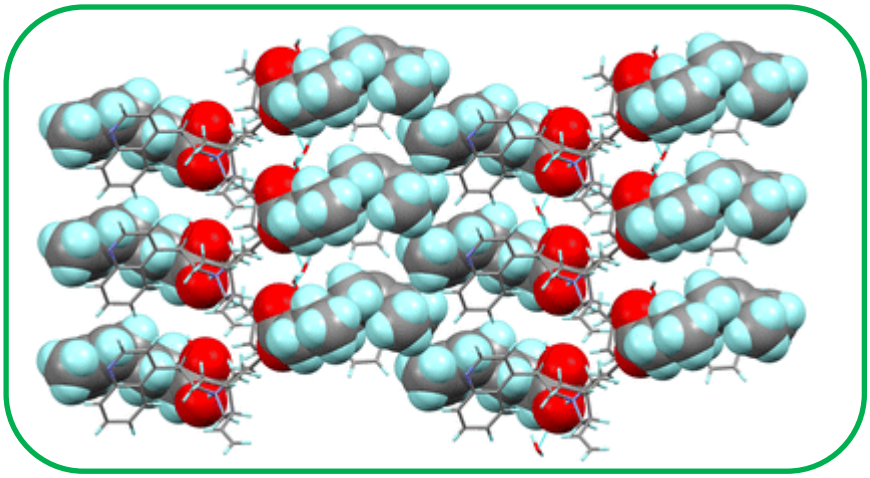

Figure 7.2 Illustration of close H···H contacts between the aliphatic tails of the citronellate anions (Anions are in space filling representation for clarity).

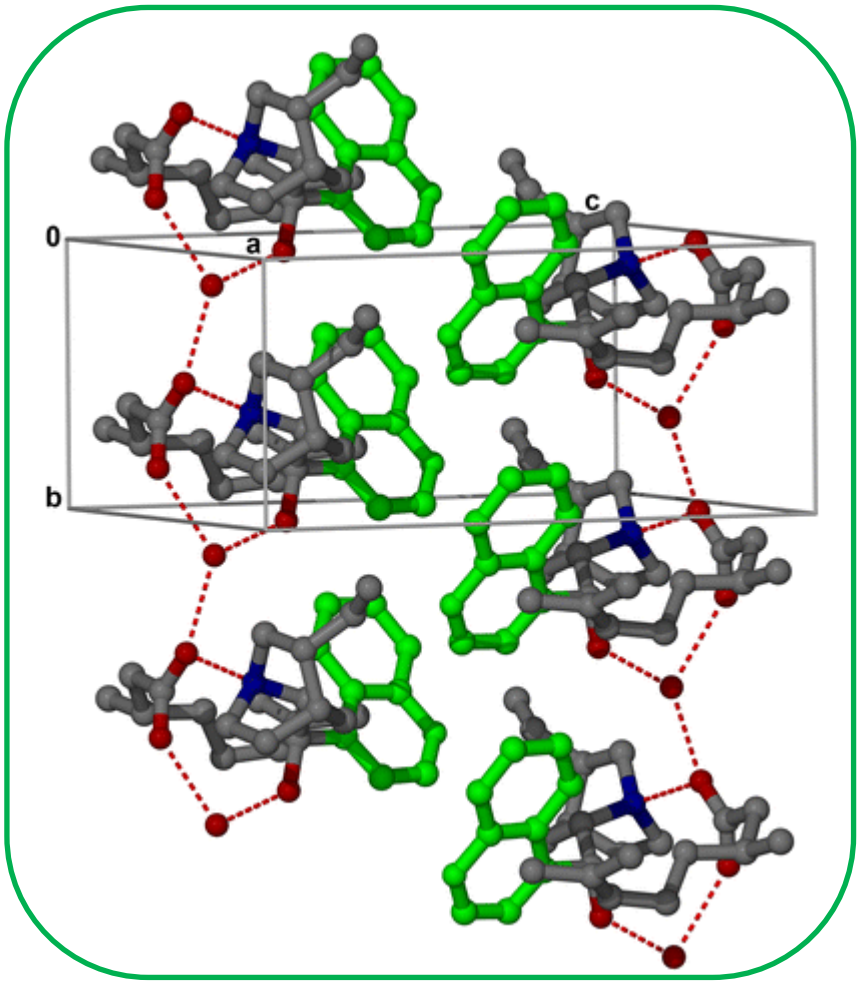


Figure 7.3 Water bridged hydrogen bonding between the ion pairs along the *b*-axis and the concomitant herringbone arrangement of the quinoline rings. The quinoline moieties are coloured green and the hydrogen atoms are omitted for clarity.

Crystallization experiments involving *R*-citronellic acid and the *Cinchona* alkaloids were also attempted. The experiments were carried out in different solvents, and only those in toluene, methanol and benzene resulted in precipitates. However, none of these samples were suitable for single crystal X-ray diffraction analysis.

Crystallization experiments using mixtures of solvents with racemic citronellic acid and the four resolving agents were also attempted. The mixtures that were used were, MeOH:$H_2O$ (8:2) and (1:1), acetone: $H_2O$ (8:2), (1:1) and (2:8), EtOH: $H_2O$ (1:1) and (8:2), MeOH:EtOAc (1:1), (8:2) and (1:9), and acetonitrile: $H_2O$ (7:3), (3:7), (9:1) and (1:1).Only a few of these experiments resulted in crystals, citronellic acid with **CIND** in MeOH:EtOAc (1:9), **QUID** in MeOH:EtOAc (8:2) and **CINC** in acetone: $H_2O$ (8:2). The DSC results showed that no new salts were formed, and the resolving agents crystallized from these solutions.

In summary, the resolving agent, (-)-cinchonidine was successfully employed to resolve racemic citronellic acid, affording the salt cinchonidinium-(*S*)-citronellate monohydrate. The

less soluble diastereomeric salt is stabilized by extensive hydrogen bonding, in which molecules of water of crystallization interlink the cation-anion pairs resulting in an infinite hydrogen-bonded chain along [010].

## 7.2 The resolution of racemic malic acid (**3.2**) (published in the *Canadian Journal of Chemistry*, **2015**, 93, 858-863, dx.doi.org/10.1139/cjc-2014-0579). Title: Resolution of malic acid by (+)-cinchonine and (-)-cinchonidine. Authors: Nikoletta B. Báthori, Ayesha Jacobs, Mawonga Mei and Luigi R. Nassimbeni.

Structure **P2**, cinchoninium-*D*-malate dihydrate, (**CINC**$^{+}$)•(*D*-**MA**$^{-}$)•2H$_2$O, was obtained by reacting cinchonine with *rac*-malic acid. The $\Delta pK_a$ for single or double deprotonation of malic acid (**MA**) are > 3. The p$K_a$ values[1] of malic acid (**MA**) are p$K_{a1}$ = 3.2 and p$K_{a2}$ = 5.1, and for the two resolving agents p$K_a$ = 9.2, for the quinuclidine N. This strongly suggests the production of salts.[2] The crystal data of the diastereomeric salts and the hydrogen bonding metrics are listed in Tables 7.3 and 7.4.

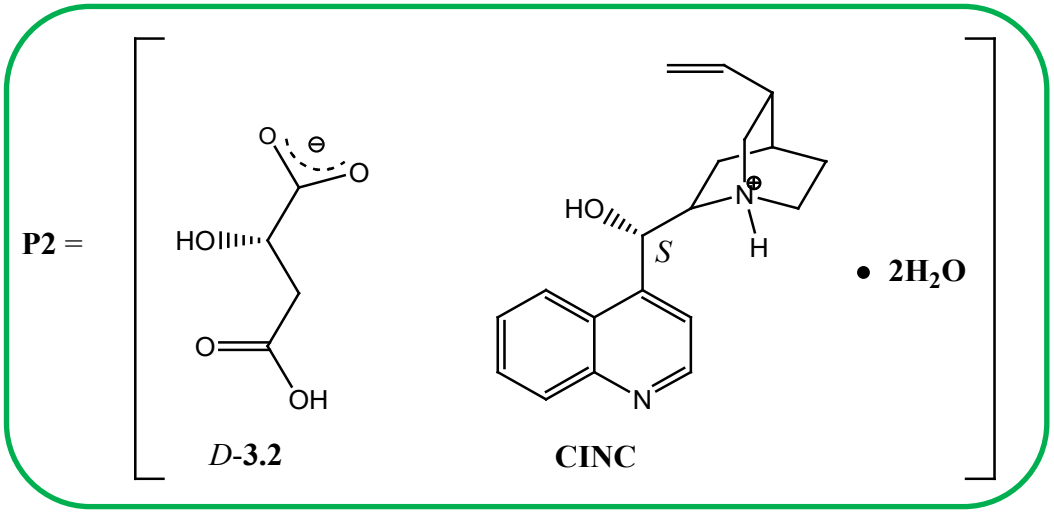


The salt crystallized in the space group $P2_1$ (No. 4) with $Z = 2$, with one of the two carboxylic acid groups having donated a proton and the structure is extensively hydrogen bonded. The packing is dominated by chains of *D*-malate anions linked by several hydrogen bonds shown in Figure 7.4a. In-between the resultant rings there are water molecules which appear as a continuous chain running along [010], and the rings may be represented in graph set notation[3] as $R_3^3(12)$ and $R_4^6(20)$.

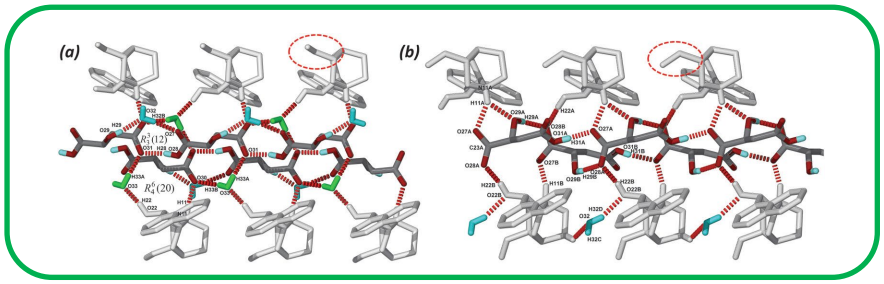


Figure 7.4 Hydrogen bonding in structures **P2** (a) and **P2a** (b). Symmetrically related water molecules are coloured green and light blue in **P2** and water molecules with 20% site occupancy are coloured light blue in **P2a**. The difference in the conformation of the vinyl group is circled with a red dotted line.

Another set of water molecules of crystallization is found between the *D*-malate anions which hydrogen bonds to the hydroxyl group of the cinchoninium cations. In addition the quinuclidinium $N^+$—H group hydrogen bonds to the carboxylate oxygen of the malic acid.

Table 7.3 Crystal data for **P2** – **P3a**.

| | **P2** | **P2a** | **P3** | **P3a** |
|---|---|---|---|---|
| Compound | (**CINC**$^+$)•(*D*-**MA**$^-$)•2$H_2O$ | 2(**CINC**$^+$)•2(*L*-**MA**$^-$)•0.2$H_2O$ | (**CIND**$^+$)•0.5(*D*-**MA**$^-$)•$H_2O$ | 2(**CIND**$^+$)•(*L*-**MA**$^-$)•2$H_2O$ |
| $M_r$ (g/mol) | $C_{23}H_{32}N_2O_8$ | $C_{23}H_{28.2}N_2O_{6.1}$ | $C_{21}H_{26.5}N_2O_{4.5}$ | $C_{42}H_{54}N_4O_9$ |
| Formula mass | 464.51 | 430.28 | 378.94 | 758.89 |
| Colour, habit | Colourless, needle | Colourless, needle | Colourless, needle | Colourless, needle |
| Crystal dimensions (mm) | 0.25x0.20x0.20 | 0.25x0.20x0.20 | 0.21x0.20x0.20 | 0.25x0.15x0.15 |
| Crystal system | Monoclinic | Triclinic | Monoclinic | Triclinic |
| Space group (No.) | $P2_1$ | $P1$ | $C_2$ | $P1$ |
| $Z$ | 2 | 2 | 4 | 1 |
| $a$ (Å) | 10.7046(6) | 7.5687(19) | 19.9466(10) | 6.5660(9) |
| $b$ (Å) | 7.2233(4) | 10.574(3) | 6.5410(3) | 10.1175(14) |
| $c$ (Å) | 15.0347(9) | 13.580(3) | 15.4264(7) | 15.415(2) |
| $\alpha$ (°) | 90.00 | 91.496(5) | 90.00 | 80.113(3) |
| $\beta$ (°) | 95.0320(10) | 91.673(5) | 106.3290(10) | 89.818(3) |
| $\gamma$ (°) | 90.00 | 93.654(5) | 90.00 | 71.728(3) |
| V (Å$^3$) | 1158.04(11) | 1083.7(5) | 1931.51(16) | 956.5(2) |
| Temperature (K) | 173(2) | 173(2) | 173(2) | 173(2) |
| ρ (calc.) (Mg/m$^3$) | 1.332 | 1.319 | 1.303 | 1.317 |
| Radiation | Mo Kα (λ = 0.71073 Å) | Mo Kα (λ = 0.71073 Å) | Mo Kα (λ = 0.71073 Å) | Mo Kα (λ = 0.71073 Å) |
| μ (mm$^{-1}$) | 0.101 | 0.096 | 0.092 | 0.093 |
| Absorption correction | Multiscan | Multiscan | Multiscan | Multiscan |
| Theta range for data collection (°) | 1.91, 28.28 | 1.93, 32.23 | 2.13, 28.37 | 2.15, 26.47 |
| Observed reflections | 11 098 | 13 971 | 8 109 | 8 499 |
| Independent reflections | 5 666 ($R_{int}$ = 0.0156) | 10 548 ($R_{int}$ = 0.0193) | 4 478 ($R_{int}$ = 0.0185) | 6 056 ($R_{int}$ = 0.0183) |
| Data/restrains/parameters | 5 666/1/324 | 10 548/5/577 | 4 478/1/258 | 6 056/3/586 |
| Maximum shift/error | 0.000 | 0.001 | 0.000 | 0.000 |
| Goodness-of-fit on $F^2$ | 1.037 | 1.023 | 1.022 | 1.042 |
| Final $R$ indices [$I > 2\sigma(I)$] | $R_1$ = 0.0387, $wR_2$ = 0.1021 | $R_1$ = 0.0491, w$R_2$ = 0.1233 | $R_1$ = 0.0339, w$R_2$ = 0.0907 | $R_1$ = 0.0521, w$R_2$ 0.1296 |
| $R$ indices (all data) | $R_1$ = 0.0417, w$R_2$ = 0.1047 | $R_1$ = 0.0625, w$R_2$ = 0.1323 | $R_1$ = 0.0363, w$R_2$ = 0.0927 | $R_1$ = 0.0567, w$R_2$ = 0.1328 |
| Largest diff. peak/hole (e Å$^{-3}$) | 0.592 and -0.360 | 0.455 and -0.255 | 0.232 and -0.164 | 0.303 and -0.253 |

Structure **P2a**, cinchoninium-*L*-malate quintahydrate, (2(**CINC**$^+$)•2(*L*-**MA**$^-$)•0.2$H_2O$), crystallized in the space group $P1$. The malic acid lost a proton from one of the COOH groups and the resulting malate anions are hydrogen bonded into columns running along [100].

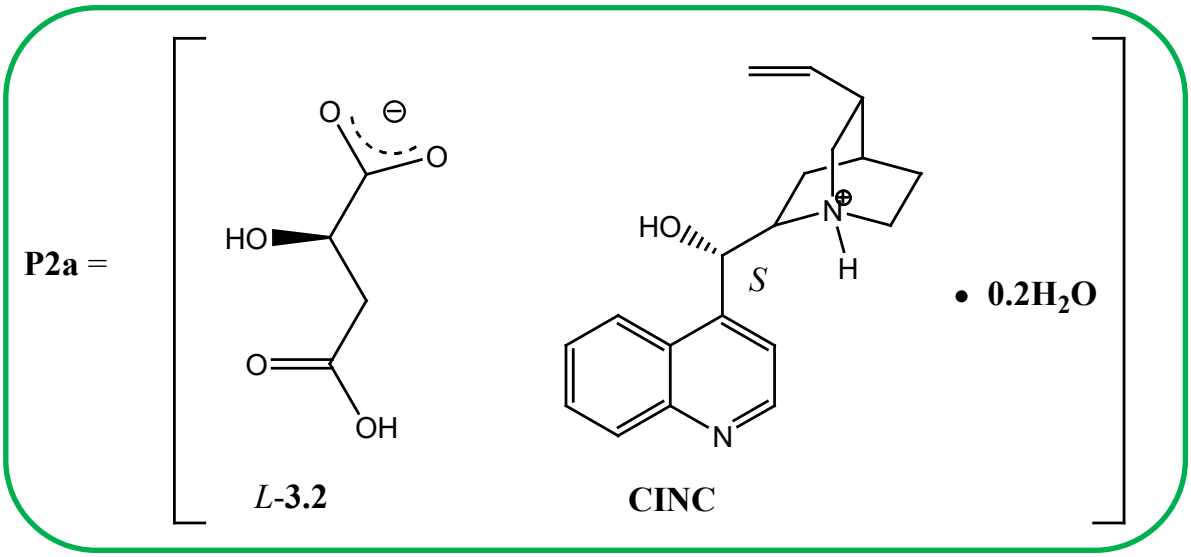


Several hydrogen bonded rings are present which may be presented as $R_4^3(15)$. The cinchoninium cation forms hydrogen bonds with the malate chain by O—H···$^-$OOC and bifurcated $N^+$—H···$^-$OOC/OH interactions. The water molecules are weakly hydrogen bonded, displaying only 20% site occupancy and form bridges between the cinchoninium cations *via* the quinoline N···H—O—H···OH hydrogen bonds (Figure 7.4b). The ethenyl group of the cinchoninium cation exist in different conformations in structures **P2** and **P2a**, (Figures 7.4 a and b).

Table 7.4 Hydrogen bond metrics for **P2** – **P3a**.

| D—H···A | D—H (Å) | H···A (Å) | D···A (Å) | D—H···A (°) | *Symmetry operator |
|---|---|---|---|---|---|
| **P2** | | | | | |
| N11—H11···O30* | 0.87 | 1.84 | 2.696(6) | 168 | 1-x, ½+ y, 1-z |
| O22—H22···O33 | 0.84 | 1.84 | 2.667(1) | 168 | |
| O28—H28···O31* | 0.84 | 1.73 | 2.554(8) | 166 | x, -1+y, z |
| O29—H29···O32 | 0.84 | 1.82 | 2.645(3) | 167 | |
| O32—H32B···O27* | 0.82 | 1.95 | 2.760(2) | 174 | x, -1+y, z |
| O33—H33A···O31 | 0.84 | 1.93 | 2.772(8) | 178 | |
| O33—H33B···O30* | 0.87 | 1.93 | 2.748(5) | 156 | 1-x, ½+ y, 1-z |
| **P2a** | | | | | |
| N11A—H11A···O27A | 0.92 | 2.02 | 2.837(7) | 148 | |
| N11A—H11A···O29A | 0.92 | 2.18 | 2.875(5) | 132 | |
| N11B—H11B···O27B* | 1.05 | 1.71 | 2.725(5) | 161 | 1+x, y, z |
| N11B—H11B···O29B* | 1.05 | 2.35 | 2.984(2) | 117 | 1+x, y, z |
| O22A—H22A···O28B | 0.84 | 1.89 | 2.727(5) | 171 | |
| O22B—H22B···O28A | 0.84 | 1.87 | 2.693(1) | 167 | |
| O29A—H29A···O28B* | 0.84 | 1.92 | 2.727(5) | 161 | 1+x, y, z |
| O29B—H29B···O28A | 0.84 | 1.97 | 2.792(7) | 165 | |
| O31A—H31A·····O27A* | 0.97 | 1.66 | 2.607(8) | 166 | x, 1+y, z |
| O31B—H31B···O27B* | 074 | 1.89 | 2.611(1) | 167 | 1+x, y, z |
| **P3** | | | | | |
| N11—H11···O25* | 0.95 | 1.75 | 2.699(8) | 175 | ½+x, -½+y, z |
| O22—H22·····O28 | 0.84 | 1.90 | 2.724(2) | 167 | |
| O28—H28C·····O26* | 0.85 | 1.97 | 2.799(2) | 159 | ½-z, ½+y, 1-z |
| O28—H28D···O25* | 0.85 | 1.86 | 2.706(5) | 171 | ½+x, -½+y, z |
| **P3a** | | | | | |
| N11A—H11A···O31B | 0.93 | 1.82 | 2.731(5) | 165 | |
| N11B—H11B···O28B* | 0.93 | 1.79 | 2.715(8) | 174 | x, 1+y, -1+z |
| O22B—H22B···O32B* | 0.84 | 1.97 | 2.739(1) | 169 | x, 1+y, -1+z |
| O22A—H22A·····O32A | 0.84 | 1.95 | 2.772(1) | 166 | |
| O29B—H29B·····O30B | 0.84 | 1.89 | 2.600(6) | 141 | |
| O32A—H32C···O31B | 0.86 | 1.83 | 2.625(3) | 153 | |
| O32B—H32F···O28B* | 0.84 | 2.22 | 2.766(4) | 123 | x, 1+y, -1+z |

Structure **P3**, cinchonidinium-*D*-malate monohydrate, (**CIND**$^{+}$)•0.5(*D*-**MA**$^{-}$)•$H_2O$, resulted from the reaction of cinchonidine with *rac*-malic acid.

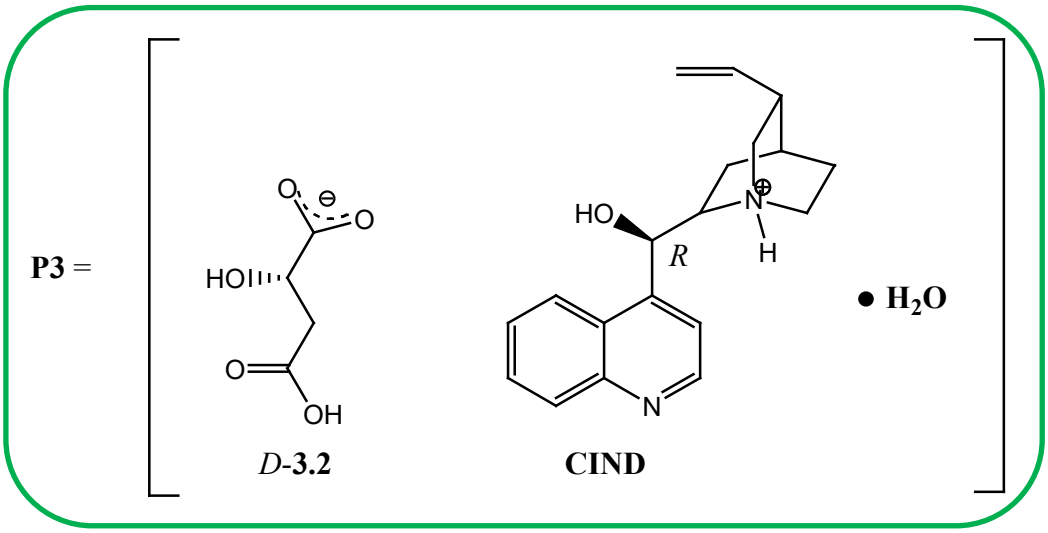


The space group of the crystallized structure is *C*2 with Z = 4. The cinchonidinium cation is in a general position, and the malate anion is located on a diad at Wykoff position *b*. The malate anions were forced to be disordered by the symmetry requirements and the hydroxyl components were refined with half site occupancy. The methylene hydrogen atom which is located adjacent to the disordered hydroxyl oxygen, could not be successfully refined and was excluded from the final model. Two malate anions and two bridging water molecules, $R_4^4(16)$, (Figure 7.5a) form hydrogen bonded rings along [010]. An $R_3^3(11)$ motif resulted due to the cations bonded to the chains of rings. The packing is indistinguishable from the packing established in the structure of the quininium-*D*-malate dihydrate, which also crystallized in the space group *C*2 and has comparable unit cell dimensions.[4]

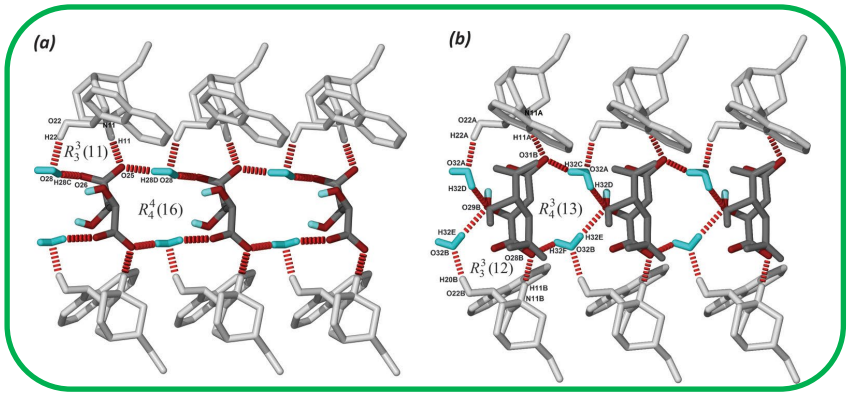


Figure 7.5 Hydrogen bonding in structures **P3** (a) and **P3a** (b). Water molecules are coloured light blue and the minor disorder of the guest is presented with grey (b).

Structure **P3a**, cinchonidinium-*L*-malate dihydrate, 2(**CIND**$^+$)•(*L*-**MA**$^-$)•2H$_2$O, crystallized in the space group $P\bar{1}$.

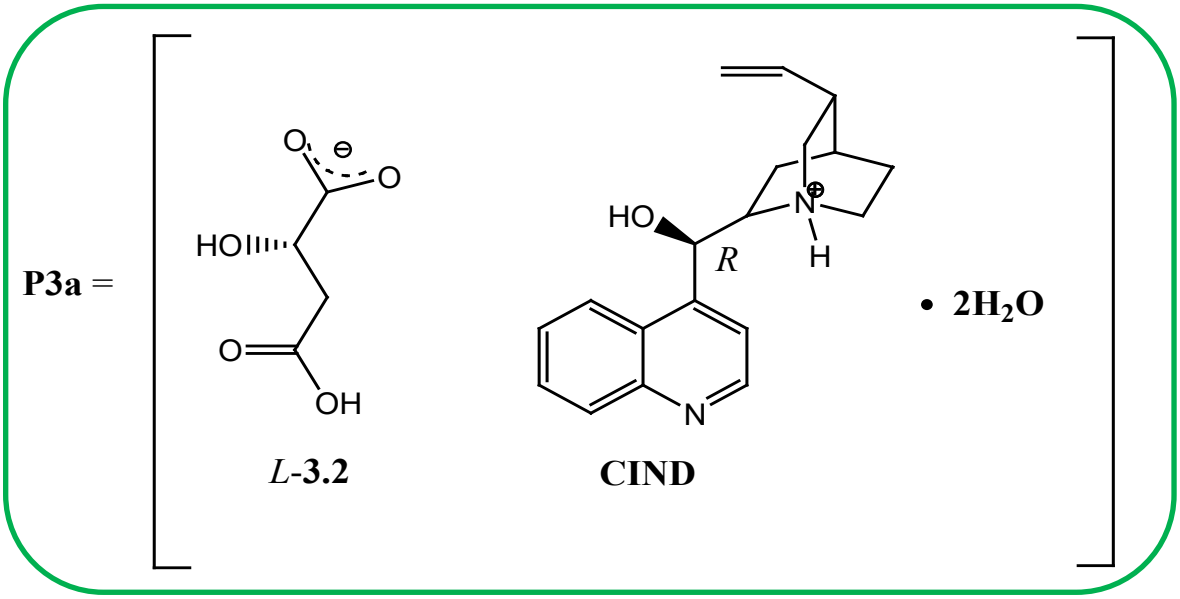


The disordered malate anion was refined to 67:33 site occupancy. The packing contains hydrogen bonded rings of malates that have water molecules in-between, described with an $R_4^3$ (13) notation, and forming chains running along [100], (Figure 7.5 (b)). The malates form $N^+$—H···$^-$OOC interactions with the cinchonidinium cations resulting in the formation of a ring motif which may be reported as $R_3^3$ (12).

Conformational analysis

In chiral discrimination experiments the different conformations of quinine have been reported.[4,5] The constant conformation of quinine was observed in the twenty-six crystal structures that were analyzed, and the flexibility of the ethenyl component has been connected to the chiral selectivity in the crystals formed from the resolution of mandelic acid. In the same manner, the conformational analysis of the cinchoninium and cinchonidinium cations in **P2** – **P3a** were carried out and the outcomes are illustrated in Table 7.5. The recorded three torsion angles (τl: C3—C4—C9—O22, τ2: O22—C9—C10—C11 and τ3: C14—C13—C18—C19) showed no drastic conformational changes in the majority of the cations, except in the position of the ethenyl component. The rotation of the quinoline group (τl) and the quinuclidine group (τ2) is very similar in all pairs of the structures. A significant change from -137° (structure **P2**) to +137° (structure **P2a**, molecule A) and -77° (in molecule B) is recorded in τ3, representing the position of the ethenyl component when cinchonine is exposed to the two opposite malate enantiomers. In regard to cinchonidine, involved in structures **P3** and **P3a**, the cation is virtually in the same conformation regardless of the malate enantiomers.

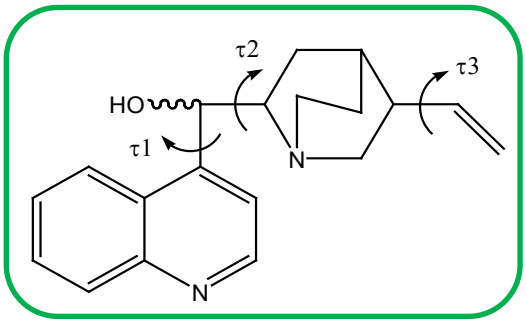


Table 7.5 Torsion angles for the cations in structures **P2** – **P3a**.

| Torsion angles | **P2** | **P2a** | | **P3** | **P3a** | |
|---|---|---|---|---|---|---|
| Molecules | | A | B | | A | B |
| τ1 (°) | 14.35 | 19.70 | 20.09 | -21.97 | -22.75 | -22.23 |
| τ2 (°) | 71.07 | 68.41 | 58.25 | -77.95 | -78.01 | -76.70 |
| τ3 (°) | -137.68 | 137.65 | -77.78 | -106.69 | -107.38 | -100.71 |

Hirshfeld surface analysis

The *Cinchona* alkaloid pairs, quinine/cinchonidine and quinidine/cinchonine are *quasi*-enantiomeric, and have been employed to isolate both enantiomers of a number of carboxylic acids.[6] Nevertheless, no crystallographic structural data was reported regarding these resolutions. In two separate studies, *N*-benzylcinchoninium chloride[7] and *N*-benzylcinchonidinium chloride[8] have been exploited to isolate the enantiomers of *rac*-2,2'-dihydroxy-1,1'-binaphthyl with both giving the (*R*)-(+)-enantiomer. The notable differences between the two structures were attributed to changes in the non-bonded interactions between the hydroxyl component and the chloride anion. Cinchonine and cinchonidine have also been used in the resolution of *rac*-mandelic acid.[9,10] Cinchonidinium-(*S*)-mandelate and cinchoninium-(*R*)-mandelate were the two less soluble diastreomeric salts. It was suggested that the steric effects of the ethenyl moiety were the cause of the differences in the packings.

The non-bonded interactions of the four malate salts were analyzed in order to understand the difference in the packing forces which stabilize their structures. The program CrystalExplorer[11] was employed to generate the relevant fingerprint plots.[12,13] The close contacts between the *D*-malate anion and the neighbouring host cations and water molecules in structure **P2** are shown in Figure 7.6(a). The O···H hydrogen bonds are represented by the spikes labelled ① and ②, with the sum of the internal and external distances ($d_i$ and $d_e$) of the Hirshfeld surfaces[14] at 1.60 Å. The H···H interactions at $d_i + d_e = 2.40$ Å are represented by the broader peak labelled ③. The two crystallographically independent malate anions' fingerprint plots are exhibited in Figures 7.6. (b) and (c).

The two show weaker O···H hydrogen bonds, the peaks labelled ③ which corresponds to close H···H contacts at 2.1 Å exhibiting partial repulsion, and the circled area of the long range contacts which corresponds to looser packing. The secondary interactions for **CIND**$^{+}$ with *D*-malate and *L*-malate are exhibited in Figures 7.6 (d) and (e). The spikes labelled ① in Figure 7.6 (d) corresponds to the carboxylate···water hydrogen bond at 1.7 Å. The disordered hydroxyl component hydrogen bonded to water is represented by the spike labelled ② at 2.28 Å. The spike labelled ③ corresponds to H···H interactions. Conversely, weaker non-bonded interactions in structure **P3a** are shown in Figure 7.6 (e), and the malate anions are disordered with the site occupancies of 67:33. Figure 7.6 (e) resembles the major component, with the spike labelled ① due to hydrogen bond O···H, with $d_i + d_e = 1.75$ Å.

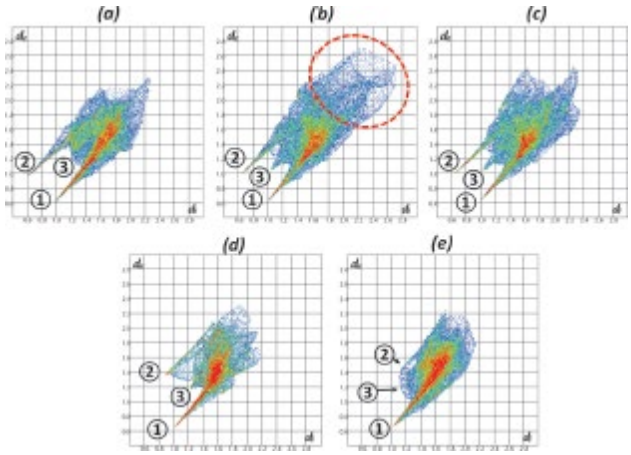


Figure 7.6 Fingerprint plots for the malate ions in structures **P2** (a), **P2a** (b and c represents the two symmetry independent ions), **P3** (d) and **P3a** (e represents the plot of the major occupancy disordered malate ion).

The longer O···H interaction (2.7 Å) is represented by the second spike labelled ②, and the H···H broad peak at ③ exhibits partial repulsion.

Conclusion

Cinchonine and cinchonidine successfully resolved the racemic *DL*-malic acid. Both of the resolving agents isolated the *D*-malate enantiomer and water was incorporated into the salts. In both salts the acid was monodeprotonated.

It is demonstrated that there is more efficient packing of the *D*-malate anions in both the cinchoninium and the cinchonidinium salts.

## 7.3 The resolution of racemic *trans*-9,10-dihydro-9,10-ethanoanthracene-11,12-dicarboxylic acid (**3.3**).

The racemic diacid was treated with the various resolving agents in different solvents, and salts were obtained giving rise to **P4** - **P8** using acetone, MeOH and acetonitrile/water as solvents (Scheme 7.1).

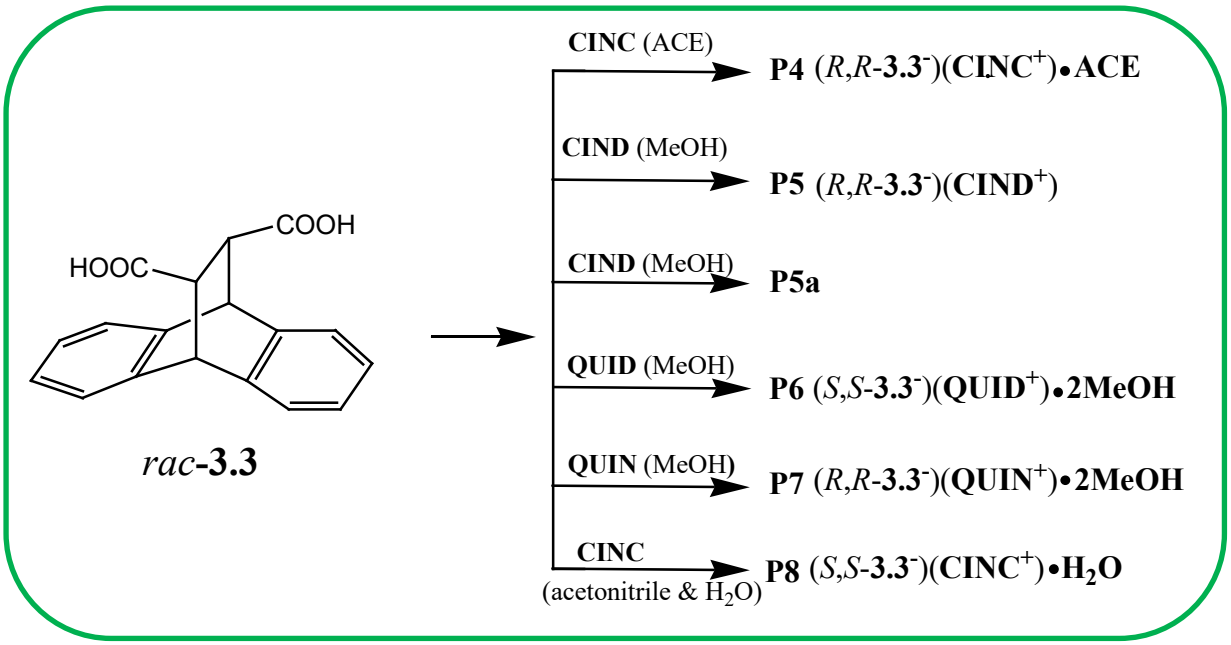


Scheme 7.1 The resolution of *rac*-**3.3** to form the diastereomeric salts **P4** – **P8,** and powdered **P5a**.

Thermal analysis

The DSC and TGA experiments were carried out in order to study the thermal behaviour of the salts in relation to the racemates and the resolving agents. The salts that formed are named as products, **P4** – **P8**. The desolvation and melting thermal events of the salts, are represented as endotherm 1 and 2 respectively. The thermal results are summarized in Figure 7.7 and Table 7.6.

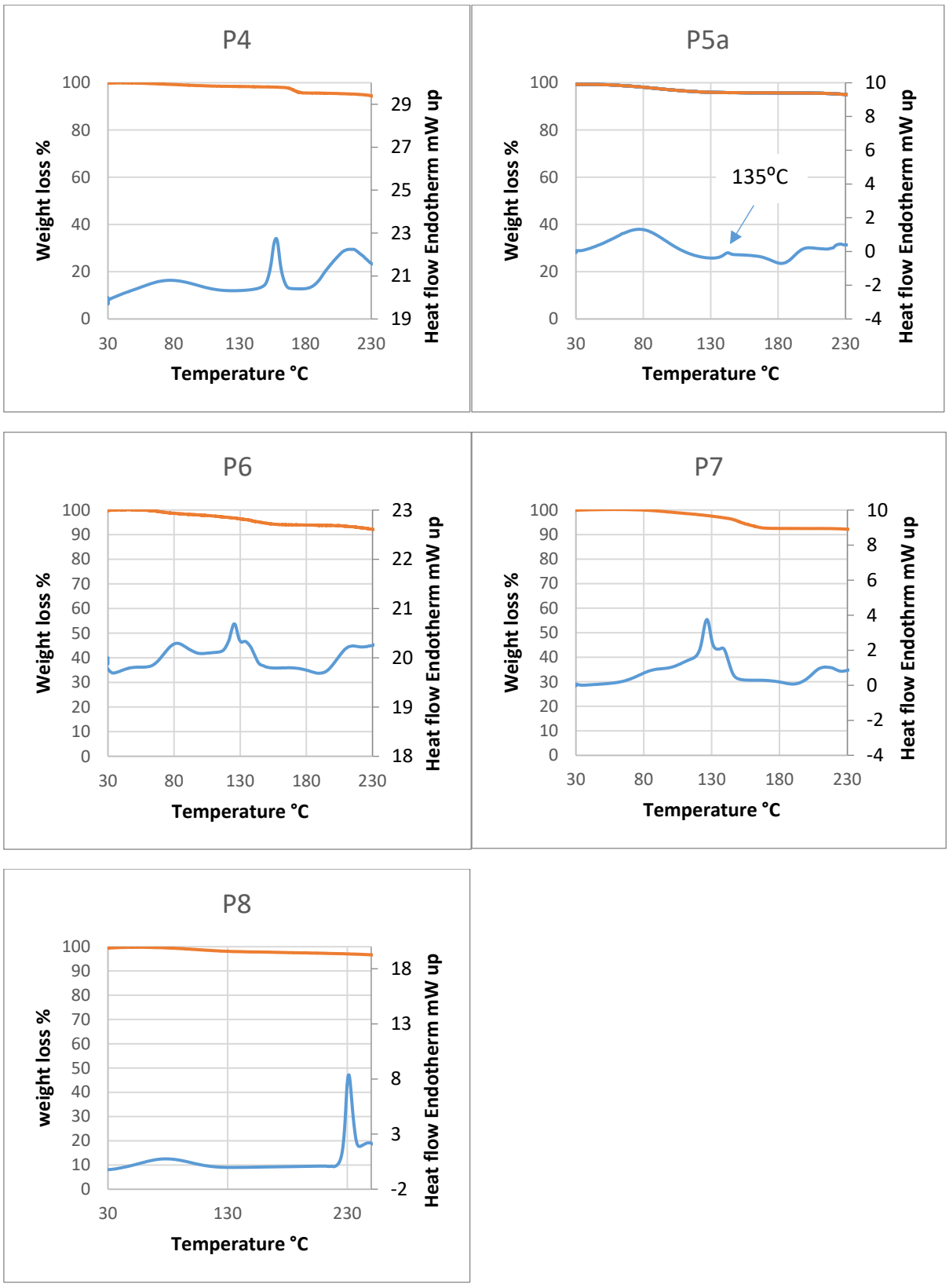


Figure 7.7 DSC and TGA curves of salts **P4** - **P8** and the powder **P5a**.

Table 7.6 Thermal analysis data of the starting materials and the products **P4, P5a, P6, P7 and P8**.

| **Reagents** | | | **Products** | **Thermal analysis** | | | |
|---|---|---|---|---|---|---|---|
| Racemate $T_{on}/T_p$ ºC | RA $T_{on}/T_p$ ºC | Solvent (bp ºC) | Salt | DSC | | TG | |
| | | | | Endo 1 $T_{on}/T_p$ ºC | Endo 2 $T_{on}$ ºC | Exp (%) | Calc (%) |
| *Rac* **3.3** 245/256 | **CINC** 248/264 | Acetone (56) | **P4** | 33/75 | 138 | 4.3 | 8.9 |
| | **CIND** 198/206 | MeOH (65) | **P5a** | 40/81 | 135 | 4.2 | 5.2 |
| | **QUID** 166/174 | MeOH (65) | **P6** | 65/81 | 115 | 7.0 | 9.4 |
| | **QUIN** 172/177 | MeOH (65) | **P7** | 59/77 | 112 | 7.8 | 9.4 |
| | **CINC** 248/264 | Acetonitrile (82) and water (100) | **P8** | 36/77 | 218 | 2.0 | 2.6 |

**RA**-resolving agents, **CINC**-cinchonine, **CIND**-cinchonidine, **QUIN**-quinine, **QUID**-quinidine, Bp-boiling point, *rac*-**3.3**-*trans*-9,10-dihydro-9,10-ethanoanthracene-11,12-dicarboxylic acid. Endo - endotherm 1 & 2 (desolvation & melt), $T_{on}$ – onset temperature, $T_p$- peak temperature, Exp-experimental and Calc-calculated.

For all the salts the DSC gave two endotherms, the first due to the loss of the solvent and the second due to the melt of the salt. The TGA results of **P4** showed a mass loss starting at 33 °C, due to the release of acetone which is highly volatile. The calculated mass loss due to one molecule of acetone was 8.97%. The experimental mass loss of 4.33% corresponds to the loss of one half of an acetone molecule. The salt also showed a lower melting temperature than the starting materials, indicating a low thermal stability.

For **P5** the crystallization experiment was repeated as there was not enough precipitate from the initial experiment to perform the DSC, TGA and FT-IR analysis. The DSC results of this precipitate (powder) henceforth referred to as **P5a** showed a broad endotherm with the onset temperature of 40 °C followed by a series of diffuse peaks, indicating a solvate. This was supported by the TGA result (exp mass loss of 4.2%) which corresponds to loss of methanol (calc 5.2%). The initial salt **P5**, did not contain any solvent in the crystal structure, however it was not possible to reproduce this salt for further analysis.

The TGA curve of **P6** showed a mass loss at low temperatures corresponding to the loss of the volatile methanol solvent molecules, with a calculated mass loss of 9.4 %, exp mass loss of 7.0%. Thereafter the salt shows a complex multistep decomposition process with broad endotherms at 65 °C and 115 °C.

The thermal analysis curves of **P7** showed a similar thermal decomposition profile as **P6**. The mass loss attributed to two moles of MeOH as in **P6** was calculated to be 9.4%, compared to the TGA experimental value of 7.8%.

The DSC thermogram of **P8** showed a broad peak with an onset at 36 °C which corresponds to the loss of water. The second endotherm is due to the melt of the salt, at an onset of 218 °C, and is immediately followed by the decomposition of the salt. The TGA results showed a mass loss of 2.0%, with a calculated mass loss of 2.6%.

For all the salts except for **P5** the thermal analysis results confirmed the formation of salt solvates. Attempts to recrystallize **P5** (non-solvated salt) were unsuccessful and a solvated precipitate **P5a** resulted. The melting points for all the salts are lower than those of the starting materials.

It has been established and documented that it is possible to obtain crystals of a particular nature different from the initial crystals, even after following the same procedure, in an attempt to prepare the same (initial) crystal.[15] Attempts to obtain **P5** following the same procedure did not yield crystals, and a powder was obtained, giving rise to **P5a**.

Hot stage microscopy (HSM) has been used as a complementary tool to assist in the characterization of solids in solid state chemistry.[16] **P5a** was analyzed using the HSM technique to assist in observing its melt at elevated temperatures.

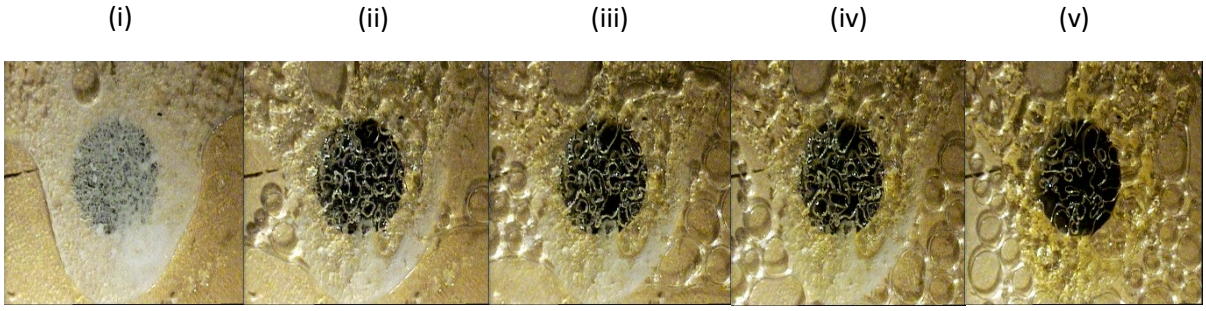


Figure 7.8 HSM photography of **P5a** at (i) 50 °C, (ii) 118 °C, (iii) 137 °C, (iv) 151 °C and (v) 160 °C.

Fig 7.8 consists of photomicrographs of **P5a** visually assayed at 50, 118, 137, 151 and 160 °C. (i) Bubbles appeared at 50 °C due to the loss of methanol. (ii) At 118 °C more bubbles are observable as well as the melt of the salt. (iii) – (v) 137 °C - 160 °C the melt continues.

Table 7.7 Desolvation temperatures ($T_{on}$) of the products compared to the solvents' boiling points.

| Salts | $T_{on}$ °C | Solvent | Bp °C | $T_{on}$ - $T_{bp}$ (°C) |
|---|---|---|---|---|
| **P4** | 33 | Acetone | 56 | -23 |
| **P5a** | 40 | MeOH | 65 | -25 |
| **P6** | 65 | MeOH | 65 | 0 |
| **P7** | 59 | MeOH | 65 | -6 |
| **P8** | 36 | $H_2O$ | 100 | -64 |

Table 7.7 shows that most of the desolvation temperatures are lower than the boiling points of the solvents except for **P6** where methanol is released at its boiling point. The results suggest that the hydrogen bonding interactions between the solvents and the salts are weak. The value of $T_{on}$ - $T_{bp}$ is often used to determine thermal stability.[17,18] The $T_{on}$ - $T_{bp}$ results indicate that **P6** is the most thermally stable of the salts, with **P8** the least stable (**P6** > **P7** > **P4** > **P5a** > **P8**).

Crystal structure analysis.

For all the structures proton transfer occurred from a carboxylic moiety of **3.3** to the quinuclidine nitrogen (N1) of the alkaloids resulting in salts. The C—O distances of the carboxylate moieties are nearly similar which clearly distinguishes the carboxylate from the carboxylic acid (Table 7.8). The crystal data and refinement details of all the diastereomeric salts are given in Table 7.9.

Table 7.8 C—O distances in the various salts.

| d(C—O)/Å | **P4** | **P5** | **P6** | **P7** | **P8** |
|---|---|---|---|---|---|
| Carboxylate | 1.227(3) | 1.242(3) | 1.252(2) | 1.254(2) | 1.248(1) |
| | 1.282(2) | 1.280(3) | 1.254(2) | 1.257(2) | 1.269(1) |
| Δd(C—O) | 0.055 | 0.038 | 0.002 | 0.003 | 0.021 |
| Carboxylic acid | 1.209(2) | 1.195(3) | 1.186(2) | 1.193(2) | 1.213(1) |
| | 1.325(2) | 1.345(3) | 1.314(2) | 1.309(2) | 1.326(1) |

(*R*,*R*-**3.3**$^-$)(**CINC**$^+$)·**ACE (P4),** (Cinchoninium *R,R*-9,10-dihydro-9,10-ethanoanthracene-11,12-carboxylic acid carboxylate acetone solvate), crystallized in the orthorhombic space group $P2_12_12_1$ with $Z = 4$, with one **3.3**$^-$ anion, one **CINC**$^+$ cation and one acetone molecule in the asymmetric unit, and the corresponding structure is depicted in Figure 7.9(a).

Table 7.9 Crystal data and refinement details of **P4** – **P8**.

| Compound | **P4** (*R*,*R*-**3.3**$^-$)(**CINC**$^+$)·**ACE** | **P5** (*R*,*R*-**3.3**$^-$)(**CIND**$^+$) | **P6** (*S*,*S*-**3.3**$^-$)(**QUID**$^+$)·**2MeOH** | **P7** (*R*,*R*-**3.3**$^-$)(**QUIN**$^+$)·**2MeOH** | **P8** (*S*,*S*-**3.3**$^-$)(**CINC**$^+$)·**H$_2$O** |
|---|---|---|---|---|---|
| Molecular formula | $C_{40}H_{42}N_2O_6$ | $C_{37}H_{36}N_2O_5$ | $C_{40}H_{46}N_2O_8$ | $C_{40}H_{46}N_2O_8$ | $C_{37}H_{38}N_2O_6$ |
| $M_r$ (g/mol) | 646.76 | 588.68 | 682.79 | 682.79 | 606.72 |
| Temperature (K) | 173 | 173 | 173 | 173 | 173 |
| Crystal size (mm) | 0.05 x 0.12 x 0.34 | 0.10 x 0.19 x 0.30 | 0.38 x 0.39 x 0.45 | 0.24 x 0.33 x 0.59 | 0.14 x 0.15 x 0.23 |
| Crystal system | Orthorhombic | Orthorhombic | Hexagonal | Hexagonal | Orthorhombic |
| Space group | $P2_12_12_1$ | $P2_12_12_1$ | $P_2$ | $P3_1$ | $P2_12_12_1$ |
| *a* (Å) | 8.9332(18) | 6.5328(13) | 10.7363(15) | 10.7536(6) | 8.8245(5) |
| *b* (Å) | 12.479(3) | 16.321(3) | 10.7363(15) | 10.7536(6) | 12.8433(7) |
| *c* (Å) | 31.390(6) | 27.258(6) | 26.456(5) | 26.5343(16) | 27.4155(17) |
| α (°) | 90 | 90 | 90 | 90 | 90 |
| *β* (°) | 90 | 90 | 90 | 90 | 90 |
| *γ* (°) | 90 | 90 | 120 | 120 | 90 |
| V (Å$^3$) | 3499.2(12) | 2906.2(10) | 2641.0(7) | 2657.3(3) | 3107.2(5) |
| *Z* | 4 | 4 | 3 | 3 | 4 |
| ρ (calcd) (g/cm$^3$) | 1.228 | 1.345 | 1.288 | 1.2780 | 1.2968 |
| Absorption coefficient *μ* (mm$^{-1}$) | 0.082 | 0.089 | 0.090 | 0.089 | 0.088 |
| Theta range for data collection (°) | 3.33 – 27.50 | 1.45 – 28.32 | 2.19 – 28.39 | 2.19 – 28.36 | 1.49 – 28.38 |
| Reflections collected | 7971 | 16441 | 27060 | 23470 | 7763 |
| No. data with $I > 2\sigma(I)$ | 6211 | 7251 | 8826 | 8830 | 6180 |
| No. parameters | 437 | 403 | 459 | 459 | 426 |
| Final R ($I > 2\sigma(I)$) | $R_1$ = 0.0463; $wR_2$ = 0.1317 | $R_1$ = 0.0484; $wR_2$ = 0.0981 | $R_1$ = 0.0425; $wR_2$ = 0.0921 | $R_1$ = 0.0428; $wR_2$ = 0.0987 | $R_1$ = 0.0477; $wR_2$ = 0.0989 |
| *R* indices all data | $R_1$ = 0.0693; $wR_2$ = 0.1556 | $R_1$ = 0.0698; $wR_2$ = 0.1090 | $R_1$ = 0.0546; $wR_2$ = 0.0984 | $R_1$ = 0.0511; $wR_2$ = 0.1034 | $R_1$ = 0.0660; $wR_2$ = 0.1088 |
| Goodness-of-fit on $F^2$ | 0.842 | 1.023 | 1.029 | 1.036 | 1.020 |

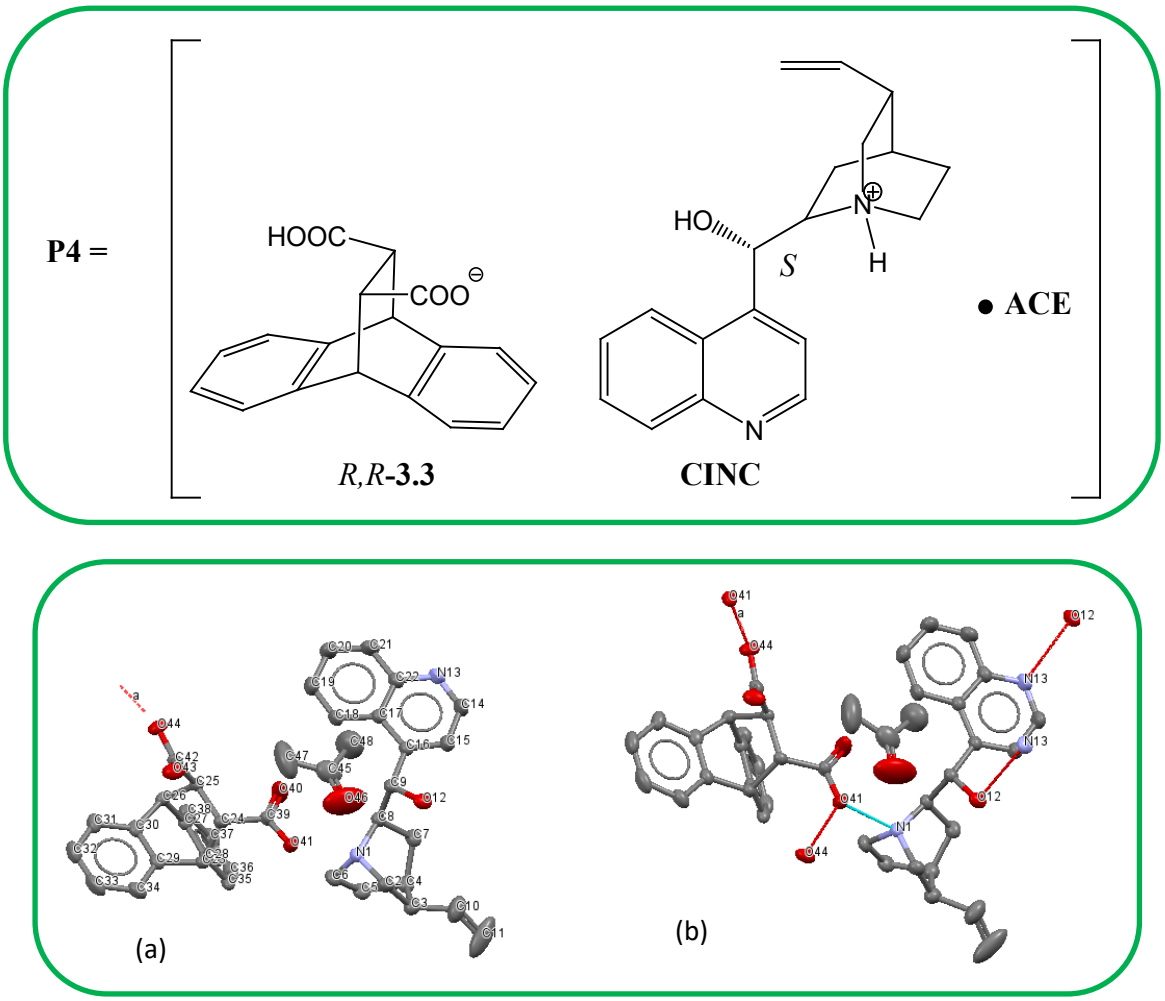


Figure 7.9 Representation of the X-ray crystal structure of **P4**, (a) showing the atom labelling and (b) showing the hydrogen bonding. Hydrogen atoms have been omitted for clarity.

The **CINC**$^{+}$ chiral C9 has an *S* configuration which was assigned accordingly and subsequently the **3.3**$^{-}$ had an (*R,R)* absolute configuration. The hydrogen bonding is characterized by the charged assisted interaction, (**CINC**$^{+}$)-N1—H1···O41-(**3.3**$^{-}$)···H—O44-(**3.3**$^{-}$). Furthermore, the quinoline nitrogen (N13) also forms hydrogen bonds with the OH of another **CINC**$^{+}$ to form $C_1^1(7)$ chains.[19] Hydrogen bonding details for all the salts are summarized in Table 7.8. The acetone carbonyl O atom, points towards the quinuclidine H atoms, therefore the acetone molecules are involved in weak C—H···O hydrogen bonding (Figure 7.10), characterized by the interactions, (**CINC**$^{+}$)-C5—H5B···O46-(**ACE**), (**CINC**$^{+}$)-C7—H7A···O46-(**ACE**) and (**CINC**$^{+}$)-C8—H8···O46-(**ACE**).

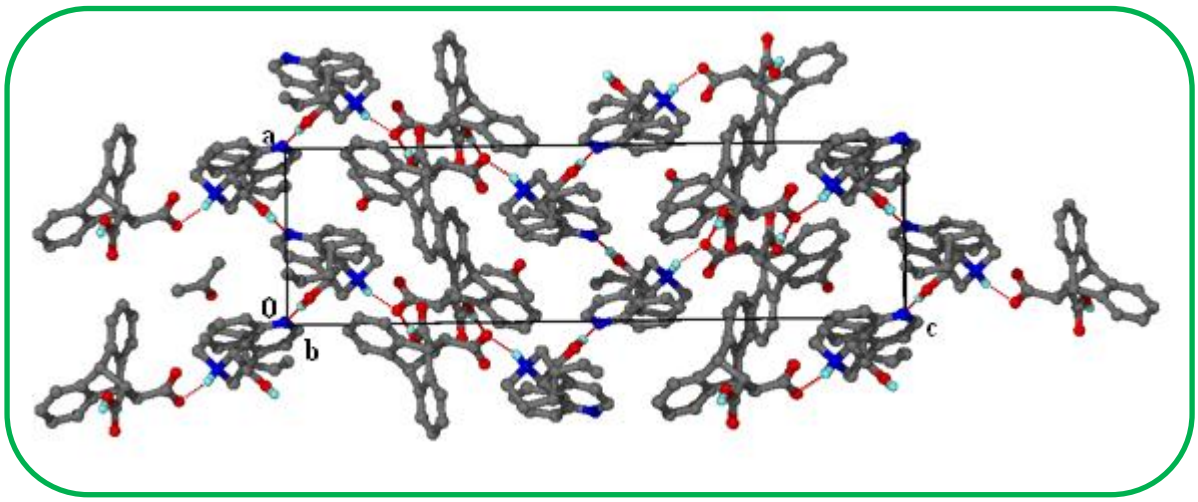


Figure 7.10 Packing diagram of **P4** along [010]. Hydrogens not involved in hydrogen bonding have been omitted for clarity.

For all the salts, **P4** – **P8**, the C—O distances of the $COO^-$ group of the **3.3**$^-$ range from 1.227(3) Å to 1.282(2) Å, with the difference between the two C—O bonds ranging from 0.002 to 0.055 Å, (Table 7.8) which suggests that the carboxyl group of **3.3** is deprotonated, and formed a salt with the resolving agents. The assignment of the products as salts is based on successful refinement of the relevant hydrogen atoms using single crystal X-ray diffraction data. The resonance of a carboxylate gives rise to the C—O bond distances of equal lengths in the absence of hydrogen bonding and other electronic perturbations. The formation of single or multiple hydrogen bonds at one oxygen atom results in the lengthening of the associated C—O bond distance.[20] The non-equivalence of the C—O bonds in **3.3**$^-$ is apparently a consequence of the classical hydrogen bond by the O atom, with one carboxylate O atom forming more hydrogen bonds compared to the other carboxylate O atom. One cation is bound to one anion through one N—H···O hydrogen bond, with an average hydrogen bond distance of 2.6822 Å.

(*R*,*R*-**3.3**$^-$)(**CIND**$^+$), **P5**, (Cinchonidinium *R,R*-9,10-dihydro-9,10-ethanoanthracene-11,12-carboxylic acid carboxylate) was successfully solved in the orthorhombic space group $P2_12_12_1$ with $Z = 4$, with one **3.3**$^-$ anion and one **CIND**$^+$ cation in the asymmetric unit. The corresponding structure is depicted in Figure 7.11(a). The **CIND**$^+$ chiral C9 has an *R* configuration and this was assigned accordingly. Therefore the **3.3**$^-$ had an *R,R* absolute configuration. The hydrogen bonding consists of (**CIND**$^+$)-N1—H1···O41-(**3.3**$^-$), (**3.3**$^-$)-O44—H44···O41-(**3.3**$^-$) and furthermore the **CIND**$^+$ OH group is linked to the other carboxylate oxygen forming (**CIND**$^+$)-O12—H12···O44-(**3.3**$^-$), see Figure 7.11(b). This results in chains along [100] which can be described as $C_2^2(9)$,[19] Figure 7.12.

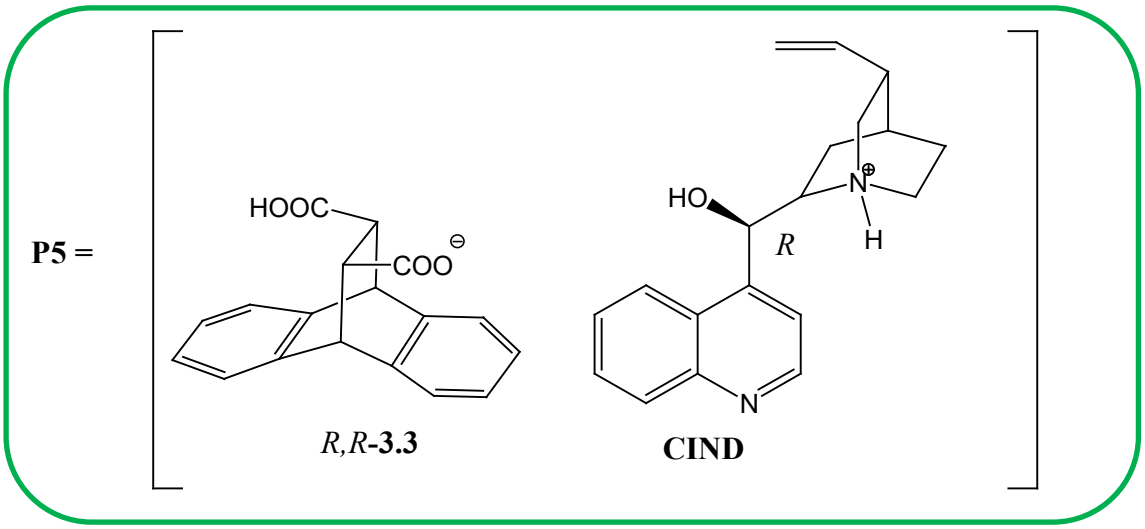


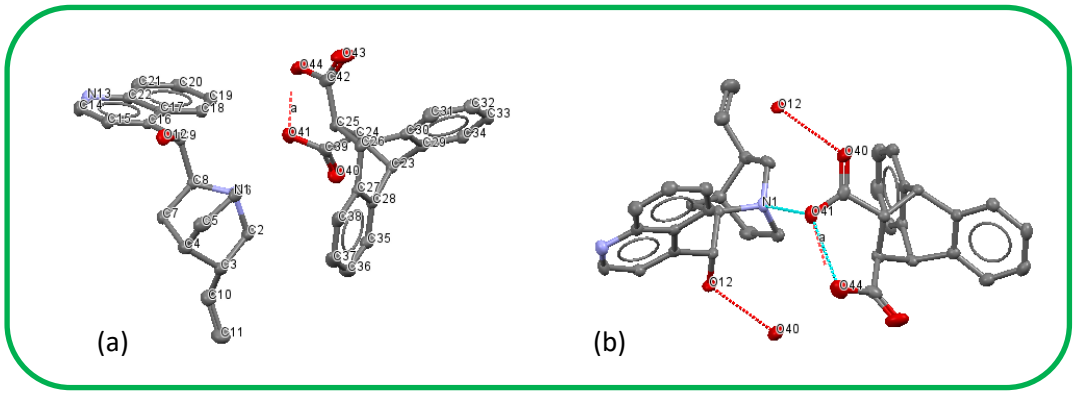


Figure 7.11 Representation of the X-ray crystal structure of **P5**, (a) showing the atom labelling and (b) showing the hydrogen bonding. Hydrogen atoms have been omitted for clarity.

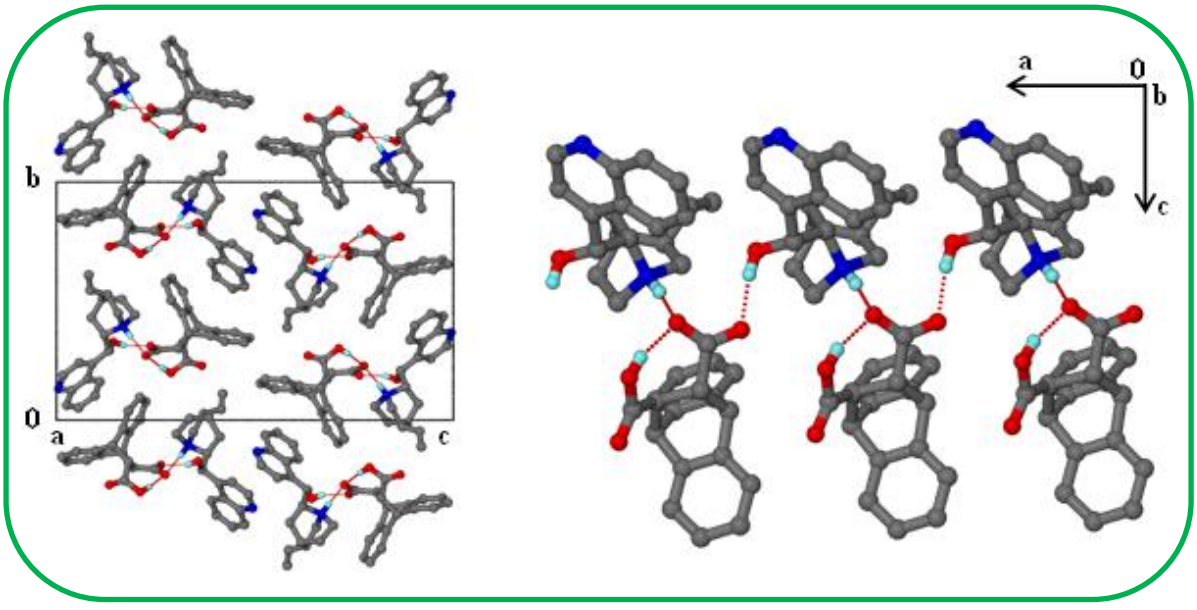


Figure 7.12 (a) Packing diagram of **P5** along [100] and (b) $C_2^2(9)$ chains of (*R*,*R*-**3.3**$^-$) and **CIND**$^+$. Hydrogens not involved in hydrogen bonding have been omitted for clarity.

(*S*,*S*-**3.3**$^-$)(**QUID**$^+$)·**2MeOH** (**P6**), (Quinidinium *S*,*S*-9,10-dihydro-9,10-ethanoanthracene-11,12-carboxylic acid carboxylate dimethanol solvate) crystallized in the hexagonal space

group $P3_2$ with $Z = 3$. The asymmetric unit consists of one **3.3**$^-$, one **QUID**$^+$ and two methanol molecules in the asymmetric unit, and the corresponding structure is depicted in Figure 7.13(a). The absolute configuration of stereogenic centres 11 and 12 of **3.3**$^-$ was assigned as (*S,S*) relative to the known absolute configuration of (*S*)-**QUID**$^+$. The supramolecular units (*S,S*-**3.3**$^-$)(**QUID**$^+$) are linked *via* two crystallographically independent methanol molecules (Figure 7.13 and 7.14). The hydrogen bonding is represented by: (**QUID**$^+$)-N1—H1···O43 (**3.3**$^-$), (**QUID**$^+$)-O12—H12···O48-(**MeOH A**), (**MeOH B**)-O50—H50···O48-(**MeOH A**), (**MeOH A**)-O48—H48···O42-(**3.3**$^-$), (**3.3**$^-$)-O46—H46···O50-(**MeOH B**), Figure 7.13(b).

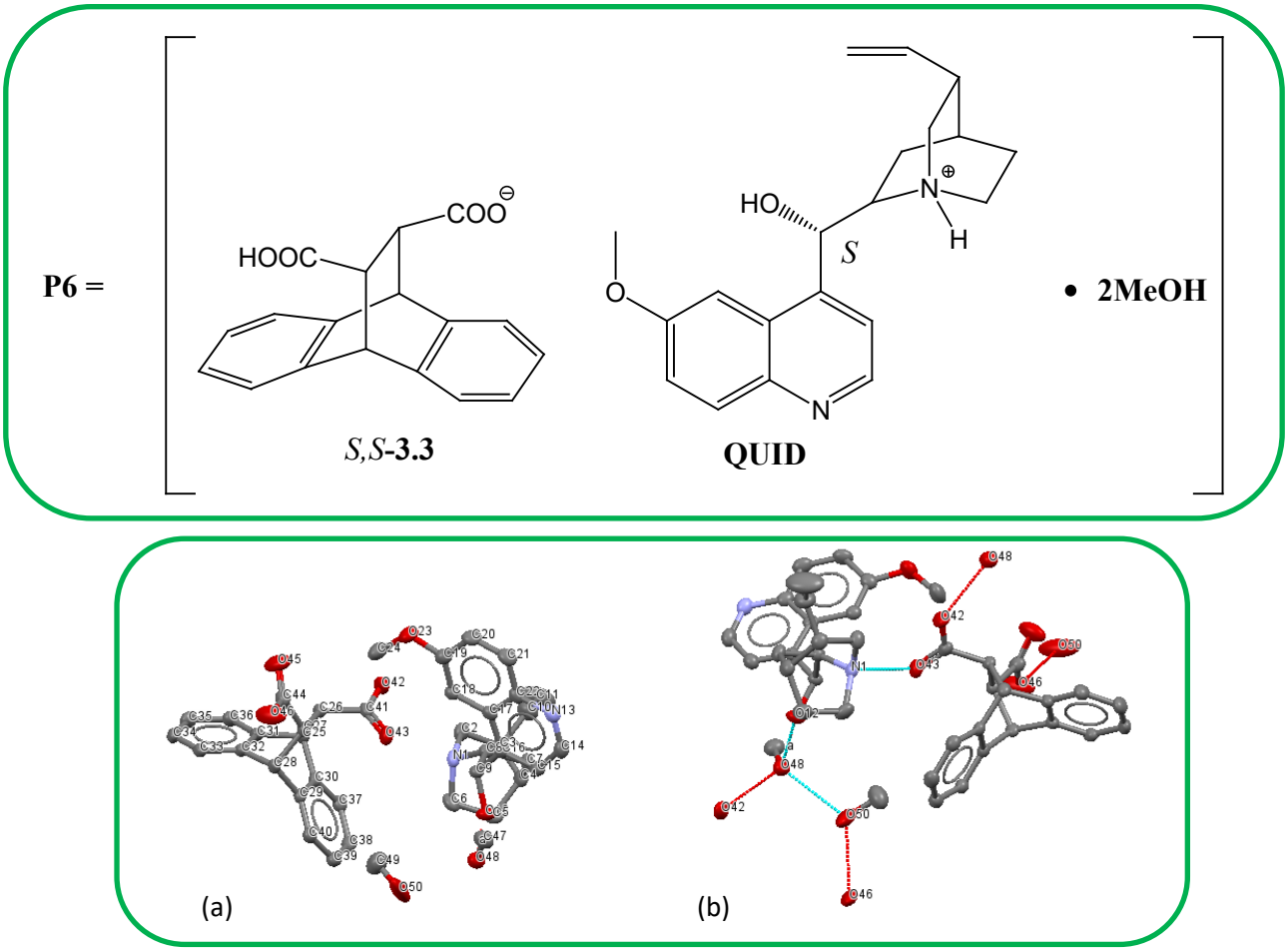


Figure 7.13 Representation of the X-ray crystal structure of **P6**, (a) showing the atom labelling and (b) showing the hydrogen bonding. Hydrogen atoms have been omitted for clarity.

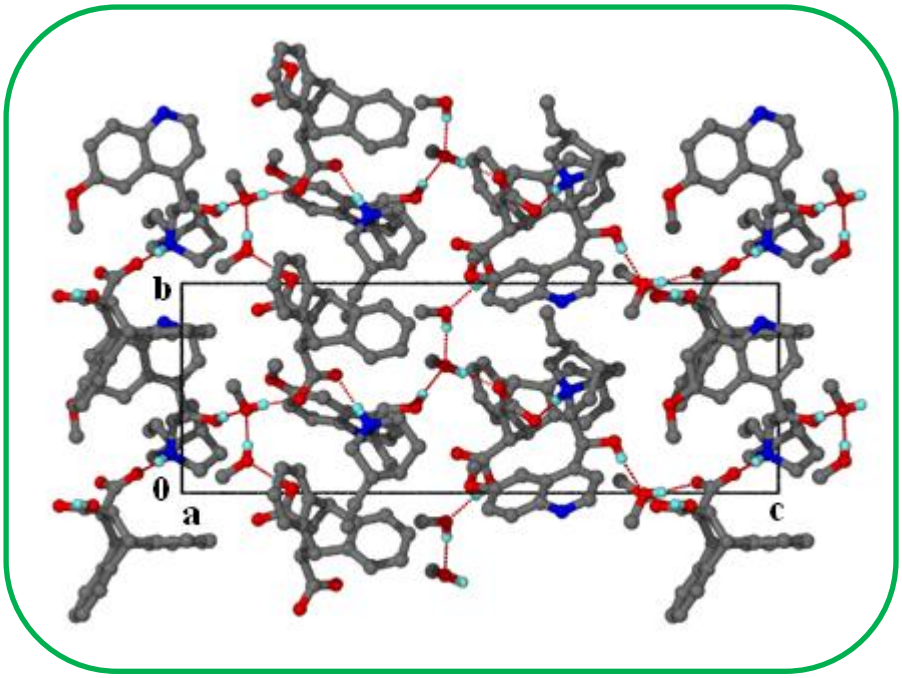


Figure 7.14 Packing diagram of **P6** along [100].

(*R*,*R*-**3.3**$^-$)(**QUIN**$^+$)·**2MeOH** (**P7**), (Quininium *R*,*R*-9,10-dihydro-9,10-ethanoanthracene-11,12-carboxylic acid carboxylate dimethanol solvate) was solved in the hexagonal space group $P3_1$ with $Z = 3$. Similar to **P6**, the asymmetric unit consists of one **3.3**$^-$, one **QUIN**$^+$ and two methanol molecules. The corresponding structure is depicted in Figure 7.15(a). The quininium chiral C9 was assigned the *R* configuration and this resulted in the (*R*,*R*-**3.3**$^-$) in the crystal structure. The hydrogen bonding is similar to that observed in **P6**. Structures **P6** and **P7** have similar unit cells and the configuration of C9 in **QUID** (*S*) and **QUIN** (*R*) allows the C9-OH moiety to hydrogen bond *via* two bridging methanol molecules to O$^-$-(**3.3**), Figure 7.16. These interactions result in the crystallization of (*S*,*S*-**3.3**$^-$) with **QUID**$^+$ and (*R*,*R*-**3.3**$^-$) with **QUIN**$^+$ allowing them to pack in enantiomeric space groups. The figure depicting the different hydrogen bonds is in Figure 7.15(b).

**P7** =

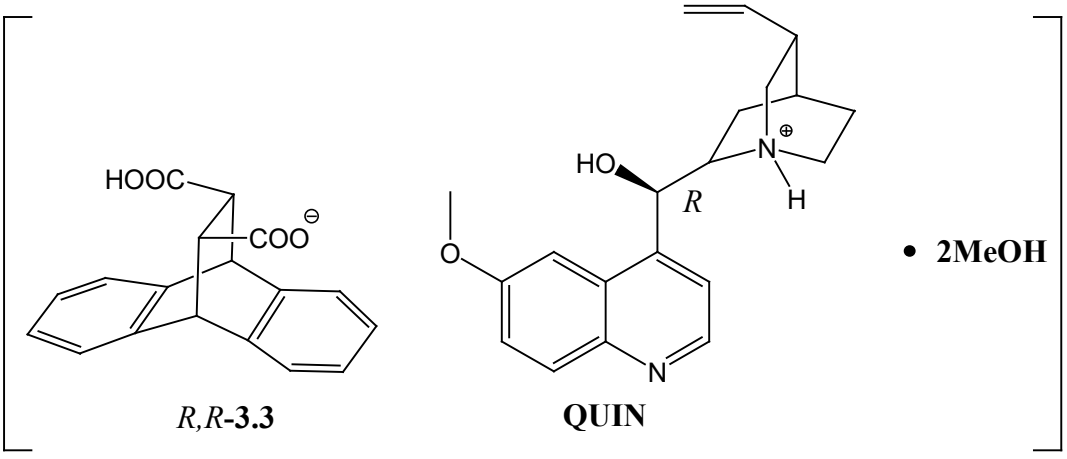


*R*,*R*-**3.3** **QUIN** • **2MeOH**

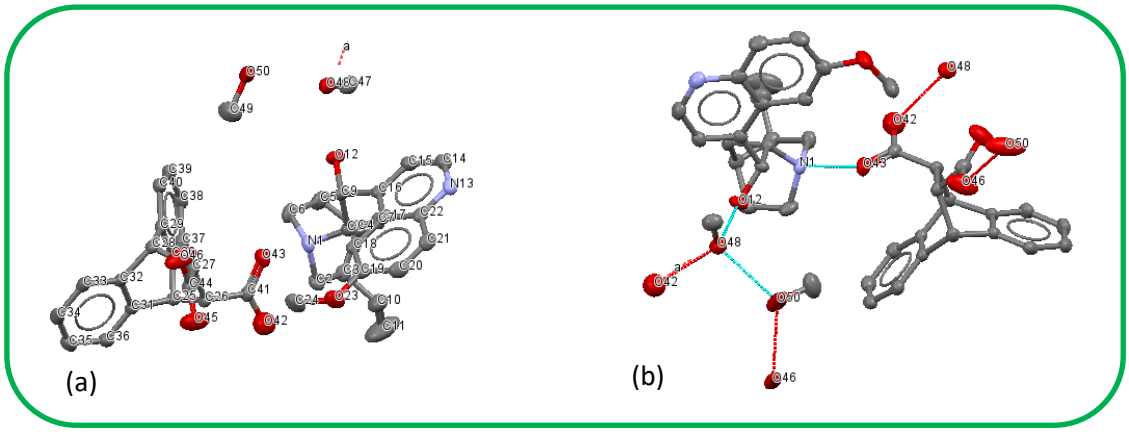


Figure 7.15 Representation of the X-ray crystal structure of **P7**, (a) showing the atom labelling and (b) showing the hydrogen bonding. Hydrogen atoms have been omitted for clarity.

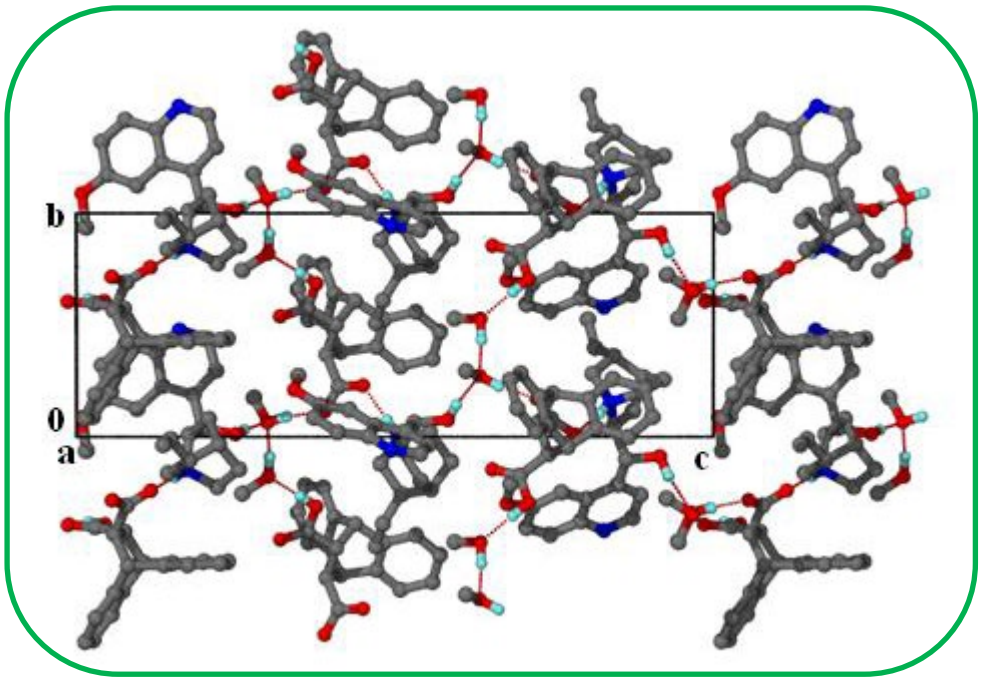


Figure 7.16 Packing diagram of **P7** viewed along [100].

(*S*,*S*-**3.3**$^{-}$)(**CINC**$^{+}$)·**H$_2$O (P8),** (Cinchoninium *S*,*S*-9,10-dihydro-9,10-ethanoanthracene-11,12-carboxylic acid carboxylate monohydrate) crystallized in the orthorhombic space group $P2_12_12_1$ with $Z = 4$, with one **3.3**$^{-}$ anion, one **CINC**$^{+}$ cation and one water molecule in the asymmetric unit, and the corresponding structure is depicted in Figure 7.17(a). The **CINC**$^{+}$ chiral C9 has an *S* configuration and subsequently the **3.3**$^{-}$ had an (*S,S)* absolute configuration. The hydrogen bonding is characterized by the charged assisted interaction, (**CINC**$^{+}$)-N1—H1···O41-(**3.3**$^{-}$)···H45A—O45-(**H$_2$O**)···H12—O12-(**CINC**$^{+}$), forming the graph set $R_3^2(9)$ notation.

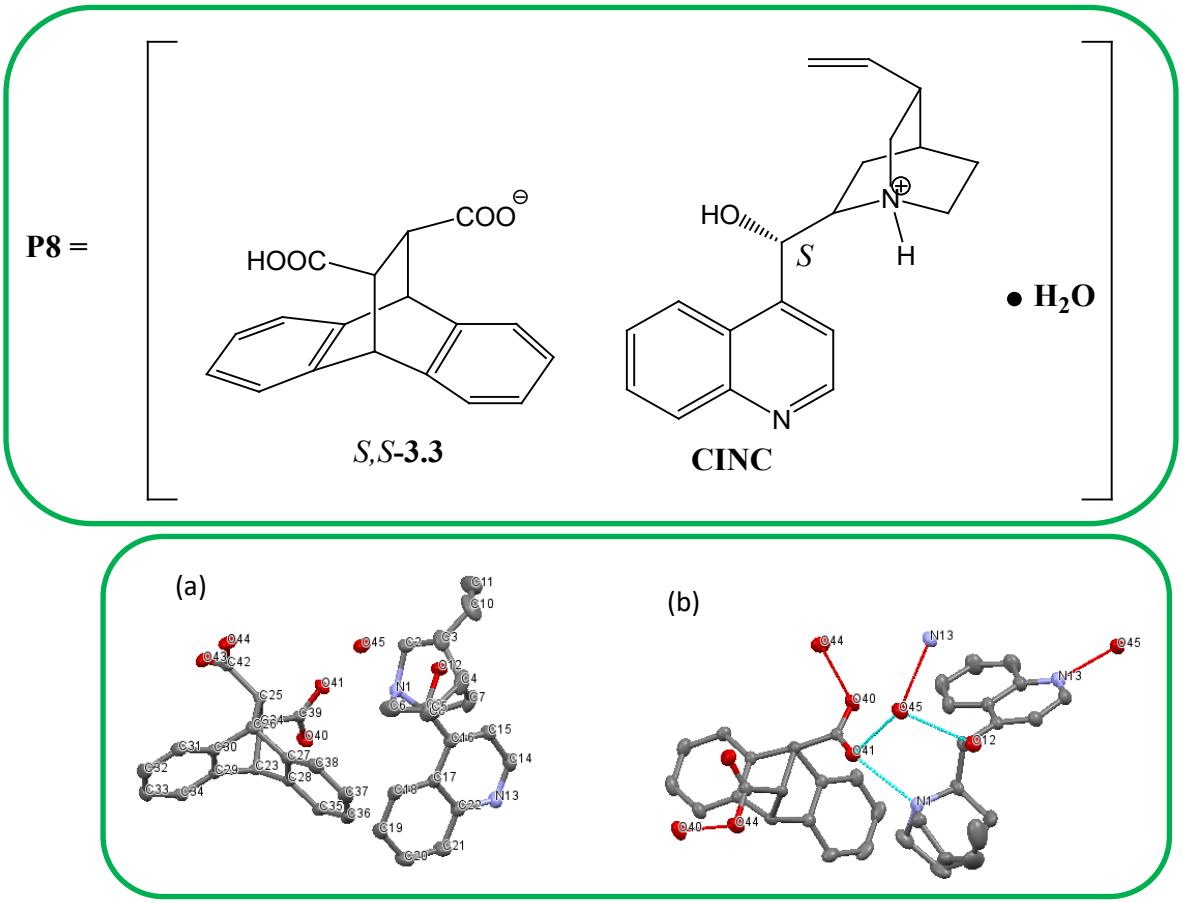


Figure 7.17 Representation of the X-ray crystal structure of **P8**, (a) showing the atom labelling and (b) showing the hydrogen bonding. Hydrogen atoms have been omitted for clarity.

The second carboxylic acid group is a hydrogen bond donor to the deprotonated carboxylate oxygen atom of another dicarboxylic acid, to form the (**3.3**$^{-}$)-O44—H44···O40-(**3.3**$^{-}$) intermolecular bond.

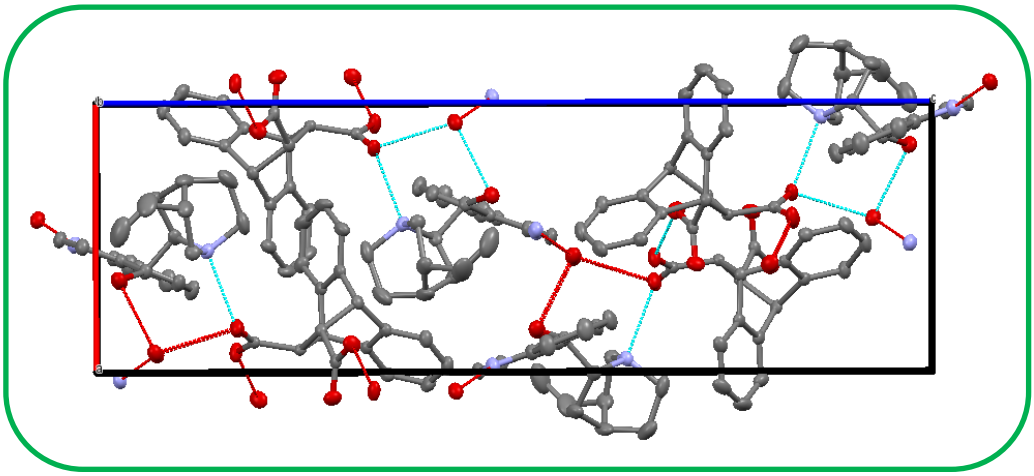

Figure 7.18 Molecular packing diagram of **P8**, a view down crystallographic *b* axis. Hydrogen atoms have been omitted for clarity.

Furthermore, the quinoline nitrogen (N13) of **CINC**$^{+}$ also forms hydrogen bonds with the $H_2O$ molecule, forming (**$H_2O$**)-O45—H45B···N13-(**CINC**$^{+}$). The corresponding structures are depicted in Figures 7.17(b) and 7.18. Hydrogen bonding details for all the salts are summarized in Table 7.10.

Table 7.10 Hydrogen bond parameters of the salts **P4** – **P8**.

| Compound | D—H···A | D—H (Å) | H···A (Å) | D···A (Å) | D—H···A (°) | Symmetry operator |
|---|---|---|---|---|---|---|
| **P4** | N1—H1···O41 | 0.93 | 1.83 | 2.690(2) | 153.1 | |
| | O12—H12···N13 | 0.84 | 1.95 | 2.782(2) | 172.8 | x-½, ½-y, -z |
| | O44—H44···O41 | 0.84 | 1.69 | 2.515(2) | 169.1 | -x, y-½, ½-z |
| **P5** | N1—H1···O41 | 0.96 | 1.75 | 2.710(2) | 174.0 | |
| | O12—H12···O40 | 0.84 | 1.85 | 2.666(2) | 162.6 | 1+x, y, z |
| | O44—H44···O41 | 0.84 | 1.86 | 2.676(2) | 164.1 | |
| **P6** | N1—H1···O43 | 0.90 | 1.76 | 2.661(2) | 174.4 | |
| | O12—H12···O48 | 0.84 | 1.96 | 2.791(1) | 171.0 | |
| | O50—H50···O48 | 0.78 | 1.91 | 2.690(2) | 172.2 | |
| | O46—H46···O50 | 0.84 | 1.80 | 2.632(3) | 171.5 | -y, x-y, z-$^{1}/_{3}$ |
| | O48—H48···O42 | 0.84 | 1.73 | 2.566(2) | 171.6 | 1-x+y, 1-x, $^{1}/_{3}$+z |
| **P7** | N1—H1···O43 | 0.90 | 1.76 | 2.665(2) | 176.2 | |
| | O12—H12···O48 | 0.93 | 1.88 | 2.797(2) | 171.3 | |
| | O50—H50···O48 | 0.99 | 1.70 | 2.688(2) | 174.5 | |
| | O46—H46···O50 | 0.88 | 1.67 | 2.638(2) | 175.3 | -x+y, 1-x, z-$^{1}/_{3}$ |
| | O48—H48···O42 | 0.91 | 1.76 | 2.571(2) | 169.8 | 2-y, 1+x-y, $^{1}/_{3}$+z |
| **P8** | N1—H1···O41 | 0.96 | 1.74 | 2.686(1) | 165.4 | |
| | O12—H12···O45 | 0.90 | 1.85 | 2.721(1) | 165.0 | |
| | O45—H45A···O41 | 0.89 | 1.963 | 2.839(1) | 166.0 | |
| | O44—H44·····O40 | 0.96 | 1.68 | 2.623(1) | 169.0 | 1-x, ½+y,$^{3}/_{2}$-z |
| | O45—H45B···N13 | 0.88 | 1.92 | 2.790(1) | 167.0 | ½+x, ½-y,2-z |

CrystalExplorer analysis

CrystalExplorer[11,12,21] was used to generate the fingerprint plots of each fragment consisting of the **3.3**$^{-}$ anion, regarding the various interactions, Figure 7.19.

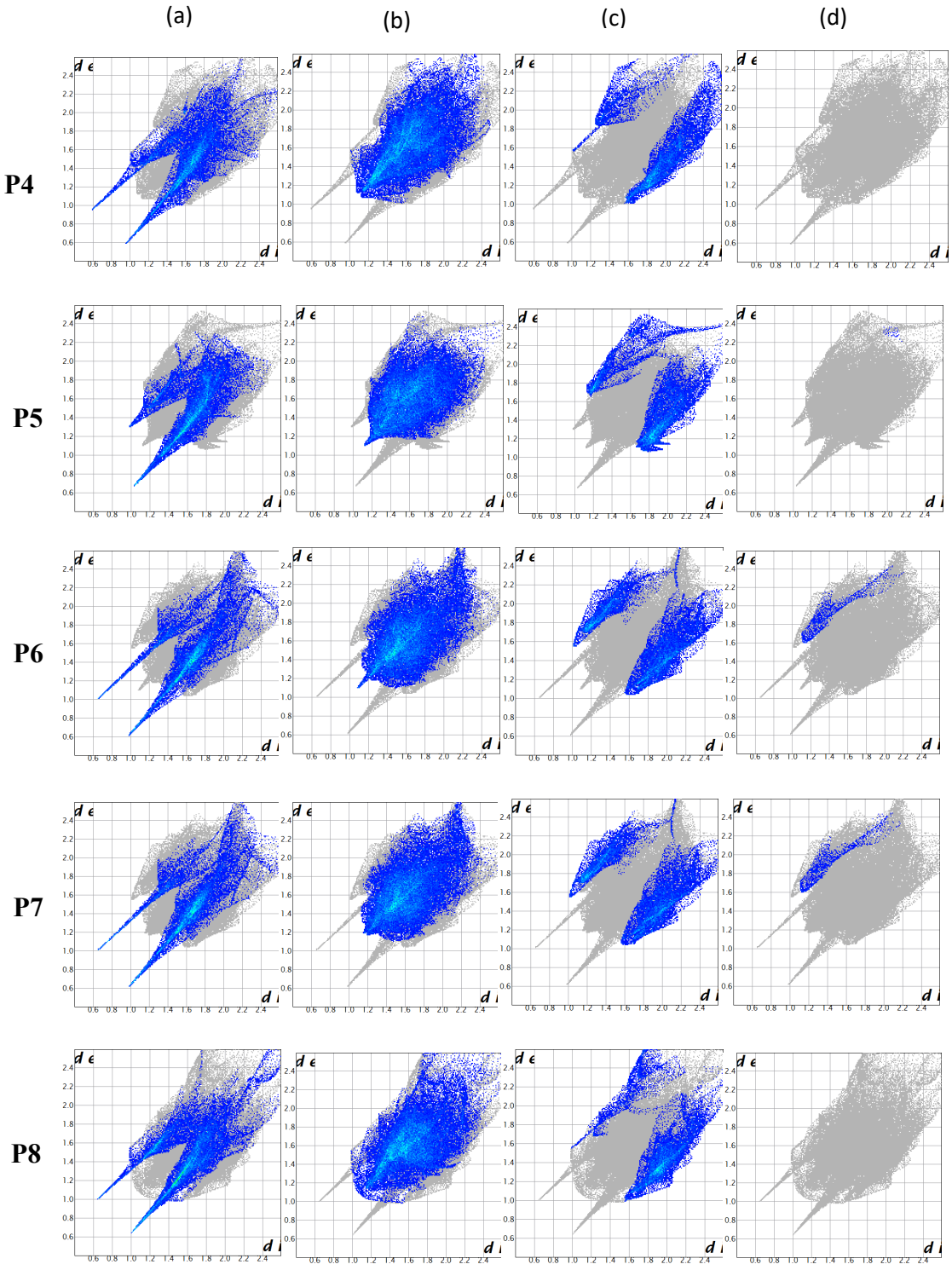


Figure 7.19 2D fingerprint plots of **P4 - P8,** showing reciprocal contacts**,** with columns (a) to (d) showing O···H, H···H, C···H and N···H contacts respectively ($d_e$ is the nearest contact point external to the Hirshfeld surface, and $d_i$ is the nearest internal distance to the surface).

The full fingerprint plots for salts **P4** - **P8** are shown in Figure 7.20 and the summary of the percentage interactions of the various interactions relative to the Hirshfeld surface are listed in Table 7.11. The main contacts for structures **P6** and **P7** are practically identical. This is expected as they are *pseudo*-enantiomeric. However, structures **P4** and **P5** differ in the H···H and the C···H contacts which are reflective of the packing differences and the observation that acetone was included in the crystal structure of **P4** whereas **P5** is a pure salt.

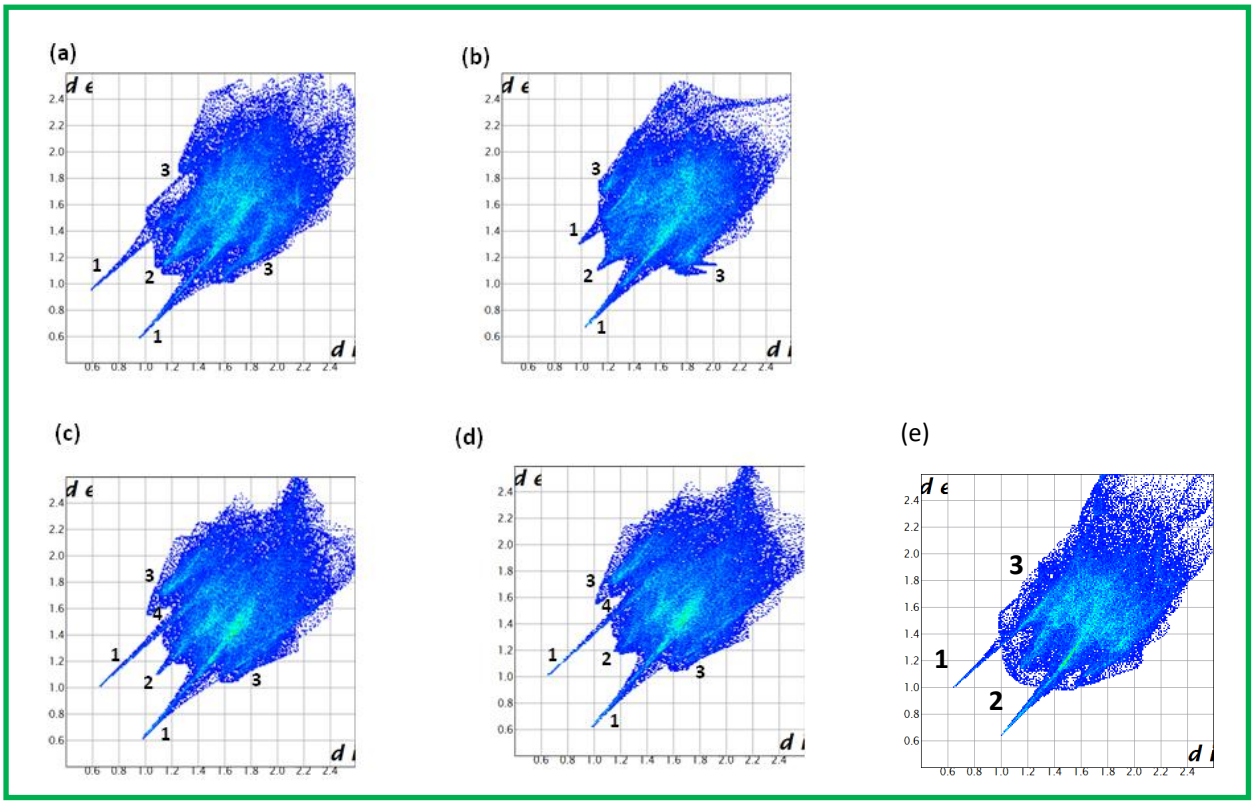


Figure 7.20 2D fingerprint plots of all the contacts in, (a) **P4**, (b) **P5**, (c) **P6**, (d) **P7** and (e) **P8**.

Table 7.11 Summary of the percentage contributions of the various contacts to the total Hirshfeld area of the products.

| Contacts | **P4** | **P5** | **P6** | **P7** | **P8** |
|---|---|---|---|---|---|
| O···H | 27.9 | 28.0 | 25.8 | 25.5 | 29.8 |
| H···H | 53.4 | 49.4 | 48.3 | 48.5 | 50.3 |
| C···H | 18.1 | 21.7 | 23.3 | 23.3 | 18.6 |
| N···H | 0.0 | 0.0 | 1.7 | 1.8 | 0.0 |
| Total | 99.4 | 99.1 | 99.1 | 99.1 | 98.7 |

The Hirshfeld surface analyses of the five salts were determined based on spherical atom electron densities. The $d_e$ and $d_i$ and the van der Waals radii of the atom were used to determine the normalized contact distance ($d_{norm}$), which helps in identifying the areas of contact inside and outside the molecule. The mixing of $d_e$ and $d_i$ in the 2D fingerprint plot gave rise to the

wide picture of intermolecular contacts in the five salts. The fingerprint plots were generated using CrystalExplorer version 3.1. Figure 7.19 shows the 2D fingerprint plots of the five salt crystals in which various spikes of various lengths and thickness, indicates different kinds of contacts, and present are also wing-like peripheral spikes. Figure 7.20 shows the full fingerprint plots (overall contribution) from the individual interactions on all five products.

The O···H intermolecular interactions appear as two distinct long and thin spikes in the 2D fingerprint plots under column (a) in Figure 7.19. The proportion of the O···H interactions is between 25.4 – 30.0% of the Hirshfeld surfaces for the five products. The contributions are similar for **P4** and **P5** (28%), **P6** and **P7** (26%) and for **P8** which is 30%.

The H···H intermolecular interactions appear as a spike between the two O···H spikes, column (b), Figure 7.19, which is the most prominent in the bulk of the fingerprint plot. The proportion of the H···H interactions is between 48.2 – 53.5% of the surfaces. This is shown by the huge central blue area in the fingerprint plots in all the products.

The C···H intermolecular interactions are represented by the thick peripheral wing-like spikes at the top left and bottom right of the fingerprint plot. The proportion of the C···H interactions is between 18.0 – 23.5% of the surfaces. The contributions are relatively similar for **P4** and **P8** (18.4%), **P6** and **P7** (23.3%) and for **P5** is in-between these two contributions, and different, contributing by 21.7%, Figure 7.19 column (c).

N···H intermolecular contacts are present for **P6** and **P7** due to C—H···N interactions between the $\mathbf{3.3}^{-}$ anion and the quinoline nitrogen which contribute an average of 1.75% to the total, Figure 7.19 column (d).

The 2D fingerprint plot can be deconstructed to simplify the specific atom pair contacts. The deconstruction gives rise to the separation of the different contributions from the various interaction types that overlap in the full fingerprint plot. In summary, the contributions can be ranked as follows: H···H contacts (average 50.0%), O···H contacts (average 27.4%), and C···H contacts (average 21.0%).

Comparison of crystal structures **P4** and **P8.**

The reaction of **3.3** with **CINC** in different solvents yielded products, **P4** and **P8**, with enantiomers of different absolute configuration found for the acid. The notable differences are the solvent used in the crystallization and the resultant solvent in the products, acetone in **P4** and water in **P8**.

In structure **P4** there are weak C—H···O interactions between the oxygen atom of acetone and the quinuclidine hydrogen atoms of **CINC.** The carbonyl group is identified as one of the leading C—H···O hydrogen bond acceptors.[22] Weak hydrogen bonds are documented as secondary interactions, and in many cases they play dominant roles in determining crystal packing and in the stabilization of inclusion complexes.[23,24]

In a study of 113 reported crystal structures, neutron diffraction results revealed that H atoms bonded to C atoms tend to form short intermolecular interactions to O atoms, and the C—H groups closer to N atoms have a tendency to take part in short C—H···O contacts, and such contacts are more attractive than repulsive. The results therefore led Taylor *et al*. to conclude that the C—H···O interactions are hydrogen bonds as far as crystallographic studies are concerned.[25] Later on Desiraju concurred in his report that the C—H···O bond is mostly electrostatic, attractive and has a long range distance character, where the C···O distance is between 3.0 – 4.0 Å.[26] He then suggested the consideration of all the strong, N—H···O and O—H···O, and the weak, C—H···O and O—H···C interactions in interpreting hydrogen bond arrangements leading to crystal packing.[27] In another study it was reported that four C—H groups participated in forming hydrogen bonds with a single carbonyl O atom, probably due to electrostatic influencies.[28] These weak C—H···O interactions do control crystal packing generally in the absence of strong hydrogen bonds.[29]

Assignment of hydrogen bonds between the acetone carbonyl group and the resolving agent's quinuclidine ring of **P4**:

The general convention in representing C—H···O distances (*D*, *d*) and angles (Θ, ϕ) is followed in the discussion, as shown in the following Figure 7.21. *D* represents the distance between C and O, and *d* the distance between the H and O atoms in the quinuclidine ring C—H group and the acetone carbonyl group. The angles Θ and ϕ symbolizes the CHO and the HOC angles. The C—H group represents the hydrogen bond donor from the quinuclidine ring, and H···O the accepting group at the carboxyl end of the acetone.

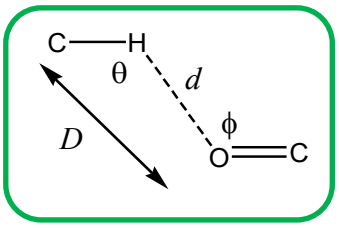


Figure 7.21 C—H···O contacts' distances and angles descriptions.

The bond lengths and angles between the carbonyl O atom and the quinuclidine C and H atoms were recorded and listed in the following Table 7.12.

Table 7.12 The recorded C—H···O contacts' lengths and angles in **P4**.

| C atoms | Distance | Contact | Distance (Å) | Angle | Contact | Angle (º) |
|---|---|---|---|---|---|---|
| 4 | *D* | C4—O46 | 3.874 | | | |
| | *d* | H4—O46 | 4.233 | | | |
| 5 | *D* | C5—O46 | 3.21 | Θ | C5—H5B—O46 | 139.04 |
| | *d* | H5B—O46 | 2.501 | ϕ | H5B—O46—C45 | 159.36 |
| 6 | *D* | C6—O46 | 3.267 | | | |
| | *d* | H6A—O46 | 3.149 | | | |
| 7 | *D* | C7—O46 | 3.303 | Θ | C7—H7A—O46 | 120.22 |
| | *d* | H7A—O46 | 2.692 | ϕ | H7A—O46—C45 | 140.92 |
| 8 | *D* | C8—O46 | 3.212 | Θ | C8—H8—O46 | 141.18 |
| | *d* | H8—O46 | 2.371 | ϕ | H8—O46—C45 | 123.15 |

According to Taylor *et al*. the C—H···O character is electrostatic and is within the C···O distance of 3.0 – 4.0 Å, with the C—H···O angle of (Θ) 110 - 180º.[21] They also indicated the distribution of the H···O=C angle (ϕ) to be around 120º. Desiraju later reported ϕ to be approximately between 120 -140º for hydrogen bond acceptors that are ketonic.[27] In cases where the carbonyl O hydrogen bonds to four C—H groups the ϕ values deviate.[28] Taylor *et al*. also reported H···O=C angles that were less than 90º which corresponded to intramolecular contacts. In addition, Desiraju indicated the cut-off for *d* to be 2.8 Å, and he reported C—H···O bonds with Θ in the range of 122 - 160º, and *d* in the range of 2.3 – 2.84 Å.[27] The carbonyl O atom in **P4** is pointing towards the quinuclidine C—H groups. Taylor *et al*. reported C—H groups next to N atoms participated in C—H···O contacts.[25] Based on the C—H···O parameters for **P4**, all the *D* values are within the specification, but quinuclidine C4 and C6 *d* distances of 4.233 Å and 3.149 Å are above the cut-off limit of 2.8 Å though C6 is next to the quinuclidine N atom, and these were not considered to participate in the weak hydrogen bond formation.

The other C contacts with the carbonyl O atom were within the expected ranges to form C—H···O interactions, and their angles are also listed, falling within the expected ranges. The

exception is the H5B—O46—C45 angle of 159.36º, having deviated from the expected range, with the other parameters falling within the expected limits. The deviation may be due to the carbonyl O atom being hydrogen bonded to the three C—H groups. C8 is also next to the quinuclidine N atom and the ϕ value is 123.15º very close to 120º. Therefore, the carbonyl O is involved in multiple hydrogen bonds with the quinuclidine C—H groups, which could explain the deviation in the ϕ value of one of the contacts, C5. The C—H···O hydrogen bond parameters are displayed below in Table 7.13.

Table 7.13 Hydrogen bond parameters due to the acetone close contact with the quinuclidine ring C—H groups.

| Compound | D—H···A | D—H (Å) | H···A (Å) | D···A (Å) | D—H···A (°) |
|---|---|---|---|---|---|
| **P4** | C5—H5B···O46 | 0.99 | 2.510 | 3.21 | 139.04 |
| | C7—H7A···O46 | 0.99 | 2.692 | 3.303 | 120.22 |
| | C8—H8···O46 | 1.00 | 2.371 | 3.212 | 141.18 |

Both salts, **P4** and **P8** display the N1—H1···O41 interaction between the resolving agent and the acid. The carboxylate oxygen (O41) is further hydrogen bonded to **3.3** in **P4** and to the water molecule in **P8** *via* the interactions, O44—H44···O41 and O45—H45A···O41 respectively. The hydroxyl groups are involved in hydrogen bonding directly to the quinoline N (**P4**) and *via* a water molecule (**P8**). Furthermore, the water molecule is hydrogen bonded to form a ring, with a graph set assignment of $R_3^2(9)$, (Figure 7.17(b)) below. In **P4** the other carboxylate oxygen (O40) is not involved in hydrogen bonding, yet in **P8** it formed the interaction, O44—H44···O40. The differences of the hydrogen bonding patterns for the two compounds are reflected on Figures 7.9(b) and 7.17(b), and in Table 7.14.

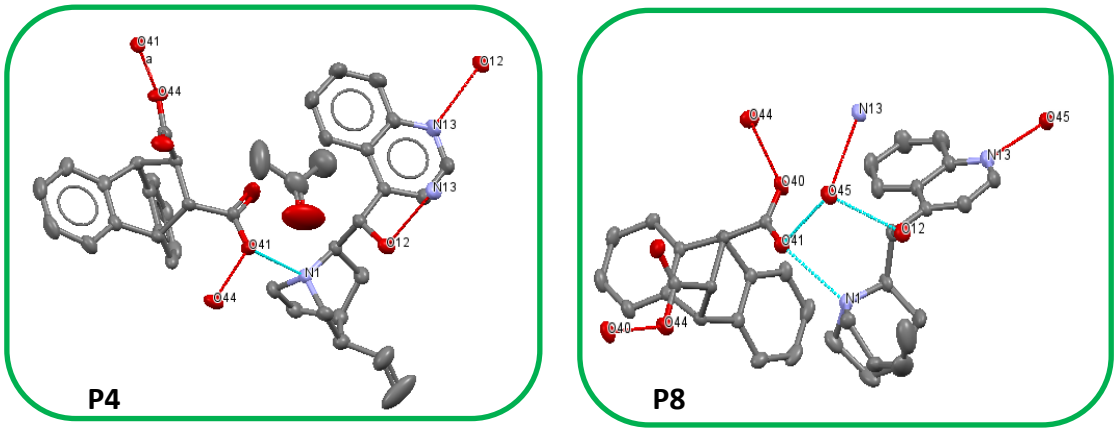


Figures 7.9(b) and 7.17(b) showing the hydrogen bonding in **P4** and **P8** respectively.

Table 7.14 Selected hydrogen bonds for **P4** and **P8**.

| **P4** | **P8** |
|---|---|
| N1—H1···O41 | N1—H1···O41 |
| O12—H12···N13 | O12—H12···O45-(water) |
| O44—H44···O41 | O44—H44···O40 |
| C5—H5B···O46-(acetone) | O45—H45A···O41 |
| C7—H7A···O46-(acetone) | O45—H45B···N13 |
| C8—H8···O46-(acetone) | |

Conformational analysis of **P4** and **P8**

In studies involving the resolution of malic acid using **CINC** and **CIND** the flexibility of the ethenyl group was associated with chiral selectivity (Section 7.2). Conformational analysis of **P4** and **P8** was conducted and the summary of the results is depicted in Table 7.15. The recorded torsion angles are, τ1: C15—C16—C9—O12, τ2: N1—C8—C9—O12 and τ3: C4—C3—C10—C11, and these are shown on the cinchonine backbone in the two products. τ1 is the rotation of the quinoline ring, τ2 is the swing motion of the bicyclic ring and τ3 is the rotation of the ethenyl group. In the two products, τ1 and τ2 show no extreme conformational changes. Regarding τ3 there is a significant change in conformation. The change may have been caused by the presence of acetone in **P4**, interacting with the hydrogen atoms of the quinuclidine ring in three non-bonding interactions, which could stabilize the product. In **P8** the water molecule could have contributed towards stabilization of the product.

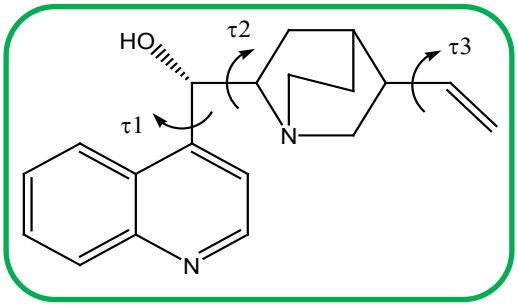


Table 7.15 The torsion angles for the **CINC** in **P4** and **P8**.

| Torsion angles | **P4** | **P8** |
|---|---|---|
| **τ1 (°)** | 22.44 | 27.51 |
| **τ2 (°)** | 73.61 | 67.38 |
| **τ3 (°)** | 119.69 | 82.50 |

The difference in the conformation of the vinyl group is also highlighted by the orientation of the group in different directions, on overlaying the two cinchonine molecules of **P4** and **P8**, in Figure 7.22.

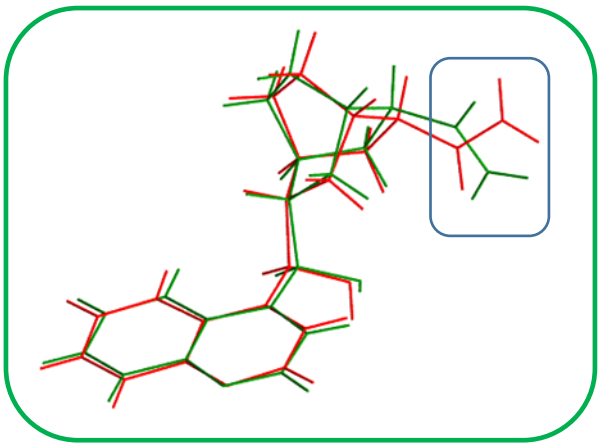

Figure 7.22 The differences in the orientation of the ethenyl groups (encircled area) in overlaying the cinchonine in **P4** and **P8**.

FT-IR analysis

IR spectroscopy was used to confirm that proton transfer had taken place between the dicarboxylic acid and the resolving agents for **P4** – **P8**. The protonated bases then behave as hydrogen bond donors and the carboxylates as hydrogen bond acceptors in the formation of the different salts. The protonated tertiary amines give rise to frequencies in the region, 2500 – 1800 $cm^{-1}$, with medium to broad peaks that are due to overtones and combinations.[30] The amine salts also show a medium to weak peak at 1670 – 1610 $cm^{-1}$. The carboxylate ions give rise to antisymmetric and symmetric frequencies between 1610 -1550 $cm^{-1}$ and 1420 – 1300 $cm^{-1}$ respectively. A distinct carbonyl stretch is found at frequencies above 1700 $cm^{-1}$. The FT-IR results also complemented the X-ray diffraction crystal structures for products **P4** – **P8**, by confirming the presence of COOH and $COO^-$ groups on the anions. The protonation of the tertiary amine is confirmed by the $N^+$—H stretch, in the strong hydrogen bond N—H···O, which occurs in the frequency range of 1800 – 2500 $cm^{-1}$,[31] and the $N^+$—H bend between 1670 – 1610 $cm^{-1}$.[32]

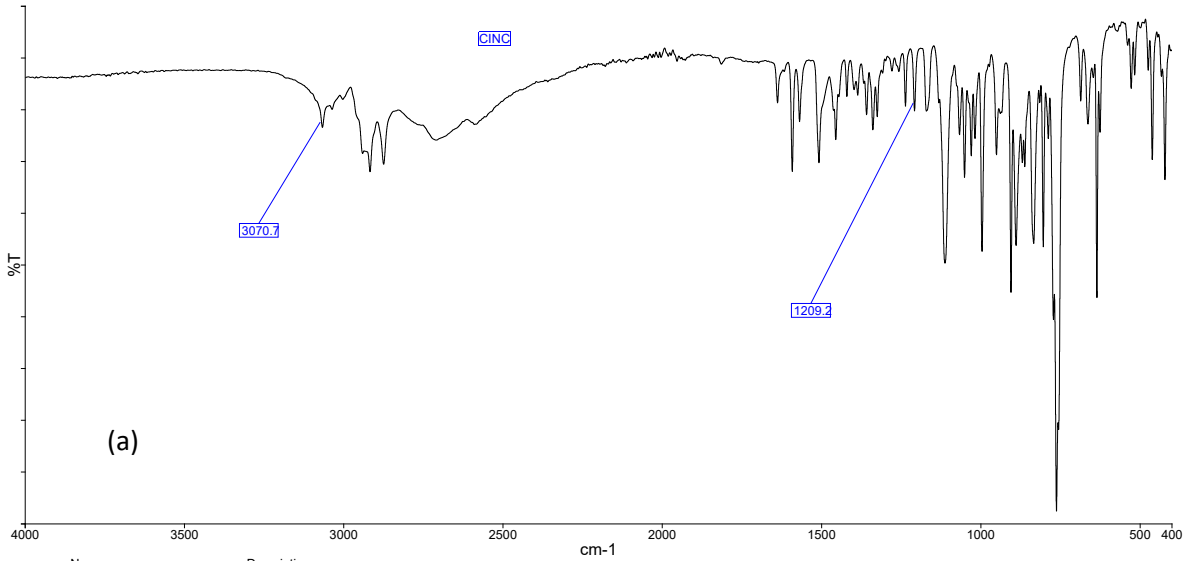
CINC
3070.7
1209.2
%T
(a)
4000
3500
3000
2500
2000
1500
1000
500
400
cm-1

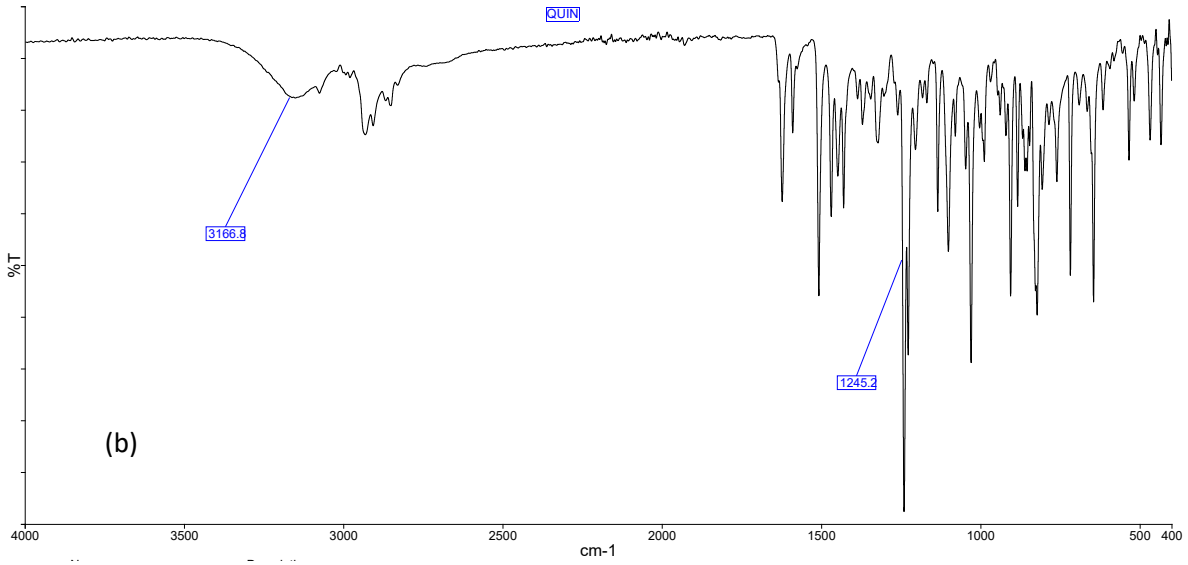
QUIN
3166.8
1245.2
%T
(b)
4000
3500
3000
2500
2000
1500
1000
500
400
cm-1

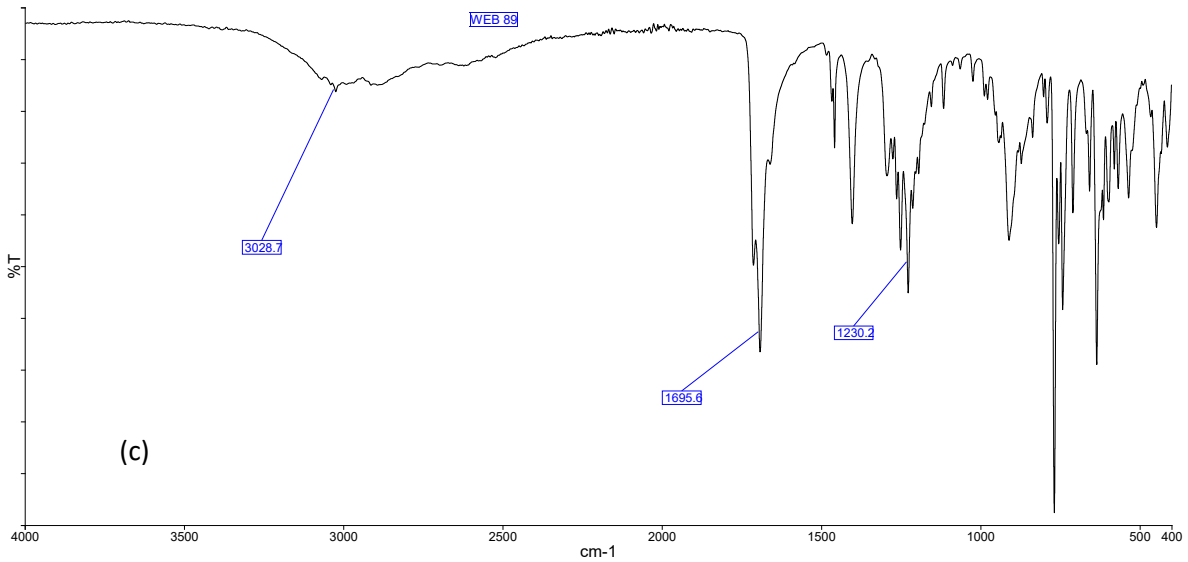
WEB 89
3028.7
1695.6
1230.2
%T
(c)
4000
3500
3000
2500
2000
1500
1000
500
400
cm-1

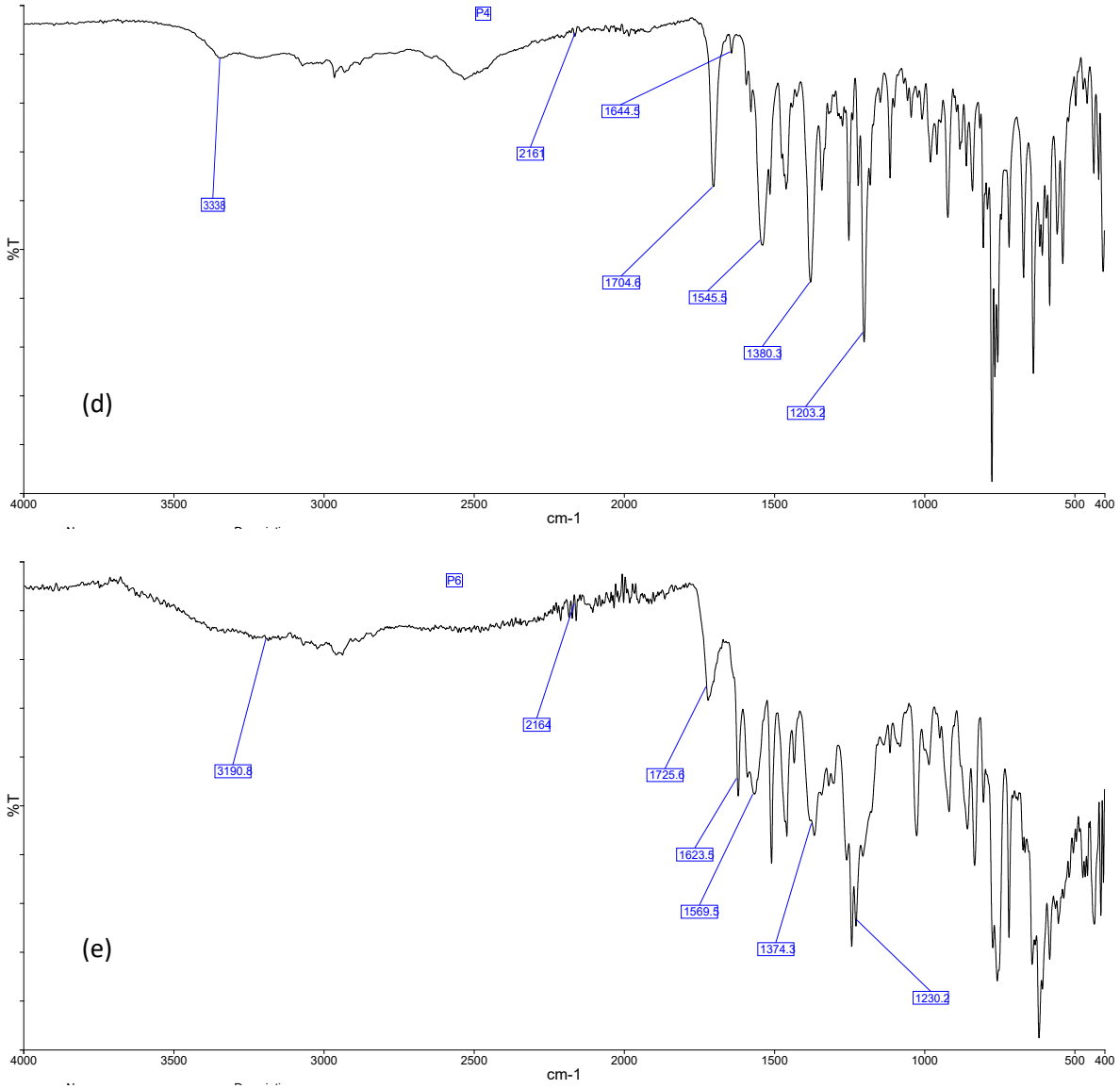


Figure 7.23 The FT-IR spectra of the resolving agents (a) **CINC** and **CIND** (b) **QUIN** and **QUID**, (c) the racemic dicarboxylic acid, (d) **P4** and (e) **P6**.

**P4** to **P8** are the salts formed *via* the reaction of the bases, **CINC**, **CIND**, **QUIN** and **QUID** with the racemic dicarboxylic acid, *trans*-9,10-dihydro-9,10-ethanoanthracene-11,12-dicarboxylic acid in different solvents. The FT-IR spectra for the pair **CINC** and **CIND** are similar, represented by (a), while the spectra for **QUIN** and **QUID** are similar, represented by (b). The infrared spectra for **P4** (d) and **P6** (e) are shown in Figure 7.23 and all these show similar spectral features. The FT-IR spectrum for **P4**, is similar to that of **P5a** and **P8**. The spectrum of **P7** resembles that of **P6.** Proton transfer in **P4** – **P8** was shown by the intensity reduction of the carbonyl peak (C=O) at 1704 $cm^{-1}$ in the spectra of the carboxylic acid group that did not transfer a proton, Figure 7.23(d), compared to the peak at 1695 $cm^{-1}$, Figure 7.23(c). This was also confirmed by the appearance of the carboxylate antisymmetric and symmetric

$COO^-$ peaks at 1545 and 1380 $cm^{-1}$ indicating that one of the carboxylic acid groups has donated a proton (d) [1569 and 1374 $cm^{-1}$ in (e)]. The appearance of the reduced carbonyl peak at 1704 $cm^{-1}$ in (d), [1725 $cm^{-1}$ (e)] confirms that the other carboxylic acid group remained neutral in the five salts. Protonation of the tertiary amine resulted in the formation of the N—H···O strong hydrogen bonds in all the products. The spectra of all the products do not convincingly show the amine salt peaks in the expected region of 2500 – 1800 $cm^{-1}$(2161 $cm^{-1}$ shown on (d)). The amine salt is also indicated by the presence of a weak peak at 1644 $cm^{-1}$ in (d) [1623 $cm^{-1}$ in (e)]. In all the salts the neutral COOH peaks are at approximately 3000 - 3400 $cm^{-1}$, represented by 3338 $cm^{-1}$ in (d) and 3190 $cm^{-1}$ in (e), the reduced carbonyl peak at 1704 $cm^{-1}$, the weak protonated tertiary amine peak at 1644 $cm^{-1}$, and the carboxylate peaks at 1545 and 1380 $cm^{-1}$ for **P4**, **P5a** and **P8**, and these are listed in Table 7.16 showing the frequency ranges corresponding to these functional groups.

The corresponding peaks for **P6** and **P7** were of slightly lower or higher frequencies compared to those of the other salts. The COOH group gave rise to a peak at 3000 - 3400 $cm^{-1}$, the carbonyl absorbed at 1725 $cm^{-1}$, the protonated tertiary amine absorbing at 1623 $cm^{-1}$ and the antisymmetric and symmetric carboxylate peaks at 1569 and 1374 $cm^{-1}$ respectively, and these are listed in Table 7.17 with their expected ranges.

From the obtained spectra it is difficult to notice the peak due to a hydrogen bonded OH group, O—H···O, due to the overlap of its peak with that of the neutral COOH peak in the salt. The peak due to a hydrogen bonded OH group appears at a lower frequency compared to that of a non-hydrogen bonded OH group.[32]

Therefore, the FT-IR confirmed the transfer of a proton resulting in salt formation due to the appearance of the carboxylate peaks, at 1545 and 1380 $cm^{-1}$ (1569 and 1374 $cm^{-1}$), and the amine salt peak at 1644 $cm^{-1}$ (1623 $cm^{-1}$). The reduction in the carbonyl peak at 1704 $cm^{-1}$ (1725 $cm^{-1}$) confirms the presence of the other carboxylic acid group as neutral.

Table 7.16 The characteristics of selected FT-IR absorptions of **P4**, **P5a** and **P8**.

| Functional groups | **P4**, **P5a** and **P8** absorptions $cm^{-1}$ | Expected absorptions ($cm^{-1}$) |
|---|---|---|
| O—H···O | 3400-3000 | 3400 – 3200 |
| COOH | 3400-3000 | 3400 – 2500 |
| C=O | 1704 | 1780 – 1670 |
| $N^+$—H | <br>1644 (weak) | 2500 – 1800<br>1670 – 1610 |
| $COO^-$ | 1545<br>1380 | 1610 – 1550<br>1420 – 1300 |
| C—O | 1203 | 1200 – 1050 |

Table 7.17 The characteristics of selected FT-IR absorptions of **P6** and **P7**.

| Functional groups | **P6** and **P7** absorptions $cm^{-1}$ | Expected absorptions ($cm^{-1}$) |
|---|---|---|
| O—H···O | 3400-3000 | 3650 – 3400 |
| COOH | 3400-3000 | 3100 – 2500 |
| C=O | 1725 | 1780 – 1670 |
| $N^+$—H | <br>1623 (weak) | 2500 – 1800<br>1670 – 1610 |
| $COO^-$ | 1569<br>1374 | 1610 – 1550<br>1420 – 1300 |
| C—O | 1230 | 1200 – 1050 |

In all the salts, salt formation was also supported by the difference in p$K_a$ values between the bases and the acid. The predicted quinuclidine N p$K_a$ values of the bases are 9.2 (**CINC** and **CIND**) and 9.1 (**QUIN** and **QUID**), and for the diacid p$K_{a1}$ and p$K_{a2}$ values are 3.82 and 5.82.[1] The $\Delta$p$K_a$ for all the salts is greater than 3, indicating the possibilty of forming salts.[2]

Turbidity test.

A turbidity test was performed to further differentiate between **P4** and **P8.** The two salts were produced from the same racemate and resolving agent, but in different solvents, **P4** in acetone and **P8** in acetonitrile and water. **P4** included acetone in the crystal structure and **P8** is a salt hydrate. The turbidity test involved heating the mixture of the racemates, resolving agents and solvents to prepare **P4** and **P8** at room temperature. The hot plate was set to heat up to 90 °C. The results are listed in Table 7.18 and illustrated in Figure 7.24.

Table 7.18 The temperature ranges at which the mixtures formed solutions, during the preparation of **P4** and **P8**.

| Trial | **P4** solution (°C) | **P8** solution (°C) |
|---|---|---|
| 1 | 36 - 50 | 50 - 60 |
| 2 | 30 - 50 | 45 - 60 |
| 3 | 34 - 50 | 50 - 60 |
| **Average** | **33 - 50** | **48 - 60** |

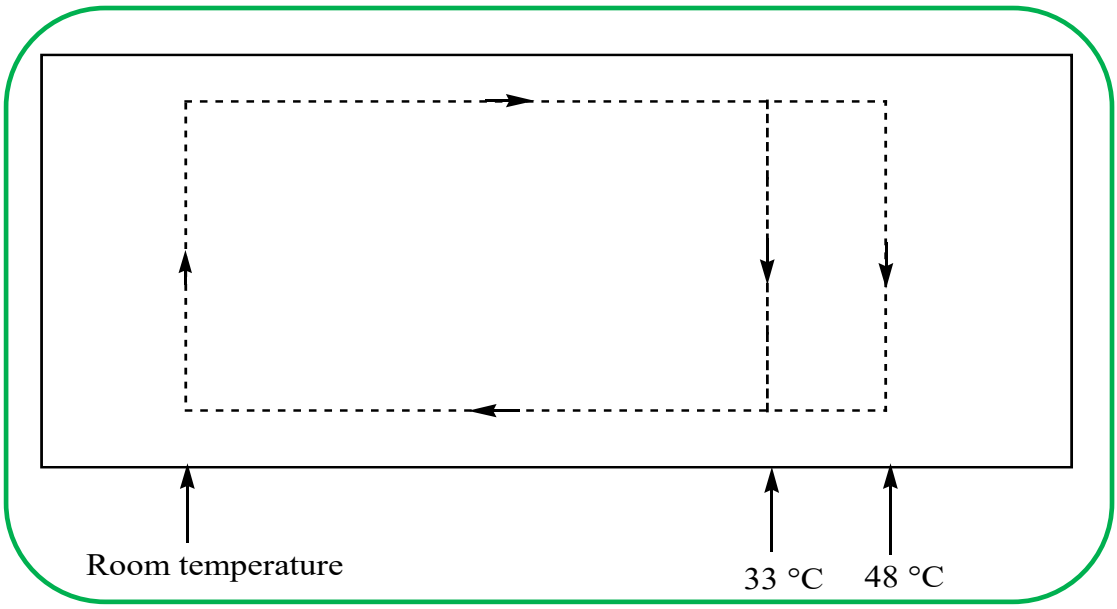


Figure 7.24 A graph depicting the heating of the mixtures into solutions, **P4** becoming a solution at 33 °C and **P8** at 48 °C.

The solutions became clear at different temperatures, when the solids totally dissolved, and were allowed to cool to room temperature. The test was performed three times, and the average temperatures were used in the analysis.

**P4** formed a solution within the average temperature range of 33 – 50 °C, and **P8** within the average temperature range of 48 – 60 °C (Figure 7.24). This shows the difference in the dissolution of the starting material in the preparation of the two different salts.

The solubility of the resolving agents, **CINC**, used in preparing **P4** and **P8** was determined in the two different solvents, acetone and acetonitrile. **CINC** is practically insoluble in water. The solubility results of **CINC** in the two solvents are tabulated in Table 7.19. The solubility tests were performed at room temperature, using stoppered vials to minimize evaporation of the solvents, with stirring of the mixtures to assist the solid in forming a clear solution. The two solvents differ greatly from each other regarding their physical properties. The boiling point of acetone is 56 °C and that of acetonitrile is 82 °C. Their densities are relatively close to each

other, acetone 0.791 g/ml and acetonitrile 0.786 g/ml. Acetone is denser and more volatile than acetonitrile.

Table 7.19 The solubility of **CINC** in acetone and acetonitrile.

| Trial | **CINC**/acetone | **CINC**/acetonitrile |
|---|---|---|
| 1 | 4.8 mg/8.17 ml | 4.8 mg/24.72 ml |
| 2 | 1.8 mg/3.62 ml | 1.8 mg/11.36 ml |

Based on the determined solubility of **CINC** in acetone and acetonitrile, the results reveal that **CINC** is three times more soluble in acetone than in acetonitrile. The resolving agent is totally insoluble in water. The acetonitrile used in preparing **P8** was mixed with three drops of water, changing the dissolution in acetonitrile by a slight margin.

The solubility of the salts from **CINC** and the dicarboxylic acid in acetone and acetonitrile were also determined. **P4** and **P8** were ground into a powder using a mortar and pestle. 2.5 mg of each salt was dissolved in increasing amounts of the solvents in vials, over a balance, stirred and sealed to minimize evaporation of the solvent, and the masses at which the powders resulted into a solution were recorded. The average results of the duplicates per test in the solvents were recorded. The masses were converted to ml according to their densities, and the results are in Table 7.20.

Table 7.20 The solubility of **P4** and **P8** in acetone and acetonitrile.

| **Solvents** | **P4** | **P8** |
|---|---|---|
| Acetone | 2.5 mg/1.38 ml | 2.5 mg/1.63 ml |
| Acetonitrile | 2.5 mg/1.31 ml | 2.5 mg/2.53 ml |

The results reveal that the salts' solubilities in the solvents are greater than the solubility of **CINC** in the same solvents. The generation of the salt therefore improved the solubility of **CINC** in acetone and acetonitrile.

The results also indicate that **P4** is soluble in less solvent volume compared to **P8,** i.e. more soluble than **P8**. **P4** is slightly less soluble in acetone than acetonitrile, and **P8** is less soluble in acetonitrile compared to acetone. Thus in both cases the less soluble salt precipitated.

Both *N*-benzylcinchoninium chloride and *N*-benzylcinchonidinium chloride have been exploited to resolve racemic 2,2'-dihydroxy-1,1'-binaphthyl.[7,8] Both of these derivatives yielded the (*R*)-(+)-enantiomer. Wang *et al.*[7] attributed this to a combination of the chirality of the resolving agent and the host-guest interactions present in the crystal structure. Gjerløv *et al.*[9] and Larsen *et al*.[10] employed **CINC** and **CIND** respectively, to resolve racemic mandelic acid.

**CINC**-*(R)*-mandelate and **CIND**-(*S*)-mandelate were the resultant products of the resolution. The differences in the packings were attributed to the steric effects of the ethenyl group. In the case of the *Cinchona* alkaloids with the host **3.3**, both **CINC** and **CIND** gave the *R*,*R*-**3.3**$^{-}$. However **QUID** preferentially crystallized with *S*,*S*-**3.3**$^{-}$ (**P6**) and **QUIN** with *R*,*R*-**3.3**$^{-}$ (**P7**). In **P8** the **CINC** crystallized with *S*,*S*-**3.3**$^{-}$. For structures **P6** and **P7**, methanol is present in both structures and is involved in hydrogen bonding to the C9-OH of the **QUID**$^{+}$ and the **QUIN**$^{+}$ respectively.

For structure **P4** involving **CINC**, acetone is present in the crystal structure and is involved in weak C—H···O hydrogen bonding (and also behaves as a space filler) to stabilize the crystal structure. The structure involving **CIND** (**P5**) does not contain any solvent. In **P8** water stabilized the structure through hydrogen bonding.

The role of the solvent in diastereomeric resolution is not clearly understood and in some cases it has been shown that the solvents are more likely to be incorporated into the less soluble salts and at the same time provide more hydrogen bond sites or become space fillers, which stabilizes these structures.[33-36] In a study by Kozma *et al*. they found that the solvated salt is the more stable, and it precipitates during the resolution process.[37] This was indicated by the results of the DSC analysis of 16 diastereomeric salt pairs. In other cases, solvents were not incorporated into the less soluble salt structures. [38,39]

Structures **P4** and **P5** resulted from different solvents, **ACE** and **MeOH**, and **P5** did not incorporate the solvent, yet they both gave rise to the same enantiomer (*R*,*R*-**3.3)**.

Structures **P6** and **P7** resulted from the same solvent, **MeOH**, both incorporated two moles of the solvent, and gave rise to the two enantiomers of **3.3**. In both cases the solvent participated in hydrogen bonding and the structures have the same hydrogen bonding network.

Structure **P8,** also incorporated water that participated in hydrogen bonding, thereby, further stabilizing the diastereomeric salt.

Strychnine and brucine are stereochemically related alkaloids, that differ by the two methoxy groups attached to the aromatic ring of brucine, similar to the resolving agent pairs, **CINC**/**QUID** and **CIND**/**QUIN**. The **QUID**/**QUIN** pair has one methoxy group per compound. According to Woodward *et al*. cited by Białońska *et al*.,[40(a)] the use of stereochemically related alkaloids that are different in the methoxy group substituent, provides access to acids of opposite configurations. This is supported by the experiments involving **CINC** and **QUID**, where **P4** and **P6**, provide access to acids of opposite configuration, albeit in different solvents.

In contrast **CIND** and **QUIN,** *via* **P5** and **P7**, resulted in acids of the same configuration, from the same solvent, however **P7** included the solvent in the crystal structure. In 2010 Zhang *et al*. demonstrated the isolation of both enantiomers of 2,6-dimethyl-5-methoxy carbonyl-4-(3-nitrophenyl)-1,4-dihydropyridine-3-carboxylic acid using **CIND** and **QUID** in the same solvent, DMF:$H_2O$ (8:5 and/or 8:8). **CIND** isolated the *S*-enantiomer and **QUID** isolated the *R*-enantiomer.[40(b)]

Gould *et al*.[41] and Białońska *et al.*[40(a)] used strychnine and brucine for the separation of racemates, *N*-benzoyl-*DL*-α-alanine and *N*-phthaloyl-*DL*-α-alanine. Gould *et al*. obtained strychninium *N*-benzoyl-*L*-α-alaninate dihydrate and brucinium *N*-benzoyl-*D*-α-alaninate $4.5H_2O$. Białońska *et al* obtained strychninium *N*-phthaloyl-*D*-α-alaninate dihydrate and brucinium *N*-phthaloyl-*L*-α-alaninate hemi hydrate. Białońska *et al.* cited the presence of the methoxy groups in the brucine as one of the obvious reasons for the different assembling of strychnine and brucine, causing the formation of various enantiomeric products. In **P4** and **P6** different enantiomers were isolated, and the incorporated solvents participated in hydrogen bonding, stabilizing the two salt solvates. The $C_1^1(7)$ chains in P**4** which allow for alternate columns of acid and base is absent in **P6**.

In another study, it was shown that introducing water molecules (a solvent) into a structure resulted in many hydrogen bonds. However, based on comparison of several diastereomeric salts where one was hydrated, the results showed that hydration does not necessarily lead to the more stable and less soluble diastereomeric salt, the hydrated salts fell almost evenly between the more and the less soluble salts.[27] In the current study, structure **P8** is stabilized by the presence of water molecules in the crystal structure.

In the structures **P4** and **P8**, the resolving agent **CINC** gave opposite enantiomers of the acid when the solvent was changed from acetone to acetonitrile and water. In 1977 Wilen *et al*. reported the influence of solvation on the solubility of diastereomeric salts of brucine and 7,8-dicarboxybicyclo[2,2,2]oct-2-ene-7,8-dicarboxylic acid. Brucine formed a salt of the (-)-acid, solvated with 3 moles of MeOH when MeOH was used as a solvent. In MeOH + water brucine formed the opposite (+)-acid hydrated with 12 water molecules.[42(a)] The configuration of the less soluble salt changed according to solvation, due to a change of solvent. In another experiment, both enantiomers of 2,2-dimethyl-3-phenylpentanoic acid were isolated by changing the solvent from EtOH to EtOH + water, using **QUIN** as a resolving agent.[42(a)]

Kozma *et al*. also observed this in the resolution of mandelic acid using **CINC** in different solvents. The configuration of mandelic acid changed when they changed the solvent from

water to other solvents in different combinations.[42(b)] Water was incorporated into the precipitating salt when in abundance. On reducing the water content in the solvent mixtures, a different solvent was incorporated with a change of configuration. Sakai *et al*. have resolved α-amino-ε-caprolactam using a single resolving agent *via* diastreomeric salt formation in various solvents, with different dielectric constants. The enantiomers were isolated based on the dielectric constants of the solvents. The salts containing (*S*)-α-amino-ε-caprolactam were obtained from solvents with dielectric constants between 29 and 58. The solvents with dielectric constants less than 25 and higher than 62 gave rise to (*R*)-α-amino-ε-caprolactam.

The results of Sakai et.al. demonstrated the effect of the dielectric constants of the solvents in controlling the molecular interactions leading to the isolation of a specific enantiomer.[43-45] In another study they established the resolution of racemates to be affected by the change in chiral spaces due to the dielectric properties of the solvents used in the resolution procedure.[46] With **P4** and **P8**, the incorporated acetone dielectric constant is 21.30 and for acetonitrile it is 36.0.[47,48] In **P4,** *R*,*R*- was isolated, the acetone dielectric constant being less than 25, in **P8,** *S*,*S*- was isolated and acetonitrile's dielectric constant is between 29 and 58. In **P8** water was incorporated with a dielectric constant of 79.99,[47] which might have affected the chiral spaces in the salt. In the production of **P8**, water was mixed with acetonitrile. The results therefore are consistent with Sakai *et al*.'s findings in relation to the effect of the dielectric constant of the involved solvent.

In other studies involving the *Cinchona* alkaloids, the two "pseudoenantiomeric" pairs, **CINC**/**CIND** and **QUIN**/**QUID**, lead to opposite product enantiomers since the pairs have opposite stereochemistry at the "working" part of the molecules, that is, positions C8 and C9.[49] This is related to the first practical resolution of BINOL, the phosphoric acid of BINOL was resolved using **CINC** and **CIND** to access the (+)- and (-)- enantiomers, respectively.[50] There are exceptions as noted earlier, *N*-benzylcinchoninium chloride and *N*-benzylcinchonidinium chloride both formed salt crystals only with (*R*)-BINOL.[7] The crystal structure **P4** contains **CINC** (C9-*S*) and the *R*,*R*-enantiomer of the diacid and similarly He *et al*. resolved sertraline with (*R*)-mandelic acid to give rise to the (1*S*,4*S*)-sertraline.[38] In the current study it was established that the **CINC**/**CIND** and **QUIN**/**QUID** pairs gave opposite products in the resolution experiments. A change of solvent in the case of **CINC** with acetonitrile/water and acetone resulted in the retrieval of both enantiomers of the acid. Thus the general trend can be altered through the choice of solvent.

Conclusion

The solvent plays an important role in chiral discrimination additional to the common role as a medium of bringing the reactants into a solution, and the diastereomeric salt crystallization process. The solvent was included in all the crystal structures except for **P5**. The hydrogen bonds associated with acetone, methanol, water molecules and the usual acid-base hydrogen bonds between the resolving agents and **3.3** play an important role in stabilizing the crystals. The role of the solvents in stabilizing diastereomeric salts is complex, as their role is greater than just providing more hydrogen bonding sites and filling empty spaces to stabilize the crystals.

Desiraju *et al*. quoted, in their textbook, "It is difficult to prescribe an ideal solvent or ideal solubility for a crystallization experiment. It is also difficult to estimate the level of supersaturation at which a crystal is likely to form".[29]

All five of the salts have the charge assisted N—H···O as well as O—H···O interactions. It is only in the case of **CINC** where the quinoline N atom participated in the formation of hydrogen bonds in **P4** and **P8**. There are also weak, C—H···O interactions between the acetone O atom and the quinuclidine C—H bonds in structure **P4**. The established intermolecular contacts enhanced the packing capacity of the products.

The DSC and TGA results confirmed the formation of new compounds. The fingerprint plots from the CrystalExplorer results revealed the dominance of: H···H, O···H and C···H interactions in all of the structures.

The FT-IR results confirmed the transfer of a proton from the dicarboxylic acid to the bases in the formation of salts. These results complemented the X-ray diffraction results.

## 7.4 The resolution of racemic 9,10-dihydro-9,10-ethanoanthracene-11-carboxylic acid (**3.4**)

The racemic acid, *rac*-**3.4** was reacted with the different resolving agents in several solvents and the salts crystallized giving rise to **P9**, **P10** and the precipitate **P10a** (Scheme 7.2). The solvents that gave crystals are MeOH and PeOH only. There was insufficient **P10** for more analysis (thermal analysis and FTIR) and on repeating the experiment, a powder **P10a** resulted.

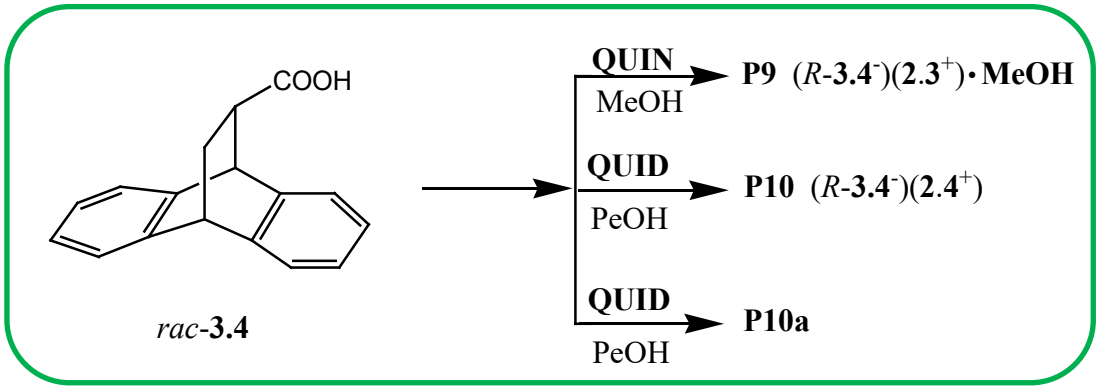


Scheme 7.2 Experimental reactions and results in the formation of the diastereomeric salts, **(*R*-3.4$^-$)(2.3$^+$)·MeOH (P9)** and **(*R*-3.4$^-$)(2.4$^+$) (P10)** and **P10a**.

Thermal analysis

The resultant crystals, **P9** and **P10a**, from the above reactions (Scheme 7.2) were analyzed on a DSC 6000 and TGA 4000 instruments, and the summary of the results are shown in Figure 7.25 and Table 7.21.

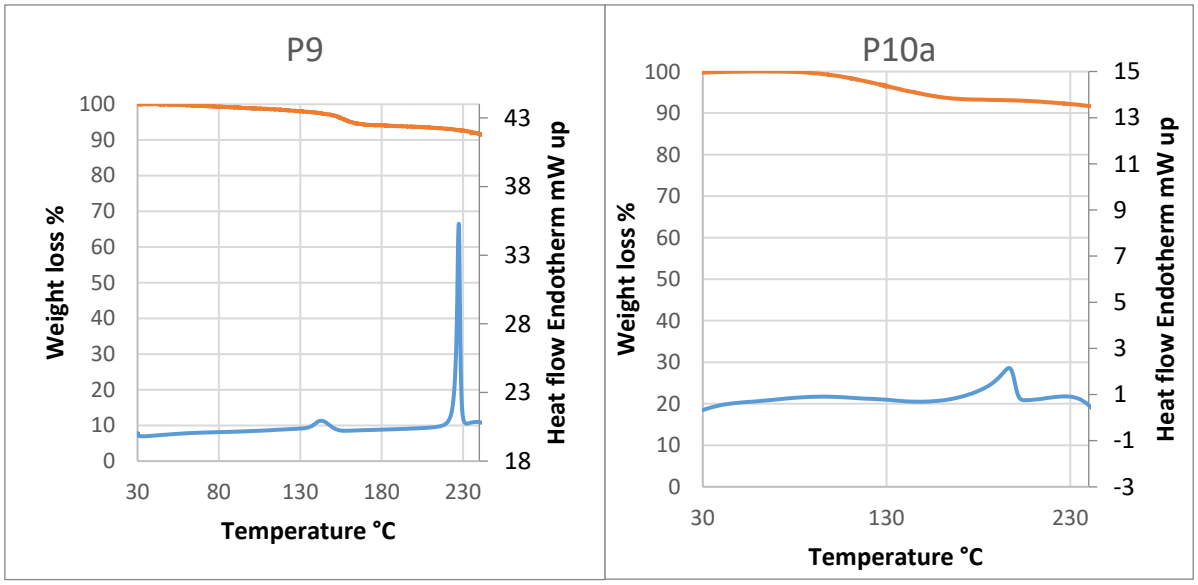


Figure 7.25 DSC and TGA curves of the salts **P9** and **P10a**.

Table 7.21 Thermal analysis data of the starting materials and the salts **P9** and **P10a**.

| **Reagents** | | | **Products** | **Thermal analysis** | | | |
|---|---|---|---|---|---|---|---|
| Racemate $T_{on}/T_p$ ºC | RA $T_{on}/T_p$ ºC | Solvent (bp ºC) | Salt | DSC | | TG | |
| | | | | Endo 1 $T_{on}/T_p$ ºC | Endo 2 $T_{on}$ ºC | Exp (%) | Calc (%) |
| *Rac* **3.4** 186/190 | **QUIN** 172/177 | MeOH 65 | **P9** | 130/143 | 214 | 5.0 | 5.3 |
| | **QUID** 166/174 | PeOH 138 | **P10a** | 161/196 | | 7.6 | 13.3 |

**RA**-resolving agents, **CINC**-cinchonine, **CIND**-cinchonidine, **QUIN**-quinine, **QUID**-quinidine, Bp-boiling point, *rac*-**3.4**-9,10-dihydro-9,10-ethanoanthracene-11-carboxylic acid. Endo - endotherm 1 & 2 (desolvation & melt), $T_{on}$ – onset temperature, $T_p$- peak temperature, Exp-experimental, Calc-calculated.

The DSC results of **P9** showed an endothermic peak with an onset temperature of 130 °C for the loss of MeOH. The second endotherm is due to the melt of the salt at 214 °C. The melting point of the salt was at a higher temperature compared to the melting points of the starting materials. The TGA results gave a mass loss of 5.0% due to the loss of MeOH, calc 5.3%.

The initial crystals of **P10** were insufficient for TGA and DSC analyses and the crystallization experiment was repeated resulting in a powder after 7 months. However, the TGA of the powder obtained from the repeated crystallization (**P10a**) showed a solvate with a mass loss of 7.6%. This mass loss is equivalent to half of a pentanol molecule. The calculated mass loss of pentanol was 13.3%. The DSC of this solvate (**P10a**) showed an onset temperature at 161 °C, corresponding to the loss of solvent and melt of the salt.

Crystal structure analysis

For both crystal structures, **P9** and **P10**, one hydrogen atom was transferred from the carboxylic acid **3.4** to the quinuclidine nitrogen (N1) of the alkaloids resulting in salts. The crystal data and refinement details of the two diastereomeric salts are summarized in Table 7.22.

Table 7.22 Crystal data and refinement details of **P9** and **P10**.

| Compound | **P9** (*R*-**3.4**$^-$)(**2.3**$^+$)·**MeOH** | **P10** (*R*-**3.4**$^-$)(**2.4**$^+$) |
|---|---|---|
| Molecular formula | $C_{38}H_{42}N_2O_5$ | $C_{37}H_{38}N_2O_4$ |
| $M_r$ (g/mol) | 606.76 | 574.72 |
| Temperature (K) | 173 | 173 |
| Crystal size (mm) | 0.160 x 0.190 x 0.250 | 0.08 x 0.09 x 0.290 |
| Crystal system | Orthorhombic | Orthorhombic |
| Space group | $P2_12_12_1$ | $P2_12_12_1$ |
| *a* (Å) | 6.5395(13) | 10.976(2) |
| *b* (Å) | 18.438(4) | 15.208(3) |
| *c* (Å) | 26.183(5) | 18.101(4) |
| *α* (°) | 90 | 90 |
| *β* (°) | 90 | 90 |
| *γ* (°) | 90 | 90 |
| V (Å$^3$) | 3157.0(11) | 3021.4(10) |
| *Z* | 4 | 4 |
| ρ (calcd) (g/cm$^3$) | 1.2764 | 1.260 |
| Absorption coefficient μ (mm$^{-1}$) | 0.84 | 0.082 |
| Theta range for data collection (°) | 1.35 -28.39 | 1.75 – 28.31 |
| Reflections collected | 7899 | 7511 |
| No. data with $I > 2\sigma(I)$ | 6466 | 5881 |
| No. parameters | 411 | 397 |
| Final R ($I > 2\sigma(I)$) | $R_1$ = 0.0422<br>$wR_2$ = 0.0886 | $R_1$ = 0.0454<br>$wR_2$ = 0.0958 |
| *R* indices all data | $R_1$ = 0.0587<br>$wR_2$ = 0.0975 | $R_1$ = 0.0656<br>$wR_2$ = 0.1056 |
| Goodness-of-fit on $F^2$ | 1.033 | 1.022 |

The C—O distances of the carboxylate moieties are similar which clearly distinguishes the $COO^-$ from the carboxylic acid (Table 7.23).

Table 7.23 C—O distances in the two salts, **P9** and **P10**.

| d(C—O)/Å | **P9** | **P10** |
|---|---|---|
| Carboxylate | 1.242(2) | 1.243(2) |
| | 1.268(2) | 1.260(2) |
| Δ d(C—O)/Å | 0.0260 | 0.0170 |

(*R*-**3.4**$^-$)(**2.3**$^+$)·**MeOH** (**P9**), (Quininium *R*-9,10-dihydro-9,10-ethanoanthracene-11-carboxylate methanol solvate) crystallized in the orthorhombic space group $P2_12_12_1$ with $Z = 4$, with one **3.4**$^-$ anion, one **2.3**$^+$ cation and one methanol molecule in the asymmetric unit (Figure 7.26(a)). The absolute configuration of the stereogenic centre 11 of **3.4**$^-$ was assigned relative to the known absolute configuration of the (*R*)-**2.3**$^+$ base. Based on this relative absolute configuration it was determined that the absolute configuration of the stereogenic centre 11 in **3.4**$^-$ is (*R*). The hydrogen bonding is characterized by the charge assisted interaction, (**2.3**$^+$)-N1—H1···O43-(**3.4**$^-$) and (**MeOH**)-O45—H45···O43-(**3.4**$^-$), and furthermore the quininium cation's OH group is linked to the other carboxylate oxygen to form (**2.3**$^+$)-O12—H12···O42-(**3.4**$^-$). The corresponding hydrogen bonds are depicted in Figure 7.26(b).

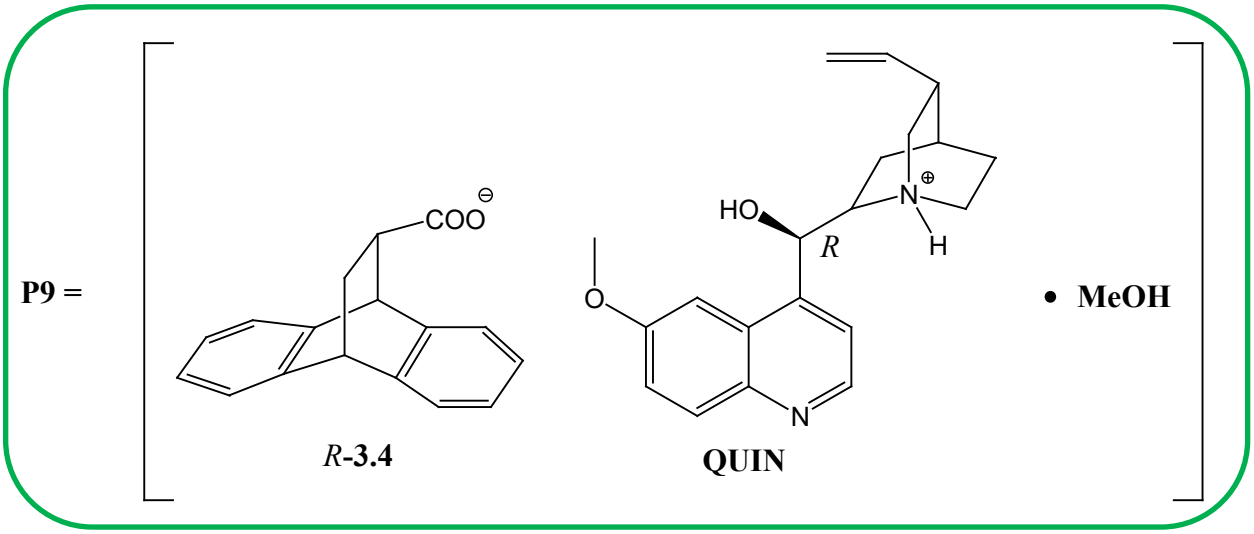


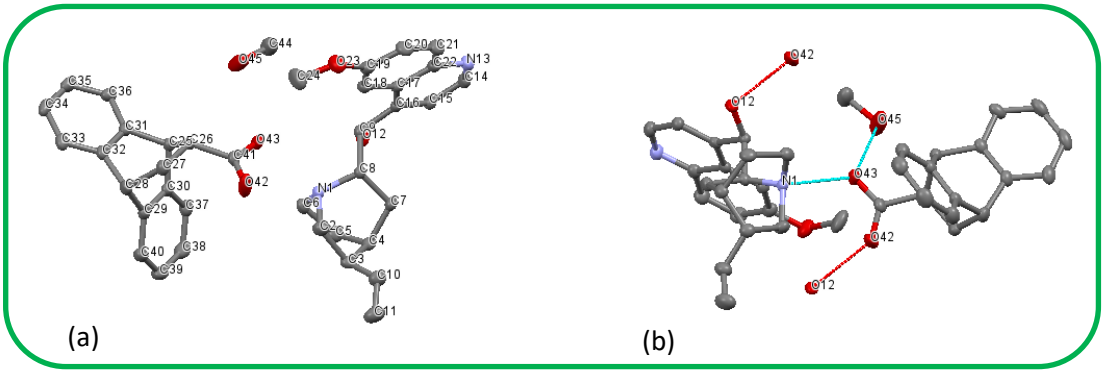


Figure 7.26 Representation of the X-ray crystal structure of **P9**, (a) showing the atom labelling and (b) showing the hydrogen bonding. Hydrogen atoms have been omitted for clarity.

Figure 7.27 shows the packing consisting of chains of the *R*-acid anions which are linked by hydrogen bonds to the quininium cations. In-between the chains the MeOH stabilizes the compound by hydrogen bonding to the *R*-acid carboxylate oxygen.

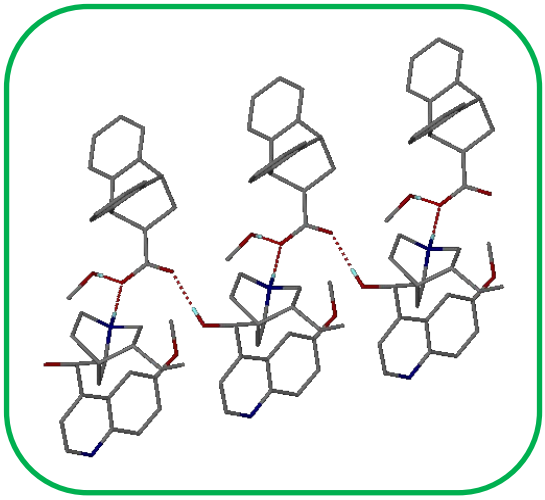

Figure 7.27 Hydrogen bonding in compound **P9** viewed along [010]. The hydrogens that are not involved in hydrogen bonding have been omitted for clarity.

The C—O distances of the $COO^-$ group of the anion, **3.4**$^-$ range from 1.242 Å (C41—O42) to 1.268 Å (C41—O43), with the difference between the two C—O bonds of 0.026 Å, which confirmed that the carboxyl group of **3.4** is deprotonated, generating an anion of **3.4**$^-$ and the cation, **2.3**$^+$. The C41—O43 bond is involved in two hydrogen bond interactions, N1—H1···O43 and O45—H45···O43 interactions, and the other one, C41—O42 is involved in one interaction, O12—H12···O42.

One **QUIN** cation is bound to one anion through $N^+$—H···$O^-$ hydrogen bonds, with d(N1···O43) = 2.7315(2) Å, the anion further bonds to a methanol molecule by the interaction, O45—H45···O43.

(*R*-**3.4**$^-$)(**2.4**$^+$) (**P10**), (Quinidinium *R*-9,10-dihydro-9,10-ethanoanthracene-11-carboxylate) was solved in the orthorhombic space group $P2_12_12_1$ with $Z = 4$. The asymmetric unit consists of one **3.4**$^-$ anion and one **2.4**$^+$ cation,[51] and the corresponding structure is shown in Figure 7.21(a). The quinidinium chiral C9 was assigned the *S* configuration and this gave rise to (*R*-**3.4**$^-$) in the crystal structure **P10**. The hydrogen bonding is similar to **P9**, with the exception of the link due to the solvent, as there is no solvent in **P10**. The hydrogen-bonding details of the salts are summarized in Table 7.24 below.

**P10** =

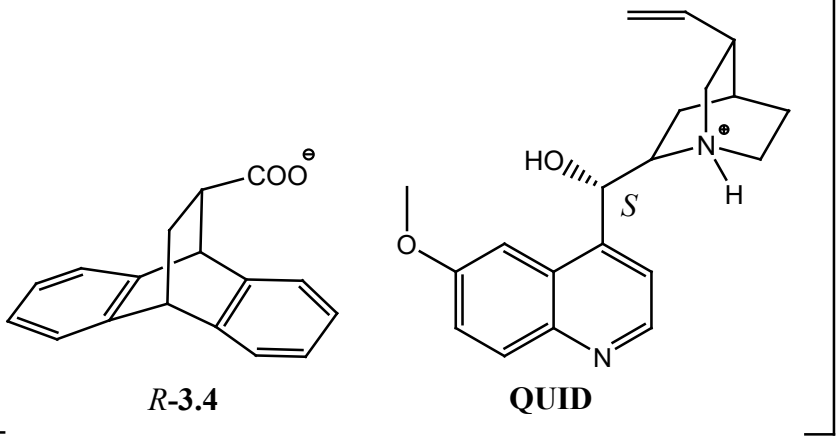


*R*-**3.4** **QUID**

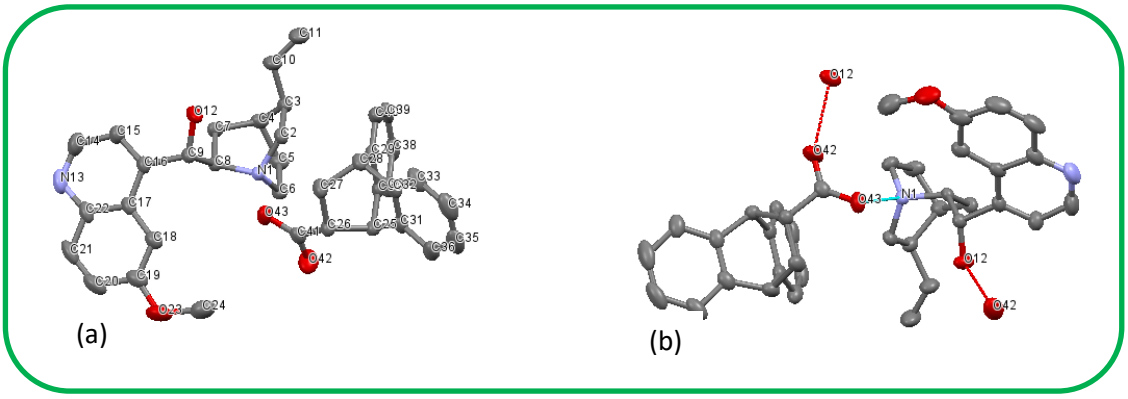


Figure 7.28 Representation of the X-ray crystal structure of **P10**, (a) showing the atom labelling and (b) showing the hydrogen bonding. Hydrogen atoms have been omitted for clarity.

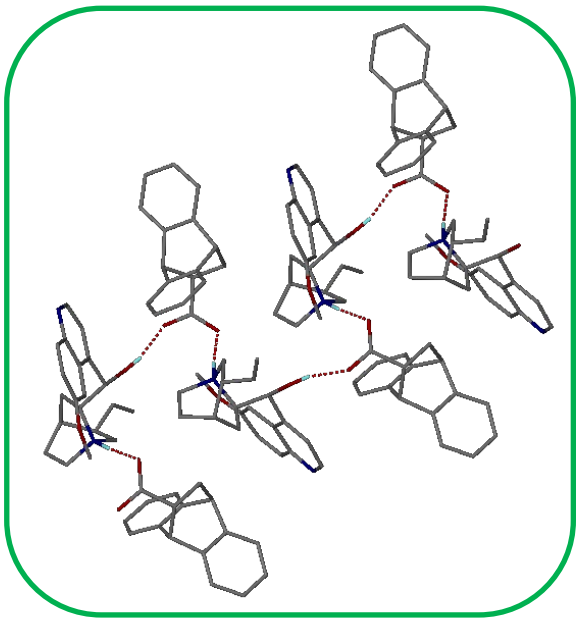

Figure 7.29 Hydrogen bonding in compound **P10,** viewed along [010]. The hydrogens that are not involved in hydrogen bonding have been omitted for clarity.

For **P10**, the C41—O43 bond is involved in hydrogen bonding by the interaction, N1—H1···O43, and the other one, C41—O42 by the O12—H12···O42 interaction. One cation is bound to one anion through $N^{+}$—H···$O^{-}$ hydrogen bonding, with d(N1···O43) = 2.6302(19) Å.

Figure 7.29 shows the packing consisting of the *R*-acids hydrogen bonded to the quinidinium cations.

In summary, both **QUIN** and **QUID** formed salts with the *R*-**3.4** enantiomer of the acid. The differences between **P9** and **P10** are the presence of the solvent in **P9**, and its contribution in the hydrogen bond formation with the acid, and the number of hydrogen bonds per salt, (Table 7.24).

Table 7.24 Hydrogen bond parameters of **P9** and **P10**.

| Compound | D—H···A | D—H (Å) | H···A (Å) | D···A (Å) | D—H···A (°) | Symmetry operator |
|---|---|---|---|---|---|---|
| **P9** | N1—H1···O43 | 0.88 | 1.85 | 2.732(2) | 175.0 | |
| | O12—H12···O42 | 0.84 | 1.75 | 2.571(2) | 167.1 | 1+x, y, z |
| | O45—H45···O43 | 0.84 | 1.87 | 2.707(2) | 176.9 | |
| **P10** | N1—H1···O43 | 1.01 | 1.64 | 2.630(2) | 165.2 | |
| | O12—H12···O42 | 0.88 | 1.75 | 2.620(2) | 167.2 | x-½, ½-y, 2-z |

CrystalExplorer analysis

The Hirshfeld surface analysis of **P9** and **P10** was conducted and the 2D fingerprint plots were generated for the individual intermolecular contacts, O···H, H···H, C···H and N···H intermolecular interactions, Figure 7.30. The full 2D fingerprint plots are illustrated in Figure 7.31. The percentage contributions of the intermolecular contacts to the total Hirshfeld surface area are listed in Table 7.25.

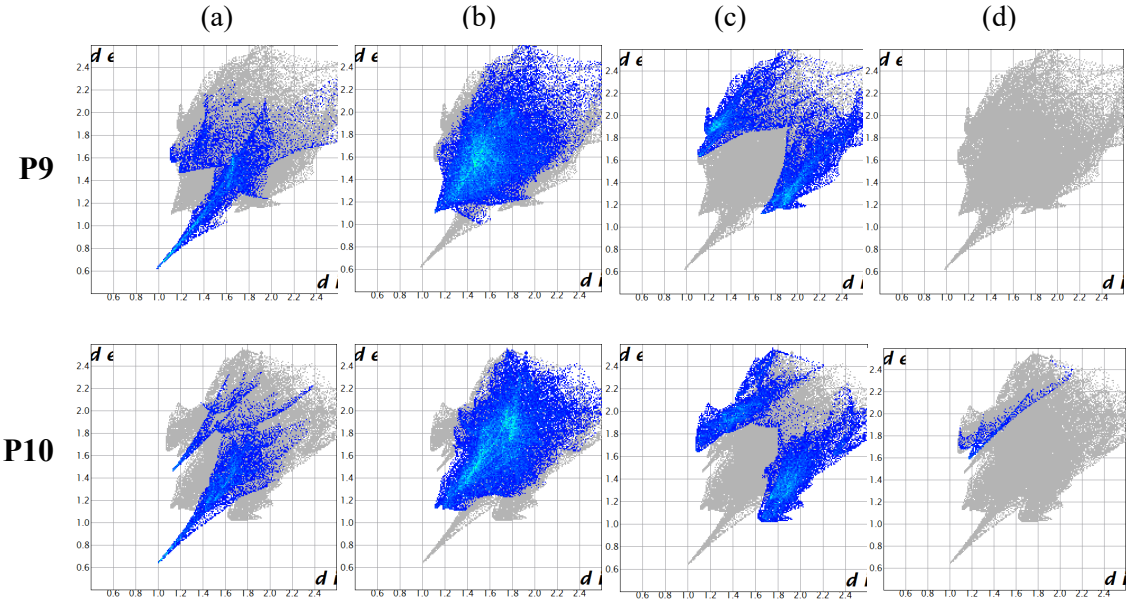


Figure 7.30 2D fingerprint plots of **P9** and **P10,** with columns (a) to (d) showing O···H, H···H, C···H and N···H contacts respectively.

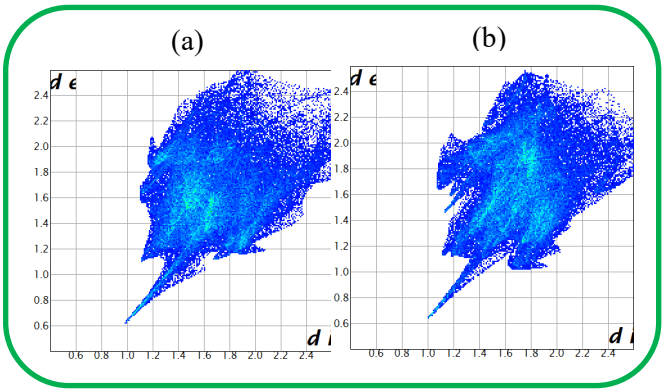


Figure 7.31 2D fingerprint plots of all the contacts in, (a) **P9** and (b) **P10**.

Table 7.25 Summary of the various contributions showing the percentages of contacts contributed to the total Hirshfeld surface area of **P9** and **P10**.

| Interactions | **P9** | **P10** |
|---|---|---|
| O···H | 16.3 | 14.8 |
| H···H | 55.6 | 56.2 |
| C···H | 26.6 | 26.8 |
| N···H | 0.0 | 1.8 |
| Total | 98.5 | 99.6 |

For **P9**, the O···H contacts are represented by the top broad spike and the sharp spike in Figure 7.30 column (a). The Hirshfeld surface area occupied by these contacts is shown by the blue colour, and the percentage contribution of this contact is 16.3%. The H···H contacts are represented by the large blue area in the centre under column (b) with a percentage contribution of 55.6%. The C···H (under column (c)) contacts are represented by the wing-like spikes at the top left and bottom right of the 2D fingerprint plot. These contacts have a reasonable contribution amounting to 26.6% to the total Hirshfeld surface. No N···H intermolecular contacts (column (d)) were found.

For **P10**, the O···H contacts are identifiable by the two thin, unequal and sharp spikes which contributed 14.8% to the total Hirshfeld surface area, Figure 7.30 column (a). The area of contribution is less compared to that in **P9.** The H···H interactions are identifiable by the broad spike in-between the two O···H sharp spikes, with the major contribution of 56.2%, Figure 7.30 column (b). The C···H contacts are represented by the wing-like spikes at the top left and bottom right in the fingerprint plot, Figure 7.30 column (c). Their contribution is relatively the same as that in **P9**, with a percentage contribution of 26.8%. The last contact shown on the top left area of the fingerprint plot is the N···H intermolecular contact, with a contribution of 1.8%, Figure 7.30 column (d).

The FT-IR analysis:

The FT-IR spectrum of **QUIN** is represented by Figure 7.32(a), and (b) for the carboxylic acid. The FT-IR of **P9** (similar to the **P10a** spectrum) is shown in Figure 7.32 (c), with the selected characteristic IR absorptions listed in Table 7.26. **P9** and **P10a** are the results of a reaction between **QUIN** and **QUID** in MeOH and PeOH with 9,10-dihydro-9,10-ethanoanthracene-11-carboxylic acid respectively. The two bases show a distinct peak on their FT-IR spectra, at 3166 $cm^{-1}$ due to the OH stretch. The carboxylic acid shows peaks due to COOH at approximately 3022 $cm^{-1}$ (within the range 3400-2500 $cm^{-1}$) though the peak is not as prominent as expected, and the distinctive carbonyl peak at 1704 $cm^{-1}$, Figure 7.32(b).

In the FT-IR spectra of **P9** and **P10a**, these show the disappearance of the carbonyl peak, confirming that the COOH group donated a proton, Figure 2.32(c). This is further confirmed by the appearance of the carboxylate peaks, antisymmetric and symmetric peaks, at 1544 and 1393 $cm^{-1}$ respectively (Fig 7.32 (c)). The COOH peaks also disappeared indicating the absence of the COOH group in the region 3400 – 2500 $cm^{-1}$, due to loss of a proton (Fig 7.36(c)). The protonated tertiary amine peak is not convincingly shown for both salts at the expected region, between 2500 and 1800 $cm^{-1}$ (Fig 7.32(c)).

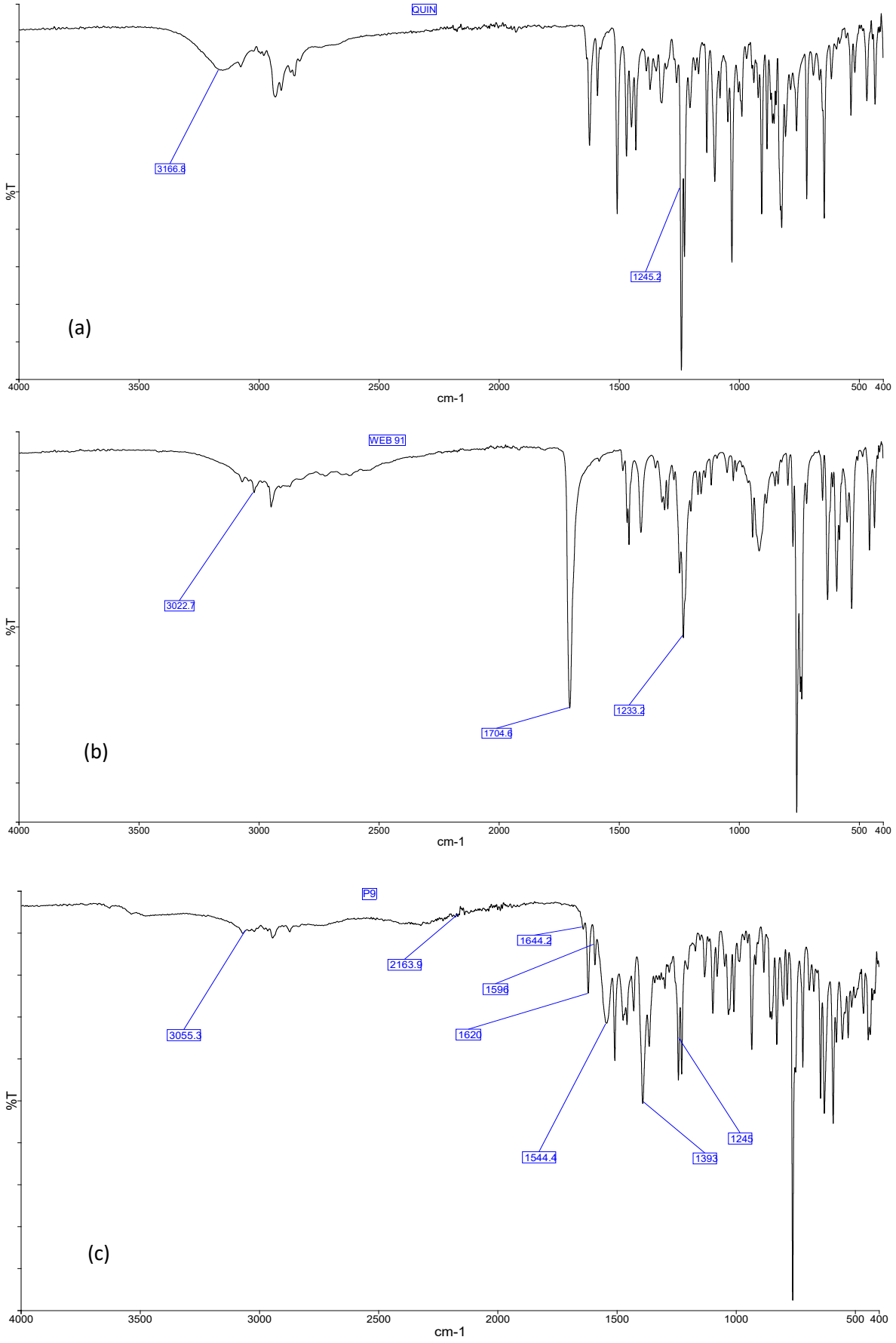


Figure 7.32 The IR spectra of, (a) **QUIN** (b) the racemate, carboxylic acid and (c) **P9**.

The FT-IR spectra do show the appearance of the other expected amine salt peak at 1620 $cm^{-1}$ in both salts (c). The appearance of the amine salt peak and the carboxylate peaks, plus the disappearance of the carbonyl peak confirmed the salt formation due to the loss of a proton, in both salts, **P9** and **P10a**. The OH peak appeared at 3166 $cm^{-1}$ for the resolving agent **QUIN**, and the reduction in frequency of the salt's peak at 3055 $cm^{-1}$ confirms that the C9 OH group is involved in hydrogen bonding.[32(b)]

Table 7.26 The characteristics of selected FT-IR absorptions of **P9** and **P10a**.

| Functional groups | **P9** and **P10a** absorptions $cm^{-1}$ | Expected absorptions ($cm^{-1}$) |
|---|---|---|
| O—H···O | 3055 (3042) | 3400 – 3200 |
| COOH | No peak | 3400 – 2500 |
| C=O | No peak | 1780 – 1670 |
| $N^{+}$—H | No peak<br>1620 (1620) | 2500 – 1800<br>1670 – 1610 |
| $COO^{-}$ | 1544 (1578)<br>1393 (1382) | 1610 – 1550<br>1420 – 1300 |
| C—O | 1245 (1227) | 1200 – 1050 |

Salt formation was also predicted due to $\Delta pK_a > 3$.[2] The $pK_a$ values of the bases is 9.1 and of the acid is 4.4,[1] with the difference = 4.7.

**QUIN** and **QUID** are stereochemically different, yet in the current resolution they yielded the same enantiomer. Previously in this work, **CIND** (**2.2**) and **CINC** (**2.1**) were employed to resolve racemic malic acid in the solvent, EtOH, and the resultant salts contained the *D*-malate anion in both salts. Both structures displayed extensive hydrogen bonding with the salts efficiently packed.[52] Gjerløv *et al*., and McKenzie (cited by Larsen) have employed **2.2** and **2.1** respectively to resolve racemic mandelic acid in water and the resultant salts had the same chirality, **2.2**-(*S*)-mandelate and **2.1**-(*S*)-mandelate.[9,10] Larsen *et al.* then prepared the diastereomeric salts of **2.1** and mandelic acid from EtOAc and found results that were different from McKenzie's, their less soluble salt was the **2.1**-(*R*)-mandelate salt.[10] The derivatives of **2.1** and **2.2**, *N*-benzylcinchoninium chloride and *N*-benzylcinchonidinium chloride yielded the same (*R*)-enantiomer on resolving the racemic 2,2'-dihydroxy-1,1'-binaphthyl in different solvents, acetonitrile and MeOH respectively.[7,8]

The selection of a good solvent is one of the main problems in optical resolution,[53] and the investigation of the role of a crystal solvate was undertaken by Kozma *et al*. in the resolution of mandelic acid by **2.1** in three different solvents and in five different solvent combinations.

The resolutions in the five solvents/solvent mixtures were markedly different, and the precipitated salts differed in configuration of the mandelic acid and in the crystal solvate.[42(a)]

In the previous section, resolution of *trans*-9,10-dihydro-9,10-ethanoanthracene-11,12-dicarboxylic acid (**3.3**), was achieved using the four *Cinchona* alkaloids, **2.1** - **2.4**.[54] A summary of related chiral resolution studies is given in Table 7.27.

Table 7.27 Summary of the above studies related to the current study.

| Refs | Resolving agents | Racemate | Solvents | Results |
|---|---|---|---|---|
| *52* | **2.1** | MaA | EtOH | (*D*-malate$^-$)(**2.1**$^+$)•2$H_2O$ |
| | **2.2** | MaA | EtOH | (0.5*D*-malate$^-$)(**2.2**$^+$)•$H_2O$ |
| *9* | **2.2** | MA | $H_2O$ | (*S*-mandelate$^-$)(**2.2**$^+$) |
| *10* | **2.1** | MA | $H_2O$ | (*S*-mandelate$^-$)(**2.1**$^+$) |
| | **2.1** | MA | EtOAc | (*R*-mandelate$^-$)(**2.1**$^+$) |
| *42(b)* | **2.1** | MA | $H_2O$ | (*S*-mandelate$^-$)(**2.1**$^+$)•$H_2O$ |
| | **2.1** | MA | $H_2O$:EtOH (4:1) | (*S*-mandelate$^-$)(**2.1**$^+$)•$H_2O$ |
| | **2.1** | MA | $H_2O$:EtOH (2:1) | (*R*-mandelate$^-$)(**2.1**$^+$) |
| | **2.1** | MA | EtOAc | (*R*-mandelate$^-$)(**2.1**$^+$)•EtOAc |
| *7* | **2.1a** | BINOL | Acetonitrile | (*R*-BINOL$^-$)(**2.1a**$^+$) |
| *8* | **2.2a** | BINOL | MeOH | (*R*-BINOL$^-$)(**2.2a**$^+$) |
| *54* | **2.1** | **3.3** | Acetone | (*R,R*-**3.3**$^-$)(**2.1**$^+$)•ACE |
| | **2.2** | **3.3** | MeOH | (*R,R*-**3.3**$^-$)(**2.2**$^+$) |
| | **2.3** | **3.3** | MeOH | (*R,R*-**3.3**$^-$)(**2.3**$^+$)•2MeOH |
| | **2.4** | **3.3** | MeOH | (*S,S*-**3.3**$^-$)(**2.4**$^+$)•2MeOH |
| | **2.1** | **3.3** | $CH_3CN$ + $H_2O$ | (*S,S*-**3.3**$^-$)(**2.1**$^+$)•$H_2O$ |
| *Current study* | **2.3** | **3.4** | MeOH | (*R*-**3.4**$^-$)(**2.3**$^+$)•MeOH |
| | **2.4** | **3.4** | PeOH | (*R*-**3.4**$^-$)(**2.4**$^+$) |

In both structures, **P9** and **P10**, the quinuclidine N and the hydroxyl O atoms contributed in the formation of hydrogen bonds, resulting in the formation of the two salts and leading to the successful resolution of the carboxylic acid, **3.4**. Studies indicating the importance of the solvents' dielectric constants as one of the decisive factors on the chiroselective molecular recognition have been reported by Sakai *et al*.[43-45] The solvents' dielectric constants at 25 ºC are, MeOH = 32.62 and PeOH = 15.03, respectively,[55] and could have contributed to the resolution observed.

In this study, the choice of solvent in the chiral resolution process is highlighted. This indicates that attention should be paid to the solvents in addition to the usual concerns for chiral resolution, such as the molecular structures of the resolving agents and racemic substrates and

their hydrogen bonding abilities. The solvent being the reaction environment or medium, is a very important factor for optimizing the resolution mechanism.

## Conclusion

The two resolving agents, **QUIN** and **QUID**, were used successfully in the resolution of racemic 9,10-dihydro-9,10-ethanoanthracene-11-carboxylic acid in different solvents, resulting in the two stable, less soluble diastereomeric salts, **P9** and **P10**. The **P10** salt could not be reproduced for further analyses and a solvate (powder) **P10a** was obtained during the recrystallization attempts. This solvate was characterized using TGA, DSC and FT-IR. The crystal structure analysis confirmed salt formation, mainly stabilized by the following interactions, N—H···O and O—H···O. The CrystalExplorer results confirmed the dominance of the O···H, H···H, and C···H contacts. Furthermore, FT-IR spectroscopy also confirmed the proton transfer from the COOH group to the nitrogen of the base resulting in the formation of salts. Both resolving agents, **QUIN** and **QUID**, in different solvents, MeOH and PeOH, gave the *R*-enantiomer of the acid.

## 7.5 The resolution of racemic 2-chloropropanoic acid (**3.5**)

Racemic 2-chloropropanoic acid (2-**CPA**) was treated with the different resolving agents in several solvents, and the salts crystallized giving rise to **P11** - **P14**, (Scheme 7.3).

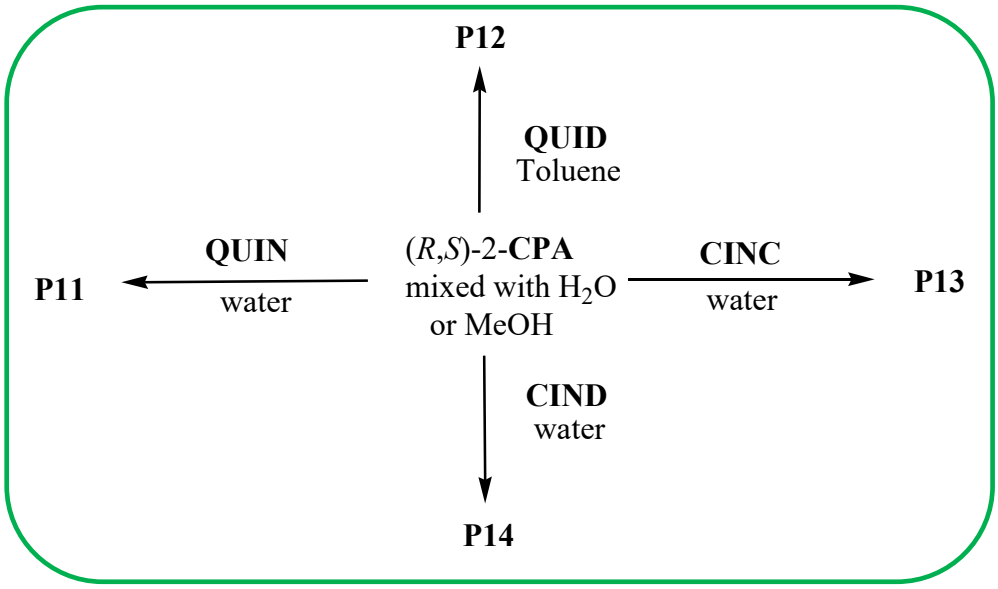


Scheme 7.3 The reaction products of the racemate, 2-**CPA** mixed with water or MeOH, with the four resolving agents, **QUIN**, **QUID**, **CINC** and **CIND** in water and toluene, **P11** (*S*-**3.5**$^{-}$)(**2.3**$^{+}$)·$H_2O$, **P12** (0.4*S*-**3.5**$^{-}$)(**2.4**$^{+}$)•$H_2O$, **P13** (0.8*S*-**3.5**$^{-}$)(**2.1**$^{+}$)·$2H_2O$ and **P14** (0.6*S*-**3.5**$^{-}$)(**2.2**$^{+}$)·$H_2O$.

Thermal analysis

The resultant salts were analyzed to determine their thermal properties regarding the desolvation and the melting points. The DSC and TGA results are summarized in Figure 7.33 and Table 7.28.

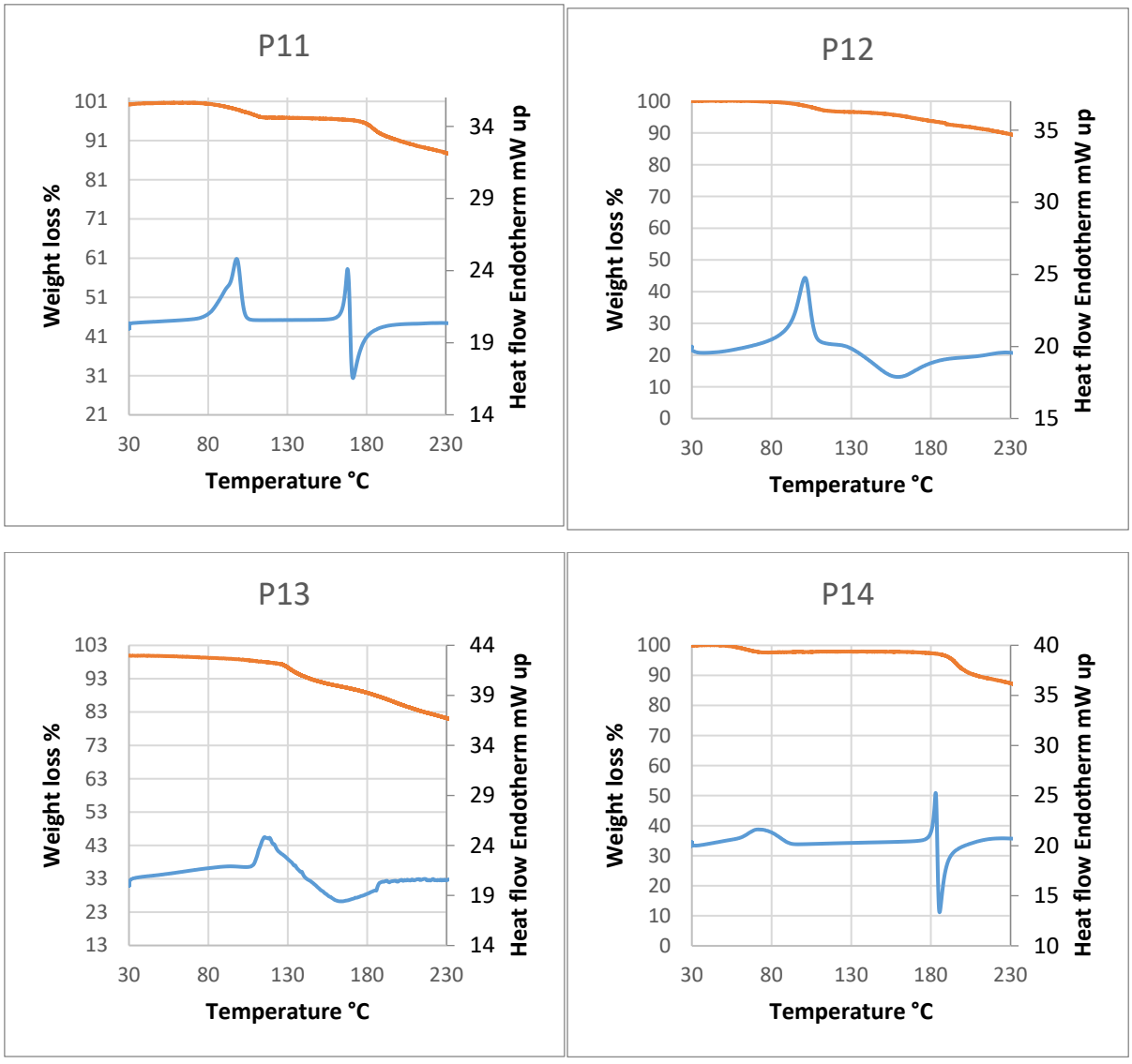


Figure 7.33 DSC and TGA curves of the salts **P11 – P14**.

Table 7.28 Thermal analysis data of the starting materials and the **P11** – **P14** salts.

| **Reagents** | | | **Products** | **Thermal analysis** | | | |
|---|---|---|---|---|---|---|---|
| Racemate (bp ºC) | RA $T_{on}/T_p$ ºC | Solvent (bp ºC) | Salt | DSC | | TG | |
| | | | | Endo 1 $T_{on}/T_p$ °C | Endo 2 $T_{on}/T_p$ ºC | Exp (%) | Calc (%) |
| *Rac* **2-CPA (**78) | **QUIN** 172/177 | Water (100) | **P11** | 70/98 | 159 | 3.1 | 4.0 |
| | **QUID** 166/174 | Toluene (111) | **P12** | 73/101 | | 3.6 | 4.0 |
| | **CINC** 248/264 | Water (100) | **P13** | 104/118 | | 5.4 | 4.3 |
| | **CIND** 198/206 | Water (100) | **P14** | 58/74 | 172 | 3.0 | 4.3 |
| **RA**-resolving agents, **CINC**-cinchonine, **CIND**-cinchonidine, **QUIN**-quinine, **QUID**-quinidine, Bp-boiling point, *rac*-**2-CPA – 2-**chloropropanoic acid. Endo - endotherm 1 & 2 (desolvation & melt), $T_{on}$ – onset temperature, $T_p$- peak temperature, Exp-experimental, Calc-calculated. | | | | | | | |

The DSC curve of **P11** demonstrated an endotherm with an onset temperature of 70 °C which is due to the loss of water. The melt of the salt occurs at 159 °C. The TGA supported the DSC results with a mass loss step of 3.1%, calculated 4.0%, corresponding to the loss of water. **P11**'s onset temperature differed from those of the starting material, with a lower onset temperature, confirming the formation of a new compound.

The DSC curve of **P12** showed the loss of water occurring together with the melt of the salt. The onset temperature of the processes was 73 °C, with the peak temperature at 101 °C. The TGA results exhibited a mass loss from about 60 °C. The calculated mass loss was 4.0%, equivalent to a mass loss due to a water molecule (exp mass loss = 3.6%).

The DSC of **P13** also shows one endotherm for the loss of water and the melt with an onset temperature of 104 °C. The TGA results showed a mass loss at about 70 °C at a slow rate, and thereafter gave a rapid mass loss between 119 and 130 °C, contributing about 5.4% of the total mass.

The calculated mass loss due to water was 4.3%, which is lower than the TGA experimental results. The difference between the calculated and the experimental percentage loss is due to the inability to locate exactly where the dehydration mass loss step stopped and where the thermal decomposition began. The salt melting point was at a lower temperature compared to that of the resolving agent. For all the salts, melting was followed by decomposition.

The thermal analysis results of **P14** resemble that of **P11**, differing in the onset and peak temperature values of endotherms 1 and 2. The first onset temperature at 58 °C corresponded to the dehydration of the salt, and endotherm 2 onset temperature at 172 °C corresponded to the melt of **P14**.

Analysis of the melting points of the dehydrated salts show that **P14** has the highest melting point and **P12** the lowest melting point, (**P14** > **P11** > **P13** > **P12**). Hydrogen bonding environments are discussed in the next section on crystal structure analysis. Both **P11** and **P12** lose water at similar temperatures and their hydrogen bonding patterns involving water are similar. **P13** loses water at a much higher temperature with **P14** showing the lowest. In **P13** the water molecule formed a hydrogen bond interacting with the quinoline nitrogen atom of **CINC**.

Crystal structure analysis.

(*S*-**3.5**$^-$)(**2.3**$^+$)•$H_2O$ (**P11**), (Quininium *S*-2-chloropropanoic carboxylate monohydrate) was prepared by the reaction of quinine with racemic 2-chloropropanoic acid in a 1:1 ratio, and crystallized in the orthorhombic system, space group $P2_12_12_1$ with $Z = 4$. There is one **3.5**$^-$ anion, one **2.3**$^+$ cation and one water molecule in the asymmetric unit. The corresponding structure is depicted in Figure 7.34(a).

The absolute configuration of the stereogenic centre of **3.5**$^-$ was assigned in relation to the known absolute configuration of the base, **QUIN**$^+$. Based on this known absolute configuration it was established that the absolute configuration of **3.5**$^-$ is (*S*). The hydrogen bonding is characterized by the charge assisted interaction, (**QUIN**$^+$)-N1—H1···O26-(**3.5**$^-$), with the hydroxyl group of **QUIN** linked to the water molecule forming the interaction, (**QUIN**$^+$)-O12—H···O31-(**$H_2O$**).

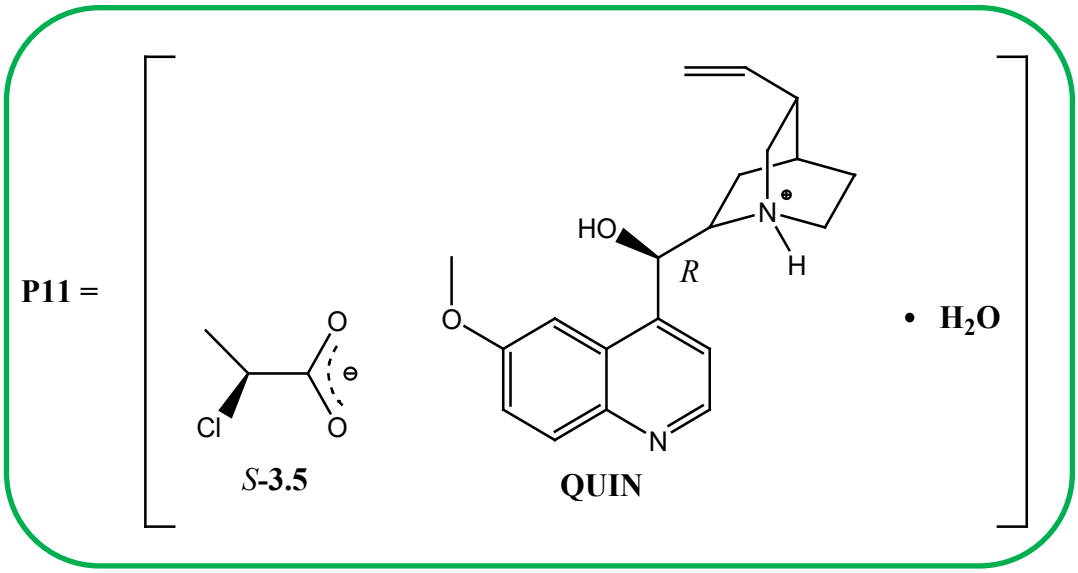

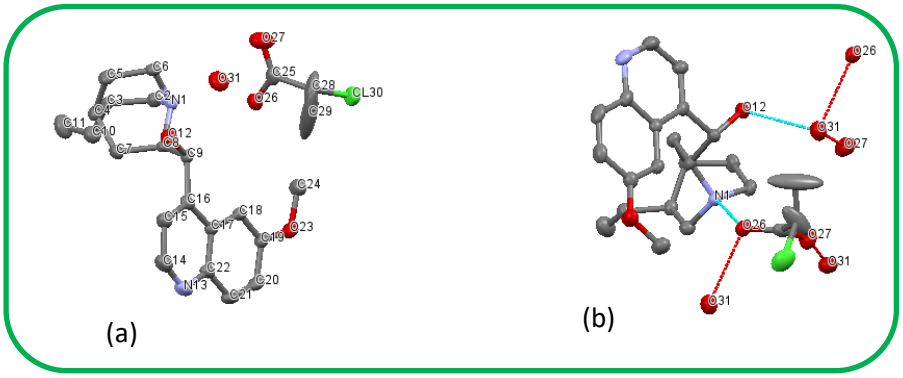


Figure 7.34 Representation of the X-ray crystal structure of **P11**, (a) showing the atom labelling and (b) showing the hydrogen bonding. Hydrogen atoms have been omitted for clarity.

The water molecule further behaves as a hydrogen bond donor to the acid forming the following interactions, (**$H_2O$**)-O31—H31A···O27-(**3.5**$^-$) and (**$H_2O$**)-O31—H31B···O26-(**3.5**$^-$). These hydrogen bonds are depicted in Figures 7.34(b) and 7.35 (packing diagram). The crystal data and refinement details are listed in Table 7.29, and the hydrogen bonding details of **P11** are summarized in Table 7.30.

Table 7.29 The crystal data and refinement details of **P11** – **P14**.

| Compound | **P11** (*S*-**3.5**$^-$)(**2.3**$^+$)·$H_2O$ | **P12** (0.4*S*-**3.5**$^-$)(**2.4**$^+$)•$H_2O$ | **P13** (0.8*S*-**3.5**$^-$)(**2.1**$^+$)·2$H_2O$ | **P14** (0.6*S*-**3.5**$^-$)(**2.2**$^+$)$H_2O$ |
|---|---|---|---|---|
| Molecular formula | $C_{23}H_{31}ClN_2O_5$ | $C_{23}H_{31}ClN_2O_5$ | $C_{22}H_{30}ClN_2O_5$ | $C_{22}H_{29}ClN_2O_4$ |
| $M_r$ (g/mol) | 450.95 | 451.79 | 437.93 | 420.9 |
| Temperature (K) | 173(2) | 173(2) | 173(2) | 173(2) |
| Crystal size (mm) | 0.14 x 0.15 x 0.16 | 0.06 x 0.07 x 0.20 | 0.08 x 0.12 x 0.23 | 0.05 x 0.12 x 0.14 |
| Crystal system | Orthorhombic | Orthorhombic | Orthorhombic | Monoclinic |
| Space group | $P2_12_12_1$ | $P2_12_12_1$ | $P2_12_12_1$ | $P2_1$ |
| *a* (Å) | 6.7183(5) | 7.0299(14) | 7.2510(15) | 12.710(3) |
| *b* (Å) | 17.7072(12) | 15.846(3) | 16.163(3) | 6.8092(14) |
| *c* (Å) | 18.8505(13) | 20.049(4) | 18.750(4) | 12.937(3) |
| $\alpha$ (°) | 90 | 90 | 90 | 90 |
| $\beta$ (°) | 90 | 90 | 90 | 107.79(3) |
| $\gamma$ (°) | 90 | 90 | 90 | 90 |
| V (Å$^3$) | 2242.50 | 2233.4(8) | 2197.6(8) | 1066.1(4) |
| *Z* | 4 | 4 | 4 | 2 |
| ρ (calcd) (g/cm$^3$) | 1.3355 | 1.344 | 1.324 | 1.311 |
| Absorption coefficient $\mu$ (mm$^{-1}$) | 0.208 | 0.209 | 0.210 | 0.210 |
| Theta range for data collection (°) | 1.58 - 27.14 | 1.64 – 25.08 | 1.66 – 27.80 | 1.65 – 27.12 |
| Reflections collected | 7763 | 3956 | 5210 | 4697 |
| No. data with $I > 2\sigma(I)$ | 3872 | 2783 | 4318 | 3472 |
| No. parameters | 287 | 330 | 309 | 302 |
| Final R ($I > 2\sigma(I)$) | $R_1$ = 0.0530<br>$wR_2$ = 0.1099 | $R_1$ = 0.0502<br>$wR_2$ = 0.0985 | $R_1$ = 0.0528<br>$wR_2$ = 0.1484 | $R_1$ = 0.0461<br>$wR_2$ = 0.0955 |
| *R* indices all data | $R_1$ = 0.0749<br>$wR_2$ = 0.1209 | $R_1$ = 0.0848<br>$wR_2$ = 0.110 | $R_1$ = 0.0905<br>$wR_2$ = 0.2103 | $R_1$ = 0.0731<br>$wR_2$ = 0.1060 |
| Goodness-of-fit on $F^2$ | 1.028 | 0.980 | 1.177 | 0.990 |

Table 7.30 Hydrogen bonding parameters of **P11** – **P14**.

| Compound | D—H···A | D—H (Å) | H···A (Å) | D···A (Å) | D—H···A (°) | Symmetry operator |
|---|---|---|---|---|---|---|
| **P11** | N1—H1···O26 | 0.90 | 1.83 | 2.725(3) | 173.0 | |
| | O12—H12···O31 | 0.84 | 1.82 | 2.655(3) | 173.0 | |
| | O31—H31A···O27* | 0.76 | 1.96 | 2.715(4) | 170.0 | ½+x,3/2-y,-z |
| | O31—H31B···O26* | 0.98 | 1.80 | 2.762(3) | 168.8 | 1+x,y,z |
| | | | | | | |
| **P12** | N1—H1···O31 | 1.08 | 1.64 | 2.688(4) | 162.0 | |
| | O12—H12···O25 | 0.97 | 1.71 | 2.659(3) | 163.3 | x-1,y,z |
| | O25—H25B···O30 | 0.94 | 1.80 | 2.713(4) | 163.2 | ½+x,3/2-y,2-z |
| | O25—H25A···O31 | 0.83 | 2.02 | 2.831(3) | 167.4 | |
| | | | | | | |
| **P13** | N1—H1···O29 | 0.93 | 1.92 | 2.789(3) | 154.6 | 3/2-x,1-y, ½+z |
| | O12—H12···O32 | 0.84 | 1.81 | 2.646(9) | 172.4 | x-½,½-y,2-z |
| | O12—H12···O33 | 0.84 | 1.87 | 2.633(6) | 150.2 | x-½,½-y,2-z |
| | O31—H31A···O12 | 0.83 | 1.99 | 2.812(5) | 172.0 | 1+x,y,z |
| | O31—H31B···N13 | 0.88 | 2.03 | 2.888(4) | 166.0 | x+½,3/2-y,2-z |
| | O32—H32···O30 | 0.86 | 1.99 | 2.785(8) | 152.0 | 2-x,y-½,3/2-z |
| | O33—H33···O29 | 0.78 | 2.00 | 2.722(6) | 154.0 | 1-x,y-½,3/2-z |
| | | | | | | |
| **P14** | N1—H1···O31 | 0.89 | 1.82 | 2.710(3) | 173.0 | 1+x,y,1+z |
| | O12—H12···O30 | 0.82 | 1.84 | 2.648(3) | 166.0 | 1+x,1+y,1+z |
| | O32—H32A···O31 | 1.07 | 1.91 | 2.832(3) | 142.1 | |
| | O32—H32B···O30 | 0.99 | 1.86 | 2.790(4) | 154.5 | x,1+y,z |

Table 7.31 The C—O distances in the salts of **P11** – **P14**.

| d(C—O)/Å | **P11** | **P12** | **P13** | **P14** |
|---|---|---|---|---|
| Carboxylate | 1.248 | 1.210 | 1.240 | 1.228 |
| | 1.269 | 1.276 | 1.258 | 1.240 |
| Δd(C—O)/Å | 0.021 | 0.066 | 0.018 | 0.012 |

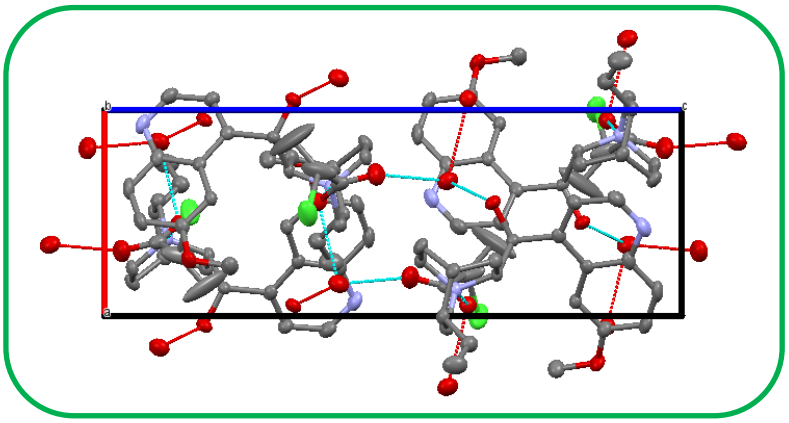

Figure 7.35 Molecular packing diagram of **P11**, a view down the crystallographic *b* axis. Hydrogen atoms have been omitted for clarity.

The C—O distances of the $COO^-$ groups are listed in Table 7.31, with the difference between the two C—O bonds of 0.021 Å, which indicates that the carboxyl group of **3.5** is deprotonated.

(0.4*S*-**3.5**$^-$)(**2.4**$^+$)•$H_2O$ (**P12**), (Quinidinium 2-chloropropanoic carboxylate monohydrate) was the result of the reaction of quinidine with racemic 2-chloropropanoic acid in a 1:1 ratio, which crystallized in the orthorhombic system, space group $P2_12_12_1$ with Z = 4. There is one disordered **3.5**$^-$ anion, one **2.4**$^+$ cation and one water molecule in the asymmetric unit. The corresponding structure is depicted in Figure 7.36(a).

The **QUID**$^+$ chiral C9 has an *S* configuration and this was assigned accordingly and the disordered **3.5**$^-$ anion refined to 0.45 *S*- and 0.55 *R*- absolute configurations. Thus **QUID** was not successful in resolving racemic 2-**CPA** compared to **QUIN**. The hydrogen bonding is characterized by the charge assisted interaction, (**QUID**$^+$)-N1—H1···O31(O37)-(**3.5**$^-$), with the hydroxyl group of **QUID** linked to the water molecule forming the interaction, (**QUID**$^+$)-O12—H12···O25-(**$H_2O$**). The water molecule further behaves as a hydrogen bond donor to the acid forming the following interactions, (**$H_2O$**)-O25—H25A···O30(O36)-(**3.5**$^-$) and (**$H_2O$**)-O25—H25B···O31(O37)-(**3.5**$^-$). These hydrogen bonds are depicted in Figures 7.36(b) and 7.37 (packing diagram). The hydrogen bonding details of **P12** are summarized in Table 7.30.

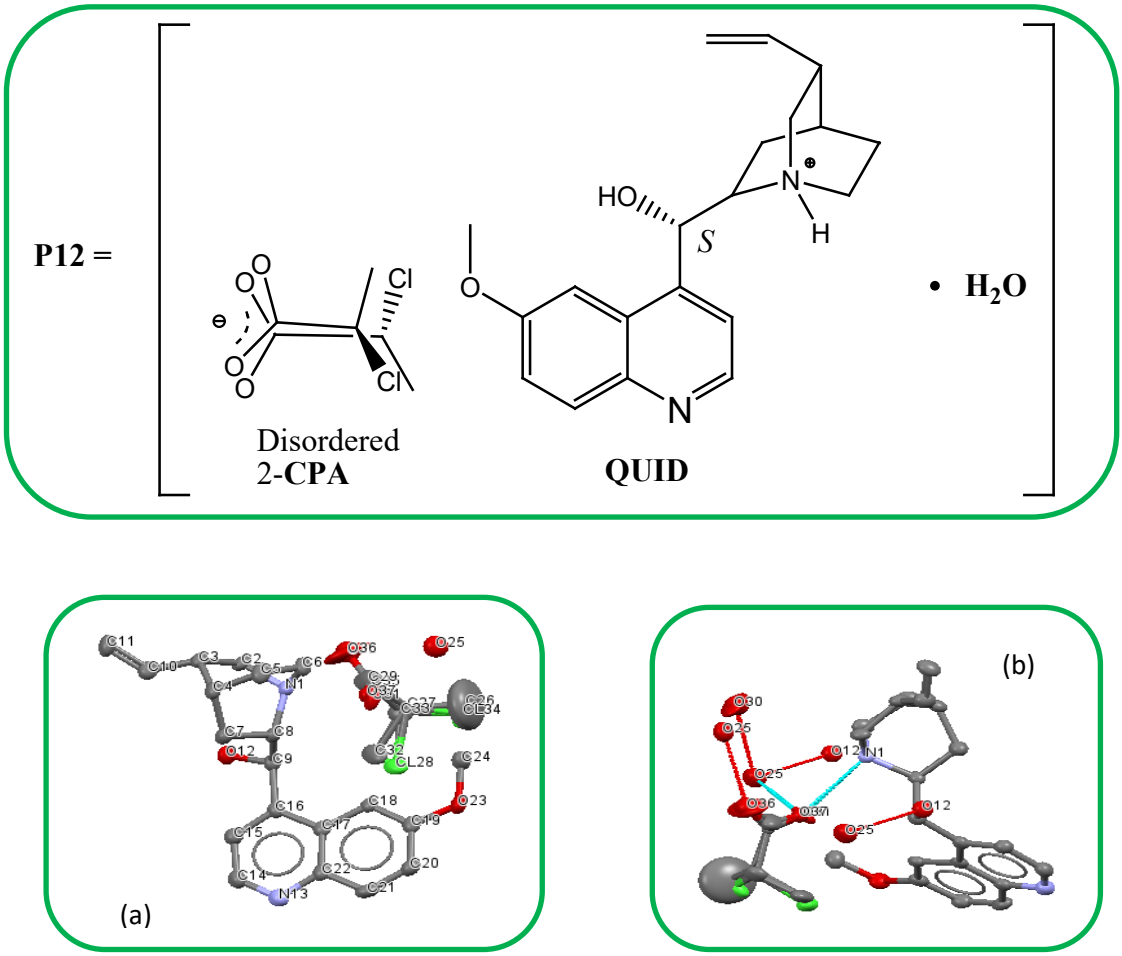


Figure 7.36 Representation of the X-ray crystal structure of **P12**, (a) showing the atom labelling and (b) showing the hydrogen bonding. Hydrogen atoms have been omitted for clarity.

The X-ray crystallographic results revealed that the molecular packing of **P12** is stabilized by the N—H···O and O—H···O interactions.

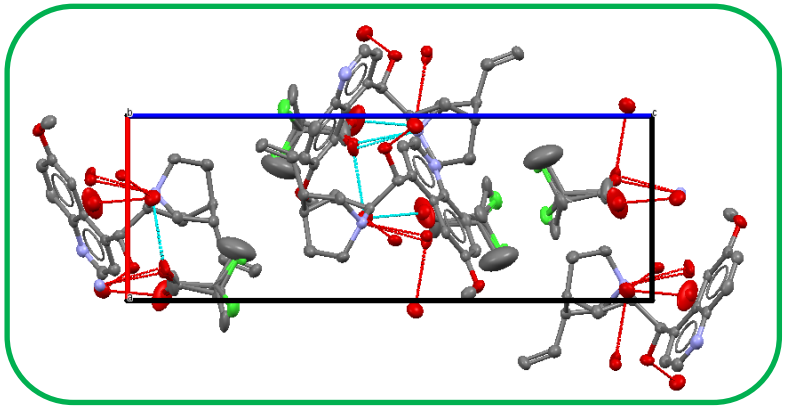

Figure 7.37 Molecular packing diagram of **P12**, a view down the crystallographic *b* axis. Hydrogen atoms have been omitted for clarity.

(0.8*S*-**3.5**$^-$)(**2.1**$^+$)•2$H_2O$ (**P13**, Cinchoninium 2-chloropropanoic carboxylate dihydrate) was the result of the reaction of cinchonine with racemic 2-chloropropanoic acid in a 1:1 ratio. Again

the crystal structure was solved in the orthorombic space group $P2_12_12_1$ with $Z = 4$. There is one disordered **3.5**$^-$ anion, one **2.1**$^+$ cation, one water molecule and a disordered water molecule in the asymmetric unit. The corresponding structure is depicted in Figure 7.33(a).

The **CINC**$^+$ chiral C9 has an *S* configuration and this was assigned accordingly and the disordered **3.5**$^-$ anion refined to 0.8 *S* and 0.2 *S* absolute configurations. Thus **CINC** partially resolved 2-**CPA**. The hydrogen bonding is characterized by the interaction, (**CINC**$^+$)-N1—H1···O29-(**3.5**$^-$), with the hydroxyl group of **CINC** linked to the disordered water molecule *via* the following interactions, (**CINC**$^+$)-O12—H12···O32-(**H$_2$O**) and (**CINC**$^+$)-O12—H12···O33-(**H$_2$O**). The hydroxyl group also behaves as a hydrogen bond acceptor forming a hydrogen bond with another water molecule through the interaction (**H$_2$O**)-O31—H31A···O12-(**CINC**$^+$). The same water molecule interacts with the quinoline N of **CINC** through (**H$_2$O**)-O31—H31B···N13-(**CINC**). The disordered water molecule behaves as a hydrogen bond donor, interacting with the carboxylate oxygens of the acid forming the interactions, (**H$_2$O**)-O32—H32···O30-(**3.5**$^-$) and (**H$_2$O**)-O33—H33···O29-(**3.5**$^-$). These hydrogen bonds are depicted in Figures 7.38(b) and 7.39.

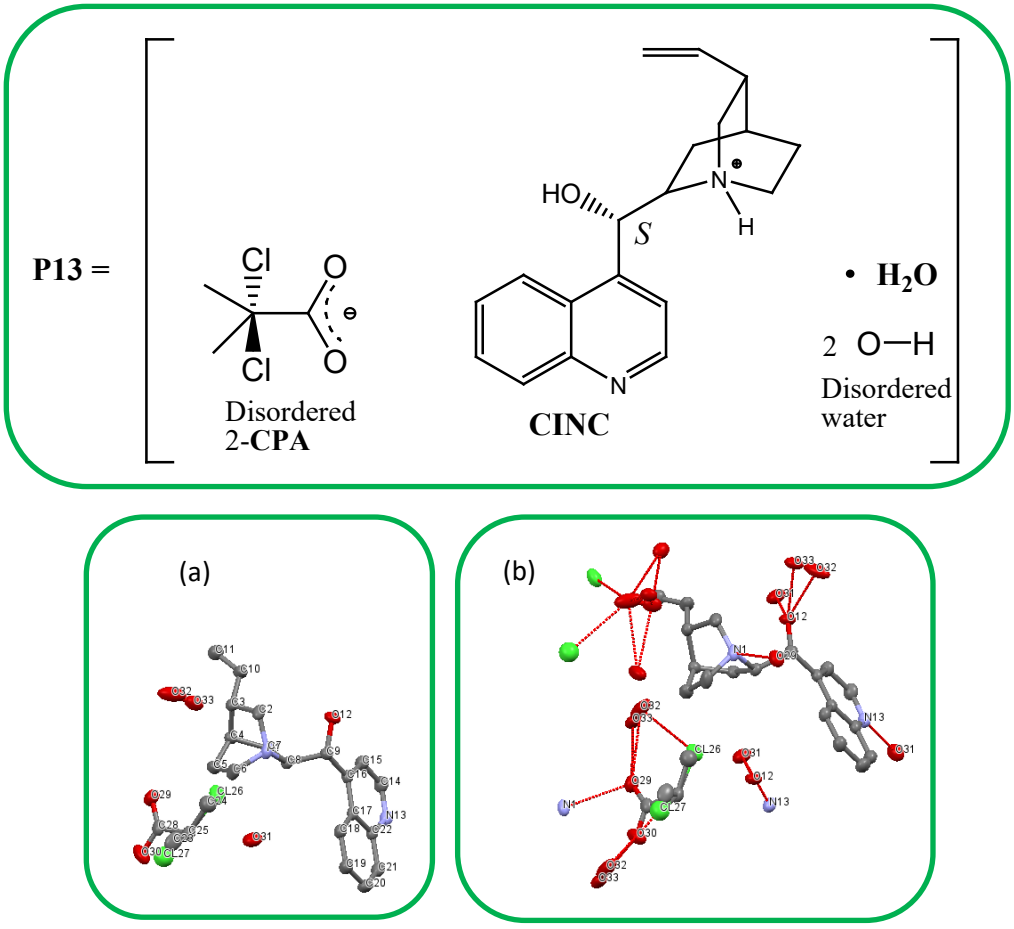


Figure 7.38 Representation of the X-ray crystal structure of **P13**, showing (a) the atom labelling and (b) the hydrogen bonding. Hydrogen atoms have been omitted for clarity.

As observed in the previous structures, the salt is stabilized by, N—H···O and O—H···O interactions.

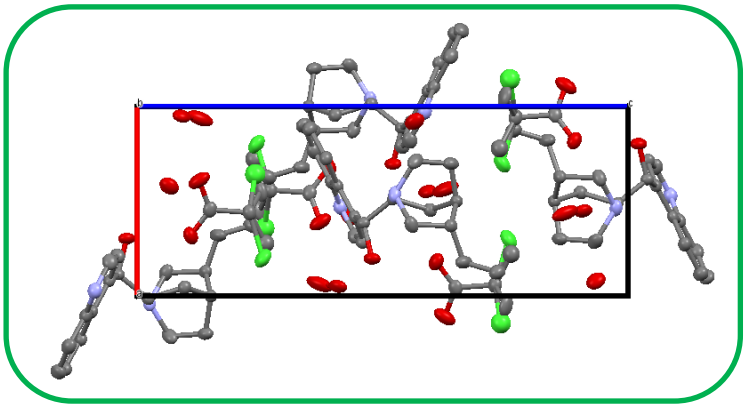

Figure 7.39 Molecular packing diagram of **P13**, a view down crystallographic *b* axis. Hydrogen bonds and atoms have been omitted for clarity.

(0.6*S*-**3.5**$^{-}$)(**2.2**$^{+}$)•$H_2O$ (**P14**, Cinchonidinium 2-chloropropanoic carboxylate monohydrate) was the result of the reaction of cinchonidine with racemic 2-chloropropanoic acid in a 1:1 ratio, which crystallized in the monoclinic system, space group $P2_1$ with $Z = 2$, with one **3.5**$^{-}$ anion, one **2.2**$^{+}$ cation and one water molecule in the asymmetric unit. The corresponding structure is depicted in Figure 7.40(a).

The **CIND**$^{+}$ chiral C9 has an *R* configuration which was assigned accordingly and the disordered **3.5**$^{-}$ refined to 0.6 *S* and 0.4 *R* absolute configurations. The hydrogen bonding is characterized by the interaction, (**CIND**$^{+}$)-N1—H1···O31-(**3.5**$^{-}$), with the hydroxyl group of **CIND** linked to the other carboxylate oxygen forming the interaction, (**CIND**$^{+}$)-O12—H12···O30-(**3.5**$^{-}$). The water molecule behaves as a hydrogen bond donor to the acid forming the following interactions, (**$H_2O$**)-O32—H32A···O31-(**3.5**$^{-}$) and (**$H_2O$**)-O32—H32B···O30-(**3.5**$^{-}$). These hydrogen bonds are depicted in Figures 7.40(b) and 7.41 (packing diagram). The crystal data and refinement details are in Table 2.29. The hydrogen bonding details of **P14** are summarized in Table 7.30.

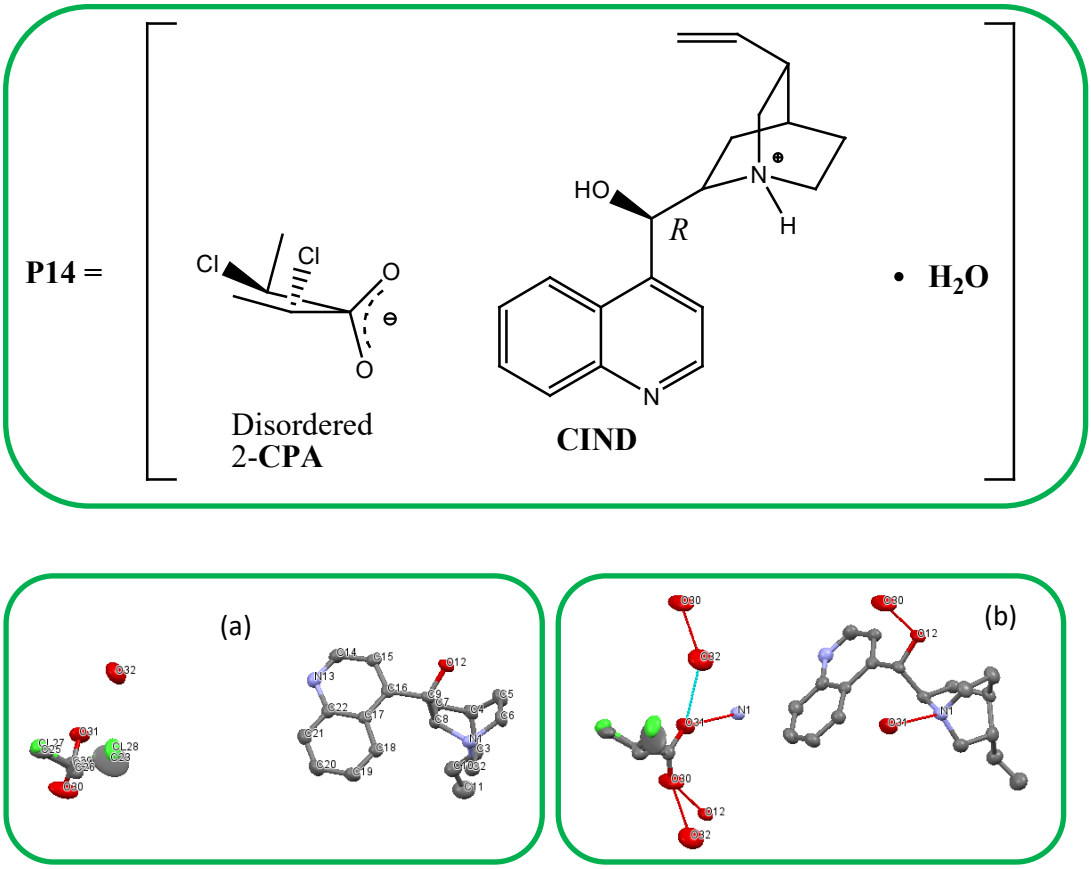


Figure 7.40 Representation of the X-ray crystal structure of **P14**, showing (a) the atom labelling and (b) the hydrogen bonding. Hydrogen atoms have been omitted for clarity.

The X-ray crystallographic results revealed that the molecular packing of **P14** is stabilized by the N—H···O and O—H···O interactions.

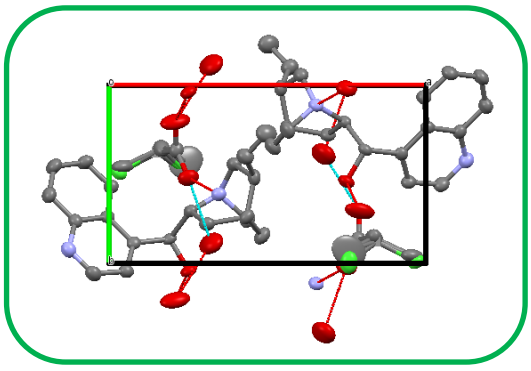

Figure 7.41 Molecular packing diagram of **P14**, a view down crystallographic *c* axis. Hydrogen atoms have been omitted for clarity.

**P11** – **P14** feature C—H···Cl contacts, which are weak hydrogen bonds.[25,26] The C—H···Cl interactions have been studied *via* the retrieval of crystallographic data from the Cambridge Structural Database of several organic crystal structures. The interactions have also been observed in coordination complexes and in organic supramolecular assemblies.[57,58] The typical

range for the H···Cl distance is between 2.5 and 3.1 Å, and the overall C—H···Cl angle is between 118 -178º, with the preferred angle close to 180º. For the salts, **P11** – **P13**, the angles are within the expected range, with the H···Cl distances slightly longer than the maximum, except for **P12**, Table 7.32.

Table 7.32 Short C—H···Cl contacts of salts **P11** – **P14.**

| Product | Contact | Distance | Angle |
|---|---|---|---|
| Salt | C—H···Cl | H···Cl/Å | C—H···Cl/° |
| **P11** | C24—H24C···Cl30 | 3.229 | 141.88 |
| **P12** | C21—H21A···Cl28 | 2.806 | 150.94 |
| | C21—H21A···Cl34 | 3.202 | 160.82 |
| **P13** | C7—H7A···Cl26 | 3.160 | 140.36 |

The flexibility or rotation of the *Cinchona* alkaloids, involving the quinoline ring (τ1), the quinuclidine ring (τ2) and the ethenyl group (τ3) were determined by measuring the torsion angles for **P13** and **P14**, Table 7.33. τ1 and τ2 for the two salts show a difference in the signs of the angles (rotation angle similar), whilst τ3 is different for the two salts. The *Cinchona* alkaloids in the two salts show a synperiplanar conformation with similar τ1in the range, -30 and 30º. τ2 indicates that both alkaloids have a synclinal conformation with τ2 falling between, -90 and -30º, and between, 30 and 90º. The *Cinchona* alkaloids differ in the rotation of the ethenyl group resulting in two different conformations. The conformation of **CINC** in **P13** is synclinal, (τ3 between 30 and 90º) and that of **CIND** in **P14** is anticlinal (τ3 between 90 and 150º). The differences in the two salts' (**CINC** and **CIND)** conformations might have been caused by the different hydrogen bond patterns involving the chlorine atom, plus the hydrogen bonds due to the water molecules. The differences resulted in the different partial isolations of 2-**CPA**.

Table 7.33 The torsion angles for the **CINC** and **CIND** in **P13** and **P14**.

| Torsion angles (º) | **P13** | **P14** |
|---|---|---|
| **τ1** | -13.75 | 15.28 |
| **τ2** | -77.89 | 81.73 |
| **τ3** | 85.89 | 131.25 |

CrystalExplorer analysis

The 2D fingerprint plots have been deconstructed to highlight specific atom pair contacts, shown on the following Figure 7.42. The deconstruction enables the separation of the contributions from different contact types that overlap in the full fingerprint plot, Figure 7.43, and the overall percentages from each interaction per compound are listed in Table 7.34.

Table 7.34 The summary of the various contributions in **P11** – **P14**.

| **Interactions** | **P11** | **P12** | **P13** | **P14** |
|---|---|---|---|---|
| Cl···H | 24.6 | 21.2 | 22.6 | 20.6 |
| O···H | 33.0 | 27.1 | 33.0 | 34.0 |
| H···H | 35.9 | 40.0 | 34.8 | 31.9 |
| C···H | 3.6 | 5.7 | 4.7 | 9.7 |
| N···H | 0.0 | 0.0 | 1.6 | 0.0 |
| Total | 97.1 | 94.0 | 96.7 | 96.2 |

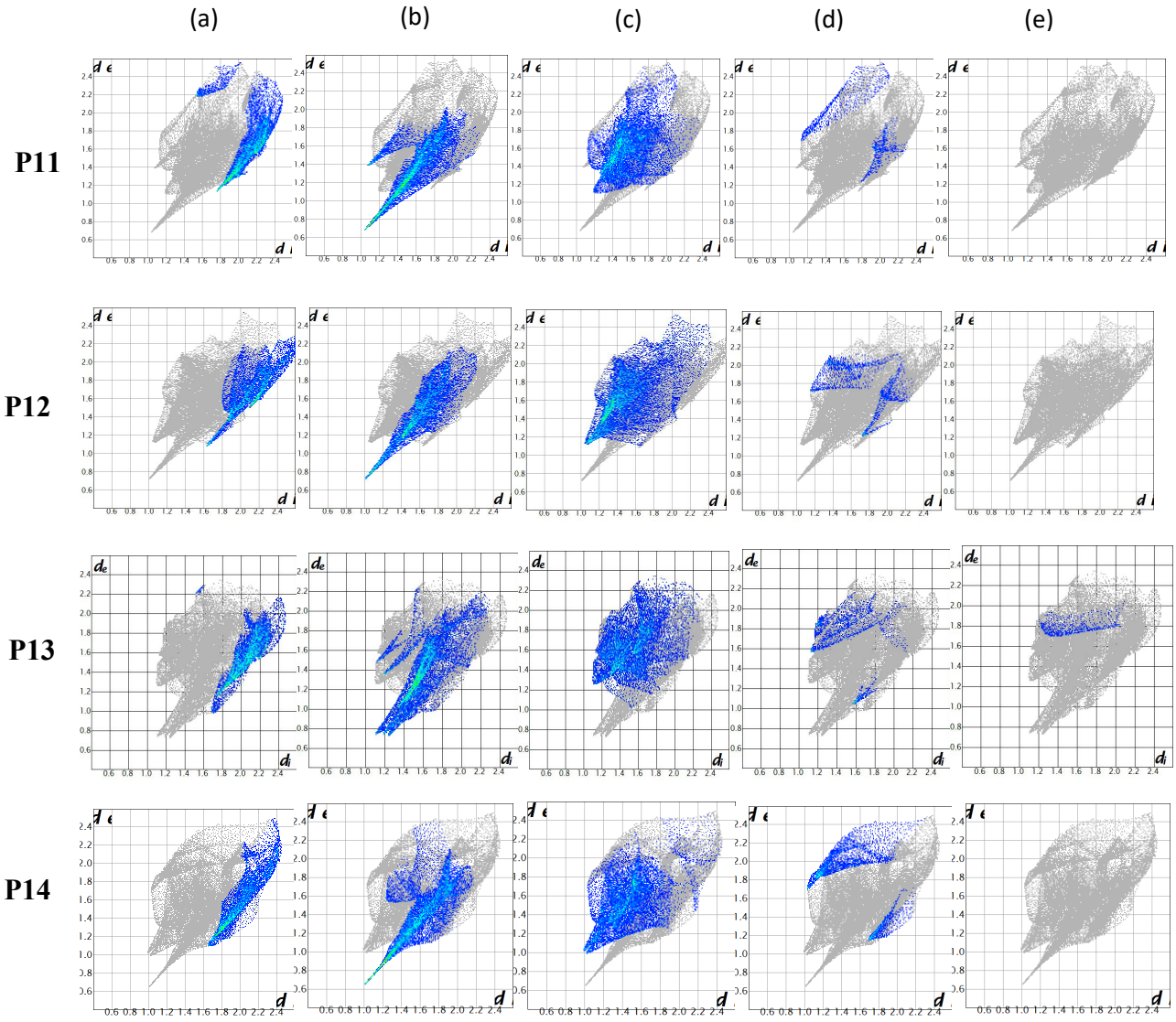


Figure 7.42 2D fingerprint plots of **P11, P12, P13** and **P14,** are shown in columns (a) to (e) showing Cl···H, O···H, H···H, C···H and N···H contacts respectively, showing the percentages of contacts contributing to the total Hirshfeld surface area.

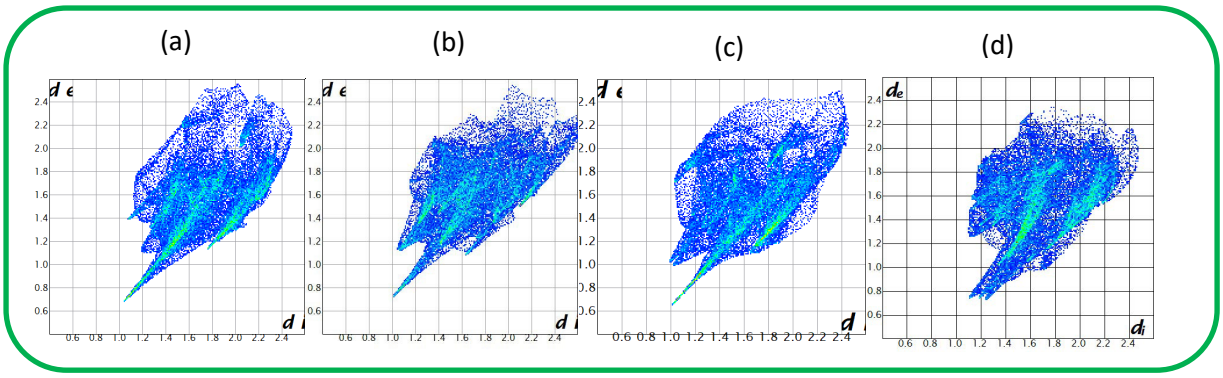


Figure 7.43 2D full fingerprint plots of (a) **P11** (b) **P12** (c) **P13** and (d) **P14**.

In **P11** the Hirshfeld surface analysis and the fingerprint plots revealed the intermolecular close contacts consisting of the Cl···H intermolecular contact, which appears at the top left and bottom right of the fingerprint plot column (a), Figure 7.42. The percentage contribution of the interaction is 24.6%. The O···H contact appears as two sharp short and longer spikes, column (b). The contribution of these contacts is 33.0%. The H···H contacts have the major contribution to the total Hirshfeld surface area, column (c), represented by the blue area at the centre of the fingerprint plot contributing 35.9% to the total Hirshfeld surface. The smallest contribution is due to the C···H contact, represented by the tiny patches at the top left and bottom right of the fingerprint plot, column (d), and the percentage contribution is 3.6%. For **P11** no contribution was observed from the N···H interaction, column (d). The contacts account for 97.1% of the total Hirshfeld surface area, as shown in Figure 7.43 showing the full fingerprint plot of **P11**.

The crystal is dominated by the Cl···H, O···H, and H···H contacts with a smaller contribution due to C···H intermolecular close contacts, which contributed to the stabilization of the crystal. The contribution from the O···H and the H···H close contacts is nearly similar with an average contribution of 35.5%, and the C···H contact contributed 3.6%.

The CrystalExplorer analysis of **P12** – **P14** were done without the contribution of the minor methyl and chlorine substituents on the disordered acid molecules.

The Hirshfeld surface analysis of **P12**, showed N···H, C···H, Cl···H, O···H, and H···H contacts of 0.00, 5.7, 21.2, 27.1, and 40.0% respectively. These are represented by the blue areas on the fingerprint plots at the right, centre and top regions of the plots. The largest region in the fingerprint plot represents the H···H contacts, which is the most significant contribution to the total Hirshfeld surface. The O···H contacts are represented by a portion at the centre extending to the bottom right spike on the fingerprint plots contributing 27.1 % to the total surface. The results show that the main intermolecular contacts are those of the H···H pair, 40.0%. The C···H contacts are shown by the smallest coloured area at the top and bottom right areas of the plot, followed by the Cl···H contacts with a larger contribution than the C···H contact. The overall total surface contribution is 94.0%, shown in Figure 7.43(b) and Table 7.33. In this structure the 2-chloropropanoate anions are disordered with site occupancies of 45:55 (*S*:*R*).

The fingerprint plots of **P13** show the intermolecular contacts consisting of the C···H and N···H pairs with small contributions of 4.7 and 1.6% respectively. These appear at the top left areas, of the fingerprint plot. The Cl···H, O···H and H···H pairs contributed in an increasing order, 22.6%, 33.0% and 34.8% respectively, as shown by the blue colouration under columns (a), (b)

and (c) in Figure 7.42. The overall contribution is 96.7%, Figure 7.43(c) and Table 7.33. The site occupancies of the disordered 2-chloropropanoate anions are 80:20 (*S*:*R*).

**P14** fingerprint plots show a reasonable contribution of the C···H pair of 9.7%, represented by the top and bottom right blue areas on the fingerprint plot. The other pairs have significant contributions, Cl···H (20.6%), O···H (34.0%) and H···H (31.9%). The Cl···H pair is represented by the right periphery of the fingerprint plot (column (a)). The O···H pair is represented by the right spike (column (b)), and the last contribution due to the H···H pair being represented by the region at the centre extending to the centre spike on the fingerprint plot (column (b)). The overall contribution is 96.2% to the total Hirshfeld surface. The 2-chloropronanoate anions are disordered with site occupancies of 60:40 (*S*:*R*).

The 2D full fingerprint plots representing the overlaps due to the individual interaction pairs are shown in Figure 7.43 and Table 7.33 for the four salts, **P11** – **P14**.

## FT-IR analysis

The FT-IR spectra per pair of **QUIN** and **QUID**, **CINC** and **CIND**, **P11** and **P12,** and **P13** and **P14** have the same features, relatively same peak intensities, with the peaks slightly different in the frequency values, Figure 7.44. The FT-IR results are summarized in Table 7.35. Each pair is represented by a spectrum of one of the compounds. The resolving agents show an OH peak at 3166 and 3070 $cm^{-1}$, Figure 7.44 (a) and (b), and the racemate shows the COOH peak at 3070 $cm^{-1}$, Figure 7.44(c). In the FT-IR spectra the COOH group of 2-**CPA** has disappeared in the salts within the range 3400 – 2500 $cm^{-1}$, indicating the absence of the COOH group in the products, Figure 7.44 (d) and (e). This is further revealed by the absence of the carbonyl peak, the disappearance of the carbonyl peak of 2-**CPA** at 1722 $cm^{-1}$. In the salts' spectra, the appearance of the carboxylate peaks confirms the loss of a proton from the COOH groups. The carboxylate peaks are at 1620 and 1386 $cm^{-1}$ (1596 and 1393 $cm^{-1}$). The amine salt peaks expected at the following ranges, 2500 – 1800 $cm^{-1}$ and 1670 -1610 $cm^{-1}$ are not convincingly shown in the spectra.

With **P11** and **P12** the peak expected in the range 1670 -1610 $cm^{-1}$ seems to be overshadowed by the carboxylate peak at 1620 $cm^{-1}$, but a slight protrusion appears at 1644 $cm^{-1}$. In **P13** and **P14** there is a small peak at 1644 $cm^{-1}$ which represents the expected amine salt peak. These results support the X-ray diffraction results in confirming the deprotonation of the carboxylic acid group of 2-chloropropanoic acid and the acceptance of the proton by the resolving agents. The discussed frequencies are illustrated in Figure 7.44 and also listed in Table 7.34 against the literature frequencies.

The hydroxyl group of the resolving agents is involved in hydrogen bonding and this is confirmed by the decrease in the frequency of the OH peak in the salts' spectra. In the spectra of the resolving agents the OH peak is noticeable at 3166 and 3070 $cm^{-1}$ for **QUIN** (**QUID**) and **CINC** (**CIND**) respectively, and for the salts the peaks are at lower frequencies, 3069 $cm^{-1}$ indicating the involvement of the OH group in hydrogen bonding.

Table 7.35 The characteristics of selected FT-IR absorptions of the salts.

| Functional groups | **P11** - **P14** absorptions $cm^{-1}$ | Expected absorptions ($cm^{-1}$) |
|---|---|---|
| O—H···O | 3069 (3069) | 3400 – 3200 |
| COOH | No peak | 3400 – 2500 |
| C=O | No peak | 1780 – 1670 |
| $N^{+}$—H | No peak<br>1644 (1644) | 2500 – 1800<br>1670 – 1610 |
| $COO^{-}$ | 1620 (1596)<br>1386 (1393) | 1610 – 1550<br>1420 – 1300 |
| C—O | 1241 (1238) | 1200 – 1050 |

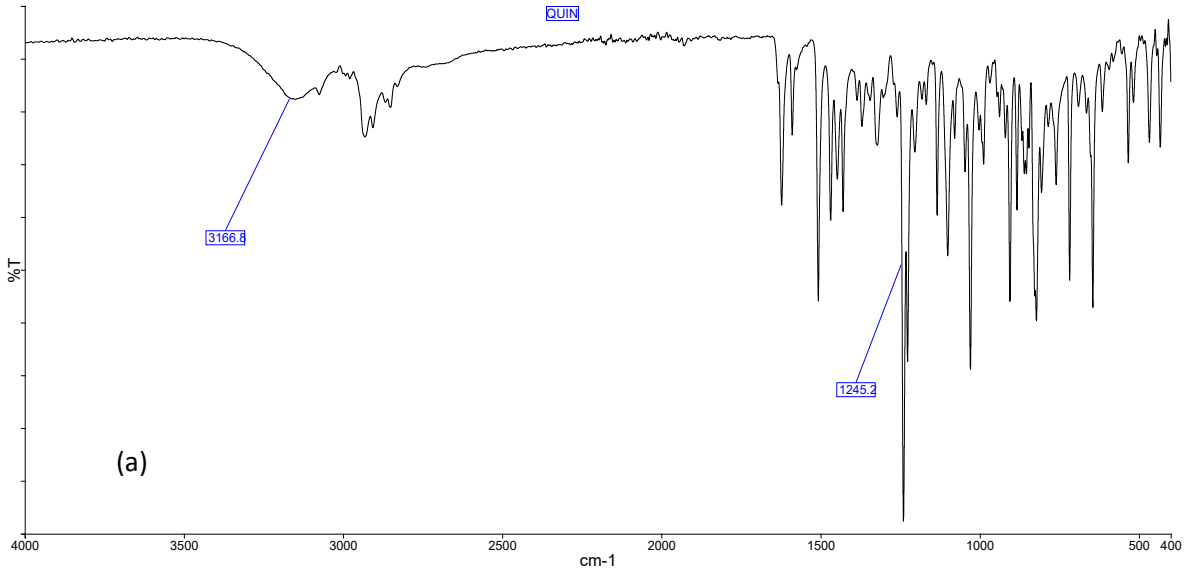
QUIN
3166.8
1245.2
%T
(a)
4000
3500
3000
2500
2000
1500
1000
500
400
cm-1

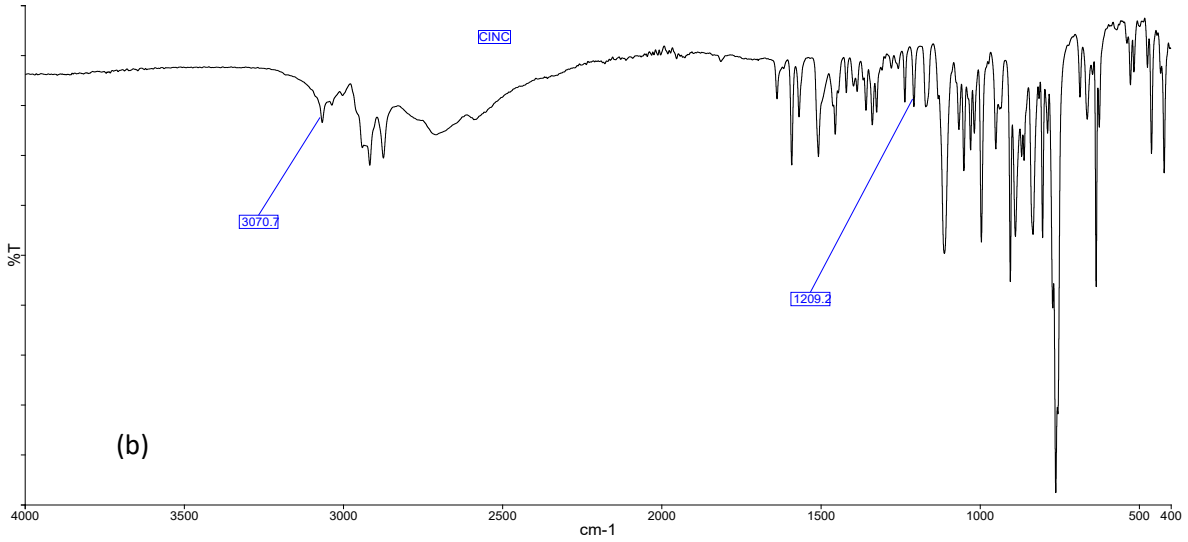
CINC
3070.7
1209.2
%T
(b)
4000
3500
3000
2500
2000
1500
1000
500
400
cm-1

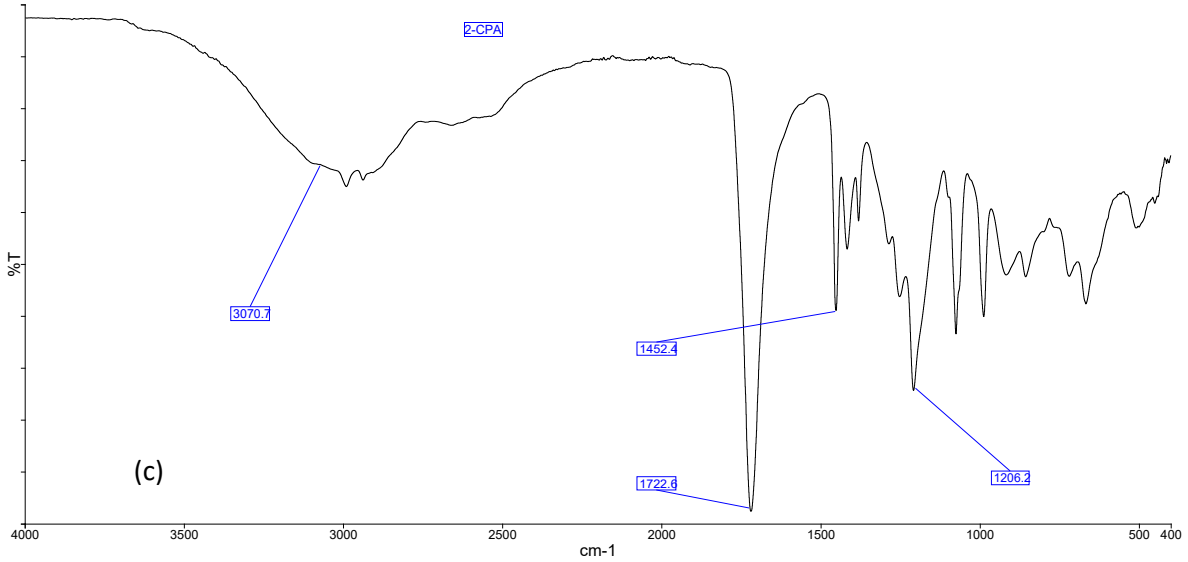
2-CPA
3070.7
1452.4
1722.6
1206.2
%T
(c)
4000
3500
3000
2500
2000
1500
1000
500
400
cm-1

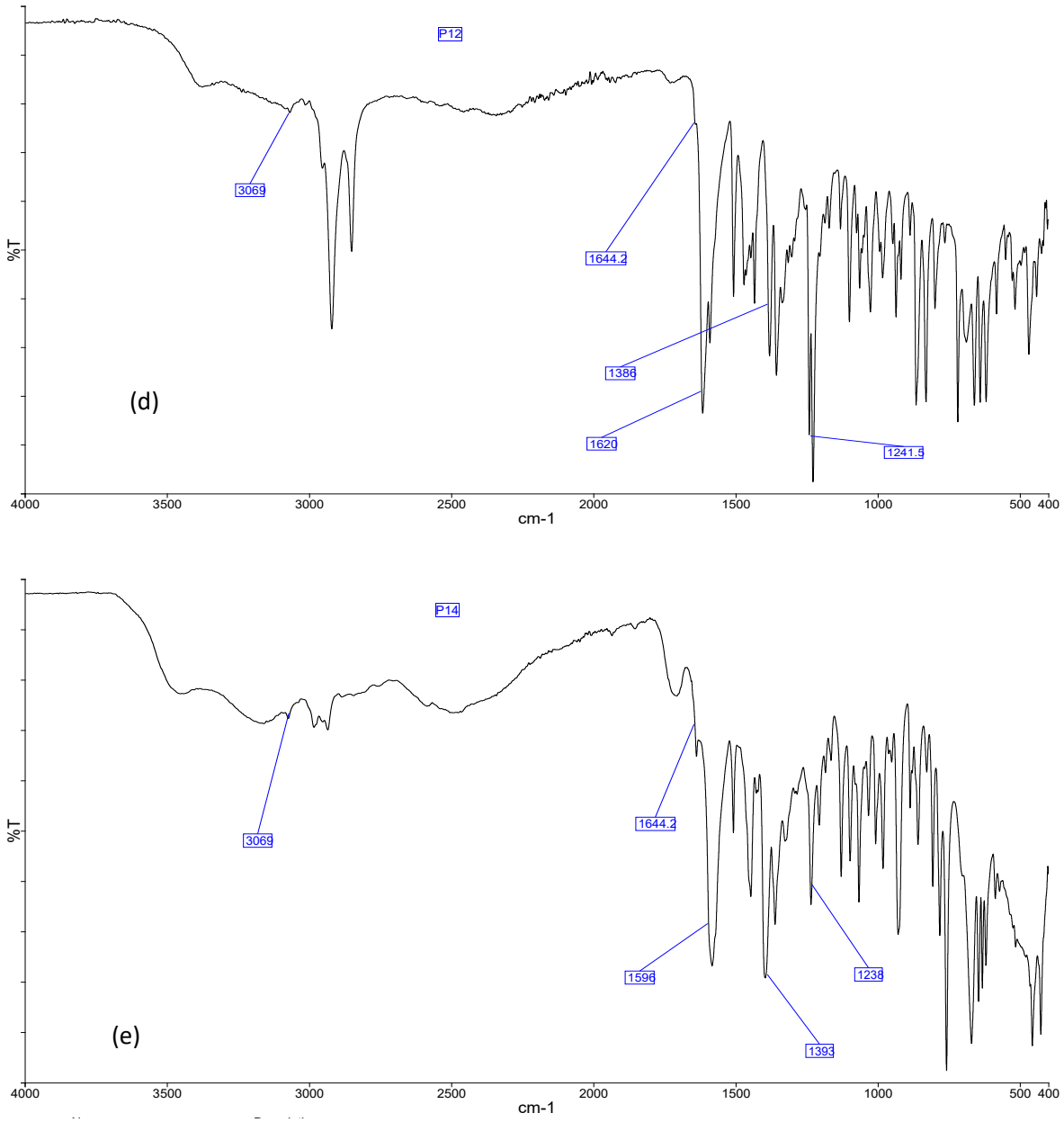


Figure 7.44 The FT-IR results of the resolving agents, (a) **QUIN** and **QUID,** (b) **CINC** and **CIND,** (c) racemic 2-chloropropanoic acid, and the salts, (d) **P11** and **P12** and (e) **P13** and **P14**.

The results confirm that the products are salts.

The p$K_a$ value of 2-chloropropanoic acid is 3.42,[1] and the difference in the p$K_a$ between the bases and the acid is > 3, which predicts salt formation.[2]

Conclusion

**QUIN** was the only resolving agent which gave complete resolution of the acid *via* the salt, **P11.** The other *Cinchona* alkaloids formed mixtures of the *R* and *S* enantiomers of the acid in various proportions. The DSC and TGA measurements revealed the formation of hydrates. Furthermore, FT-IR spectroscopy showed the formation of salts based on the presence of the carboxylate peaks. This was confirmed by the single crystal X-ray diffraction results which also showed that the products are salts.

**QUIN** successfully isolated the *S*-**3.5** enantiomer and formed the hydrated salt **P11**. All the salt hydrates demonstrated N—H···O and O—H···O hydrogen bonds. CrystalExplorer further revealed that the salt hydrates are dominated by Cl···H, O···H, H···H interactions with smaller contributions due to C···H.

In **P12 - P14** the resolving agents gave mixtures of 2-**CPA**. In **P13** there is another kind of hydrogen bond that is absent in the other salts, the O—H···N interaction, involving the quinoline ring of **CINC**. In all the salts the chlorine participated in hydrogen bonding, in the formation of weak C—H···Cl hydrogen bonds.

The findings also show the differences in the resolution abilities of these resolving agents on the 2-chloropropanoic acid in water and one in toluene. **QUIN** in water gave 100 % of (*S*)-2-**CPA** compared to **QUID** in toluene/water which gave 40% (*S*)-2-**CPA**. It is difficult to compare these results due to the different solvents used which could have influenced the outcome, (Table 7.36).

Table 7.36 The resolution results of the four *Cinchona* alkaloids in the resolution of 2-chloropropanoic acid.

| Salt | RA | Enantiomer | % |
|---|---|---|---|
| **P11** | **QUIN** | *S*-2-**CPA** | 100 |
| **P13** | **CINC** | *S*-2-**CPA** | 80 |
| **P14** | **CIND** | *S*-2-**CPA** | 60 |
| **P12** | **QUID** | *S*-2-**CPA** | 40 |

The Dutch Resolution method was employed by treating the mixture of **QUIN** and **QUID** with 2-**CPA**/water using the solvent, water. The resultant precipitate was **P11** which confirms that it is the least soluble salt. Other experiments (with 2-**CPA**/water and 2-**CPA**/MeOH) in several solvents with two or three resolving agents, in different combinations, did not give rise to crystals for further analysis.

## 7.8 References


1. Calculator Plugins were used for structure property prediction and calculation, MarvinSketch, Version 20.9, ChemAxon (http://www.chemaxon.com).
2. Cruz-Cabeza AJ. Acid-base crystalline complexes and the p$K_a$ rule. *CrystEngComm,* **2012**, 14, 6362-6365.
3. Etter MC, MacDonald JC and Bernstein J. Graph-set analysis of hydrogen-bond patterns in organic crystals. *Acta Cryst. B*, **1990**, 46, 256-262.
4. Bàthori NB, Jacobs A, Nassimbeni LR and Sebogisi BK. Quininium malates: Partial chiral discrimination *via* diastereomeric salt formation. *S. Afr. J. Chem*., **2014**, 67, 160-166.
5. Bàthori NB, Nassimbeni LR and Oliver CL. Quininium mandelates- a systematic study of chiral discrimination in crystals of diastereomeric salts. *Chem. Commun*., **2011**, 47, 2670-2672.
6. Jaques J, Collet A and Wilen SH. *Enantiomers, Racemates and Resolution*, Krieger Publishing Company, Malabar, Florida, **1991**.
7. Wang Y, Sun J and Ding K. Practical method and novel mechanism for optical resolution of BINOL by molecular complexation with *N*-benzylcinchoninium chloride. *Tetrahedron,* **2000**, 56, 4447-4451.
8. Toda F, Tanaka K, Stein Z and Goldberg J. Optical resolution of binaphthyl and biphenanthryl diols by inclusion crystallisation with *N*-alkylcinchonidium halides. Structural characterization of the resolved materials. *J. Org. Chem.,* **1994**, 59, 5748-5751.
9. Gjerløv A and Larsen S. A study of diastereomeric mandelate salts of cinchonidine and the relation to their quasidiasteremeric analogues. *Acta Cryst.,* **1997**, B53, 708-718.
10. Larsen S, De Diego HL and Kozma D. Optical resolution through diastereomeric salt formation: The crystal structures of cinchoninium (*R*)-mandelate and cinchoninium (*S*)-mandelate at low temperature. *Acta Cryst*., **1993**, B49, 310-316.
11. CrystalExplorer (Version 3.1), Wolf SK, Grimwood DJ, McKinnon JJ, Turner MJ, Jayatilaka D andSpackman MA. University of Western Australia, **2012**.
12. Spackman MA and McKinnon JJ. Fingerprinting intermolecular interactions in molecular crystals. *CrystEngComm.,* **2002**, 4, 378-392.
13. McKinnon JJ, Jayatilaka D and Spackman MA. Towards quantitative analysis of intermolecular interactions with Hirshfeld surfaces. *Chem. Commun.,* **2007**, 37, 3814-3816.

14. Spackman MA and Jayatilaka D. Hirshfeld surface analysis. *CrystEngComm*., **2009**, 11, 19-32.
15. (a) Dunitz JD and Bernstein J. Disappearing polymorphs. *Acc. Chem. Res*., **1995**, 28, 193-200. (b) Bučar D-K, Lancaster RW and Bernstein J. Disappearing polymorphs revisited. *Angew. Chem. Int. Ed*., **2015**, 54, 6972-6993.
16. (a) Mura P, Faucci MT, Manderioli A, Bramanti G and Ceccarelli L., Compatibility study between ibuproxam and pharmaceutical excipients using differential scanning calorimetry, hot-stage microscopy and scanning electron microscopy, *Pharm. Biomed. Anal*., **1998**, 18, 151-163. (b) Vitez IM, Newman AW, Davidovich M and Kiesnowski C. The evolution of hot-stage microscopy to aid solid-state characterisations of pharmaceutical solids, *Thermocimica Acta*, **1998**, 324, 187-196. (c) Panna W, Wyszomirski P and Kohut P. Application of hot-stage microscopy to evaluating sample morphology changes on heating, *Therm. Anal. Calorim*., **2016**, 125, 1053-1059. (d) Bouanga Boudiombo JS and Jacobs A. Salts of mefenamic acid with amines: Structure, thermal stability, desolvation and solubility, *J. Pharm. Sci*., **2018**, 107, 3014-3021.
17. Atwood JL, Barbour LJ and Jerga A. Storage of methane and Freon by interstitial van der Waals confinement. *Science*, **2002**, 296, 2367-2369.
18. Nassimbeni LR. Physicochemical aspects of host-guest compounds. *Acc. Chem. Res*., **2003**, 36, 631-637.
19. Bernstein J, Davies RE, Shimoni L and Chang N-L. Patterns in hydrogen bonding: Functionality and graph set analysis in crystals. *Angew. Chem. Int. Ed. Engl.,* **1995**; 34, 1555-1573.
20. MacDonald JC, Dorrestein PC and Pilley MM. Design of supramolecular layers *via* self-assembly of imidazole and carboxylic acids. *Cryst. Growth Des*., **2001**, 1, 29-38.
21. McKinnon JJ, Spackman MA and Mitchell AS. Novel tools for visualizing and exploring intermolecular interactions in molecular crystals. *Acta Cryst.,* **2004**, B60, 627-668.
22. Desiraju GR. The C—H···O hydrogen bond: Structural implications and supramolecular design. *Acc. Chem. Res.,* **1996**, 29, 441-449.
23. Berkovitch-Yellin Z and Leiserowitz L. The role played by the C—H···O and the C—H···N interactions in determining molecular packing and conformation. *Acta Cryst.,* **1984**, B40, 159-165.
24. Grootenhuis PDJ, van Eerden J, Dijkstra PJ, Harkema S and Reinhoudt DN. Complexation of neutral molecules by preorganized macrocyclic hosts. *J. Am. Chem. Soc.,* **1987**, 109, 8044-8051.

25. Taylor R and Kennard O. Crystallographic evidence for the existence of C—H···O, C—H···N and C—H···Cl hydrogen bonds. *J. Am. Chem. Soc*., **1982**, 104, 5063-5070.
26. Desiraju GA. The C—H···O hydrogen bond in crystals: What is it? *Acc. Chem. Res*., **1991**, 24, 290-296.
27. Desiraju GR, Kashino S, Coombs SS and Glusker JP. C—H···O packing motifs in some cyclopenta[*a*]phenanthrenes. *Acta Cryst*., **1993**, B49, 880-892.
28. Desiraju GR. *Crystal Engineering. The design of organic solids*. Elsevier: Amsterdam, **1989**, 142-164.
29. Desiraju GR, Vittal JJ and Ramanan A. *Crystal Engineering: A textbook*. Singapore: World Scientific Publishing, **2011**, p94.
30. Williams DH and Fleming I. Spectroscopic Methods in Organic Chemistry, 5th Edition, McGraw Hill, London, **1995**, 28-62.
31. MacDonald JC, Dorrestein PC and Pilley MM. Design of supramolecular layers *via* self-assembly of imidazole and carboxylic acids. *Cryst. Growth Des*., **2001**, 1, 29-38.
32. (a) Pavia DL, Lampman GM, Kriz GS and Vyvyan JR. Introduction to spectroscopy, 4th Edition, Brooks/Cole, **2009**, 15-81. (b) Basavoju S, Boström D and Velaga P. Indomethacin-saccharin cocrystal: Design, synthesis and preliminary pharmaceutical chaeacterization. *Pharm. Res*., **2008**, 25, 530-541.
33. Kozma D, Novák Cs, Tomor K, Pokol G and Fogassy E. Mechanism of optical resolution *via* diastereomeric salt formation. *J. Therm. Anal. Calorim.,* **2000**, 61, 45-50.
34. Morimoto M, Yamakawa A, Katagiri H and Sakai K. Resolution of racemic 1-benzyl-5-oxo-3-pyrrolidinecarboxylic acid with enantiopure (*S*)-phenylalanine *N*-benzylamide *via* diastereomeric salt formation. *Tetrahedron: Asymmetry,* **2007**, 2869-2875.
35. Białońska A and Ciunik Z. When in the presence of the strong hydrogen bonds, the weak hydrogen bonds gain an importance. *CrystEngComm,* **2006**, 8, 66-74.
36. Sakai K, Sakurai N and Nohira H. New resolution technologies controlled by chiral discrimination mechanisms. *Novel optical resolution technologies*, Vol. 269, Topics in Current Chemistry Series **2007**, 199-231.
37. Kozma D, Ács M and Fogassy E. Predictions of which diastereomeric salt precipitates during an optical resolution *via* diastereomeric salt formation. *Tetrahedron,* **1994**, 6907-6912.
38. He Q, Rohani S, Zhu J and Gomaa H. Resolution of Sertraline with (*R*)-mandelic acid: Chiral discrimination mechanism study. *Chirality,* **2012**, 24, 119-128.

39. Langkilde A, Oddershede J and Larsen S. Diastereomeric salts of lactic acid and 1-phenyl-ethylamine, their structures and relative stabilities. *Acta Cryst.,* **2002**, B58, 1044-1050.

40. (a) Białońska A and Ciunik Z. Racemic resolution of *N*-protected alanine by strychnine and brucine *versus* donor/acceptor capability. *CrystEngComm,* **2004**, 6, 276-279. (b) Zhang B-l, He W, Shi X, Huan M-l, Huang Q-j and Zhou S-y. Synthesis and biological activity of the calcium modulator (*R*) and (*S*)-3-methyl 5-pentyl 2,6-dimethyl-4-(3-nitrophenyl)-1,4-dihydropyridine-3,5-dicarboxylate. *Bioorg. Med. Chem. Lett.*, **2010**, 20, 805-808.

41. Gould RO and Walkinshaw MD. Molecular recognition in model crystal complexes: The resolution of D and L amino acids. *J. Am. Chem. Soc*., **1984**, 106, 7840-7842.

42. (a) Wilen SH, Collet A and Jacques J. Strategies in optical resolution. *Tetrahedron*, **1977**, 33, 2725-2736. (b) Kozma D, Nyéki Á, Ács M and Fogassy E. Optical resolution of mandelic acid by Cinchonine in different solvents. *Tetrahedron: Asymmetry,* **1994,** 5**,** 315-316.

43. Sakai K, Sakurai R, Yuzawa A and Hiramaya N. Practical continuous resolution of α-amino-ε-caprolactam by diastereomeric salt formation using a single resolving agent with a solvent switch method. *Tetrahedron: Asymmetry*, **2003**, 3713-3718.

44. Sakai K, Sakurai R and Hiramaya N. Chiral discrimination controlled by the solvent dielectric constant. *Tetrahedron: Asymmetry*, **2004**, 1073-1076.

45. Sakai K, Sakurai R, Akimoto T and Hirayama N. Molecular mechanism of dielectrically controlled optical resolution (DCR). *Org. Biomol. Chem.*, **2005**, 360-365.

46. Sakai K, Sakurai R and Hiramaya N. Molecular mechanism of DCR phenomenon observed in (*RS*)-1-cyclohexylethylamine-mandelic acid resolution system. *Tetrahedron: Asymmetry*, **2006**, 1812-1816.

47. Moshen-Nia M, Amiri H and Jazi B. Dielectric constants of water, methanol, ethanol, butanol and acetone: Measurement and computational study. *J. Solution Chem*., **2010**, 39, 701-708.

48. Coetzee JF and Padmanabhan. Dissociation and homoconjugation of certain phenols in acetonitrile. *J. Phys. Chem*., **1965**, 69, 3193-3196.

49. Hughes DL. Resolution of 1,1'-binaphthol, (*R*)-(+)- and (*S*)-(-)-2,2'-*bis*(diphenylphosphini)-1,1'-binaphthyl (BINAP). *Org. Synth*., **2014**, 91, 1-11.

50. Jacques J, Fouquey C and Viterbo R. Enantiomeric cyclic binaphthyl phosphoric acids as resolving agents. *Tetrahedron Letters*, **1971**, 12, 4617-4620.

51. Lee T and Wang PY. Screening, manufacturing, photoluminescence, and molecular recognition of co-crystals: Cytosine with dicarboxylic acids. *Cryst. Growth Des*., **2010**, 10, 1419-1434.
52. Nikoletta Báthori, Ayesha Jacobs, Mawonga Mei and Luigi R. Nassimbeni. Resolution of malic acid by (+)-cinchonine and (-)-cinchonidine. *Canadian J. Chem*., **2015**, 93, 858-863.
53. Kozma D, Pokol G and Ács M. Calculation of the efficiency of optical resolutions on the basis of the binary phase diagram for the diastereomeric salts. *J. Chem. Soc., Perkin Trans 2*, **1992**, 435-439.
54. To be submitted for publication, 2021.
55. Bezman RD, Casassa EF and Kay RL. The temperature dependence of the dielectric constants of alkanols. *J. Mol. Liquids*, **1997**, 73, 397-402.
56. Aakeröy CB, Evans TA, Seddon KR and Pálinkó I. The C—H···Cl hydrogen bond: Does it exist? *New J. Chem*., **1999**, 145-152.
57. Balamurugan V, Hundal MS and Mukherjee R. First systematic investigation of C—H···Cl hydrogen bonding using inorganic supramolecular synthons: Lamellar, stitched stair-case, linked-ladder, and helical structures. *Chem. Eur. J*., **2004**, 10, 1683-1690.
58. Hartwar VR, Roopan SM, Subashini R, Khan FN and Row TNG. Analysis of Cl···Cl and C—H···Cl intermolecular interactions involving chlorine in substituted 2-chloroquinoline derivatives. *J. Chem. Sci*., **2010**, 122, 677-685.

# Chapter 8

## Conclusion

The research was intended to investigate the mechanism involved in the resolution of racemic acids, using the *Cinchona* alkaloids as resolving agents with various racemic acids. This process is based on the phenomenon of molecular recognition, which, in this case is analyzed by a number of analytical techniques. In particular, refined crystal structures yield the strength and directions of non-bonded interactions which occur between a resolving agent and the resulting product. The analysis of the close contacts was achieved by the program Crystal Explorer, and the thermal stability of the crystalline products were further analyzed by differential scanning calorimetry, thermal gravimetry and infra-red spectroscopy.

The five racemates, **3.1** – **3.5**, were successfully resolved using the four resolving agents, **CINC**, **CIND**, **QUIN** and **QUID**, in different solvents, acetone, methanol, pentanol, acetonitrile mixed with water, water and toluene (Table 8.1). The resolutions obtained are, **3.1** and **3.5** resolved by one resolving agent, **3.2** and **3.4** by two, **3.3** by four and one of those resolving agents resolved **3.3** in a different solvent. **3.5** was also partially resolved by the other resolving agents in different proportions. The results confirmed that the change of solvent yields opposing results, and strong hydrogen bonds stabilized the salts.

The mixtures of the resolving agents (1:1 and 1:1:1) were also employed to resolve the racemates, in different solvents, a method called the Dutch Resolution Method, and the results were not suitable for further analysis.

In order to resolve the racemates, the resolving agents, racemates and solvents were brought to a solution under heat, on evaporation of the solvent, crystals formed, and were analyzed using DSC, TGA, single crystal X-ray diffraction and FT-IR spectroscopy. The results obtained from these techniques complimented each other to confirm the products as salts, **P1** – **P14**. Only two products of the salts were impossible to reproduce, **P5** and **P10**, on reproducing them they resulted into powders, giving rise to **P5a** and **P10a** products.

The ability of a resolving agent to resolve a racemate, in a suitable solvent, is different in all the different racemates. With **3.1** only one resolving agent gave a positive result yet all of the *Cinchona* alkaloids were able to resolve **3.3** though in different solvents. Incorporation of the solvent did not occur in only two salts, **P5** and **P10**. In the majority of the salts water was incorporated, followed by MeOH. This then shows the propensity of polar solvents in stabilizing crystal structures.

Table 8.1 Overall summary of all the salts with the incorporated solvents and the isolated enantiomers from the racemates.

| Salt | RA | Racemate | Solvent incorporated | Isolated enantiomer |
|---|---|---|---|---|
| **P1** | **CIND** | **3.1** | $H_2O$ | (*S*)-**3.1** |
| **P2** | **CINC** | **3.2** | $H_2O$ | (*D*)-**3.2** |
| **P3** | **CIND** | **3.2** | $H_2O$ | (*D*)-**3.2** |
| **P4** | **CINC** | **3.3** | Acetone | (*R,R*)-**3.3** |
| **P5** | **CIND** | **3.3** | - | (*R,R*)-**3.3** |
| **P6** | **QUID** | **3.3** | MeOH | (*S,S*)-**3.3** |
| **P7** | **QUIN** | **3.3** | MeOH | (*R,R*)-**3.3** |
| **P8** | **CINC** | **3.3** | $H_2O$ | (*S,S*)-**3.3** |
| **P9** | **QUIN** | **3.4** | MeOH | (*R*)-**3.4** |
| **P10** | **QUID** | **3.4** | - | (*R*)-**3.4** |
| **P11** | **QUIN** | **3.5** | $H_2O$ | (*S*)-**3.5** |
| **P12** | **QUID** | **3.5** | $H_2O$ | (0.45*S*)-**3.5** |
| **P13** | **CINC** | **3.5** | $H_2O$ | (0.8*S*)-**3.5** |
| **P14** | **CIND** | **3.5** | $H_2O$ | (0.6*S*)-**3.5** |
| Resolving agents (RA), **CINC**-Cinchonine, **CIND**-Cinchonidine, **QUIN**-Quinine and **QUID**-Quinidine<br>Racemates, **3.1** Citronellic acid, **3.2** Malic acid, **3.3** *Trans*-9,10-dihydro-9,10-ethanoanthracene-11,12-dicarboxylic acid, **3.4** 9,10-Dihydro-9,10-ethanoanthracene-11-carboxylic acid **3.5** 2-Chloropropanoic acid. | | | | |

**P5a** and **P10a** powders were only analyzed using DSC, TGA and FT-IR spectroscopy.

In **P2** and **P3**, **P4** and **P5** the pair **CINC**/**CIND** isolated the same enantiomer in accord with the findings obtained by Wang et al. and Toda et al.[1,2,3] In most applications the "pseudoenantiomeric" pairs of **CINC**/**CIND** and **QUIN**/**QUID** gave rise to products of opposite enantiomers due to their different stereochemistries at C8 and C9.[4,5] For **P6** and **P7**, the pair **QUIN**/**QUID** isolated different enantiomers in line with Gjerløv et al. and Larsen et al.'s findings,[6,7] yet in **P9** and **P10** the pair **QUIN**/**QUID** isolated the same enantiomer.

In **P4** and **P8**, **CINC** isolated different enantiomers and the solvents used are different, and this is supportive of Kozma et al.'s findings.[8] The results also indicate the importance of solvents in relation to the type of enantiomer isolated from a racemate.[9,10,11]

It was also established that stereochemically related resolving agents are able to isolate acids of opposite configurations,[12,13] and in the current results **CINC**/**QUID** afforded this type of results in **P4** and **P6**. The same concept is contradicted by the current results in **P5** and **P7**, **CIND/QUIN** isolated enantiomers of the same configuration.

In **P11** – **P14** the resolving agents isolated the (*S*)-enantiomer in the order **QUIN** > **CINC** > **CIND** > **QUID**, with **QUIN** as the best in resolving 2-chloropropanoic acid. Therefore, the pairs **CINC/CIND** and **QUIN/QUID** isolated the same enantiomers but in different proportions. The findings are also broadly in line with Wang *et*. *al*. and Toda *et*. *al.*'s results.[1,2]

The salts were stabilized by strong and weak hydrogen bonds, where the solvents contributed in the stabilization except in **P5** and **P10**. The weak hydrogen bonds act as secondary interactions and have been shown to play dominant roles in the determination of crystal packings.[13,14]

The findings show the difficulty in predicting the expected outcomes before actually performing the experiments and analyzing the results.

Different resolving agents resolve different racemates, isolate enantiomers in different proportions, in different solvents, all this affirm the fact that the choice of a good resolving agent or solvent in the resolution of racemates is still a trial and error experimental exercise.

The findings of the study are restricted to the diastereomeric salts obtained, without reducing them to the enantiomers and the bases. The thermal analysis concentrated only on the desolvation and the melting temperatures in characterizing the salts.

The study shows that repeat crystallization experiments to obtain **P5** and **P10** did not yield suitable single crystals, instead solvated powders were formed. This confirms that the process of crystallization can be difficult and is an art as well as a science.[15,16]

Recommendations- It is imperative that in future research attention be paid to the solvents being used, regarding the resolution outcomes. In cases where individual solvents do not yield results, solvent mixtures in different ratios should be utilized. If a particular resolving agent is unsuccessful, their derivatives should be employed.

Reflexion- Undertaking a research study has been an invaluable experience. I now understand the nature of research, the gruesome processes involved in research, and the patience needed regarding the obtaining of suitable results for processing. I have an experience that expected results sometimes do not materialise, research is frustrating and tedious, but at the end of it all rewarding and fulfilling. The experience has instilled some discipline, allowed me to examine my professional conduct and guidelines for changes to my future research. I plan to explore further the process of the resolution of organic compounds since I have more knowledge to apply. The experience and knowledge will be passed on to the postgraduate students in my department for future scientists. The research study has encouraged me to view my own

research abilities within the broader research field, provided a wealth of resources from which we can learn in order to improve the quality of development, research and teaching in the institution.

Contribution- The findings of the undertaking will contribute to the crystallography research towards understanding the factors involved in a successful resolution, especially the effect of solvents besides dissolution. The study will have an impact in the pharmaceutical industry in the preparation of enantiomeric drugs.

## 8.1 References


1. Wang Y, Sun J and Ding K. Practical method and novel mechanism for optical resolution of BINOL by molecular complexation with *N*-benzylcinchoninium chloride. *Tetrahedron,* **2000**, 56, 4447-4451.
2. Toda F, Tanaka K, Stein Z and Goldberg J. Optical resolution of binaphthyl and biphenanthryl diols by inclusion crystallisation with *N*-alkylcinchonidium halides. Structural characterization of the resolved materials. *J. Org. Chem.,* **1994**, 59, 5748-5751.
3. Bàthori N, Jacobs A, Mei M and Nassimbeni L. Resolution of malic acid by (+)-cinchonine and (-)-cinchonidine. *Canadian J. Chem*., **2015**, 93, 858-863.
4. Jacques J, Fouquey C and Viterbo R. Enantiomeric cyclic binaphthyl phosphoric acids as resolving agents. *Tetrahedron Letters*, **1971**, 12, 4617-4620.
5. Hughes DL. Resolution of 1,1'-binaphthol, (*R*)-(+)- and (*S*)-(-)-2,2'-*bis*(diphenylphosphini)-1,1'-binaphthyl (BINAP). *Org. Synth*., **2014**, 91, 1-11.
6. Gjerløv A and Larsen S. A study of diastereomeric mandelate salts of cinchonidine and the relation to their quasidiasteremeric analogues. *Acta Cryst.,* **1997**, B53, 708-718.
7. Larsen S, De Diego HL and Kozma D. Optical resolution through diastereomeric salt formation: The crystal structures of cinchoninium (*R*)-mandelate and cinchoninium (*S*)-mandelate at low temperature. *Acta Cryst*., **1993**, B49, 310-316.
8. Kozma D, Nyéki Á, Ács M and Fogassy E. Optical resolution of mandelic acid by Cinchonine in different solvents. *Tetrahedron: Asymmetry,* **1994,** 5**,** 315-316.
9. Sakai K, Sakurai R, Yuzawa A and Hiramaya N. Practical continuous resolution of α-amino-ε-caprolactam by diastereomeric salt formation using a single resolving agent with a solvent switch method. *Tetrahedron: Asymmetry*, **2003**, 3713-3718.
10. Sakai K, Sakurai R and Hiramaya N. Chiral discrimination controlled by the solvent dielectric constant. *Tetrahedron: Asymmetry*, **2004**, 1073-1076.
11. Sakai K, Sakurai R, Akimoto T and Hirayama N. Molecular mechanism of dielectrically controlled optical resolution (DCR). *Org. Biomol. Chem.*, **2005**, 360-365.
12. Białońska A and Ciunik Z. Racemic resolution of *N*-protected alanine by strychnine and brucine *versus* donor/acceptor capability. *CrystEngComm,* **2004**, 6, 276-279.
13. Gould RO and Walkinshaw MD. Molecular recognition in model crystal complexes: The resolution of D and L amino acids. *J. Am. Chem. Soc*., **1984**, 106, 7840-7842.

14. Berkovitch-Yellin Z and Leiserowitz L. The role played by the C—H···O and the C—H···N interactions in determining molecular packing and conformation. *Acta Cryst.,* **1984**, B40, 159-165.
15. Grootenhuis PDJ, van Eerden J, Dijkstra PJ, Harkema S and Reinhoudt DN. Complexation of neutral molecules by preorganized macrocyclic hosts. *J. Am. Chem. Soc.,* **1987**, 109, 8044-8051.
16. Dunitz JD and Bernstein J. Disappearing polymorphs. *Acc. Chem. Res*., **1995**, 28, 193-200.
17. Bučar D-K, Lancaster RW and Bernstein J. Disappearing polymorphs revisited. *Angew. Chem. Int. Ed*., **2015**, 54, 6972-6993.

# Appendices

## Chapter 1

### Appendix A

The top 10 single enantiomer drugs' usage and structures that were reported:[1]

Atorvastatin (**1**), (3*R*,5*R*)-7-[2-(4-Fluorophenyl)-3-phenyl-4-(phenylcarbamoyl)-5-propan-2-ylpyrrol-1-yl]-3,5-dihydroxyheptanoic acid, and administered as Atorvastatin calcium, a lipid lowering medication.

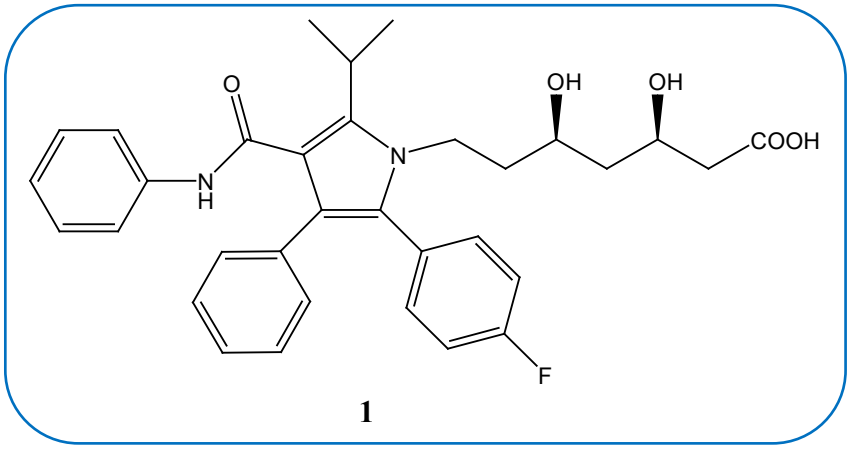


**1**

Simvastatin (**2**) [(1*S*,3*R*,7*S*,8*S*,8a*R*)-8-[2-[(2*R*,4*R*)-4-hydroxy-6-oxooxan-2-yl]ethyl]-3,7-dimethyl-1,2,3,7,8,8a-hexahydronaphthalen-1-yl] 2,2-dimethylbutanoate (a lipid lowering medication). Pravastatin (**3**), (3*R*,5*R*)-3,5-dihydroxy-7-((1*R*,2*S*,6*S*,8*R*,8a*R*)-6-hydroxy-2-methyl-8-{[(2*S*)-2-methylbutanoyl]oxy}1,2,6,7,8,8a-hexahydronaphthalen-1-yl)-heptanoic acid, administered as Pravastatin sodium to lower cholesterol.

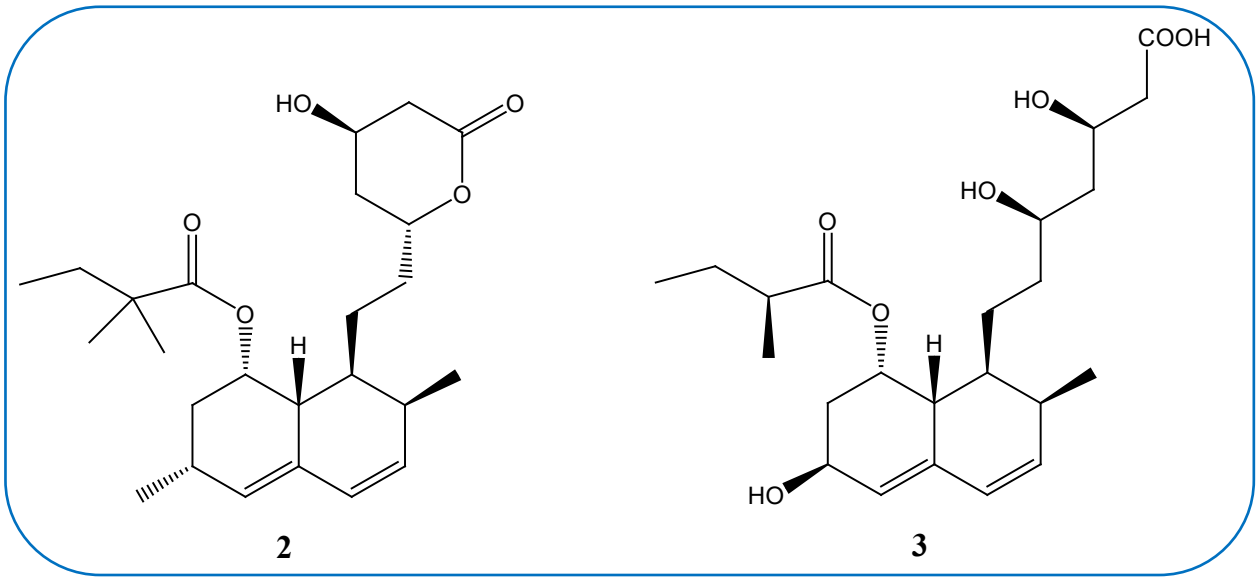


**2** **3**

Paroxetine (**4**) (3*S*,4*R*)-3-[(2H-1,3-benzodioxol-5-yloxy)methyl]-4-(4-fluorophenyl)piperidine, administered as a Paroxetine hydrochloride as an anti-depressant. Clopidogrel (**5**) (+)-(*S*)-methyl 2-(2-chlorophenyl)-2-(6,7-dihydrothieno[3,2-c]pyridine-5-(4H)-yl)acetate, administered as Clopidogrel bisulphate as an anti-platelet agent, to inhibit blood clot.

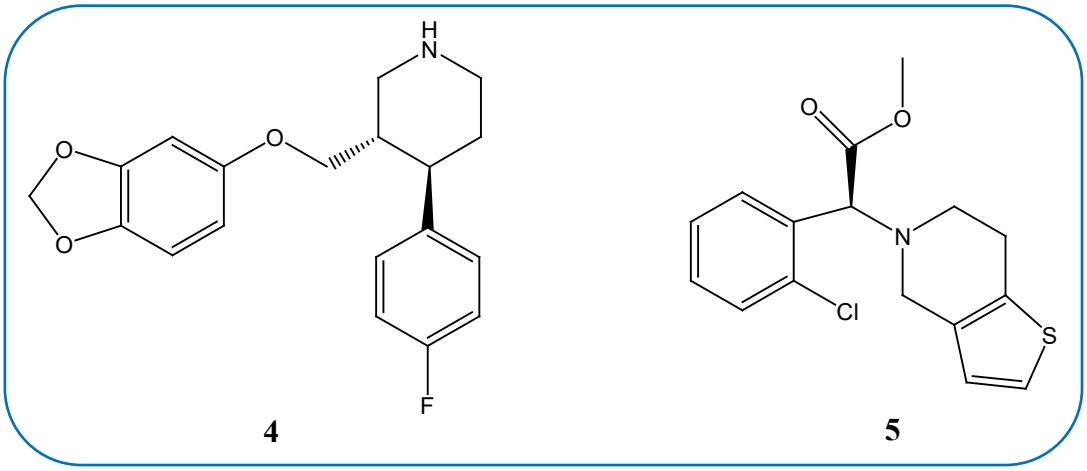


**4** **5**

Setraline (**6**), (1*S*,4*S*)-4-(3,4-dichlorophenyl)-N-methyl-1,2,3,4-tetrahydronaphthalen-1-amine, taken as hydrochloride tablet as an anti-depressant. Fluticazone (**7**), S-Fluoromethyl (6*S*,8*S*,9*R*,10*S*,11*S*,13*S*,14*S*,16*R*,17*R*)-6,9-difluoro-11,17-dihydroxy-10,13,16-trimethyl-3-oxo-6,7,8,11,12,14,15,16-octahydrocyclopenta[a]phenanthrene-1,7-carbothioate, taken as a propionate as an anti-inflammatory.

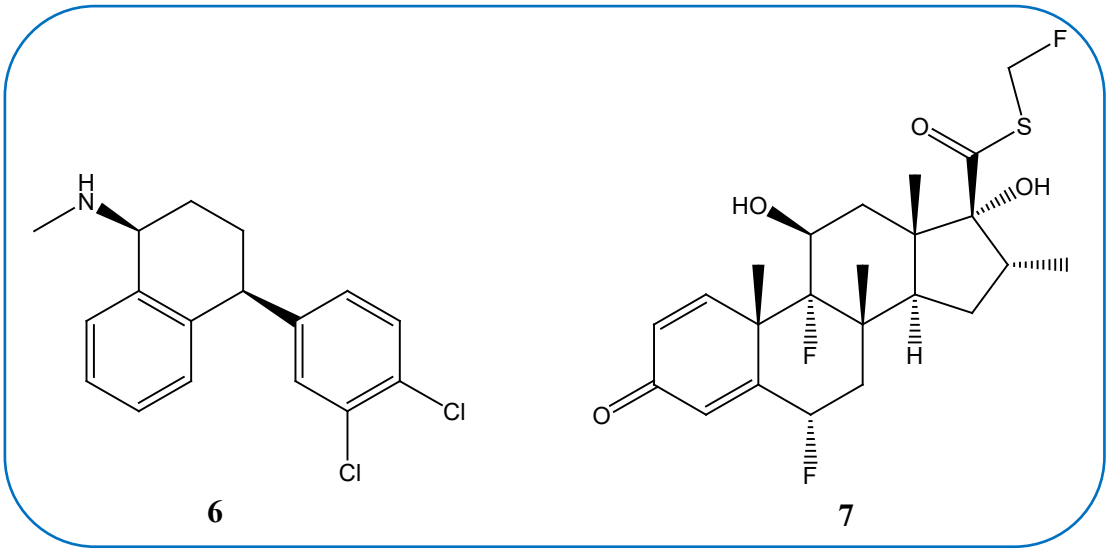


**6** **7**

Esomeprazole (**8**), (*S*)-(-)5-Methoxy-2-[(4-methoxy-3,5-dimethylpyridin-2-yl)methylsulfinyl]-3H-benzoimidazole, used to reduce stomach acid. Amoxicillin (**9**), (2*S*,5*R*,6*R*)-6-{[(2*R*)-2-(4-hydroxyphenyl)-acetyl]amino}-3,3-dimethyl-7-oxo-4-thia-1-azabicyclo[3.2.0]heptane-24-carboxylic acid, used as an antibiotic.

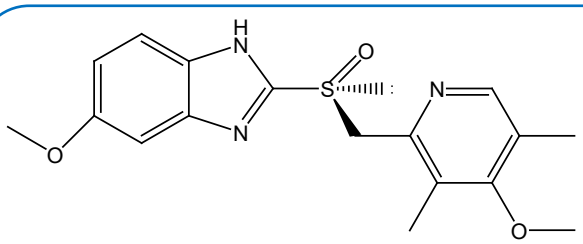

**8**

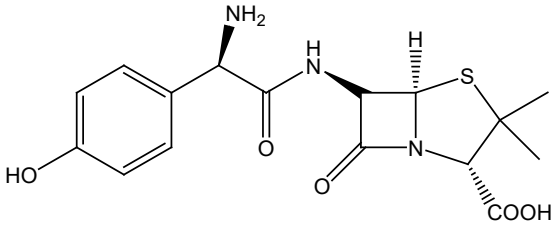

**9**

Valsartan (**10**), (*S*)-3-methyl-2-(*N*-{2'-(2H-1,2,3,4-tetrazol-5-yl)biphenyl-4-yl]methyl}pentanamido)butanoic acid, and it is an angiotensin(II) receptor antagonist, for the treatment of high blood pressure.

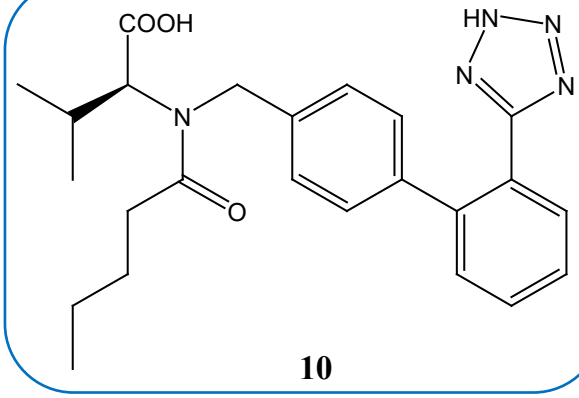

**10**

## Reference

1. Caner H, Groner E and Levy L. Trends in the development of chiral drugs. *Drug Discov. Today*, **2004**, 9, 105-110.

# Chapter 2

## Appendix B

Table 1 The CSD (version 5.41, November 2019) hits for the cinchonine fragments.

| Col | Refcode | Compound name |
|---|---|---|
| 1 | CAVTUO | α-1',2,3',4',10,11-Hexahydrocinchonine dihydrochlorate |
| 2 | CINCHO10 | Cinchonine |
| 3 | CINCHO11 | Cinchonine |
| 4 | EFUSII | O-Methoxycinchonine |
| 5 | EJELEL | Catena-(*bis*(μ$_3$-cinchonine-N,N',O)-hexamethyl-di-aluminium-zinc toluene solvate |
| 6 | ELELIP | Catena-(tetrakis(μ$_3$-cinchonine)-dodecamethyl-tetra-aluminium-di-zinc toluene solvate) |
| 7 | EZEDET | O-Tosyl cinchonine |
| 8 | EZEDIX | O-Tosyl cinchonine |
| 9 | FACDIW | Cinchoninie dihydrochloride dichloro-zinc dihydrate |
| 10 | FACDOC | Cinchoninie dihydrochloride dichloro-cobalt dihydrate |
| 11 | FACFEU | *Bis*(cinchonine) *bis*(tetrachloro-copper) trihydrate |
| 12 | FOYTES | β-1',2,3',4',10,11-Hexahydrocinchonine β-9-deoxy-1',2,3',4',10,11-hexahydrocinchonine |
| 13 | INECIO | Cinchonine-trihydridoborate |
| 14 | LOBWEE | *N*-(9-Deoxyepicinchonine-9-yl)phthalimide |
| 15 | LOBWII | 3-Nitro-*N*-(9-deoxyepicinchonine-9-yl)benzamide monohydrate |
| 16 | LOBWOO | Ferrocenylcarboxylic acid *N*-(9-deoxyepicinchonine-9-yl)amide |
| 17 | QOXMAS | 3-(2-Methoxyphenyl)-4-methyl-2-thioxo-2,3-dihydro-1,3-thiazol-1-ium-5-carboxylate cinchonine |
| 18 | XEXQEW | 9-Epi-10,11-dihydrocinchonine |
| 19 | YEMWAQ | (-)-*Trans*-tetrahydro-isohumulone (+)-cinchonine chloroform solvate |
| 20 | ZUDNUH | Chloro-(cinchonine)-(η$^6$-*p*-cymene)-ruthenium(ii) |
| 21 | ZZZANV | Cinchonine dihydrochloride mercury(ii) chloride dihydrate |

Table 2 The CSD (version 5.41, November 2019) hits for the cinchoninium fragments.

| Col | Refcode | Compound name |
|---|---|---|
| 1 | CEGWEQ | *N*-Benzylcinchoninium chloride |
| 2 | CINCDC | Cinchoninium tetrachloro-cadmium(ii) dihydrate |
| 3 | DAPJAF | (8*S*,9*R*)-9-Hydroxy-6'-methoxy-1-methylcinchoninium iodide |
| 4 | DAPJEJ | (8*S*,9*R*)-9-Hydroxy-6'-methoxy-1-methylcinchoninium methanolclathrate |
| 5 | FACFEU01 | *Bis*(Cinchoninium tetrachloro-copper(ii)) trihydrate |
| 6 | FACFEU02 | *Bis*(Cinchoninium tetrachloro-copper(ii)) trihydrate |
| 7 | FACFEU04 | Cinchoninium tetrachloro-copper(ii) trihydrate |

| | | |
|---|---|---|
| 8 | HEXPOQ | O-(1-adamantoyl)-*N*-(9-anthracenylmethyl)dihydrocinchoninium 4-nitrophenolate acetonitrile solvate tetrahydrate |
| 9 | HEXTUA | Cinchoninium (*R*)-*t*-butylphenylphosphinous acid borane |
| 10 | JORQIQ | (Cinchoninium)-trichloro-zinc methanol solvate |
| 11 | LABXOB | Cinchoninium (*S*)-mandelate |
| 12 | LABXUH | Cinchoninium (*R*)-mandelate |
| 13 | MEJQOI | Cinchoninium 1-methyl-6-(1-methylethylidene)-3-oxotetrahydro-1H-cyclopenta(c)furan-3a(3H)carboxylate |
| 14 | MEVXOA | Cinchoninium L-tartrate tetrahydrate |
| 15 | NEXPEM | (9-Epi-10,11-dihydrocinhoninium)-trichloro-cobalt(ii) |
| 16 | OFANIV | 9-Hydroxycinchonan-1-ium 3-carboxy-2-hydroxypropanoate hydrate |
| 17 | OHUZOG | Cinchoninium (6*R*)-6-allyl-8-(phenylsulfonyl)-1,4-dioxa-8-azaspiro(4.5)decane-6-carboxylate |
| 18 | PUQTIF | Cinchoninium violurate monohydrate |
| 19 | PUQTOL | Cinchoninium squarate hydrate |
| 20 | QASDIY | Catena-(*bis*(μ$_2$-bromo)-(μ$_2$-*N*,*N*'-bis(cinchoninium)-*p*-xylene)-bromo-di-copper(i) bromide trihydrate) |
| 21 | QEDZAC | *N*-(2-Bromobenzyl)cinchoninium bromide |
| 22 | SESYUL | Cinchoninium 3-carboxybenzoate |
| 23 | UNOBUU | (11*S*)-(+)-*N*,*N*'-Dimethylcinchoninium *bis*(iodide) |
| 24 | UYAGEH | Cinchoninium serine phosphate dihydrate |
| 25 | WATFUT | *Bis*(cinchoninium) tetrachloro-cadmium(ii) tetrachloro-copper(ii) |
| 26 | WOMQUK | (*R*)-(+)-1,1'-bi-2-naphthol benzylcinchoninium chloride |
| 27 | WUXQIP | Cinchoninium-trichloro-cobalt(ii) |
| 28 | WUXQOV | Cinchoninium-trichloro-cobalt(ii) ethanol solvate |
| 29 | ZZZDRG | *Bis*(cinchoninium) sulphate dihydrate |

Table 3 The CSD (version 5.41, November 2019) hits for the cinchonidine fragments.

| Col | Refcode | Compound name |
|---|---|---|
| 1 | CINDIN | Cinchonidine |
| 2 | CINDIN10 | Cinchonidine |
| 3 | CUNQOS | 4,4'-Dicarboxy-1,1'-bi-2-naphthol *bis*(cinchonidine) methanol solvate |
| 4 | CUZVOJ | (8*S*,9*SRS*)-9-(Phenylsulfinyl)-epi-cinchonidine |
| 5 | DASMEQ | 11-(Triphenylsilyl)-10,11-dihydrocinchonidine |
| 6 | DIXMIH | (+)-(*P*)-4-Cyclohexyl-2-methyl-buta-2,3-dienoic acid cinchonidine monohydrate |
| 7 | FEXGIZ | (3*R*,8*S*,9*R*)-10,11-dihydro cinchonidine |
| 8 | FIZVIU | (-)-Cinchonidine (*S*)-indole-3-succinate |
| 9 | GOGZUY | O-Methoxycinchonidine |
| 10 | GOHBAH | O-phenoxycinchonidine |
| 11 | INECEK | Cinchonidine-trihydroborate acetone solvate |

| | | |
|---|---|---|
| 12 | JAPNUJ | A-*N*-nitroso-1',2',3',4,10,11'-hexahydrocinchonidine hydrochloride |
| 13 | NODWUZ | 10*R*-Cinchonidine dibromide |
| 14 | PEPDUK | Cinchonidine benzene clathrate |
| 15 | PIGWEI | Catena-(μ2-bromo)-*tris*(μ2-cyano-(*N*-(cyanobenzyl)cinchonidine-)di-copper |
| 16 | UGEWEI | 6-(Neopentyloxy)-9-O-(*t*-butylcarbamoyl)cinchonidine (*S*)-N-(3,5-dinitrobenzoyl)leucine ethyl acetate solvate |
| 17 | VIGKOM | 11-Triethylsilyl-10,11-dihydrocinchonidine |
| 18 | YEMVAP | (4*S*,5*R*)-3,4-dihydroxy-5-(3-methylbutyl)-4-(4-methylpentanoyl)-2-(2-methylpentanoyl)cyclopent-2-en-1-one (-)-cinchonidine 2-methoxy-2-methylpropane solvate |
| 19 | YEMVET | (4*S*,5*R*)-3,4-dihydroxy-2-[(2*S*)-2-methylbutanoyl]-5-(3-methylbutyl)-4-(4-methylpentanoyl)cyclopent-2-en-1-one (-)-cinhonidine diethyl ether propan-1-ol solvate |
| 20 | YEMVIX | (+)-*Cis*-isohumulone (-)-cinchonidine |
| 21 | YOLFOV | *Bis*(μ2-*N*-(4-(Tetrazol-5-yl)benzyl)cinchonidine)-tetrakis(azido)-di-zinc monohydrate |
| 22 | YOLFOV01 | *Bis*(μ2-*N*-(4-(Tetrazol-5-yl)benzyl)cinchonidine)-tetrakis(azido)-di-zinc monodeuterate |
| 23 | ZZZEPC | Cinchonidine sulfate octahydrate |
| 24 | ZZZICY | Cinchonidine dihydrobromide dihydrate |
| 25 | ZZZTZW | Cinchonidine hydrochloride monohydrate |
| 26 | ZZZZUGK | Cinchonidine hydrobromide monohydrate |

Table 4 The CSD (version 5.41, November 2019) hits for the cinchonidinium fragments.

| Col | Refcode | Compound name |
|---|---|---|
| 1 | ADIKII | Cinchonidinium diperchlorate |
| 2 | BEFPEI | 4-Vinylbenzylcinchonidinium chloride |
| 3 | BEFPIM | Catena-(hexakis(μ-chloro)-*bis*(μ-4-vinylbenzylcinchonidinium-penta-copper ethanol solvate |
| 4 | CIYKEB | ((*R*)-Benzylcinchonidinium)-trichloro-copper(ii) |
| 5 | GAJBOJ | (*R*)-9,9'-Spirobixanthene-1,1'-diol *N*-benzylcinchonidinium chloride acetonitrile solvate |
| 6 | GAJBOJ01 | (*R*)-9,9'-Spirobi[xanthene]-1,1'-diol *N*-benzylcinchonidinium chloride acetonitrile solvate |
| 7 | GARJUF | *N*-Benzylcinchonidinium (Δ)-*bis*(3,4,5,6-tetrachlorobenzene-1,2-diolato)(3-fluorobenzene-1,2-diolato)phosphate acetone solvate |
| 8 | GAWSUT | *N*-Benzylcinchonidinium (Δ)-*bis*(3,4,5,6-tetrachlorobenzene-1,2-diolato)(4-fluorobenzene-1,2-diolato)phosphate acetone solvate |
| 9 | HATHEQ | Trichloro-(cinchonidinium-*N*)-cobalt(ii) |
| 10 | HUSBIG | *Bis*((3R,4S,8S,9R)-Cinchonidinium) (2*R*,3*R*)-tartrate dihydrate |
| 11 | HUSBIG01 | (18*R*,19*S*,21*S*,25*S*)-Cinchonidinium) (2*R*,3*R*)-tartrate monohydrate |
| 12 | IROVUG | (11*R*)-(-)-*N*,*N*'-dimethylcinchonidinium diiodide |

| | | |
|---|---|---|
| 13 | JAPGIR | (*R*)-(+)-1-(2-Hydroxy-1-naphthyl)-3-(2-hydroxyphenyl)isoquinoline *N*-benzylcinchonidinium chloride |
| 14 | JAPGIR01 | (*R*)-(+)-1-(2-Hydroxy-1-naphthyl)-3-(2-hydroxyphenyl)isoquinoline *N*-benzylcinchonidinium chloride |
| 15 | MICLOZ | *N*-Fluorocinchonidinium tetrafluoroborate monohydrate |
| 16 | MOZHOY | (*S*)-(-)-1,1'-Spirobi-indane-7,7'-diol *N*-benzylcinchonidinium chloride |
| 17 | NAHVOH | Cinchonidinium pyrucic acid oxime |
| 18 | NEDDAB | O-Allyl-9-anthacenylmethyl cinchonidinium bromide diethyl ether solvate |
| 19 | NEDDEF | O-Allyl-9-anthracenylmethyl cinchonidinium *p*-nitrophenoxide dichloromethane solvate |
| 20 | OFANOB | *Bis*(9-hydroxycinchonan-1-ium) 2-hydroxysuccinate dihydrate |
| 21 | OFANUH | *Bis*(9-hydroxycinchonan-1-ium) 2-hydroxysuccinate dihydrate |
| 22 | OGANER | (-)-Cinchonidinium-(-)-(*S*)-citronellate monohydrate |
| 23 | OSAJEZ | *N*-Methylcinchonidinium iodide |
| 24 | QASDEU | Dibromo-(*N*-3-cyanobenzylcinchonidinium)-copper(i) methanol solvate |
| 25 | QOMFON | (*R*)-(-)-2,2'-Diamino-1,1'-bianthryl (-)-*N*-benzylcinchonidinium chloride |
| 26 | RANPUS | Cinchonidinium tetrakis(4-(2-(4,6-diamino-1,2,5-triazinyl))phenyl)borate dimethylsulfoxide toluene clathrate |
| 27 | RERXUH | Cinchonidinium (*S*)-mandelate |
| 28 | RERYAO | Cinchonidinium (*R*)-mandelate |
| 29 | SIGWIP | 1-*N*-(9-Anthrylmethyl)-6'-hydroxy-10,11-dihydrocinchonidinium chloride dichloromethane solvate |
| 30 | SIGWUB | 1-*N*-(9-Anthrylmethyl)-9-O-benzyl-6'-hydroxy-cinchonidinium chloride chloroform solvate |
| 31 | SIGYAJ | 1-*N*-(9-Anthrylmethyl)-6'-isopropoxy-10,11-dihydrocinchonidinium chloride hemihydrate |
| 32 | TURJIZ | Cinchonidinium *tris*(tetrachlorobenzenediolato)phosphate ethyl acetate solvate |
| 33 | TUZDAV | Cinchonidinium 4-hydroxyphenylacetate hemihydrate |
| 34 | TUZDEZ | Cinchonidinium 4-hydroxyphenylacetate isopropanol solvate monohydrate |
| 35 | VELWUF | Cinchonidinium *bis*(4-methylbenzenesulfonate) monohydrate |
| 36 | XAZPAP | Cinchonidinium *bis*(2,3-naphthalenediyl)orthoborate acetone solvate |
| 37 | QUNXIG | *N-(*2-Fluorobenzyl)cinchonidinium bromide sesquihydrate |
| 38 | ZZZTZW01 | Cinchonidinium chloride monohydrate |

Table 5 The CSD (version 5.41, November 2019) hits for the quinine fragments.

| Col | Refcode | Compound name |
|---|---|---|
| 1 | BOMDUC01 | Quinine |
| 2 | CAGMAB | 6'-methoxy-10,11-didehydrocinchonan-9-ol |

| | | |
|---|---|---|
| 3 | CAGMAB01 | 6'-methoxy-10,11-didehydrocinchonan-9-ol |
| 4 | CETTOM | Quinine-ferriprotoporphyrinIX acetonitrile unknown solvate |
| 5 | DADCUG | 10-Hydroxy-10-methyl-10,11-dihydroquinine |
| 6 | DBZEQU | Dibenzoequinine |
| 7 | DUMQUY | 1-Butylquinine tetrafluoroborate |
| 8 | ECAMOK | 10,11-Dihydroquinine hydrochloride |
| 9 | ECAQAD | Quinine acesulfame |
| 10 | EACQAD01 | Quinine acesulfame |
| 11 | ELIPAQ | Quinine quinidine dehydrate |
| 12 | HOPGEY | 2-(1,5-dimethyl-4-hexenyl)-6-amino-3-hydroxy-5-methyl-1,4-benzoquinine |
| 13 | IGATOC | (*R*)-(-)-2-Fluoro-a-methyl-4-biphenylacetic acid (8a,9*R*)-6'-methoxycinchonana-9-ol salt |
| 14 | IMEWOM | O-Ferrocenoyl-10,11-dihydroquinine |
| 15 | INECOU | Hydroquinine-trihydridoborate monohydrate |
| 16 | INECUA | Hydroquinine-trihydridoborate |
| 17 | JEJZEE | 9-(4-methoxycarbonyl-1H-1,2,3-triazoyl)-9-dehydroxyepiquinine |
| 18 | JIFYOM | Diquinine biphenyl-2,2'-dicarboxylic acid monohydrate |
| 19 | JORHON | (Ethane-1,2-diamine)-(quinine)-palladium(ii) nitrate monohydrate |
| 20 | JORQEM | ($\mu_2$-Quinine)-bis(triethylphosphine)-trichloro-di-palladium(ii) chloroform solvate monohydrate |
| 21 | JORQOW | ($\eta^2$-Quinine)-trichloro-platinum(ii) hydrochloride hydrate |
| 22 | KAMDAD | Quinine toluene solvate monohydrate |
| 23 | LIQBAP | Catena-[($\mu_2$-Sulfato-O,O')-(quinine-N)-chloro-zinc(ii) |
| 24 | MOHBOA | (8*S*,9*R*,10*R*)-10-Bromo-10,11-dihydroquinine |
| 25 | MOHBUG | (8*S*,9*R*,10*S*)-10-Bromo-10,11-dihydroquinine benzene solvate |
| 26 | QIQMUY | 10(*R*), 11-Dihydroxydihydroquinine |
| 27 | QIQNAF | 10(*S*), 11-Dihydroxydihydroquinine hydrate |
| 28 | RAKJES | 9-epi-Quinine mesylate |
| 29 | SARGEY | (3*S*)-3-Hydroxyquinine 9-acetate dichloromethane solvate |
| 30 | TIKBEX | *Bis*(9-hydroxy-6'-methoxycinchonan-1-ium) 2-hydroxysuccinate dihydrate |
| 31 | TIKBIB | *Bis*(9-hydroxy-6'-methoxycinchonan-1-ium) 2-hydroxysuccinate dihydrate |
| 32 | TIKBOH | 9-Hydroxy-6'-methoxycinchonan-1-ium 3-carboxypropanoate monohydrate |
| 33 | TIKBUN | *Bis*(9-hydroxy-6'-methoxycinchonan-1-ium) 2-hydroxysuccinate dihydrate |
| 34 | TOPXED | Quininedi-ium sulphate *bis*(thiourea)monohydrate |
| 35 | VICCUF | 9-Desoxy-9-chloroquinine |
| 36 | VIVMIX | 9-epi-Bromoquinine |
| 37 | XEFVAH | Catena-(*tris*($\mu_3$-iodo)-*tris*($\mu_2$-quinine)-*bis*($\mu_2$-iodo)-penta-copper(i)) |
| 38 | XUWTUE | (Quinine)-trichloro-cobalt(ii) |

| | | |
|---|---|---|
| 39 | YAFHUL | Quinine acesulfame monohydrate |
| 40 | YAFJAT | Quinine acesulfame |
| 41 | YAJHAV | Quinine thiosaccharin |
| 42 | ZZZFHU | Quinine benzenate |
| 43 | ZZZMNM | Quinine selenite dihydrate |
| 44 | ZZZMNO | Quinine sulfate dihydrate |
| 45 | ZZZMNO01 | Quinine sulfate dihydrate |
| 46 | ZZZQUK | Quinine acid sulphate iodine complex hexahydrate |
| 47 | ZZZQYU | Quinine dihydrobromide trihydrate |

Table 6 The CSD (version 5.41, November 2019) hits for the quininium fragments.

| Col | Refcode | Compound name |
|---|---|---|
| 1 | BEYTIJ | Quinininium (*R*)-4,12-dibromo(2.2)paracyclophane-7-carboxylate |
| 2 | DOZMAJ | 9-Hydroxy-6'-methoxycinchonan-1-ium 2,4-dinitrophenolate |
| 3 | FEQZEG | (3"*R*,4"*S*,8"*S*,9"*R*)-(-)-Quininium (3a*R*,4*S*,8a*R*)-(-)-decahydro-3a-methoxycarbonyl-8-oxo-3,5-(2'-oxapropanediylidene)azulene-4-carboxylate |
| 4 | FIJSUM | (-)-Quininium (+)-2,2'-dimethylcyclopropanecarboxylate monohydrate |
| 5 | FISDOB | 1,3-*bis*(Quininium-N-methyl)-2-fluorobenzene *bis(*hexafluorophosphate) dihydrate |
| 6 | IROQEL | *bis*(18*R*,19*S*,21*S*,25*S*-Quininium) (2*R*,3*R*)-tartrate monohydrate |
| 7 | JORKOQ | *Bis*(*N*-Methylquininium) *bis*(tetraflyuoroborate) monohydrate |
| 8 | JORQAI | (Quininium)-dichloro-($\eta^5$-pentamethyl-cyclopentadienyl)-iridium tetrafluoroborate |
| 9 | JUBBOX | 9-Epiquininium chloride dihydrate |
| 10 | LEVSIP | (*R*)-9,9'-Spirobixanthene-1,1'-diol *N*-benzyl(6-methoxy)quininium chloride acetonitrile solvate |
| 11 | LIVWOC | (-)-Quininium *N*-benzoyl-*trans*-2-aminocyclohexenanecarboxylate dihydrate |
| 12 | NEXPOW | Epiquininium-trichloro-cobalt(ii) ethanol solvate monohydrate |
| 13 | PUVTUV | Quininium (*S*,*S*)-hydrgen tartrate hemihydrate |
| 14 | ROHJAZ | Quininium (*S*)-mandelate |
| 15 | ROHJAZ01 | Quininium (*S*)-mandelate |
| 16 | SIGWOV | 1-*N*-(9-Anthrylmethyl)-9S-epi-quininium chloride |
| 17 | SIGXAI | 1-*N*-(9"-((1",8"-S:4",5"-R)-1",2",3",4",5",6",7",8"-Octahydro-1",4":5"8"-dimethanoanthacenyl)methyl)quininium chloride acetone solvate |
| 18 | SIGXEM | 1-*N*-(9"-((1",8"-R:4",5"-S)-1",2",3",4",5",6",7",8"-Octahydro-1",4":5"8"-dimethanoanthacenyl)methyl)quininium chloride acetone solvate monohydrate |
| 19 | TUZDOJ | Quininium 4-hydroxyphenyl acetate |

| | | |
|---|---|---|
| 20 | UJOCAX | Catena-*bis*($\mu_2$-$\eta^2$-Quininium)-oktakis($\mu_2$-chloro)-dichloro-octa-copper(i)) |
| 21 | UJOCEB | Catena-*bis*($\mu_2$-$\eta^2$-Quininium)-oktakis($\mu_2$-bromo)-dibromo-octa-copper(i)) |
| 22 | UMUPIB | Catena *bis*(Quininium) oktakis($\mu_2$-chloro)-chloro-penta-copper(i)) |
| 23 | UMUPOH | Catena (*bis*(Quininium)-pentakis($\mu_2$-bromo)-dibromo-tri-copper(i) monohydrate) |
| 24 | URIYAW | *Bis*(Quininium) (S)-1,1'-binaphthyl-2,2'-dicarboxylate dihydrate |
| 25 | UYEZII | 9-Hydroxy-6'-methoxycinchonal-1-ium hydroxyl(phenyl)acetate |
| 26 | UYEZOO | 9-Hydroxy-6'-methoxycinchonal-1-ium hydroxyl(phenyl)acetate |
| 27 | UYEZOO01 | 9-Hydroxy-6'-methoxycinchonal-1-ium hydroxyl(phenyl)acetate |
| 28 | UYIBAG | Quininium (*R*)-mandelate |
| 29 | VAZCUV | Quininium (*S*)-2-chloro-n-butyrate |
| 30 | VIYROM | Quininium *p*-coumarate *p*-coumaric acid methanol solvate monohydrate |
| 31 | WANTOU | Quininium salicylate monohydrate |
| 32 | WIXWUW | O-9-(2,6-Di-isopropylphenylcarbamoyl)quininium (1*R*,3*R*)-(+)-*cis*-permethrinic acid chloroform clathrate |
| 33 | WIXXAD | O-9-(2,6-Di-isopropylphenylcarbamoyl)quininium (1*S*,3*R*)-(+)-*trans*-permethrinic acid n-heptane clathrate |
| 34 | WIXXEH | O-9-(2,6-Di-isopropylphenylcarbamoyl)quininium (1*S*,3*S*)-(+)-*cis*-permethrinic |
| 35 | WOBGEA | O-9-(2,6-Di-isopropylphenylcarbamoyl)quininium (1*R*,3*S*)-(+)-*trans*-permethrinic acid chloroform clathrate |
| 36 | YANNIL | Quininium saccharinate |
| 37 | YUCXIE | Quininium tetrachloride-zinc(ii) |
| 38 | YUKMOG | Diquininium (fluoro(hydroxyphenylphosphinyl)phosphonate acetone solvate sesquihydrate |

Table 7 The CSD 2020 (version 5.41, November 2019) hits for the quinidine fragments.

| Col | Refcode | Compound name |
|---|---|---|
| 1 | BOMDUC | (*S*)-(6-Methoxyquinolin-4-yl)(2*R*,4*S*,8*R*)-8-vinylquinuclidin-2-yl)methanol |
| 2 | BRHEPQ | (+)-10-Bromo-10,11-dihydro-epi-quinidine |
| 3 | CAGMIJ | 10,11-Didehydroquinidine |
| 4 | CETTUS | Quinidine-ferriprotoporphyrin IX unkown solvate |
| 5 | DADCUH | 10-hydroxy-10-methyl-10,11-dihydroquinidine |
| 6 | EJUKAV | M-(-)-9,9'-Biabthryl-2,2'-dicarboxylic acid *bis*((+)-quinidine) acetone solvate |
| 7 | ELIPAQ | Quinine quinidine dihydrate |
| 8 | GANYID | 10*R*, 11-Dihydroxy-10,11-dihydroquinidine monohydrate |
| 9 | INEDAH | Quinidine-trihydridoborate |
| 10 | INEDEL | Quinidine-trihydridoborate methanol solvate |

| | | |
|---|---|---|
| 11 | JEYZIX | Quinidine sequihydrate |
| 12 | KAXTAE | (*p*-Chlorobenzoyl)dihydroquinidine |
| 13 | KIPPUU | 10,11-Dihydroquinidine sesquihydrate |
| 14 | KOLWAJ | (3*S*)-3-Hydroxyquinidine methane sulfonate |
| 15 | MUHZUM | (2*R*,4*S*,5*R*,9*S*)-6'-methoxycinchonan-9-ol methanol solvate |
| 16 | PIWGIM | Catena-(($\mu_3$-bromo)-tetrakis($\mu_2$-cyano)-($\mu_2$-N-(4-cyanobenzyl)quinidine)-di-copper) |
| 17 | QMFERC | Quinidine(-)-1,1'-dimethylferrocene-3-carboxylate monohydrate |
| 18 | QUINDE | Quinidine ethanol solvate |
| 19 | QINDE01 | Quinidine ethanol solvate |
| 20 | SARDUK | (Dimethylcarbamoyl)dihydroquinidine osmium tetroxide toluene solvate |
| 21 | SIFJUM | (*S*)-10-Bromo-10,11-dihydroquinidine |
| 22 | SUDWIX | 9-Epiquinidine hydrochloride monohydrate |
| 23 | TORNOD | Dihydroquinidine-9-O-(9'-phenanthryl)ether monohydrate |
| 24 | VUGSUL | Diquinidine 5,5'-dinitrodiphenic acid acetonitrile clathrate |
| 25 | YUYFUU | (11*S*,12*R*)-Quinidine methyl paraben |
| 26 | ZZZNKI | Quinidine sulphate dihydrate |
| 27 | ZZZNKI01 | Quinidine sulphate dihydrate |
| 28 | ZZZAQC | Quinidine benzenate |

Table 8 The CSD 2020 (version 5.41, November 2019) hits for the quinidinium fragments.

| Col | Refcode | Compound name |
|---|---|---|
| 1 | APAKIM | Quinidinium *p*-hydroxybenzoate |
| 2 | BUWYIB | (+)-(3*R*,4*S*,8*R*,9*S*)-QuinidiniumΔ-(-)$_{546}$-*bis*(oxalato0-(1,10-phenanthroline)-chromium(ii) monohydrate |
| 3 | DOZLUC | 9-Hydroxy-6'-methoxycinchonan-1-ium 2,4-dinitrophenolate |
| 4 | HATHAM | Trichloro-(quinidinium-N)-cobalt(ii) |
| 5 | MEKGUE | (8*R*,9*S*)-Quinidinium (*S*)-4-nitrobenzilate ethyl acetate solvate |
| 6 | NEXPIQ | (Epiquinidinium)-trichloro-cobalt(ii) monohydrate |
| 7 | NEXPIQ01 | (Epiquinidinium)-trichloro-cobalt(ii) monohydrate |
| 8 | SIGXIQ | 1-*N*-(9"-((1",8"-*S*:4",5"-*R*)-1",2",3",4",5",6",7",8"-Octahydro-1",4":5"8"-dimethanoanthacenyl)methyl)quinindinium chloride methanol solvate |
| 9 | SIGXOW | 1-*N*-((*R*)-2-(1,1'-binaphthyl)quinidinium bromide |
| 10 | SIGXUC | 1-*N*-((*S*)-2-(1,1'-binaphthyl)quinidinium bromide dichloromethane solvate |
| 11 | TUZDID | Quinidinium 4-hydroxyphenylacetate monohydrate |
| 12 | WEYDEJ | *Bis*(quinidinium) tetraoxo-molybdenum(iv) monohydrate |

| | | |
|---|---|---|
| 13 | WEYDIN | Quinininium chloride monohydrate |